Synthesis of Heat Integrated Gas Separation Systems Incorporating Absorption

The University of Manchester

Synthesis of Heat Integrated Gas Separation Systems Incorporating Absorption

A thesis submitted to

The University of Manchester

For the degree of

Doctor of Philosophy

In the Faculty of

Engineering and Physical Sciences

Margarita Martin

School of Chemical Engineering and Analytical Science

2009

List of Contents

List of Figures

List of Tables

Abstract

There is an economic incentive to substitute energy and capital-intensive conventional gas separation schemes based on cryogenic distillation. Absorption has potential advantages over low-temperature schemes as it does not rely on high refrigeration requirements to perform the separation.

An optimisation-based synthesis framework has been developed that integrates distillation and absorption-desorption schemes. This methodology is able to quantitatively resolve the numerous tradeoffs between the various capital and operating factors and systematically suggest new design configurations.

A multilevel modelling approach enables the accommodation of absorption-desorption separation options in the distillation orientated framework supported by COLOM® (©Centre for Process Integration, University of Manchester). Improved shortcut models for reboiled absorption and distillation columns have been proposed, which are suitable for exploitation in the developed synthesis framework.

A new methodology for heat integration is proposed that achieves efficient heat recovery and proposes a configuration of the heat exchanger network. This methodology works in harmony with the optimisation framework. Simultaneous optimisation of the separation system, the heat exchanger network and the refrigeration system offers the opportunity of achieving a superior overall configuration.

The structural and operating variables of the separation system are optimised by Simulated Annealing. As a stochastic optimisation method, SA can deal with the large scale of the problem and its discontinuous and non-linear nature imposed by the feasibility limits of the separations and the model equations. The optimal separation configurations are selected on the grounds of minimum capital and operating costs. An analysis of costing methods is provided which aims at rationalising the basis for cost estimation.

The application of the developed synthesis methodology is illustrated by a number of examples of relevance to the natural gas processing and refinery gas processing. Results will emphasise the functionality of the methodology as a tool for quantitative evaluation of preliminary designs and realisation of highly integrated and efficient process concepts. - TOTAL WORD COUNT: 64,374.

Declaration

No portion of the work referred to in this thesis has been submitted in support of an application for another degree or qualification of this or any other university, or other institute of learning.

Margarita Martin

Copyright Statement

Dedication

This thesis is dedicated to my family.

Acknowledgements

I acknowledge the financial support of the European Mobility Marie Curie committee, which funded my PhD research.

I would like to thank the founders and coordinators of the ExPERT programme for allowing me to pursue my PhD in this institution. Over the past years I have had the honour and privilege to work with top world-class academics and professionals.

I wish to thank Dr. Megan Jobson for her continued supervision and consistent support. As an outstanding communicator and a hands-on researcher, Dr. Jobson has inspired me to develop skills transcending my PhD discipline.

I am really grateful to Prof. Robin Smith and Dr. Nan Zhang for their supervision. Prof. Smith identified visionary opportunities that marked a turning point in my PhD research. Dr. Zhang's vast expertise in large scale optimisation problems helped me select research tools and methods.

Thanks to Prof. Peter J. Heggs for his supervision and mentoring prior to his retirement. His academic excellence and charming character are profoundly missed.

I am indebted to Steven Doyle for enabling and supporting the development of my methodology within the COLOM® environment.

Thanks to the students of the Centre for Process Integration for making my time more enjoyable. I really appreciate their genuine efforts to help me accomplish my PhD research.

I am really thankful to my work colleagues of the Warrington group of AspenTech Ltd. and to my former manager, Ian Moore, for their trust and support.

Last but not least, I wish to thank my friends and family for their patience and consistent encouragement. Without them, this work would not have been possible.

Nomenclature

Absorption-desorption model (flowsheet level) (§3.4)

B_1	=	Molar flowrate of absorber bottoms
D_1	=	Molar flowrate of lighter product from absorption-desorption system
D_2	=	Molar flowrate of heavier product from absorption-desorption system
F	=	Molar flowrate of feed to absorption-desorption system
i	=	Generic component of multicomponent system
M	=	Molar flowrate of solvent make-up to absorption-desorption system
R	=	Molar flowrate of gas recycle (optional) within absorption-desorption system
R_D	=	Recycle-to-overhead internal gas recycle ratio
$Rec(i)$	=	Recovery of component i in specified product
R_T	=	Recycle-to-product external gas recycle ratio
$x_{B1}(i)$	=	Molar fraction of absorber bottoms
$x_M(i)$	=	Molar fraction of solvent make-up feed to absorption-desorption system
$y_{D1}(i)$	=	Molar fraction of lighter product from absorption-desorption system
$y_{D2}(i)$	=	Molar fraction of heavier product from absorption-desorption system
$y_F(i)$	=	Molar fraction of feed to absorption-desorption system
$y_R(i)$	=	Molar fraction of gas recycle within absorption-desorption system

Absorption-desorption model (column level) (§3.5)

Individual or component related variables

A_B	=	bottom stage absorption factor
A_e	=	effective absorption factor
A_i	=	absorption factor on stage i of absorber section
A_j	=	absorption factor on stage j of stripper section
A_T	=	top stage absorption factor
b	=	individual liquid molar flowrate from reboiler of exhauster
d	=	individual vapour molar flowrate in reboiled absorber overhead
ΔH_{vap}	=	component molar enthalpy of vaporisation

K_i = equilibrium constant on stage i
l_0 = individual molar flowrate in solvent feed
l_i = individual liquid molar flowrate on stage i of absorber section
l_j = individual liquid molar flowrate on stage j of stripper section
P^0 = component vapour pressure in reboiled absorber column
P_1^0 = component vapour pressure at temperature T_1 in Kelvin
P_2^0 = component vapour pressure at temperature T_2 in Kelvin
S_B = bottom stage stripping factor
S_e = effective stripping factor
S_i = stripping factor on stage i of absorber section
S_j = stripping factor on stage j of stripper section
S_R = stripping factor in reboiler
S_T = top stage stripping factor
v_F = individual vapour molar flowrate of feed to reboiled absorber
v_i = individual molar flowrate on stage i of absorber section
v_j = individual molar flowrate on stage j of stripper section
v_{TX} = individual vapour molar flowrate from reboiled absorber top section
x_i = liquid molar fraction on stage i of absorber section
y_i = vapour molar fraction on stage i of absorber section

Greek letters

φ_A = fraction of feed gas component flowrate, v_{n+1}, that remains unabsorbed
φ_{AA} = fraction of feed gas component flowrate, v_{n+1}, that remains unabsorbed in exhauster
φ_{AX} = fraction of feed gas component flowrate, v_{n+1}, that remains unabsorbed
φ_S = fraction of the given component in the liquid feed, l_0, that is remains in the liquid
φ_{SA} = absorption section stripping factor
φ_{SX} = exhausting section stripping factor
ψ_A = fraction of liquid feed component flowrate, l_0, that is lost to the gas
ψ_S = fraction of feed gas flowrate, v_{n+1}, that is absorbed
π_A = absorption factor product
Σ_A = absorption factor series

Overall variables

B = liquid molar flowrate from reboiler
L_i = liquid molar flowrate on stage i of absorber section
m = number of stages of stripper section (excluding reboiler)
n = number of stages of absorber section
P = pressure in reboiled absorber column

R = gas constant (8.314 J $mol^{-1}K^{-1}$)
R_{Boilup} = boilup ratio
T_i = temperature on stage i of absorber section
V_F = vapour molar flowrate of feed to reboiled absorber
V_i = vapour molar flowrate on stage i of absorber section
V_{m+1} = vapour molar flowrate from reboiler of exhauster

Distillation model (§3.7)

B = bottom flowrate
D = is the distillate rate
h_L = molar enthalpy of the liquid at the top of the column
$h_{L\infty}$ = enthalpy of the liquid at the rectifying pinch
H_V = molar enthalpy of the vapor at the top of the column
$H_{V\infty}$ = enthalpy of the vapour at the rectifying pinch
$K_{i,\infty}$ = equilibrium constant of component i at the rectifying pinch
L = liquid reflux
L'_{min} = minimum reflux ratio at the column bottoms
L_∞ = liquid flowrate at the rectifying pinch
N = number of components
q = feed quality
Q_{COND} = condenser duty
$R_{\infty min}$ = minimum reflux ratio at the rectifying pinch
R'_{min} = minimum reflux ratio at the column bottoms
V = vapor flowrate at the top of the column
V_∞ = vapor flowrate at the rectifying pinch
$x_{i,\infty}$ = liquid mole fraction of component i at the rectifying pinch
$x_{i,B}$ = liquid mole fraction of component i in bottoms
$x_{i,D}$ = vapour mole fraction of component i in distillate
$x_{i,F}$ = liquid mole fraction of component i at the feed
$y_{i,\infty}$ = vapour liquid mole fraction of component i at the rectifying pinch

Greek letters

$\alpha_{HNK,HK}$ = relative volatility of the component below the heavy key
α_{ij} = relative volatility of component i with respect to j
$\alpha_{ij,\infty}$ = relative volatility of component i with respect to j at the rectifying pinch
θ_j = parameter of the Underwood method

Heat exchanger network design (Chapter 4)

C_j = hot stream j
H_i = hot stream i
I_{Cl} = cold-side interval
I_{Hk} = hot-side interval

L'_m = level m in the composite level list
L_{Cl} = hot-side temperature level l
L_{Hk} = hot-side temperature level k
m = number of cold streams
n = number of hot streams
Q_{evap} = heat absorbed by the refrigerant from the heat source
$T_{cond.}$ = condenser temperature in Kelvin
$T_{evap.}$ = evaporator temperature in Kelvin
ΔT_{min} = minimum temperature approach
U_{Ci} = hot utility i
U_{Cj} = cold utility j
η = mechanical efficiency of the compressor

Chapter 1. Introduction

1.1 Definitions

- LPG (Liquified Petroleum Gas)

Petroleum or natural gas-derived mixture of propane (C_3H_8) and butane (C_4H_{10}), which is primarily used as fuel.

- NGL (Natural Gas Liquids)

Natural gas-derived mixture of ethane (C_2H_6), propane (C_3H_8), butanes (n-C_4H_{10}, i-C_4H_{10}), pentanes and higher molecular weight hydrocarbons.

- Light naphtha

A mixture consisting mainly of straight-chained and cyclic aliphatic (non-aromatic) hydrocarbons having from five to nine carbon atoms per molecule (Meyer (1998)).

- Olefins or alkenes

Unsaturated hydrocarbons containing at least one carbon-to-carbon double bond, such as ethylene and propylene.

1.2 Scope of work

This work will primarily focus on the development of a systematic synthesis framework for the quantitative evaluation of absorption-desorption and distillation gas separation options.

Over the past decades, patented process technology developments have emerged to address one or more of the following issues: increased process efficiency, reduced capital cost, improved operability, increased product purity. While the implementation of low-temperature gas separation systems have achieved certain level of maturity, physical absorption-desorption systems have not yet reached the same level of penetration across industry.

A number of publications are in favour of the application of absorption-desorption technology to gas separation processes that are historically dominated by cryogenic distillation. This work is motivated by the lack of a design methodology that is able to account for the numerous economic and operational trade-offs of the different separation options in a quantitative manner.

1.3 Background

1.3.1 Gas separations

A separation process allows a segregation of feed stream components between two or more separation product streams. The separation of multicomponent gases for industrial processing or distribution to end users is generally motivated by economic, environmental and health and safety considerations. Frequently, component recovery from gas streams or purification of gas streams is driven by the increased total value of the resulting final products. Also very often, one or more components occurring in a gas stream are hazardous or environmental pollutants or

simply undesirable in the product stream and must be removed from the bulk of the gas stream before the gas stream is further processed or distributed.

Sequences or trains of separations are usually encountered in industrial applications to allow the separation of one or more gas feeds into various products. The separation is driven by the added value of the end products, and intermediate separation tasks in the sequence are required to achieve the overall train separation targets. An approach to the analysis of the economic value of intermediate processing streams can be found elsewhere (Sadhukhan (2002)).

The traditional classification of gas separations by typical separation objectives of King (1980) is reviewed by Barnicki and Fair (1992). Gas purification and bulk separation between main constituents of the gas are common objectives. Sharp separations achieve a practically complete split of feed components between product streams, while sloppy separations achieve a partial recuperation of the component group of interest with a consequent enrichment of one of the products. Some representative examples of gas separation objectives are introduced below.

1.3.1 (i) Natural gas separations

Example 1. Nitrogen naturally occurs in associated natural gas (produced in association with crude oil extraction) or non-associated natural gas, but may also result from nitrogen injections employed for reviving oil wells. Pipeline natural gas must meet various specifications regarding dew point, heating value, acid gas content and total inert content, among others. According to Gaskin (2009), nitrogen content in natural gas for distribution is often limited to 2-4 mol%, because it dilutes the fuel value of the natural gas. In cases where natural gas nitrogen content exceeds the allowable limit, nitrogen must be removed to meet this specification.

Example 2. Natural gas is a mixture of hydrocarbons, predominantly methane, ethane, propane, butane and pentane. Some natural gas processing plants have the facility to recover NGLs from a rich natural gas feed that is rich in C2+. Isolation of ethane and propane is motivated by the favourable economics of using these components for synthesis of olefins as opposed to using them for fuel in the bulk of the natural gas.

1.3.1 (ii) Refinery gas processing

Example 1. Hydrogen is a common constituent of gas streams in refinery processing. Some refinery operations require hydrogen as reactant while others generate hydrogen as a side-product. Hydrogen recovery from refinery off-gases is therefore desirable because it may be reused within the plant. Surplus of hydrogen is typically sold to external users due to the higher value of hydrogen for synthesis than for fuel.

Example 2. In a refinery, the unsaturates gas plant, also known as coker gas plant, performs the separation of light naphtha, LPG olefins and fuel gas from the overhead streams from a fluid catalytic cracking unit. Light naphtha is a primary feedstock for producing olefins in steam crackers.

1.3.2 Typical gas separation technologies - Propane-plus recovery from natural gas

Existing technologies for performing the separation examples of section 1.3.1 involve cryogenic systems such as turboexpanders, Joule-Thompson valves and cascaded refrigeration plants, and non-cryogenic systems, such as oil absorption systems and enhanced absorption systems. Other established technologies including adsorption processes such as pressure swing adsorption, membrane separation processes, incineration, thermal oxidiser, and catalytic incinerator processes are primarily suited to purification separations rather than bulk separations (Barnicki and Fair (1992)).

Different recovery scenarios are encountered in natural gas processing. Typical specifications include gas transportation specifications. In plants where NGLs are recovered from rich natural gas feeds, the design specifications of the separation system are on the ethane recovery.

The most widely applied technology to extract ethane from natural gas is low-temperature separation, which involves partial condensation of the gas feed into a liquid fraction predominantly rich in ethane and other NGLs. According to Farry (1998), Joule-Thompson throttling valves, turboexpanders and mechanical refrigeration are the principal mechanisms employed in these separations. Farry (1998) also indicates that recovery of NGLs by oil absorption, with a gas-oil fraction and usually refrigerated is an older method, still used occasionally.

Farry (1998) recommends the ethane extracted from associated gas as one of the cheapest ways to produce ethylene, despite the large size of the NGLs recovery process to supply a world-scale ethylene cracker. The advantages of cracking ethane into ethylene over cracking other feedstocks, such as naphtha and LPG, is that formation of byproducts, such as propylene, butylene and pyrolysis gasoline, is prevented. The presence of byproducts requires a more complex downstream separation train than usual trains for ethylene derivatives from ethane feeds.

The calorific value of ethane is approximately 1.8 times that of methane. According to Farry (1998), this means that a typical natural gas stream with 5% ethane content, will have a 4% higher calorific value than a stream consisting of methane only. As a result, ethane does not make a significant difference to the natural gas properties at average concentration levels; therefore, there is no general minimum ethane recovery target. The consequence of this is that the decision to recover ethane from natural gas is primarily imposed by ethane market economics.

In periods of adverse economic conditions, the price of liquid ethane as petrochemical feedstock may be less than its equivalent fuel price, and the operators of natural gas plants may prefer to maximise the propane recovery while minimising the ethane recovery. Under these circumstances, operational process flexibility to switch from the common 80-90% propane recovery mode to an ethane rejection mode may be advantageous.

Different technologies for C3+ recovery have evolved historically to improve separation performance. In the early days of natural gas LPG recovery, two types of processes were the commonest: absorption with circulated heavy lean oil for C3+ recovery at ambient conditions (Figure 1.1), and refrigeration of the gas for C3+ extraction (Figure 1.2). First process improvements combined the two concepts by refrigerating the absorption lean oils, which required installation of complex sponge-oil systems to reduce solvent losses.

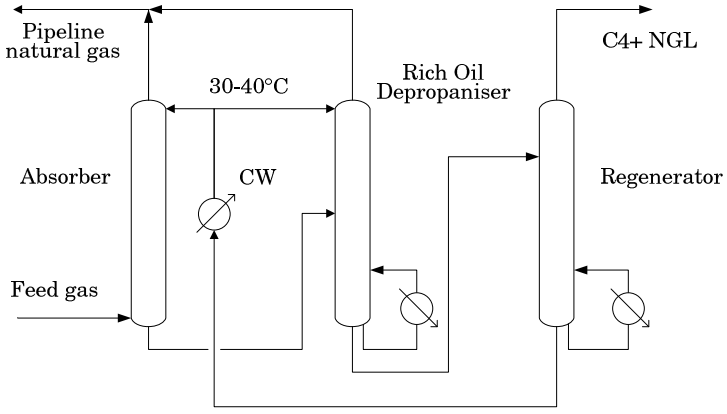

Figure 1.1: Lean oil absorption system.

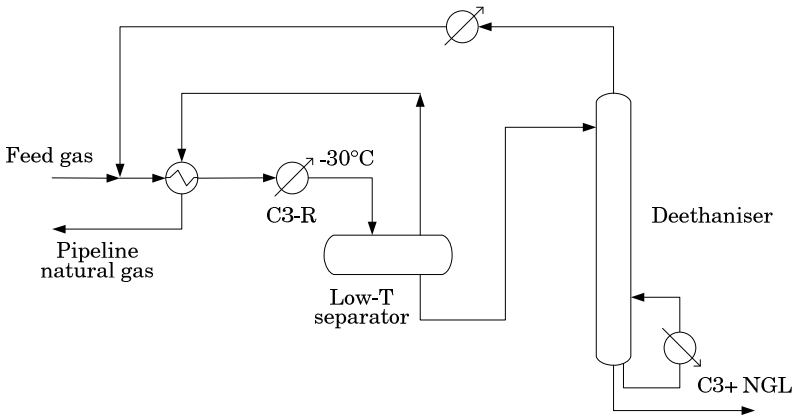

Figure 1.2: Refrigerated system.

The refrigerated low temperature separation system of Figure 1.2 can achieve low propane recoveries of less than 50%, which is usually sufficient to meet the dew point control specifications for gas transportation. With a cascaded refrigeration cycle, higher recoveries can be achieved.

In Joule-Thompson processes, primarily developed for C2+ recovery, refrigeration is avoided by letting down the pressure of the gas feed in through expansion in a JT valve. When the fuel gas delivery pressure specification is high, recompression costs may become prohibitive.

Cryogenic turboexpander processes were developed primarily for recovery of C2+ or demethanisation, whereby the expansion of the gas feed through an expander produces the formation of a condensate that is rich in NGLs. Further enrichment of the separated phases can be achieved in a cryogenic distillation unit, which consists of a complex distillation column with multiple feeds and pumparounds.

For identical separation specifications, cryogenic turboexpander processes feature lower compression demands than Joule-Thompson processes, because a portion of the total recompression of the fuel gas is provided by the turboexpander. Further efficiency improvements were realised with

the introduction of the Gas Sub-cooled Process (GSP) in the 1970s (Figure 1.3) by Ortloff Engineers Inc., and the use of dephlegmators.

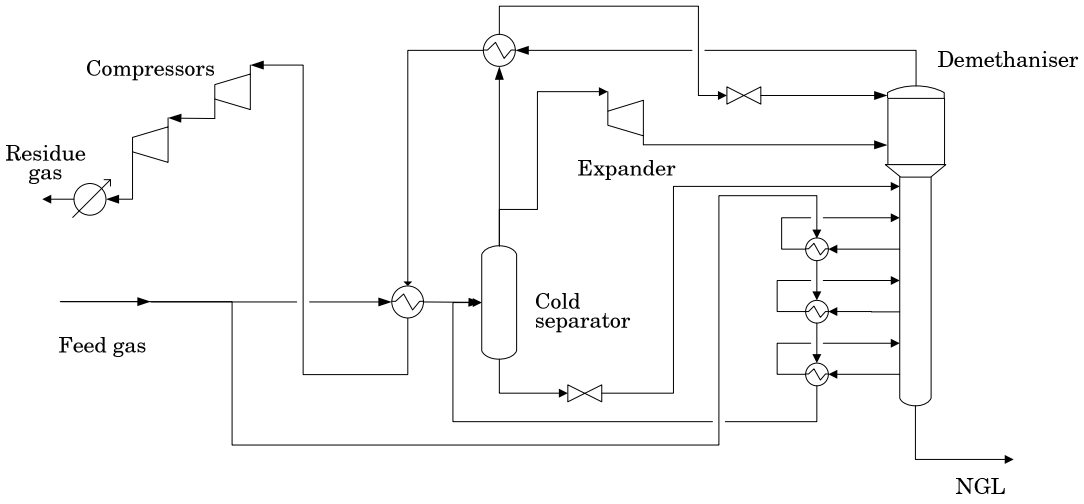

Figure 1.3: GSP Ortloff system.

Expander-based cryogenic processes require a high inlet pressure to achieve through the expansion a sufficiently low temperature leading to the desired propane recovery. As a result, the feed gases must be frequently compressed prior to expansion. For small feed compression ratios, if the turboexpander discharge pressure is considerably lower than the compressor inlet pressure, the need for a separate compressor can be eliminated by using a pre-boost turboexpander with a loaded booster compressor (Bloch and Soares (2001)). Alternatively, any remaining cooling demand can be supplemented with refrigeration.

Substantial evolution of the cryogenic turboexpander scheme allowed this technology to achieve C3+ recovery levels through the introduction of residue-reflux systems, two-tower systems (Figure 1.4), and enhancements to the original GSP process.

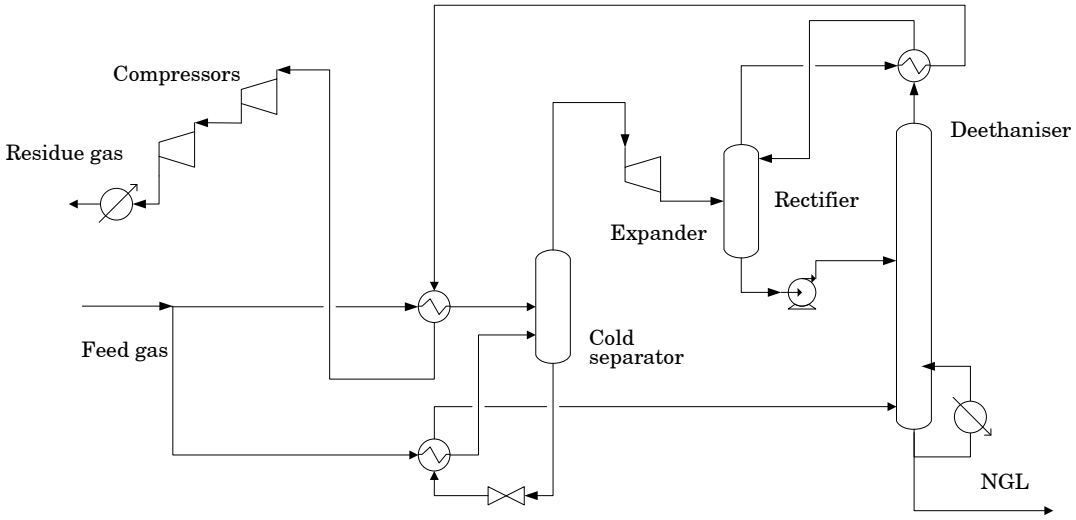

Figure 1.4: Two-tower system.

1.3.3 Enhanced absorption-desorption process technology

Absorption entails counterflow circulation of a multicomponent gas feed and a lean solvent in an absorber column to produce an overhead stream that is enriched in one or more feed components and a loaded, rich solvent stream that is enriched in the remaining feed components. In physical absorption with an absorption oil or with a lighter C5+ organic solvent, the solvent typically absorbs the heavier feed component(s) of the multicomponent stream, hence generating an overhead stream which is predominant in the lighter feed component(s). The split between feed components is given by the solvent composition, the solvent circulation, the dimensions of the absorber and the conditions within the absorber.

Desorption consists in the regeneration of the rich solvent by releasing the absorbed component(s) using one or more flash vessels, using heat, using a distillation column, a stripping gas column, a reboiled stripping column or a combination of these standard methods. Other options than distillation are suited to situations where there is a large difference of volatilities between the solvent and the solute or where solvent losses to the overhead product are not an issue.

There is a limited number of publications in the open literature that relate to the application of absorption-desorption to gas separation processes that are traditionally accomplished by cryogenic distillation. A summary of two main contributions is provided below.

1.3.3 (i) Absorption-desorption enhancements in Mehra process

The Mehra process is a patented absorption-desorption process that enhances the process performance through reboiled absorption, presaturation and adequate selection of chilling locations (Figure 1.5). The Mehra Process is described in several US Patents, including Mehra (1986), (1989), Wood and Mehra (1996). These patents describe systems for absorption-desorption systems where physical solvent used is internally generated from the feed gas and systems where the physical solvent used is external. Improvements to these processes by Gaskin (2009) address the use of cryogenic temperatures in processing gases in solvent absorption systems.

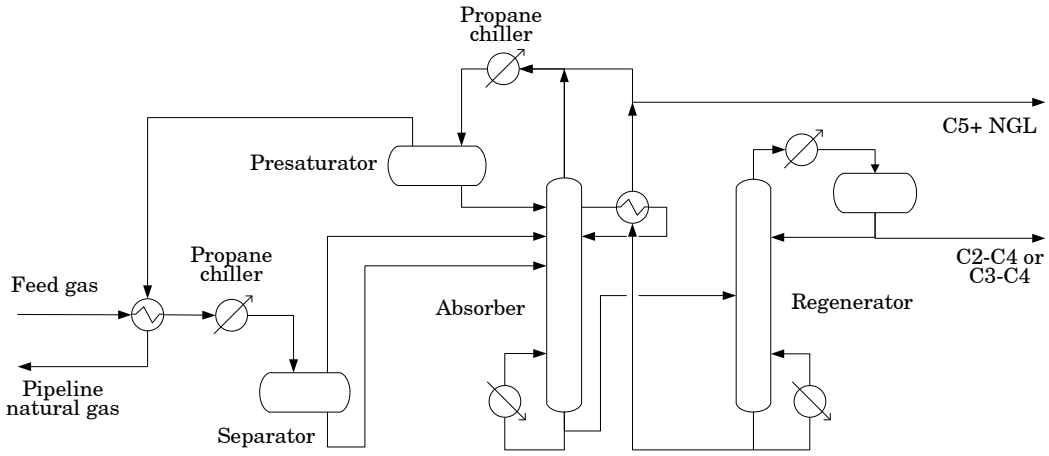

Figure 1.5: Mehra absorption system.

It is recognised that solvent absorption-desorption (Gaskin (2009)) is well suited to applications of separation of natural gas streams into light and heavy products, typically nitrogen and methane and refinery gas components into light and heavy products, typically hydrogen and

methane. Commercial technologies based on the Mehra proprietary technology are also available for ethylene and heavier and LPG recovery from refinery off-gases, hydrogen recovery from refinery streams and recovery of reactants from purge gases (Advanced Extraction Technologies, Inc. homepage, Mehra (2009)).

In order to prevent the contamination of the heavier product by the lighter component(s) through co-absorption of the light components into the solvent, the Mehra process features a reboiler at the bottom of the absorber, which strips out the absorbed light component. In a modified version of the Mehra process described by Gaskin (2009), shown in Figure 1.6, the rich solvent is subjected to multiple flash stages and a portion of the gas released from one or more of the early flash stages is recycled to the absorber (at a point in the absorber that is equal to or below the feed gas stream). This process provides a higher purity product stream but requires recompression of the recycle gas and an additional flash stage.

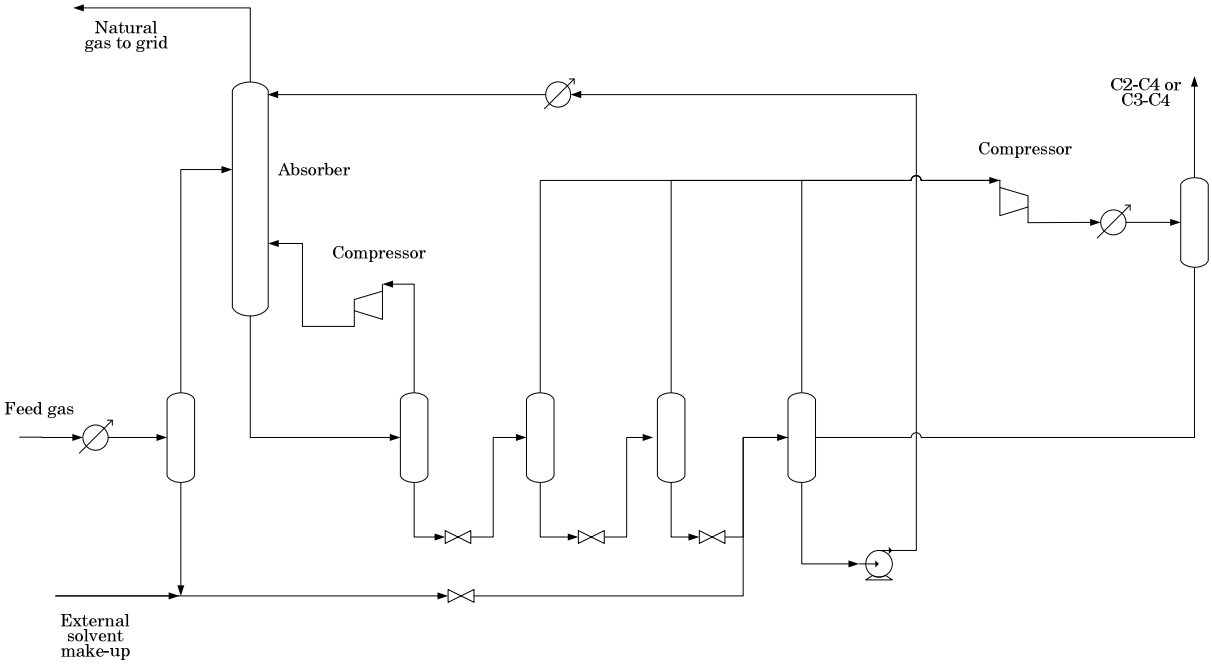

Figure 1.6: Absorption process followed by solvent regeneration in series of flashes (Gaskin (2009)).

Typical operating pressures of Mehra absorption processes are lower than 30 bar. Relatively low pressures ensure high relative volatilities and adequate solvent retention, which improves separation performance and energy efficiency. It is common to use a C5+ solvent that can be recovered from the process itself.

According to Mehra (1987), presaturation allows the use of lighter C5+ NGL components as the preferred solvent. Essentially, in the presaturator drum of Figure 1.5, the chilled mix of overhead absorber gas and lean solvent come in contact and leave the drum in saturated conditions, which reduces solvent losses and the solvent avidity for light components in the column. By chilling the overhead gas at the inlet of the presaturator, the heavy key separation efficiency improves, due to the knockout of the heavy key fraction that otherwise would escape unabsorbed.

1.3.3 (ii) Absorption-desorption enhancements by Becker and Bauer (1996)

Becker and Bauer (1996) describe an alternative patented process for the recovery of C2+ hydrocarbons, in particular, ethylene and ethane from FCC (Fluid Catalytic Cracking) fluid catalytic cracking waste gas.

The process presented by Becker and Bauer (1996) allows for co-extracted methane removal by use of reboiled absorption. The novelty of this process with respect to the Mehra process resides in that it incorporates chilling of the desorber overhead, which condensates partially. The resulting condensate is fed back to the desorber for reducing the losses of solvent and increasing the C2-C3 cut on the desorber overhead product.

In various cracking gas processes, a gas mixture is obtained which comprises ethylene and ethane and C3 and C4 hydrocarbons. In most refineries the heavier C5+ fraction is first separated from the waste gas by fractional distillation. Subsequently, the C3+ fraction is recovered in a Gas Coker Plant by oil absorption, whereas the bulk of C2 and a proportion of

C3 and C4 hydrocarbons are discharged into the fuel gas grid. If the economic drivers for C2 recovery suggest that this is desirable, this is generally implemented by partial condensation of the FCC waste gas in a low temperature process.

Refineries generally contain a large number of small to medium size off-gas streams with variable amounts hydrogen and hydrocarbons, which are usually sent to the fuel utility systems. A summary of numerous hydrogen source streams can be found elsewhere (Wang *et al.* (1984)). In most of the reactions where hydrogen participates, a purity of above 95% in the hydrogen reactant is required. The purification processes cited by Wang *et al.* (1984) include cryogenic separation, pressure swing absorption, catalytic purification and membrane separation.

According to Becker and Bauer (1996), because the FCC waste gases inevitably contain traces of higher polyunsaturated hydrocarbons, nitrogen oxides and oxygen, the low temperatures in cryogenic ethane recovery, involves the risk of explosive resins formation.

In the process presented by Becker and Bauer (1996), NGLs are recovered from the cracking gas by absorption using a physical paraffinic solvent, such as a C4+ or a mixture of pentanes, with an optimal molecular weight between 60 and 75 g/mol (for reference, molecular weight of n-/iso-butane is 58 g/mol and that of n-/iso-pentane is 72 g/mol). This solvent is characterised by a very high solvent power for C2+. Light gasoline directly obtained from the existing fractional distillation is an adequate and readily available solvent.

This is in agreement with the work of Schutt and Zdonik (1956), whereby it is possible to recover ethylene from hydrocarbon mixtures by using lean oils with molecular weights ranging from 30 to 72 such as ethane, propane, butane, or pentane. These require solvent inlet temperatures in the order of 4.45 to -34.44°C (40 to -30°F), as opposed to relatively non-

volatile lean oils of molecular weight between 80 and 120, which operate at normal inlet-oil temperatures to the absorber of 21.11 to 43.33°C (70° to 110°F).

Recommended absorber operating pressures in the system described by Becker and Bauer (1996) range from 4 to 50 bar, with an optimal range between 10 and 30 bar. According to Becker and Bauer (1996), a pressure increment of 26 bar (from 4 to 30 bar) can reduce by 50% the solvent flowrate demands. While it may be possible for the regeneration column to operate at a higher or lower pressure than the absorption column, a lower pressure is recommended. Recommended solvent feed temperature ranges between 0 and -50°C, with -35 to -45°C as an optimal subinterval. Lower temperatures could increase the solvent affinity for the gas components; however, it could induce formation of nitrous oxides. This fact may place a restriction on the lower temperature limit for feeds with a high NOx content. Recommended maximum temperature at the bottom of the regenerating column is in the 105-120°C range. This recommendation could prevent undesired incipient polymerisation into butadiene at higher temperatures.

1.4 Guidelines for technology selection

The issue of technology selection arises after the gas separation examples of Sections 1.3.2 and 1.3.3 highlighted the application of different technologies to the same gas separations. These separations are traditionally accomplished by low-temperature separations.

Economic and operational factors need to be taken into account in the design of a gas separation system. However, a comprehensive exploration of the numerous trade-offs involved that enables a quantitative comparison of the alternative technologies is not available in the literature.

Some authors have provided guidelines for gas separation technology selection. Their recommendations are discussed in this section.

According to Mehra and Gaskin (1999), Mehra (2001), it is possible to incorporate absorption-desorption processes to most of the gas processing applications which are dominated by cryogenic systems. Additionally, Mehra and Gaskin (1999), suggest that absorption can compete with (and occasionally outperform) cryogenic systems in most of the separations domain where cryogenic systems prevail, and recommend a thorough evaluation of separation options during separation synthesis. According to Mehra and Gaskin (1999) a balance between the numerous factors including feed compositions, pressure, flexibility of operation and recovery specifications will dictate the selection of the most adequate technology.

Mehra (2002) attributes a number of advantages to absorption-desorption over other available technologies for C3 or C3+ recovery:

- Energy efficiency. Mehra (2002) claims that enhanced absorption features significantly lower compression costs than cryogenic distillation systems, with respect to C3 or C3+ recovery.

- Carbon dioxide freezing. At typical temperatures for C3+ recovery, carbon dioxide freezing does not become an issue for typical separation systems. However, according to Mehra (2002), carbon dioxide can freeze in the C2+ recovery process. For the Mehra absorption process, carbon dioxide freezing is not an issue because the lowest operating temperature in the process is greater than the carbon dioxide freezing point of -78.5°C at 1 atm.

- Process flexibility. Because the economics of ethane-recovery frequently rely on the difference between ethane's fuel value and its value as chemical feedstock, the ability to reject or recover ethane may be important to the profitability of a gas-processing plant. On

occasions where it may be desirable to recover ethane from the gas feed with a system designed for high C3+ recovery, the enhanced absorption system may provide capacity for incidental recovery of ethane. According to Mehra and Gaskin (1999), a cryogenic plant for C3+ can also recover ethane, but less efficiently. On the other hand, all processes for C2+ recovery are suitable for recovering less ethane when required. Mehra and Gaskin (1999) defend that ethane rejection is possible through enhanced absorption at lower energy use due to the reduction of solvent circulation rate, by opposition to the energy increase in a cryogenic plant.

The energy-efficiency advantage is discussed next. Intuitively, absorption-desorption will incur in lower compression costs due to not relying on the gas feed letdown for the separation and to the less severe refrigeration temperatures. However, it is expected that the circulation of solvent in the system will introduce a negative effect on the energy use of the separation system due to solvent regeneration requirements. The work presented in this thesis proposes to investigate these trade-offs in a quantitative framework that accounts for all the interactions simultaneously. In terms of the capital costs of absorption-desorption systems, smaller compressors are allowed at the expense of the installation of two large absorption and desorption columns. A quantitative framework is needed to effectively analyse the interaction between capital and operating costs.

The flexibility advantage is discussed next. While it is expected that under ethane rejection the solvent circulation will be reduced and the regeneration duties will decrease, it is arguable that the overall energy consumption can be reduced, since it is expected that the reboiler duty will increase substantially in order to achieve high ethane rejections. Once again, a systematic quantitative analysis is necessary to resolve the trade-offs between the numerous factors.

The authors' extensive experience in process design allows Mehra and Gaskin (1999) to formulate technology recommendations of a number of commercial separation schemes for a wide range of operating conditions and various design factors for natural gas processing. Table 1.1 adapted from Mehra and Gaskin (1999) contains a set of optimal conditions for the two considered separation systems.

	Cryogenic	**Absorption-Desorption**	**No clear advantage**
		Propane recovery	
Pressure, bar	80+	18-30	0-18, 30-80
Propane recovery, %	-	0-80, 95+	80-95
Gas richness	Low	High	Medium
Products desired	-	Separate liquids	C3+
% C5+ recovery	>85%	-	<80%
Water content	-	High	Medium/low
Feed stability	High	Low	Medium
		Ethane recovery	
Pressure, bar	80+	18-40	40-80
Ethane recovery, %	60-85	0 - 45, 92+	45-60, 85-92
Gas richness	Low	High	Medium
Inlet CO_2 mol %	-	> 0.2	0 - 0.2
N2 mol %	-	> 2	< 2
Water content	-	High	Medium/low
Feed stability	High	Low/medium	-

Table 1.1: Recommended range of conditions for cryogenic and absorption-based systems.

The assumption of Mehra and Gaskin (1999) that the choice of gas separation technology is linked to recovery specifications and inlet gas conditions is questionable. These recommendations ignore complex tradeoffs between capital and operating costs, scale of the process, energy costs and annualisation factors. Practical design of separation process requires careful consideration of a broader range of factors. Furthermore, the process recommendations of Mehra and Gaskin (1999) are restricted to commercial separation schemes of fixed configuration and fixed heat integration matches. Additional heat recovery options could be exploited by use of a systematic and integrated design approach.

In conclusion, the shortage of quantitative design methods in the literature for systems where distillation and absorption-desorption option

are possible alternatives is the motivation behind the development of a methodology for design of gas separation systems.

1.5 Objectives of this work

The two-fold objective of this work is to develop an optimisation-based synthesis methodology for the design of gas separation networks that integrate distillation and absorption-desorption options, and to demonstrate the capabilities of the developed methodology.

This objective will be achieved by targeting the following areas:

1. Modelling. A modelling strategy is required to represent: (A) the separation blocks (distillation and absorption-desorption); (B) the sequence of separation blocks; (C) the refrigeration system (if necessary). For the given separation specifications, models must be able to estimate equipment dimensions, which are then translated into annualised costs, and preliminary energy demands.

2. Heat integration. Distillation and absorption-desorption units are heavy energy users, and any practical design methodology must contemplate heat integration to reduce the process utility demands. A heat integration strategy is needed that fulfills the following requirements: (A) to be integrated with the design of the refrigeration system; (B) to target for minimum or (near minimum) utility costs; (C) to provide a practical configuration of the heat exchanger network and its associated capital costs.

3. Optimisation. An optimisation strategy for the optimal design of the separation system on the basis of minimum capital and operating costs is required to simultaneously optimise the split sequence, the technology allocation to each split in the sequence, the operating conditions for each separation, the heat exchanger network and the refrigeration system. This

strategy must be robust given the large scale of the problem, the feasibility limits of the separations and the non-linearity of the model equations.

4. Cost estimation. A costing mechanism is needed to reflect the desired trade-offs between capital and operating contributions to the total cost of the separation system.

The demonstration of the developed methodology will be achieved by application of it to a number of case studies.

1.6 Contributions of this work

This work contributes with advancements to the area of computational synthesis of effective and integrated separation systems and optimisation, and to the area of process research and development by pioneering a quantitative and systematic comparison between highly integrated process alternatives to the traditional low-temperature separation options.

This work will achieve progress in the following areas:

1. Modelling

    a. Improved shortcut models for reboiled absorption and distillation columns

    b. Accommodation of absorption-desorption separation options in the distillation orientated framework supported by COLOM® (©Centre for Process Integration, University of Manchester) via development of a multilevel absorption-desorption block modelling approach

2. Heat integration

c. A new heat integration strategy that minimises utility demands while providing a practical configuration of the heat exchanger network

d. A new strategy that does not rely on mathematical programming but instead is optimised at the same time as the separation system and the refrigeration system

3. Optimisation

e. A stochastic Simulated Annealing framework that is tailored to the synthesis of gas separation systems involving distillation and absorption-desorption options and is capable of optimising discrete and continuous variables

4. Cost estimation

a. A survey of costing methods and real prices

The results of applying the developed methodology to different case studies will illustrate its capabilities to generate highly efficient process systems during conceptual design.

1.7 Publications and presentations

- Papers in international peer reviewed conferences

Martin, M., Jobson, M., Zhang, N. and Heggs, P.J. (2006). "Shortcut Evaluation of Absorption for Synthesis of Gas Separation Networks". *Distillation and Absorption 2006 Conference Proceedings*, pp. 88-99.

- Presentations in national/international non peer reviewed conferences/workshops

Martin, M, Jobson. M., Smith, R. (2007). "Design of Gas Separation Networks". XXIV Process Integration Research Consortium Annual Meeting, Manchester, UK.

Martin, M, Jobson, M., Zhang, N., Heggs, P.J. (2006). "Design of Gas Separation Networks". 111th International Summer Course. BASF Aktiengesellschaft, Ludwigshafen, Germany.

Martin, M, Jobson, M., Zhang, N. (2006). "Design of Gas Separation Networks". XXIII Process Integration Research Consortium Annual Meeting. Manchester, UK.

Martin, M., Jobson, M., Zhang, N., Heggs, P.J. (2006). "Shortcut Evaluation of Absorption for Synthesis of Gas Separation Networks". E.U. Marie Curie ExPERT Showcase. CEAS, The University of Manchester, Manchester, UK.

Martin, M., Jobson, M., Zhang, N., Heggs, P.J. (2005). "Shortcut Evaluation of Absorption for Synthesis of Gas Separation Networks". Fluid Separation Processes Research Event, IChemE. BP Sunbury, London, UK.

Martin, M, Jobson, M., Zhang, N., Heggs, P.J. (2005). "Design of Gas Separation Networks". XXII Process Integration Research Consortium Annual Meeting. Manchester, UK.

Martin, M., Jobson, M., Zhang, N., Heggs, P.J. (2005). "Shortcut Evaluation of Absorption for Synthesis of Gas Separation Networks". E.U. Marie Curie ExPERT Showcase. CEAS, The University of Manchester, Manchester, UK.

1.8 Conclusions

This chapter has presented the background and the scope of this contribution to the design of gas separation systems. Examples of gas separations of industrial relevance have been provided, along with a review of some of the commonest gas separation system technologies.

Low-temperature distillation based processes have traditionally dominated large scale bulk gas separations, such as NGL recovery from natural gas or ethylene recovery from refinery off-gases. However, the review of published material has provided evidence of the proven application of absorption-desorption systems to some of these separations.

Separation system design is a multifaceted complex problem that needs to resolve quantitatively the many trade-offs existing in distillation and absorption-desorption systems. Existing technology recommendations for natural gas separations are simple generalisations and a methodology that assists with the design of the optimal gas separation system is unavailable. The development of such a methodology is the object of this work.

Chapter 2. Literature review

2.1 Introduction

This chapter offers a review of the relevant publications concerning process synthesis. Reviews of the existing publications that relate to different aspects of this work are provided in the next chapters.

Process synthesis, including separation system synthesis, occupies a central place in process engineering literature. On the one hand, process synthesis sets the economics for the process for a large part of its lifetime (Koolen (2001)). On the other hand, process synthesis plays a key role in supporting the development of new process systems (Umeda (2004)) and the shift of raw materials and chemical routes (Li and Kraslawski (2004)) for tighter environmental regulations, effective use of resources and process sustainability.

In process synthesis, the design of the separation system remains the most challenging task, together with the design of the reactor system (Koolen (2001)).

This section first introduces key objectives and current challenges for process synthesis. A review of the available process synthesis approaches (specific and non-specific to gas separations) is then provided. A subsequent subsection focuses on the topic of technology selection, which has been covered by an important number of publications. Finally, this section establishes the connections between an existing synthesis framework (Wang (2004)) and the synthesis methodology proposed in this work.

2.2 Separation system synthesis outputs

Whereas for liquid separations, distillation is the dominant separation technology, no technology dominates gas separations. On some occasions, more than one separation technology can perform a given separation task in a feasible and economically attractive way (Barnicki and Fair (1992)). Selecting the optimal separation technology to accomplish a separation task is a key synthesis objective. Extending the separation synthesis problem to allow for various separation technologies increases the complexity of the problem. Heuristic rules for preselection of alternative separation options are available but with limited applicability and validity (Koolen (2001)).

Typical separation systems often involve various separation tasks in sequence. Hence, the synthesis problem must establish the best sequence of separation tasks. The synthesis of distillation sequences has received great deal of attention in the open literature (Andrecovich and Westerberg (1985), Aggarwal and Floudas (1990), Viswanathan and Grossmann (1990), Yeomans and Grossmann (1999)).

Another key output of separations synthesis is the selection of operating conditions of each of the separation tasks as these affect the separation performance.

2.3 Process synthesis challenges

The separation system synthesis problem is an open-ended activity that involves a number of interlinked decisions (Douglas (1995)). An important process synthesis challenge is the complexity of the problem due to decision-making at different levels, such as the reactor system, the separation system, the heat exchange network and the utility system. When synthesis decisions at different levels are made sequentially, important opportunities for process improvement originating from the

interactions between levels may be missed. The layered model for synthesis of chemical processes presented by Linnhoff and Boland (1982), Smith and Linnhoff (1988) and the hierarchical approach of Douglas (1988) attempts to reduce the number of missed opportunities by using heuristics to guide the decisions at different synthesis levels. Douglas (1995) revisits the popular hierarchical synthesis procedure presented by Douglas (1988) and suggests using component physico-chemical properties and economic short-cut calculations for preliminary screening of separation alternatives. The sequential nature of this procedure, however, does not allow for interaction between decisions at the different levels of the hierarchy, offering no guarantee of finding the best possible design.

An significant weakness of the synthesis process is the lack of a structured set of design alternatives, with the creativity and experience of the designer (Koolen (2001)) being instrumental in the development of process design alternative options.

In addition, process system synthesis is a challenging problem because of the lack of commercial tools for the synthesis of large-scale flowsheets (Douglas (1995)). Commercial process simulation software may assist with process design, heat exchanger network design, utility system design and control system design. However, the practicalities of the use of commercial process simulation tools make it inadequate for comparison of a large number of process configuration options, due to the limitation of simulating only one configuration at a given time. Within a flowsheet of a fixed structure however, these process simulation tools are capable of exploring variable ranges and optimising operating variables. Commercial tools for general process synthesis are relatively uncommon. The software packages at the Centre for Process Integration of the University of Manchester (1985-2009) cover a wide range of functions in process integration. For separation systems synthesis, COLOM® may assist with the thermodynamic analysis of distillation columns, column sequencing, design of complex columns and azeotropic distillation. The software

package of the Computer Aided Process-Product Engineering Centre of the Technical University of Denmark (ICAS©, Integrated Computer-Aided System) is orientated to heuristic pre-screening of separation technologies and its interaction with solvent design.

Despite the available synthesis tools, these are heavily restricted to a few aspects of the design of the process and generally account for simple economic objectives. In order to reflect trade-offs between various objectives, some of which are difficult to quantify, final process design decisions must be made in the real world practice.

2.4 Separation system synthesis approaches

Traditionally, synthesis methods are classified into two groups: knowledge-based and optimisation methods.

Common knowledge-based synthesis methods are rule-driven: heuristics and facts are used to help generate flowsheet alternatives. Heuristics often provide a useful guide to preliminary process design; however, because heuristics are based on generalisations of abstracted common process properties, occasionally may be misleading. The work of Barnicki and Fair (1990), (1992) contains a comprehensive set of heuristics for application to separations of liquids and gas/vapour mixtures. Barnicki and Fair (1990), (1992) offer advice on separation technology selection and sequencing.

Traditional optimisation synthesis methods are based on mathematical programming. In these methods, the direct application of mathematical programming approaches is possible because of the manageable complexity of the problems; in general, a limited number of variables is involved and the alternatives may be manually enumerated for superstructure construction. The concept of superstructure is described later in more detail.

A number of studies have been carried out on the development of hybrid methods that combine heuristic and optimisation synthesis approaches. Kheawhom and Hirao (2004) employ a heuristic approach that applies experience-based rules and thermodynamic rules to reduce the complexity of the search space. Mathematical programming is then used to solve the remaining multicriteria optimisation problem, consisting of environmental and economic objectives. Hostrup *et al.* (1999), Hostrup *et al.* (2001) develop a hybrid methodology integrating mathematical modelling with heuristic approaches for simultaneous solvent and separation process design to meet environmental objectives. A heuristic approach based on thermodynamic rules is employed for screening out infeasible technologies. Subsequently, alternative flowsheets for the remaining options are represented by a superstructure to be solved by Mixed Integer Non-Linear Programming (MINLP). The methodology of Hostrup *et al.* (2001) was implemented into the ICAS© software package (Integrated Computer-Aided System 7.1, CAPEC, Technical University of Denmark), with the objective of providing an interactive environment for separation synthesis.

Siirola (1996), Barnicki and Siirola (2001) refer specifically to the following three methods for separation systems synthesis:

i. Evolutionary modification.

This strategy generates a flowsheet from an existing standard flowsheet pattern for a similar separation by incorporating the necessary adaptative modifications to align the new process with the existing one. Although rarely resulting in novel designs, this approach is a frequently used separations synthesis approach because of the available repertoire of design heuristics (Nadgir and Liu (1983), Cheng and Liu (1988), Fien and Liu (1994)) and flowsheet encyclopaedias.

The basic concept of using an existing design as a reference for a new design is the basis for most current industrial design projects. In such

cases, prior knowledge of feasible combinations related to the choice of separation technologies for a separation task, the sequencing of the separation tasks, and the operating conditions for the separation tasks is available. The main limitation of this experience-based approach is that it ignores the potential of alternative novel process configurations and operating strategies. Therefore, re-using process design expertise is detrimental to process innovation.

Seuranen *et al.* (2005) proposed a framework to reuse systematically existing design experience for new designs. Design information is extracted from a database for the most similar separation design and applied to the new problem. The strong influence from old cases implies that little or no process improvements are realised.

ii. Systematic generation.

The flowsheet is formed out of a set of unit operations, using process and thermodynamics constraints for the selection and interconnection arrangements (Siirola (1996)). This flowsheet is synthesised by progressively transforming a given feed stream into one or more target products. The synthesis strategy presented by Siirola (1996) systematically applies artificial stream processing operators in sequential order to evolve from the initial feed to the product streams.

In a similar approach to separation synthesis (O'Young *et al.* (1997)), separation is viewed as movements in composition space, from the feed state to the product specifications. However, emphasis is placed on bypassing the boundaries hindering the transitions through the composition space, such as thermodynamic boundaries (eutectics, azeotropes) and equipment operating limits.

iii. Superstructure optimisation.

Douglas and Stephanopoulos (1995) introduced the general separation system superstructure. Superstructure optimisation methods can provide a systematic framework for a variety of process synthesis problems.

In superstructure methods, from a known feed composition, desired product compositions and a set of separation methods, a hypothetical flowsheet is constructed, which includes the candidate separation technologies interconnected in various possible ways so as to represent a large number of flowsheet alternatives. The optimum is located among the starting superstructure of options. Thus, absolute global optimality depends upon the completeness of this set.

Li and Kraslawski (2004) argue that the applicability of this approach is limited by the insufficient ability to automatically generate a flowsheet superstructure and the extensive computational requirements. For large scale problems, optimisation methods may incur extensive computation times. Optimisation algorithms often need to be tailored to the size and nature of the problem to achieve a sufficiently fast execution.

This synthesis method requires an explicit or implicit superstructure representation using a mathematical formulation. The explicit representation is limited to small problems, where the existence of each piece of equipment in a specific location can be represented by binary variables and the connectivity of all pieces of equipment can be rationalised. For some simplified classes of design problems, such as the synthesis of heat exchanger networks, the set of process alternatives, which is known as a superstructure, admits a mathematical formulation. This may be solved by the available mathematical programming optimisation methods.

In the representation of the separation problem as a mass exchange network (El-Halwagi and Manousiouthakis (1989)), the synthesis is approached via mathematical programming using a superstructure

representation of the network, analogous to the one adopted for heat exchange networks.

In this category of simple problems, an optimisation strategy for membrane-based separations is developed by Kookos (2002). The presented superstructure allows simultaneous optimisation of the process, including continuous and discrete variables, such as operation conditions, module configurations and membrane material. More recently, Kookos (2003) extends the representation of the pure membrane-based separation network to develop a methodology for optimisation of combined separation systems consisting of distillations columns and membrane units, where the use of membranes is prescribed to overcome thermodynamic limitations, such as close boiling points or azeotropes. The new superstructure is formulated for the structural and parametric optimisation of the combined separation system with respect to an economic indicator.

In the work of Caballero and Grossmann (2001), (2006) for the design of thermally coupled-heat-integrated distillation sequences a superstructure of the feasible options is generated systematically by the mathematical formulation of the problem, which consists of logical relationships. A programming approach is then proposed for optimisation of the superstructure.

For general separation synthesis problems, however, the set of process alternatives cannot be represented formally. The synthesis approach becomes a strategy of eliminating systematically the less desirable combinations within the set, simultaneously optimising the design and operating variables of the remaining options using stochastic methods.

In this category of complex problems, Wang and Smith (2005) present a sequence-based superstructure to accommodate all separation process options for the synthesis of low-temperature heat-integrated separation

systems. The optimisation is then carried out using a genetic algorithm, a stochastic method.

Linke and Kokossis (2003) describe the application of stochastic optimisation methods (simulated annealing and Tabu search) to the synthesis of integrated reaction and separation process superstructures.

Uppaluri *et al.* (2006) present a superstructure-based methodology for simultaneous optimisation of pressure and network configurations of gas separation membrane permeators. This superstructure is optimised using the simulated annealing algorithm, a stochastic method.

2.5 Shortcuts to separation technology selection

Typical synthesis problems are based on the exploration of a large number of design options. Screening of the design options may serve to reduce the number of alternatives at an early stage and thus, to simplify the synthesis problem. Screening provides a quick estimate of alternatives without requiring a detailed simulation-based analysis; hence it may be used to make early decisions.

Separation technologies exploit the differences in certain physicochemical properties between the chemical components of a mixture. These differences may be quantified for prediction of a separation technology ability to perform the separation of a given gas multicomponent feed.

Barnicki and Fair (1992) published the most complete set of rules for screening of gas-vapour separations (Douglas (1995)). The considered technologies include condensation, cryogenic distillation, physical absorption, chemical absorption, membrane permeation, molecular sieve adsorption and equilibrium-limited adsorption. The appropriateness of a given technology depends on specific process requirements, such as the quantity and extent of the desired separation, and physico-chemical

properties of the mixture components. This heuristic-based procedure employs qualitative and quantitative indicators of the performance of the various separation technologies. Quantitative indicators are used to generate a ranked list of the feed components with respect to a certain physicochemical property exploited by the separation technology. The suitability of a given technology to separate the components of a multicomponent stream is connected with the relative position of the key components of each group in the ranked list. However, the proposed method is orientated to preliminary feasibility screening, and is not suitable for process design as this requires a design methodology for the relevant separation equipment.

Jaksland *et al.* (1995) developed a synthesis methodology aimed at addressing the issues of physical feasibility and economic viability. Similarly, feasibility assessment of separation technologies is supported in their methodology by analysis of the component physicochemical properties, and the operating conditions. Quantitative indicators are calculated for the feed components and then compared with certain feasibility limits for each separation technology. The outcome of this comparison is a preliminary estimate of the suitability of a given separation technology. Feasibility limits are reportedly derived from a combination of physical insights and simulation exercises; however, insufficient evidence of the connection between these limits and the issue of economic viability is provided, due to the lack of a quantitative synthesis framework.

For Material Separation Agent (MSA) based methods, which involve an external agent, such as absorption and adsorption, separation feasibility is affected by the choice of the external agent or MSA. The work of Jaksland and Gani (1996) integrates the problems of process design and solvent design. Their methodology combines the process synthesis algorithm of Jaksland *et al.* (1995) and the product design algorithm of Constantinou *et al.* (1996). Initially, candidate molecule types (with desirable functional

groups and target properties) are generated based on the pure component properties of the species in the feed to be processed at given operating conditions. The candidate molecule types are screened further using mixture properties. The Computer-Aided Molecular Design (CAMD) methodology (Gani *et al.* (1991), Harper *et al.* (1999)) is finally applied to select the final set of molecules matching the specified property target values. This synthesis approach produces a set of preliminarily feasible separation technologies for the given separation objectives, suggests suitable MSAs, and provides an estimated range of adequate operating conditions of the relevant separation technologies. However, this approach does not serve all the purposes of process synthesis because it does not offer a methodology for equipment design or a quantitative evaluation of the proposed separation technologies. Similar output regarding technology selection and operating conditions for known processes may also be surveyed from the relevant information resources.

Bek-Pedersen *et al.* (2000) suggest that component concentration differences between two co-existing phases in a separation device or driving forces are directly related to the use of energy and feasibility of the separation technologies, and use this information to make decisions regarding process synthesis. However, the assumption that feasibility may be attributed to the magnitude of driving forces has not been fully demonstrated.

2.6 Synthesis framework legacy

Wang (2004), Wang and Smith (2005) present a synthesis framework for synthesis and optimisation of heat-integrated low temperature gas separation systems. The design of the refrigeration system is accomplished simultaneously.

In the terms employed by Wang (2004), a simple separation task features a single feed with two products and a single light and heavy key

component respectively. In a five-product separation system (A/B/C/D/E), there are in total 20 discrete simple tasks, as illustrated in Figure 2.1. A practical separation sequence may be generated from selection of a group of tasks in the task matrix, as shown in Figure 2.1.

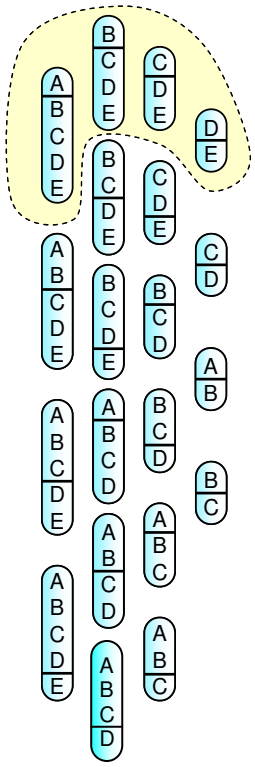

Figure 2.1: Simple task matrix for a 5-product separation and sequence example.

Wang (2004) employs task representation to accommodate a large number of separation options, including simple and complex distillation columns.

In the terms used by Wang (2004), the separation equipment in which a simple separation task may be implemented is defined as a simple task representation. The task representations considered by Wang (2004), which act as building blocks, are single flash drums, dephlegmators and single distillation columns (Figure 2.2).

Besides these basic separation options in Figure 2.2, a simple split may also be performed by separation options which are generated from direct combination of the three initial building blocks. Therefore simple task

representations are extended to account for pre-flash distillation columns, dephlegmator-columns, and columns with post dephlegmators. In total six simple task representations are considered.

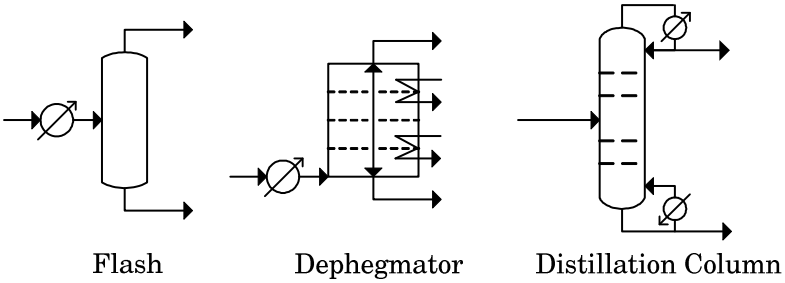

Figure 2.2: Building blocks for separation schemes in low-temperature processes.

A hybrid separation task may be subsequently generated from two different ordered combinations of simple tasks (the direct and the indirect sequence), and features a single feed and three products. Complex separation options can provide high energy efficiency at the cost of increased capital investment. For a hybrid separation task (A/B/C), there are three hybrid task representations:

- Side-columns: side-rectifiers and side-strippers
- Side-draw columns: vapour side-draw columns and liquid side-draw columns
- Prefractionating arrangements: columns with thermal coupling, Petlyuk columns and dividing-wall columns; columns without thermal coupling, prefractionators.

Wang (2004) provides shortcut models for all the separation options. The shortcut models for combined separation representations are formulated using the models of the simple ones. The shortcut models of the hybrid task representations are obtained by decomposing each complex configuration into an assembly of simple columns.

The essence of the synthesis methodology presented by Wang (2004) is the representation of the separation problem as a sequence of separation tasks which can morph into different task representations. A superstructure that embeds all the separation options is developed and solved by a Genetic Algorithm, a stochastic optimisation method. The optimisation framework for the synthesis methodology presented by Wang (2004) is provided by COLOM® (©CPI, University of Manchester 1985-2009).

The work covered by the present thesis is forged within the COLOM® framework and re-uses the available internal tools and procedures. In accordance with the terminology of Wang (2004), the work presented in this thesis expands the array of simple task representations through the incorporation of an additional separation alternative to the framework, i.e. absorption-desorption. Nonetheless, the synthesis methodology presented in this work remains largely detached from the methodology of Wang (2004) due to a different scope of work.

The motivation for excluding the vast enumeration of hybrid task representations from the scope of this thesis is that this work concentrates on the robustness and the accuracy of the separation models, at column and flowsheet level, with the aim to capture the key interactions in the absorption-desorption system. The absorber-desorber arrangement features an increased complexity over the distillation-based options, which is associated with the circulation of the solvent and the regeneration system. However, some of the existing separation models in COLOM® for the task representations of Wang (2004) require further tuning for increased confidence in the results and for alignment of these models with the proposed absorber-desorber models. A modification of the distillation column model is implemented under the scope of the work of this thesis.

Finally, the methodology proposed in this work departs from the optimisation framework of by Wang (2004) by being supported by a

Simulated Annealing optimisation framework, which has proven to offer great control and robustness.

2.7 Conclusions

This chapter has introduced some of the perennial synthesis challenges that have been addressed in the literature. Only partial solutions exist to the open-ended synthesis problem. Most synthesis strategies are dominated by replication of proven process systems. Completely general separation synthesis strategies do not exist; the available quantitative approaches make compromises with universality by restricting themselves to one or two separation technologies and imposing connectivity constraints between separations.

In relation with the above, the synthesis methodology presented in this thesis achieves quantitative status by focusing on distillation and absorption-desorption gas separation options, and supporting systematic investigation of these by an adequate optimisation framework.

Due to this synthesis methodology being implemented in COLOM®, the terms “separation task” and “task representation” introduced by Wang (2004) to describe the COLOM-based synthesis framework, are applicable to this work.

Chapter 3. Separations modelling

3.1 Definitions

- Component recovery

Fraction of the feed flowrate of a component which is isolated in a given product stream by a separation system. The recovery of component i in product k is given by Equation (3.1):

$$Rec_k(i) = \frac{Flowrate\ of\ 'i'\ in\ 'k'}{Flowrate\ of\ 'i'\ in\ feed} \tag{3.1}$$

3.2 Introduction

The synthesis methodology presented in this thesis requires design models for the relevant separation technologies. Improved shortcut models are proposed in this chapter for reboiled absorption and distillation columns. A full-column reboiled absorber is recommended to achieve the light key specifications in the bottom product.

Adequacy of the models to the synthesis framework is critical for model selection. Because these models are integrated in an optimisation framework, it is essential that they allow a rapid execution while offering a sufficiently accurate representation of the process. In this chapter, the suitability of some of the most common models in the literature to the synthesis methodology is investigated and improvements are suggested. Models and improvements are validated using commercial simulation software.

Models are used by the proposed synthesis methodology to generate a preliminary design of the separation equipment that achieves the given separation objectives. Thereafter, capital cost estimates of the selected separation equipment combined with the total utility consumption, enables quantitative comparison between a large number of separation alternatives for optimisation of the separation system.

This section provides a description of the existing models and the adaptation to this work. A number of modifications are applied to the original models to improve accuracy without an adverse effect on the computation time.

3.2.1 Constant column pressure profiles assumption

Throughout this work, the pressure is assumed to be a constant along the column. In reality, a pressure profile is developed along the column due to the stages liquid loading and the pressure drop due to friction. The pressure profile in a column may affect the separation efficiency and the reboiler and condenser duties due to the sensitivity of the relative volatilities and the enthalpy of vaporisation to the pressure.

Because the design methodology proposed in this work is aimed at conceptual design, pressure changes in the column are neglected. This argument is also supported by the uniformity of column pressure profiles across separation columns, which is linked to a minimal propagation of the pressure factor to the comparison of alternative separation schemes.

A subsequent study of the resulting preliminary design, which will involve rigorous modelling tools to account for additional effects such as pressure variation, is recommended for validation purposes and for further refinement.

3.3 Basics of absorption-desorption

Absorption is a basic chemical engineering operation and is very well-established for most areas of gas separations including gas purification. Absorbers can handle a range of feed rates; thus, an advantage of absorption is its flexibility.

Absorption involves transferring gas components to a contacting solvent. To maximise the mass-transfer driving force (the difference in concentrations between the gas and liquid phases), the absorber operates in a countercurrent fashion.

The transfer occurs when the component vapour pressure in the gas phase is higher than its vapour pressure in equilibrium with the solvent. The solution of a gas component in the solvent results in an increase of the entropy of the system. Additionally, in real systems, the molecular interactions between the absorbent and the solute may result in heating or cooling of the solution.

In physical absorption, the components are dissolved in a solvent and can be desorbed for recovery. The absorption of hydrocarbons by absorption oils and the absorption of ammonia by water are examples of physical absorption. Physical absorption is generally characterised by observance of Henry's law, dictated by relatively linear absorption isotherms over a range of partial pressures.

Some factors affecting the operation of the absorber include temperature, feed solvent loading and feed gas composition. Firstly, as the temperature is reduced, the capacity of a solvent to absorb the solute gas components generally increases, the limit being the freezing point of the solvent. Secondly, solvent absorption capacity is improved by reducing the component concentration in the solvent to a low level. Thirdly, a highly

concentrated feed gas will require a higher solvent flowrate and number of stages to achieve the same gas product purity.

3.3.1 Solvent selection

Solubility is the most important consideration in solvent selection for absorption. The higher the solubility, the lower the amount of solvent required to remove a given amount of gas component. Absorption selectivity is sometimes sought in solvents in order to control co-absorption. The solvent should also be relatively non-volatile to prevent a significant solvent residue in the gas product. Other favourable properties include low flammability and viscosity, high chemical stability, low freezing point, good rheological properties, acceptable corrosiveness, low toxicity and pollution potential and, finally, low cost of fresh solvent.

According to England (1986), because of the interactions between physical solvents are relatively minor, mixed solvents may be screened for use in new separation processes.

3.4 Absorption-desorption flowsheet modelling

3.4.1 Introduction

The optimisation and synthesis framework proposed in this work is supported by a new three-level modelling methodology that reconciles individual column model objectives with separation sequence synthesis objectives.

At Level 1 of the methodology in Figure 3.1, or sequence level, the mass and energy balances around the separation block are solved, which enables the characterisation of the block inlet and outlets. Inputs to Level 1 calculations include feed composition and conditions, product recoveries and designated key components, as well as feed and temperature specifications on the separation products.

At Level 2 or block level, mass balances are established within the absorption-desorption cycle in order to characterise each of the intermediate and recycle streams in the block. The calculations at Level 2 will be presented in section 3.4.3.

At Level 3 or column level, the design of the individual columns is carried out. Inputs to Level 3 calculations include the stream conditions at the block boundaries and the conditions of the internal streams, as well as the operating variables necessary for column design from the optimiser.

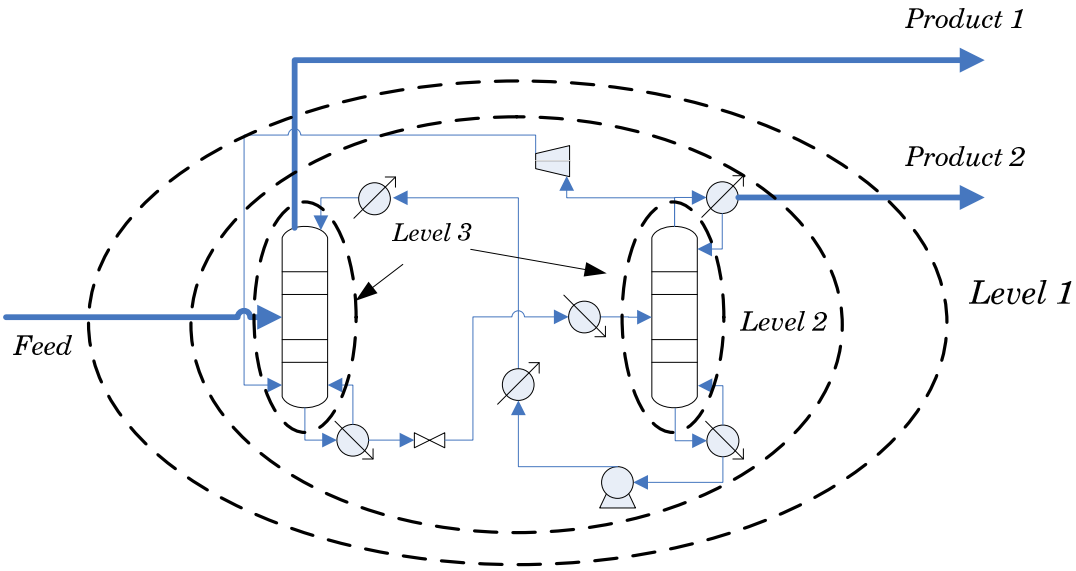

Figure 3.1: Schematics of the three-level modelling methodology

It is important to observe that for a simple separation task that is carried out by a simple distillation column, the boundaries of the three levels overlap with each other, as the distillation column is the only constituent of the separation block.

This three-level methodology fulfils a double requirement. Firstly, it provides stream characterisation, which is necessary prior to the design of the absorption and solvent regeneration columns and heat exchange equipment. Secondly, it serves to reconcile the concentration of solvent and other non-key components at the boundaries of Level 1 with the

calculated values of these magnitudes at Level 3. This latter point is discussed in section 3.4.2.

3.4.2 The *solvent-free* boundary approach

As a Material Separation Agent based method, absorption relies on the contact of the gas feed with a solvent stream, which acts as a vehicle in the segregation of components based on their differential solubility. Due to the contact with the solvent, the gas separation products will carry a small amount of solvent components, which in common applications must be replenished by continuous addition of fresh solvent to the circuit.

High-quality predictive column models will agree on the contamination of product streams by the solvent. In this work, the reboiled absorber design model for calculation of the number of theoretical stages and the required solvent circulation for a given boilup ratio, the details of which will be presented in section 3.5.2 (v), predicts the presence of marginal amounts of solvent on the column overhead, which is consistent with real absorber operation.

For the purposes of separation sequence synthesis, however, the proposed absorption-desorption cycle must conform to the sequencing framework introduced in section 2.6. In this framework, previously utilised by Wang (2004) and implemented in COLOM® (©CPI, University of Manchester 1985-2009), the separation sequence is perceived as a series of single separation tasks, each of which is treated as a "black box" by the Level 1 mass balance calculations.

An example of separation sequence options is shown in Figure 3.2, extracted from Wang (2004). A single separation task achieves a simple split between the components in the feed to the task, whereby two product streams are generated from a single feed. Then, it is the role of the separation scheme in the "black box" to achieve the separation targets

imposed by the overall mass balance. Because the idea of contamination of the gas products with solvent does not fit in with this sequencing framework, the proposed multilevel modelling methodology prevents the Levels 2 and 3 model-derived solvent concentrations from propagating beyond the block boundaries to the rest of the sequence or to the final products, which would result in unreconciled overall recovery specifications.

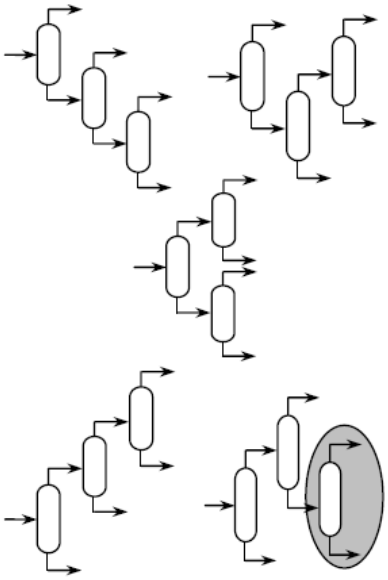

Figure 3.2: Sequencing options for a five-product separation train from Wang (2004).

The result is that within the proposed design methodology, the solvent does not leave the separation block with the products. For consistency, this assumption must be reflected by the formulation of the mass balances at Level 2, which have the function of reconciling column calculations with the specifications on the products from the block. The first implication of this assumption is that allowance for solvent make-up is not required for the system design.

The second implication of the "solvent-free boundary" assumption is related to the presence of solvent in the desorber overhead. For consistency between calculations at different levels, any remaining solvent in the desorber overhead is artificially separated from the top product and

recycled to the absorber. Since the solvent is the desorber heavy key, solvent overhead recovery is imposed (arbitrarily 0.01%). This recovery acts as an input to the Level 2 mass balances prior to column design calculations.

Differently, any residual solvent in the absorber overhead, as predicted by the reboiled absorber model, is simply neglected. The reason for this is that the concentration of solvent at the top product of the absorber is unknown until the column design algorithms are executed. Because this concentration is usually very small due to the low temperature operation and typical heavier-than-C4+ solvent, iteration on the overhead solvent concentration is not considered appropriate for conceptual synthesis objectives.

3.4.3 Overall mass balance of generic absorption-desorption flowsheet

In the absorber-desorber flowsheet of Figure 3.3, feed and products flowrates are represented by F and D_1 and D_2, respectively. Absorber bottoms and gas recycle flowrates are represented by B_1 and R.

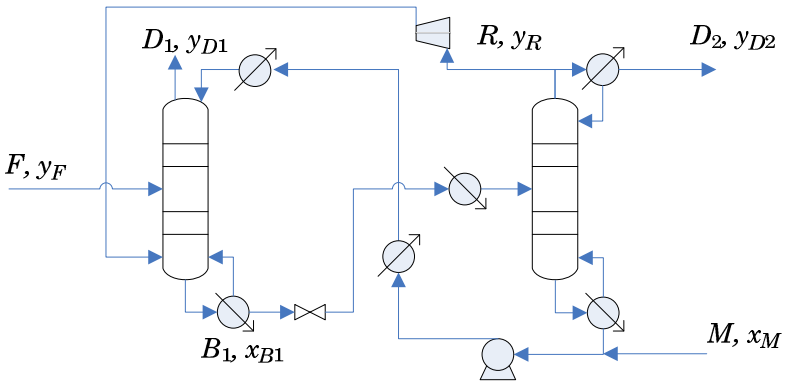

Figure 3.3: Absorption-desorption cycle for material balance.

The separation achieved by the desorber column is decisive as it controls the composition of the lean solvent, and therefore the absorption performance, as well as the composition of one of the products. Because of the finite number of stages of the regenerator, it is not possible to achieve

a perfect separation between the solvent and the product. As a result, the solvent feed to the absorber will contribute to the total inflow of components that originated from the gas feed into the separation block.

Another possible contribution to the total feed to the absorber occurs when the boilup is replaced or supplemented with a gas product recycle from the desorber overhead; however, this configuration will not be analysed in the context of this thesis.

As a result of these additional contributions to the net absorber feed, it is not possible to estimate the molar flowrate of feed components in the bottoms stream, B_1 in Figure 3.3, as $B_1 x_{B1}(i) = Rec(i) F y_F(i)$, where $Rec(i)$ is the overall recovery of component i by D_2, defined by:

$$Rec(i) = \frac{D_2 y_{D2}(i)}{F y_F(i)} \tag{3.2}$$

The recovery frequently is expressed as a percentage, however, in this derivation, it has been normalised to range between zero and one.

For components in the feed that do not naturally appear in the fresh solvent, an overall material balance may be written as:

$$F y_F(i) = D_1 y_{D1}(i) + D_2 y_{D2}(i) \tag{3.3}$$

From the definition of recovery, it follows that:

$$D_1 y_{D1}(i) = \left(1 - Rec(i)\right) F y_F(i) \tag{3.4}$$

$$D_2 y_{D2}(i) = Rec(i) F y_F(i) \tag{3.5}$$

Where $Rec(i)$ is the overall recovery of component i by D_2.

For the components that are exclusive to the solvent, no overall recovery exists as such because these components are not contained in the feed.

The gas recycle, R, if there is any, is characterised by having the same composition as the overhead product from the desorber. A recycle-to-overhead or internal recycle ratio R_D recycle ratio is defined as:

$$R_D = \frac{R}{D_2} \tag{3.6}$$

Equation (3.6) allows to determine the ratio R_D for a specified recycle rate R.

The flowrate of a component in the recycle is given by:

$$Ry_R(i) = R_D D_2 y_2(i) \tag{3.7}$$

A recycle-to-product or external recycle ratio R_T is defined as:

$$R_T = \frac{R}{D_2 + R} \tag{3.8}$$

The recycle ratios are related one another by the following equations:

$$R_T = \frac{R_D}{1 + R_D} \tag{3.9}$$

$$R_D = \frac{R_T}{1 - R_T} \tag{3.10}$$

For all the components in the system, including the solvent-specific components, another recovery, which is relative to the desorber feed and

the desorber overhead, $Rec_2(i)$, allows to write the flowrate of these components in the desorber overhead as:

$$D_2 y_{D2}(i) = Re c_2(i)\, B_1 x_{B1}(i)\,(1 - R_T) \tag{3.11}$$

The individual flowrates of gas feed components in the rich solvent may be determined from the equation below, which is derived from Equations (3.5) and (3.11):

$$B_1 x_{B1}(i) = \frac{Re c(i) F y_F(i)}{Re c_2(i)(1 - R_T)} = \frac{Re c(i) F y_F(i)}{Re c_2(i) \dfrac{1}{1 + R_D}} \tag{3.12}$$

Equation (3.12) is applicable to all feed components including the light key since $Rec_2(i) > 0$. For components lighter than the absorber light key component, $B_1 x_{B1}(i) = 0$, since $Rec(i) = 0$. Once the Level 3 calculations for the absorber are complete, an updated concentration of the rich solvent stream is obtained, which is then used as the new feed to the desorber Level 3 design calculations.

3.5 Absorption and desorption column models

3.5.1 Introduction

Models principal requirement is to provide a reliable representation of the real process. In most applications of design models, however, accuracy is traded off with simplicity, and a balance between factors is desired. In the proposed optimisation framework, it is desirable that models can be computed rapidly, due to the combinatorially large number of iterations executed during optimisation.

For this reason, complex separation models involving detailed mathematical apparatus are outside the scope of this work. Such models

include the semi-rigorous conventional stage-by-stage equilibrium and mass and energy balance model (MESH). According to Kister (1992), the steady-state operation of a distillation column is described by the MESH equations. MESH stands for: (1) Material of flowrate balance equations, both component and total; (2) Equilibrium equations including the bubble point and dew point calculations; (3) Summation or stoichiometric equations of composition constraints; and finally, (4) Heat or enthalpy or energy balance equations. These equations are completely general and can be applied to multistage fractionation systems including absorption and stripping columns.

The Edmister model, which will be presented in detail in section 3.5.2, effectively combines staged component molar balances into a relationship that is useful for design and performance rating purposes. The derivation of the Edmister model is based on the only assumption that equilibrium is achieved in each of the stages. In fact, the Edmister model and the MESH (Kister (1992)) column models are equivalent, provided that the correct estimates of the internal liquid and gas flowrates and equilibrium constants are used as inputs to the Edmister model. However, these values can only be calculated from mass and enthalpy balances, which would automatically convert the Edmister model into the more laborious MESH equations.

To achieve equilibrium in each stage in reality, highly favourable mass and heat transfer is required, which would also prevent gradients of concentration or other intensive properties within each stage. In practice, the stage efficiency for absorbers can be in the range 0.3-0.4 out of a maximum efficiency of 1. This is equivalent to a 60-70% deviation from the equilibrium. However, the model is useful as it can predict the required number of theoretical stages, which will then be turned into actual stages using a typical efficiency value.

3.5.2 Background

The concept of absorption and stripping factors was introduced by Kremser (1930) and subsequently used by other authors (Horton and Franklin (1940), Edmister (1943), (1957)). The difference between the numerous models of absorption and stripping factors is in the assumptions involved in the derivation of the performance functions. Kremser model assumes constant overflow throughout the column and leads to appreciable error in applications where variation of flowrates along the column is encountered (Horton and Franklin (1940)), which is in the majority of the commercial absorbers. Kremser model does not account for temperature variations along the column and assumes constancy of the equilibrium relationship between the compositions in both phases. Nonetheless, the Kremser model has been favoured over stage-by-stage calculation design methods because of its ease of use.

Completely general absorption and stripping functions were derived by Horton and Franklin (1940), Edmister (1943) with the only assumption of equilibrium between gas and liquid prevailing on each theoretical stage of the column. However, in the evaluation of these performance functions, it is required to iterate on the individual stage absorption factors or alternatively, to make the necessary assumptions to facilitate this evaluation, albeit with some loss of accuracy.

This work adopts the modelling methodology of Edmister (1957) for various types of columns and makes a selection of the most adequate rules for model simplification. These rules will be presented after the model equations.

The model of Edmister (1957) for prediction of performance and design of absorption and desorption columns applies absorption and stripping factor functions to multicomponent separators such as reboiled absorbers, refluxed strippers, distillation columns and columns with side strippers.

The methodology of Edmister (1957) is characterised by a unified perception of all multistage separation processes as combinations of common separation zones or building blocks: condensing, absorbing, feed flash, stripping and reboiling, which may be arranged to form absorbers, enrichers (absorber plus condenser), strippers and exhausters (i.e. stripper plus reboiler). Condensing, feed flash and reboiling consist of a single equilibrium stage, while absorbing and stripping are multistage zones. Each of these multistage zones features two feeds and two products.

In commercial applications, in any of these multistage zones, the vapor feed is subject to absorption by the liquid flowing down the column and the liquid feed is subject to stripping by the rising vapors. However, even though absorption and stripping occur simultaneously in a given zone, absorption predominates in the absorber section and stripping predominates in the stripping section.

Multicomponent separation performance, usually given by feed component recoveries, is determined by the number of stages, the interstage vapour and liquid flowrates and the vapour-liquid equilibrium constants, and this is reflected in the model equations shown below. For prediction of separation performance, flowrates and equilibrium constants may be grouped in the definition of absorption and stripping factors:

$$A_i = \frac{1}{K_i}\frac{L_i}{V_i} \tag{3.13}$$

$$S_i = \frac{1}{A_i} \tag{3.14}$$

Where K_i, A_i and S_i represent the equilibrium constant ($K_i = y_i/x_i$), the absorption and stripping factors respectively for a fixed component on stage i, and L_i and V_i are the liquid and vapour molar flowrates on stage i.

The distributions of a component in the tower may be computed using functions of these factors and the number of stages.

Edmister (1957) provides rigorous relationships for separation performance and design as functions of absorption and stripping factors for the various fractionation building blocks: absorber, enricher, stripper and exhauster. In the following subsection the models are presented for these blocks with the exception of an enricher, which is outside the scope of this work.

3.5.2 (i) Absorber section

The equations of the absorber model of Edmister (1957) may be derived by combination of individual component molar balances and equilibrium relationships. A component molar balance around the top of the absorber in Figure 3.4 including stages 1 through i gives:

$$l_i + v_1 = v_{i+1} + l_0 \tag{3.15}$$

Combining this equation with the equilibrium relationship:

$$v_{i+1} = \frac{l_{i+1}}{A_{i+1}} \tag{3.16}$$

And rearranging gives:

$$l_{i+1} = A_{i+1}\left(l_i + v_1 - l_0\right) \tag{3.17}$$

Equation (3.17) relates the liquid leaving stage i+1 to the liquid leaving stage i.

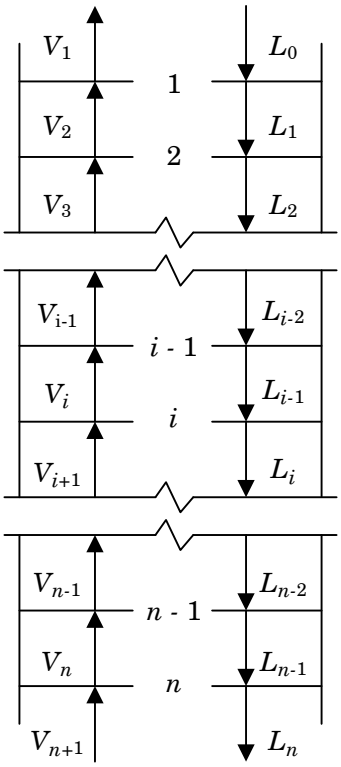

Figure 3.4: Schematics of an absorber section.

An equation for a multistage absorber is obtained by combining relationships similar to Equation (3.17) for each stage:

$$l_1 = A_1 v_1 \tag{3.18}$$

$$l_2 = A_2 \left(l_1 + v_1 - l_0 \right) \tag{3.19}$$

…

$$l_{n-1} = A_{n-1} \left(l_{n-2} + v_1 - l_0 \right) \tag{3.20}$$

$$l_n = A_n \left(l_{n-1} + v_1 - l_0 \right) \tag{3.21}$$

To give:

$$l_n = v_1\left(A_1A_2A_3\ldots A_n + A_2A_3\ldots A_n + A_3\ldots A_n + \ldots + A_n\right) - l_0\left(A_2A_3\ldots A_n + A_3\ldots A_n + \ldots + A_n\right) \tag{3.22}$$

Equation (3.22) is the basic relationship between the section products and the solvent feed.

3.5.2 (ii) Stripper section

In the following, the Edmister (1957) equations for the stripper section are presented.

A component molar balance around the bottom of the stripper in Figure 3.5 including stages j through m gives

$$v_j + l_m = l_{j-1} + v_{m+1} \tag{3.23}$$

Combining with the equilibrium relation:

$$l_{j-1} = \frac{v_{j-1}}{S_{j-1}} \tag{3.24}$$

And rearranging gives:

$$v_{j-1} = S_{j-1}\left(v_j + l_m - v_{m+1}\right) \tag{3.25}$$

Equation (3.25) is the relationship between the vapor leaving stages j - 1 and j.

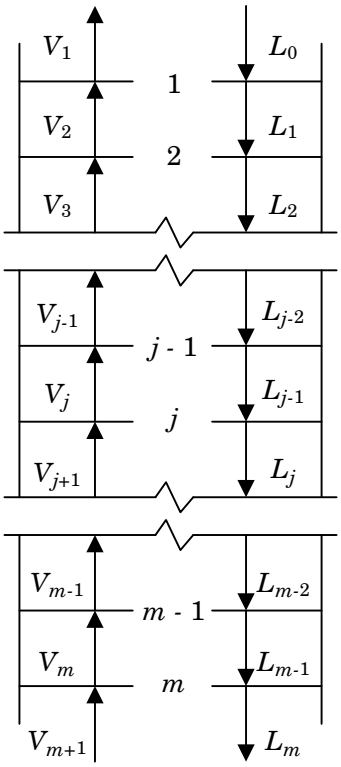

Figure 3.5: Schematics of a stripper section.

An equation for the multistage stripper is obtained by combining relationships similar to Equation (3.25) for each stage:

$$v_1 = S_1\left(v_2 + l_m - v_{m+1}\right) \tag{3.26}$$

$$v_2 = S_2\left(v_3 + l_m - v_{m+1}\right) \tag{3.27}$$

…

$$v_{m-1} = S_{m-1}\left(v_m + l_m - v_{m+1}\right) \tag{3.28}$$

$$v_m = S_m l_m \tag{3.29}$$

To give:

$$v_1 = l_m\left(S_m S_{m-1} S_{m-2} \ldots S_1 + S_{m-1} S_{m-2} \ldots S_1 + S_{m-2} \ldots S_1 + \ldots + S_1\right) - v_{m+1}\left(S_{m-1} S_{m-2} \ldots S_1 + S_{m-2} \ldots S_1 + \ldots + S_1\right) \tag{3.30}$$

3.5.2 (iii) Stripper section plus reboiler (exhauster)

A component material balance around the reboiler of Figure 3.6 gives:

$$l_m = v_{m+1} + b \tag{3.31}$$

For a partial reboiler such as the kettle reboiler pictured in Figure 3.6, the equilibrium relationship holds:

$$v_{m+1} = S_R b \tag{3.32}$$

Using this relationship it is possible to transform Equation (3.30) into:

$$v_1 = b\left(S_R S_m S_{m-1} S_{m-2} \ldots S_1 + S_m S_{m-1} S_{m-2} \ldots S_1\right) + \left(S_{m-1} S_{m-2} \ldots S_1 + S_{m-2} \ldots S_1 + \ldots + S_1\right) \tag{3.33}$$

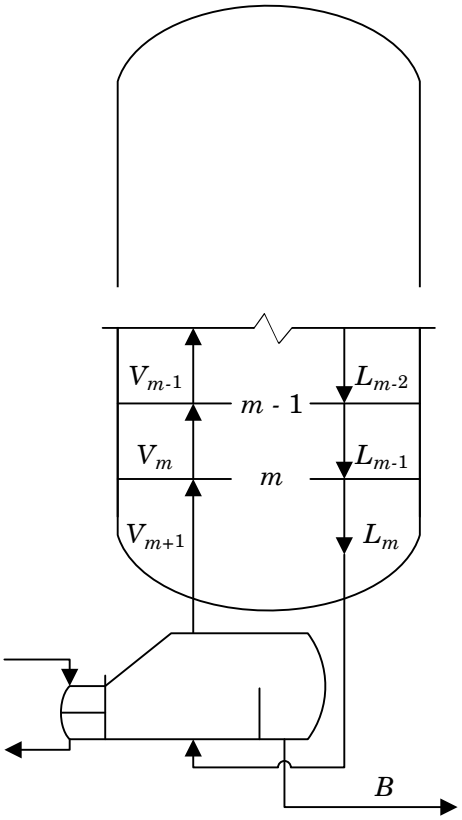

Figure 3.6: Schematics of a kettle reboiler at the bottom of the stripper.

For a total reboiler, such as the thermosyphon reboiler pictured in Figure 3.7, there is no equilibrium relationship between liquid and vapour, however, there is still a relationship between v_{m+1} and b. Because the liquid feed to the reboiler has the same composition as the vapour from the reboiler, the boilup ratio may be expressed as the ratio between the component molar flowrates, v_{m+1} and b:

$$R_{Boilup} = \frac{V_{m+1}}{B} = \frac{v_{m+1}}{b} \tag{3.34}$$

As a result, R_{boilup} replaces the reboiler stripping factor, S_R, in Equation (3.32), and the result is:

$$\begin{aligned} v_1 = R_{Boilup}\left(S_R S_m S_{m-1} S_{m-2} \ldots S_1 + S_m S_{m-1} S_{m-2} \ldots S_1\right) \\ R_{Boilup}\left(S_{m-1} S_{m-2} \ldots S_1 + S_{m-2} \ldots S_1 + \ldots + S_1\right) \end{aligned} \tag{3.35}$$

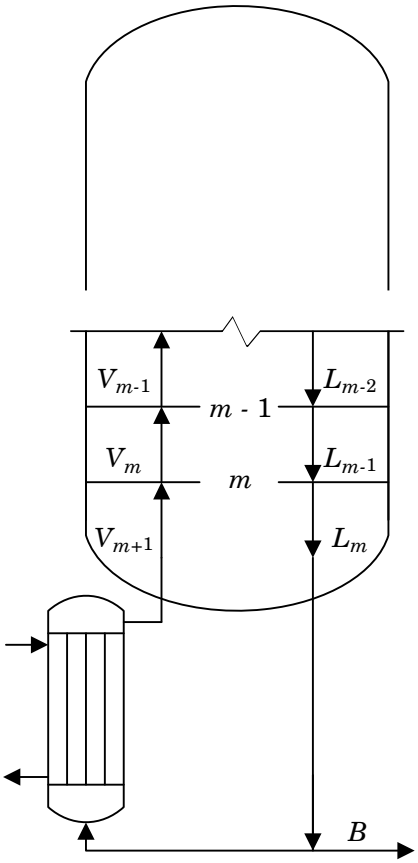

Figure 3.7: Schematics of a thermosyphon reboiler at the bottom of the stripper.

3.5.2 (iv) Normalisation of Edmister equations

The Edmister model equations may be formalised using the following definitions. Edmister (1957) groups the absorption factor series and the product using the following variables:

$$\Sigma_A = A_1A_2A_3\ldots A_n + A_2A_3\ldots A_n + A_3\ldots A_n + \ldots + A_n \tag{3.36}$$

$$\pi_A = A_1A_2A_3\ldots A_n \tag{3.37}$$

Then, the absorber equation (3.22) becomes

$$l_n = v_1\Sigma_A - l_0\left(\Sigma_A - \pi_A\right) \tag{3.38}$$

By inspection of Equations (3.36) and (3.37), it is predicted that parameters Σ_A and π_A will be in the range of nearly zero to very large values, depending on the component absorption factors. The form of Equation (3.38) is too sensitive to small differences in the absorption factor, and hence requires further manipulation.

Equation (3.38) combined with an overall component material balance for the entire absorber:

$$l_n = v_{n+1} + l_0 - v_1 \tag{3.39}$$

Gives:

$$v_{n+1} + l_0 - v_1 = v_1\Sigma_A - l_0\left(\Sigma_A - \pi_A\right) \tag{3.40}$$

$$v_{n+1} + l_0\left(1 + \Sigma_A - \pi_A\right) = v_1\left(\Sigma_A + 1\right) \tag{3.41}$$

$$v_1 = v_{n+1}\frac{1}{\Sigma_A + 1} + l_0\left(1 - \frac{\pi_A}{\Sigma_A + 1}\right) \tag{3.42}$$

Two new absorption factor functions may be identified which now have numerical values between zero and one regardless of the values of A and the number of stages. These factors are:

$$\varphi_A = \frac{1}{\Sigma_A + 1} \tag{3.43}$$

$$\psi_A = 1 - \frac{\pi_A}{\Sigma_A + 1} \tag{3.44}$$

Equation (3.42) becomes:

$$v_1 = v_{n+1}\varphi_A + l_0\psi_A \tag{3.45}$$

Equation (3.45) by Edmister (1957), is now applicable to all components. Factors φ_A and ψ_A may be given a physical interpretation. By looking at Equation (3.45), Edmister (1957) arrived at the conclusion that φ_A represents the fraction of feed gas flowrate, v_{n+1}, that remains unabsorbed, while ψ_A is the fraction of the given component in the liquid feed, l_0, which is lost to the gas.

By an analogous procedure a similar equation was obtained from Equation (3.30) for a stripper:

$$l_m = l_0\varphi_S + v_{m+1}\psi_S \tag{3.46}$$

The examination of the definition of φ_A and ψ_A reveals the following relationships:

$$\psi_A = 1 - \varphi_S \tag{3.47}$$

$$\psi_S = 1 - \varphi_A \tag{3.48}$$

$$\varphi_A = \frac{1}{A_1A_2A_3\ldots A_n + A_2A_3\ldots A_n + A_3\ldots A_n + \ldots + A_n + 1} \tag{3.49}$$

$$\varphi_S = \frac{1}{S_mS_{m-1}S_{m-2}\ldots S_1 + S_{m-1}S_{m-2}\ldots S_1 + S_{m-2}\ldots S_1 + \ldots + S_1 + 1} \tag{3.50}$$

A similar relationship for the stripper section plus a reboiler is obtained by combining Equation (3.46) with the reboiler mass balance of Equation (3.31) and an overall mass balance. For a partial reboiler:

$$\frac{v_1}{b} = \frac{S_R\varphi_{AX} + 1}{\varphi_{SX}} - 1 \tag{3.51}$$

Or

$$\frac{l_0}{b} = \frac{S_R \varphi_{AX}}{\varphi_{SX}} + \frac{1}{\varphi_{SX}} \qquad (3.52)$$

Where subscript X designates the exhausting section and φ_{SX} ranges between 0 and 1.

For a total reboiler, S_R is replaced with the boilup ratio, $\frac{V_{m+1}}{B}$.

3.5.2 (v) Reboiled absorber

A reboiled absorber configuration may adequately reduce the co-absorption of light components. In general, unless the light key component is much more volatile than the heavy key component or the separation specifications for the light key are unusually relaxed, the present design methodology will recommend a reboiled absorber configuration.

Figure 3.8 represents a reboiled absorber, which is a combination of the absorber of Figure 3.4 and the exhauster (stripper with reboiler) of Figure 3.6.

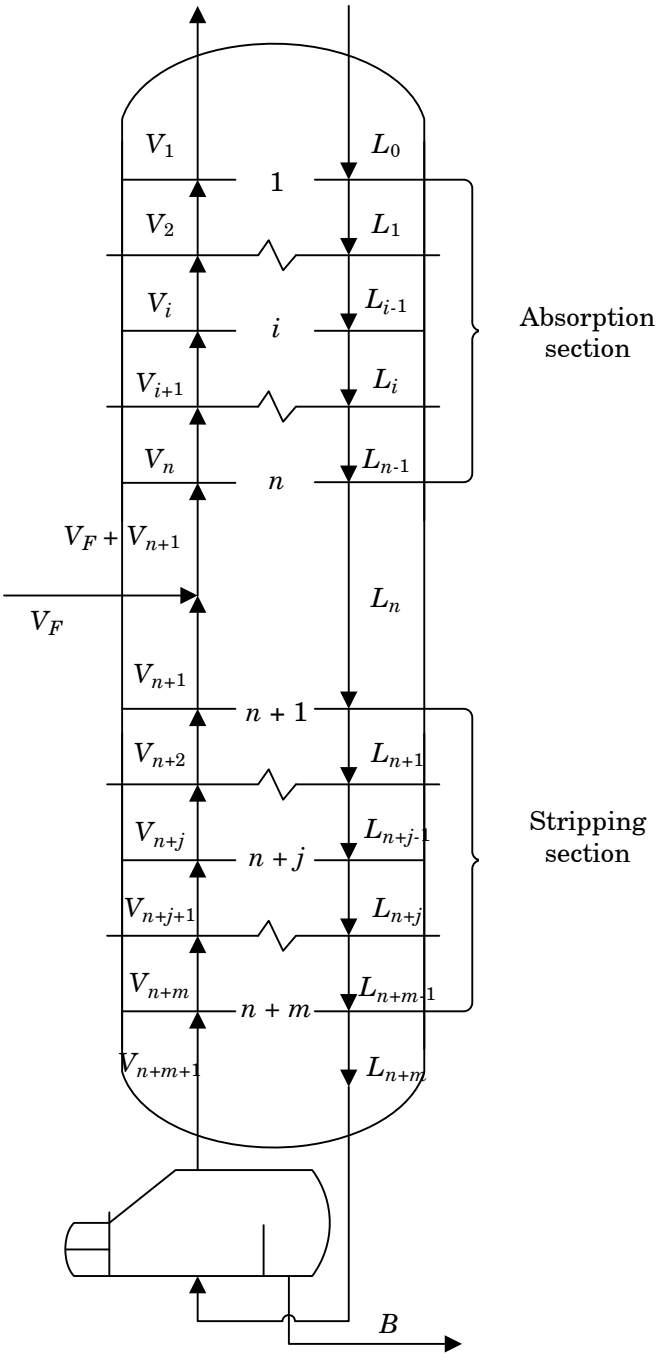

Figure 3.8: Schematics of a reboiled absorber column.

The recovery equation for the reboiled absorber column is obtained by combining Equation (3.45) for the absorber with Equation (3.51) for the exhauster. For this particular case, Equation (3.45) may be written as:

$$d = \varphi_{AA}\left(v_{TX} + v_F\right) + \left(1 - \varphi_{SA}\right) l_0 \tag{3.53}$$

Equation (3.51) for this case becomes

$$\frac{v_{TX}}{b} = \frac{S_R \varphi_{AX} + 1}{\varphi_{SX}} - 1 \tag{3.54}$$

Combining these equations and rearranging gives:

$$\frac{d}{b} = \frac{\varphi_{AA} \dfrac{S_R \varphi_{AX} + 1}{\varphi_{SX}} + \left(1 - \varphi_{SA} - \varphi_{AA}\right) \dfrac{l_0}{b}}{1 - \varphi_{AA}} \tag{3.55}$$

Solvent inlet flowrate, reboiler duty or boilup rate or ratio, absorber number of theoretical stages for top and bottom section and absorber key component recoveries are interrelated through Equations (3.53) and (3.54), where the various $\varphi-$fractions are implicitly related to the number of stages through Equations (3.49) and (3.50). With typical recovery specifications on the two key components, the problem features two independent equations and four variables, which leaves two degrees of freedom, one per section. Said equations are Equation (3.53) for the top section, which is formulated for the heavy key, and Equation (3.54) for the bottom section, which is formulated for the light key.

Selecting the solvent inlet flowrate and the boilup rate as the degrees of freedom, the respective number of stages of the sections can be derived from Equations (3.53) and (3.54) . Theoretically, it is possible to find different pairs of values of the selected degrees of freedom for a given feasible reboiled absorber design. However, the problem may be treated as a problem with a single degree of freedom. This is due to a higher boilup rate demanding a higher solvent flowrate and viceversa. Aside from the secondary impact on the number of stages and column height, the relationship between solvent flowrate and boilup rate is trivial. Therefore, the problem can be reduced to the selection of the minimum feasible solvent flowrate for a given boilup rate.

The strategy for solving the reboiled absorber column model in the proposed synthesis framework is described in more detail in section 3.9.1.

3.5.2 (vi) Evaluation of recovery equations

The recovery fractions of Edmister (1957) may be evaluated using assumed trial values of K, V, and L on each stage. When the correct values of A and S are used, this method is as rigorous as the MESH model. Edmister (1957) defends the rigor of this model because of the only assumption imposed is the equilibrium at column stages. In effect, this assumption is generally a reasonable approximation in preliminary column design.

Effective absorption and stripping factors, A_e and S_e, are defined as follows:

$$\varphi_A = \frac{1}{A_e^{\,n} + A_e^{\,n-1} + \ldots + A_e^{\,2} + A_e + 1} = \frac{A_e - 1}{A_e^{\,n+1} - 1} \tag{3.56}$$

$$\varphi_S = \frac{1}{S_e^{\,m} + S_e^{\,m-1} + \ldots + S_e^{\,2} + S_e + 1} = \frac{S_e - 1}{S_e^{\,m+1} - 1} \tag{3.57}$$

The effective factors are useful because of the simplicity they offer with respect to the evaluation of the recovery equations. A_e and S_e are intermediate values in the range of absorption and desorption factors encountered within the column, such that may represent the separation performance of the process without information on individual stages, thus leading to the same result for φ_A and φ_S from Equations (3.56) and (3.57) as it is obtained from (3.49) and (3.50) using the values of A and S on each stage.

For two-stage columns, Edmister (1943), (1957) shows that the effective factors are given by the following relationships:

$$A_e = \sqrt{A_B\left(A_T + 1\right) + 0.25} - 0.5 \tag{3.58}$$

$$S_e = \sqrt{S_T\left(S_B + 1\right) + 0.25} - 0.5 \tag{3.59}$$

Where subscripts B and T designate the bottom and top stages, respectively. According to Edmister (1957), the estimates from (3.58) and (3.59) provide a convenient approximation for multistage separation columns. Edmister (1957) maintains that the effective factors are strongly correlated to the values of A and S at the top and bottom stages and are relatively independent of the number of stages. As a result, A_e is closer to A_B and that S_e is closer to S_T.

The alternative method of Horton and Franklin (1940) for estimating the values of A_e and S_e, suggests a correspondence between the effective factor and the local absorption factor at a certain stage of the absorber. This method is concerned with determining the location within the column where $A = A_e$ and $S = S_e$. In this method, the location of the effective factor depends on an overall column value of A (or S). According to Horton and Franklin (1940), the effective absorption factor, A_e, for the very light components will correspond to the value of A at a position near the bottom of the absorber and for the very heavy components, to the value of A at a position near the middle of the tower. A guide to the location of effective absorption factors by overall column absorption or desorption factors is presented by Horton and Franklin (1940) and is shown in Table 3.1.

A or S	m/n
0.0 to 0.1	1.0
0.1 to 0.4	0.9
0.4 to 1.0	0.8
1.0 to 4.0	0.7
> 4.0	0.6

m = stage corresponding to effective factor; n = number of total theoretical stages

Table 3.1: Location of effective absorption factors, Horton and Franklin (1940).

According to this method, the effective absorption factor corresponds to the corresponding absorption factor at the position in the column obtained from Table 3.1.

Because intermediate stage absorption factors are usually unknown, the relevant stage absorption factor must be estimated from top and bottom values. Edmister (1957) provides linear relationships to obtain the absorption factor at an intermediate stage from the values at top and bottom for use in combination with the method of Horton and Franklin (1940). These relationships are shown in Table 3.2.

A or S	A_e	S_e
0.0 to 0.1	A_B	S_B
0.1 to 0.4	$A_B + 0.1\,(A_T - A_B)$	$S_T + 0.1\,(S_B - S_T)$
0.4 to 1.0	$A_B + 0.2\,(A_T - A_B)$	$S_T + 0.2\,(S_B - S_T)$
1.0 to 4.0	$A_B + 0.3\,(A_T - A_B)$	$S_T + 0.3\,(S_B - S_T)$
> 4.0	$A_B + 0.4\,(A_T - A_B)$	$S_T + 0.4\,(S_B - S_T)$

Table 3.2: Method of Horton and Franklin (1940) with contribution of Edmister (1957).

The methods for estimating the effective factors from Edmister (1957) and Horton and Franklin (1940) are tested in section 3.5.4 (i).

3.5.3 Estimation of absorption factor column profile

In this work, a distinct approach is proposed, which is shown to overcome the difficulties of the presented approaches for calculation of effective factors, as will be illustrated by section 3.5.4 (i). Instead of using the effective factor version of the Edmister equation, the proposed approach resorts to the initial formulation based on stage-by-stage absorption factors.

Horton and Franklin (1940) present a set of simple rules to estimate flowrate and temperature column profiles from terminal stage values and suggest that the use of these rules was satisfactory in a number of cases studied. The internal flowrate profile estimation proposed by Horton and

Franklin (1940), assumes constant percent vapour flowrate contraction due to absorption in each stage:

$$\left(\frac{V_1}{V_{n+1}}\right)^{1/n} = \frac{V_j}{V_{j+1}} \tag{3.1}$$

Where n represents the total number of stages and j represents an intermediate stage number.

Or alternatively:

$$V_j = V_1^{\frac{n+1-j}{n}} \tag{3.2}$$

For the temperature:

$$\frac{V_{n+1} - V_{j+1}}{V_{n+1} - V_1} = \frac{T_n - T_j}{T_n - T_0} \tag{3.3}$$

These rules assume constant percent absorption on each stage throughout the tower and temperature change proportional to the contraction of the vapour flowrate upwards of the column. In order to generate the temperature profiles, a number of assumptions are made:

- The vapour being absorbed is entirely responsible for the temperature change.

- The temperature change in one stage is proportional to the amount of vapour being absorbed in the stage, which is underpinned by constant latent heat and constant liquid heat capacity assumptions (and negligible or constant heat of solution).

- The temperature change in one stage is a fraction of the overall temperature change between column top and bottom.

According to Horton and Franklin (1940), the predicted stage flowrates and temperatures may differ considerably from those in a real absorber, but use of these predictions gives an overall absorption efficiency for each component which is in closely agreement with stage-to-stage calculations.

Use of the above empirical rules will enable the calculation of vapour and liquid flowrates and stage temperatures. The effective absorption factors may be subsequently calculated from the L-to-V ratios and temperatures.

Finally, for estimating the absorption factor column profiles, it is necessary to establish the species equilibrium constant column profile. A method for calculation of the equilibrium constant profiles has been developed in this work. This constant, $K = y/x$, relates the stage vapour phase molar fraction to the stage liquid phase molar fraction of the considered species. According to the Gibbs phase rule, in a two-phase multicomponent system with n components, n independent variables are required to identify the state of equilibrium and to retrieve component K-values. Consequently, knowledge of the composition of one of the phases and another intensive variable (temperature or pressure) is necessary to fully specify the equilibrium of the system.

Alternatively, since the phase compositions inside the column are not readily available, the component K-value profile may be approximated from top and bottom values. This approximation is based on the assumption that the K-value is exclusively dependent on the stages temperature. This relationship between K-value and temperature is obtained by combining an equilibrium relationship between phases with a relationship for the partial vapour pressure as a function of the temperature.

Raoult's law is the simplest vapour-liquid equilibrium relationship and it applies to ideal mixtures. Raoult's law postulates that the K-value of a

component in the equilibrium mixture is the ratio of the component vapour pressure to the total pressure of the system:

$$Py = P^0 x \tag{3.4}$$

$$K = \frac{y}{x} = \frac{P^0}{P} \tag{3.5}$$

For non-ideal mixtures, accuracy is improved by incorporating the activity coefficient to the Raoult's law, which allows for the deviations from the ideal liquid. Similarly, the incorporation of the fugacity coefficient allows for the deviations from the vapour phase ideal behaviour. However, for subsequent calculation of the absorption factor column profiles, a highly accurate estimate of the *K*-value profile is unnecessary because of the crude estimates of the profiles of liquid and vapour flowrates, which also intervene in the calculation.

The Clausius-Clapeyron equation for the vapour-liquid equilibrium of a pure component is given by:

$$ln\left(\frac{P_1^0}{P_2^0}\right) = \frac{\Delta H_{vap}}{R}\left(\frac{1}{T_2} - \frac{1}{T_1}\right) \tag{3.6}$$

Where $P_1{}^0$ and $P_2{}^0$are the vapour pressures corresponding to temperatures T_1 and T_2 respectively (in Kelvin), ΔH_{vap} is the component molar enthalpy of vaporisation and R is the gas constant (8.314 J $mol^{-1}K^{-1}$).

It is possible to combine Equations (3.5) and (3.6) to obtain a relationship between component *K*-values at two different temperatures, T_1 and T_2:

$$ln\left(\frac{K_1}{K_2}\right) = \frac{\Delta H_{vap}}{R}\left(\frac{1}{T_2} - \frac{1}{T_1}\right) \tag{3.7}$$

Provided that the enthalpy of vaporisation is sufficiently constant throughout the column, the constant $\frac{\Delta H_{vap}}{R}$ may be evaluated from application of Equation (3.7) to the terminal stages of known *K*-values. Equation (3.7) may be then manipulated to obtain the basic relationship between the *K*-value at an intermediate absorber stage *j* and a known *K*-value, such as the top stage *K*-value:

$$K_j = K_1 \left(\frac{K_1}{K_n} \right)^{\frac{\frac{1}{T_1} - \frac{1}{T_j}}{\frac{1}{T_n} - \frac{1}{T_1}}} \tag{3.8}$$

With the estimated column internal profiles of vapour and liquid flowrates, temperatures and vapour-liquid equilibrium constants from Equations (3.1) or (3.2), (3.3) and (3.8), it is possible to calculate approximate internal absorption / stripping profiles, which may then be used to solve the Edmister equations.

This proposed method allows estimation of absorption factor profiles and effective factors and illustration of its application is provided in section 3.5.4 (i).

3.5.4 Model validation

3.5.4 (i) Validation of methods for estimation of effective factors

A paraffinic solvent saturated with a mix of light hydrocarbons is stripped off the light components in a reboiled stripper column section. The characteristics of this stream from Table 3.3 are typical of a C8 absorption oil loaded with NGL from natural gas absorption, albeit simplified because in practice, such a stream would also contain butane and heavier components. Because of the high molecular weight of the solvent, the regeneration can take place in a reboiled stripper without significant C8 overhead losses of C8.

The reboiled stripper consisting of eight theoretical stages was simulated in Aspen Plus® Version 2004.1. The composition of the saturated liquid feed is given in Table 3.3. The reboiler duty was adjusted to achieve a recovery of 99.9% of propane in the gas product.

	Molar fractions
Methane	0.0524
Ethane	0.130
Propane	0.0517
n-Octane	0.766
Flowrate, kmol/h	33.46

Table 3.3: Stripper feed composition for model validation.

Stripper internal profiles calculated by the simulation software are presented in Table 3.4 and Table 3.5.

Stage number	Temperature	Liquid flowrate	Vapor flowrate	Pressure	Heat duty
	°C	kmol/h	kmol/h	bar	kW
1	32.5	42.4	7.9	10	0
2	128.8	51.6	16.8	10	0
3	208.6	84.2	26.0	10	0
4	228.8	104.4	58.6	10	0
5	232.7	109.6	78.8	10	0
6	233.5	110.7	84.0	10	0
7	233.7	110.9	85.1	10	0
8	233.7	25.6	85.3	10	557

Table 3.4: Flowrates and general conditions profiles in the stripper column.

Stage number	*K-value*s			
	Methane	Ethane	Propane	n-Octane
1	20.26	3.95	1.13	0.00
2	25.22	9.28	4.25	0.15
3	19.90	10.51	6.33	0.72
4	16.99	9.76	6.27	0.95
5	16.37	9.55	6.22	0.99
6	16.24	9.51	6.20	1.00
7	16.22	9.50	6.20	1.00
8	16.22	9.50	6.20	1.00

Table 3.5: Vapour-liquid *K*-value profiles in the stripper column.

These data may be employed to obtain the column effective absorption factor of the column light key, propane, from the following equation derived from Equation (3.52), for a reboiled stripper (exhauster):

$$\frac{l_0}{b} = S_R S_e^{\,m} + \frac{S_e^{\,m+1} - 1}{S_e - 1} \tag{3.9}$$

Because Equation (3.9) is not explicit on the effective stripping factor, the value of this is found by trial and error. Table 3.6 contains a summary of the results.

Parameter	Value
Recovery, fraction	0.99977
A_e	0.216
S_e	2.000

Table 3.6: Calculation of effective stripping factor from simulation profiles.

The estimation method of Equation (3.59) attributed to Edmister (1943), requires the stripping factor values at the top and bottom stages, while the combined method of Horton and Franklin (1940), Edmister (1943) of Table 3.2 requires a rough average of the stripping factors within the column, as well as those at the top and bottom. Simulated absorption and desorption factor profiles are provided in Table 3.9 for reference. The results of the comparison between the rigorous value of S_e from the simulation (Table 3.6) with the methods of prediction of S_e for these estimates are shown in Table 3.7.

Estimation method	S_e
Equation (3.59) from Edmister (1957)	0.708
m/n = 0.7 for $1 < S < 4$ from Table 3.1 and Table 3.2	1.574

Table 3.7: Estimates of S_e from available approximations in literature.

Table 3.7 shows that the approximations of Horton and Franklin (1940), Edmister (1943) and Edmister (1957) departure from the reported S_e of 2.0 from simulation in a different degree. The unsatisfactory predictions for the case in question may be attributed to the prominent variations in temperature and flowrates profiles within the column.

The alternative approach presented in this work for calculation of effective absorption and desorption factors by estimating the column profiles for absorption and desorption factors is tested for agreement with the effective factors from the simulation. Estimated flowrates and temperature column profiles are included in Table 3.8. These allow calculation of absorption and desorption factor profiles, shown in Table 3.9. Using these profiles, it is possible to determine effective factors and the consequent recovery. The result of this calculation is provided in Table 3.10.

Stage number	Simulation (rigorous)			Approximation		
	Liquid flow kmol/h	Vapor flow kmol/h	Temperature °C	Liquid flow kmol/h	Vapor flow kmol/h	Temperature °C
1	42.4	7.9	32.5	42.4*	7.9*	32.5*
2	51.3	16.8	128.8	48.8	16.8*	128.8*
3	62.2	25.7	208.6	57.7	23.2	148.0
4	75.4	36.6	228.8	70.0	32.1	171.2
5	91.4	49.8	232.7	87.1	44.4	199.4
6	110.7	65.8	233.5	110.7*	61.5	233.5
7	110.9	85.1	233.7	110.9*	85.1*	233.7*
8	25.6	85.3	233.7	25.6*	85.3*	233.7*

* Inputs to developed estimation method.

Table 3.8: Simulated and estimated column profiles.

Stage number	Simulation (rigorous)		Approximation	
	S Propane	*A* Propane	*S* Propane	*A* Propane
1	0.21	4.77	0.21	4.77
2	1.38	0.72	1.39	0.72
3	1.96	0.51	1.96	0.51
4	3.52	0.28	2.54	0.39
5	4.47	0.22	3.12	0.32
6	4.71	0.21	3.69	0.27
7	4.76	0.21	4.76	0.21
8	20.68	0.05	20.68	0.05
φ	0.784	0.004	0.010	0.763

Table 3.9: Simulated and estimated absorption/stripping factor profiles.

Parameter	Simulation (rigorous)	Approximation
Recovery, fraction	0.99977	0.99943
A_e	0.216	0.237
S_e	2.000	1.719

Table 3.10: Simulated and estimated effective stripping factor.

The comparison provided in Table 3.10 between simulation and rigorous data reveals that the proposed basis for the column modelling improve the prediction of the effective stripping factor with respect to the existing approaches in the literature.

In conclusion, by incorporating approximated but individual stage-by-stage information in the Edmister equation, the column model is noticeably more accurate than by simply using an effective absorption factor which is merely derived from top and bottom conditions (Equation (3.59)) or from top and bottom conditions and a linear interpolation of the two (Table 3.2).

3.5.4 (ii) General strategy for model validation

Process simulation software is the accepted benchmark for model validation. However, the separation models employed in this work are orientated to design, which is the reverse of the typical operating mode of commercial simulation software. Simulation software does not generally run on design mode but on the simulation mode. On simulation mode, the design configuration of the separation equipment is known, and models are used for predicting separation performance.

Because of the different purpose of these models, agreement between these and commercial simulation models cannot be straightforwardly tested on the same mode, and one set of models must be transformed to operate in the reverse mode. In certain cases, models may require substantial manipulation to switch from design mode to simulation mode, and viceversa.

In this work, the simulated separation performance of the considered separation equipment is used as the basis for comparison between models.

3.5.4 (iii) Reboiled absorber column model validation

The previous validation example has indicated that the Edmister model with the proposed profile estimation methodology is capable of yielding an improved prediction of the recovery achieved by a column simulated by commercial simulation software.

In a new example, the proposed shortcut model is tested for assessment of predicted key design variables, primarily the solvent feed and the boilup requirements. The composition of the gas feed to the reboiled absorber column is provided in Table 3.11. In this example, the shortcut model is used to propose a design of a reboiled absorber column that meets certain recovery specifications. Application of the shortcut model generates a prediction of the solvent flowrate and the boilup rate and the number of stages of each section of the column. Other model outputs, also used by intermediate model calculations, are the column flowrates, *K*-values and temperature profiles.

	Molar fractions
Methane	0.014
Ethane	0.550
Propane	0.257
n-Butane	0.178
Flowrate, kmol/h	1917

Table 3.11: Reboiled absorber feed composition.

In the two tests illustrated by Figure 3.9 and Figure 3.10, feed composition and flowrate, and recoveries are constant, while the column pressure and the corresponding feed temperature (saturated vapour at the column pressure) vary from one case to another. The predicted number of theoretical stages and feed location by the model is then used to set up a RadFrac® model in Aspen Plus® 2004.1, which is able to find the solvent

flowrate and boilup rate that meet the desired recovery specifications. The number of trays in Figure 3.9 and Figure 3.10 are theoretical stages.

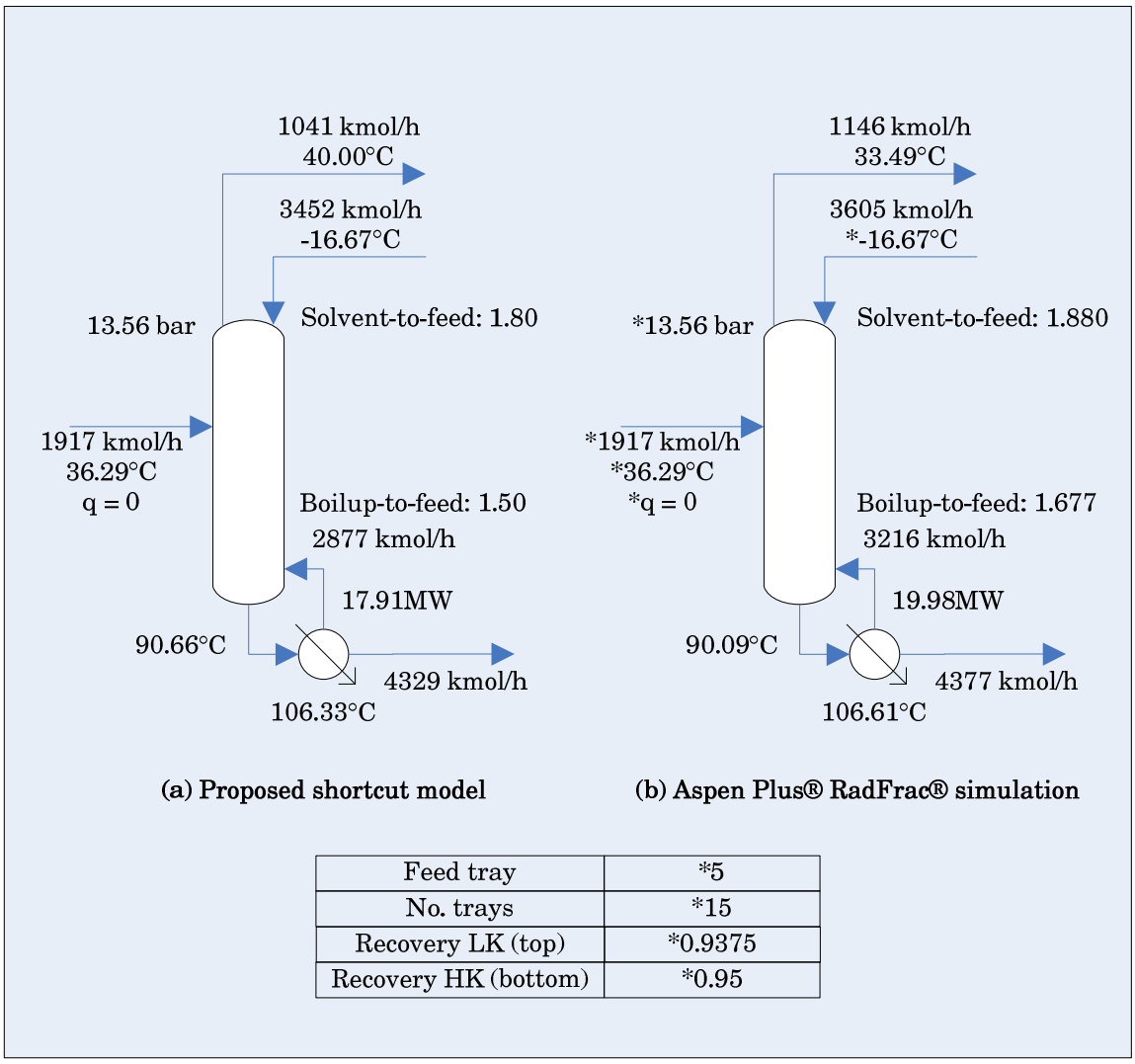

(a) Proposed shortcut model

(b) Aspen Plus® RadFrac® simulation

Feed tray	*5
No. trays	*15
Recovery LK (top)	*0.9375
Recovery HK (bottom)	*0.95

* Fixed inputs to Aspen Plus® simulation

Figure 3.9: Validation of key design and operating variables for reboiled absorber (Case (i)).

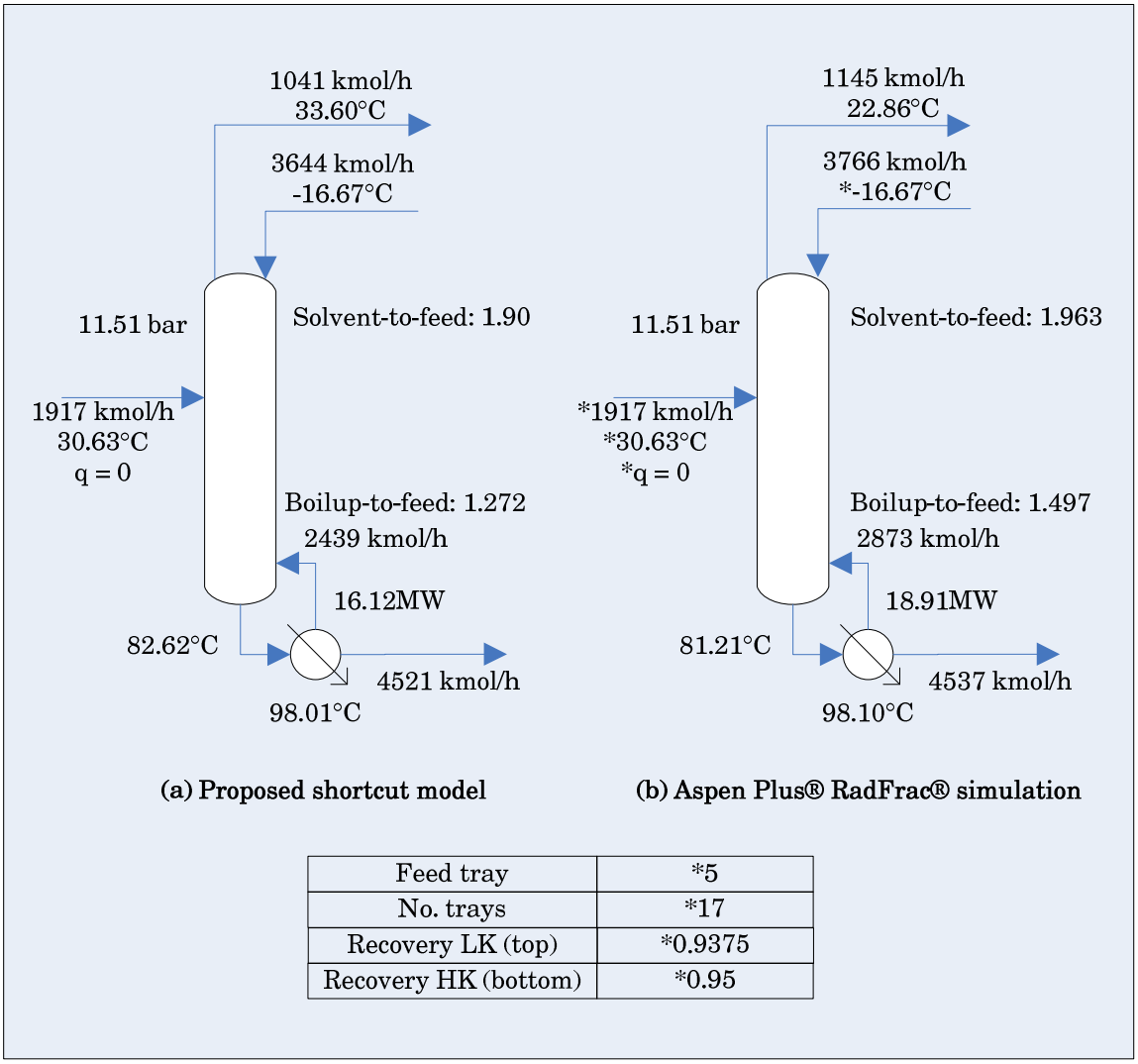

Feed tray	*5
No. trays	*17
Recovery LK (top)	*0.9375
Recovery HK (bottom)	*0.95

* Fixed inputs to Aspen Plus® simulation

Figure 3.10: Validation of key design and operating variables for reboiled absorber (Case (ii)).

Table 3.12 summarises the key discrepancies between the shortcut model and Aspen Plus®. Case (i) corresponds to Figure 3.9 and Case (ii) corresponds to Figure 3.10. Solvent flowrate estimates are within a 4.2% deviation of the simulation data. The boilup flowrate shortcut predictions for Cases (i) and (ii) are respectively 10.4 and 15.1% lower than Aspen Plus® results. There is a direct correlation between the reboiler duty and the boilup rate; hence the deviations shown in Table 3.12 for these parameters are qualitatively the same.

		Case (i)	Case (ii)
Inlet solvent flowrate kmol/h	Shortcut	3452	3644
	Aspen Plus®	3605	3766
	Deviation (%)	**4.2**	**3.2**
Boilup flowrate kmol/h	Shortcut	2877	2439
	Aspen Plus®	3216	2873
	Deviation (%)	**10.5**	**15.1**
Reboiler duty MW	Shortcut	17.91	16.12
	Aspen Plus®	19.98	18.91
	Deviation (%)	**10.4**	**14.8**

Table 3.12: Shortcut validation using commercial simulation software.

The 4.2% higher solvent flowrate required to achieve the desired recovery of heavy key in the bottoms is logically accountable for the increased reboiling requirements. This may be explained by considering that a higher solvent flowrate will remove a greater amount of light key and lighter components, which will only be stripped off by a larger reboiler duty. It may be concluded that the reboiler requirements are highly sensitive to the solvent inlet flowrate, which is responsible for the apparent disagreement between models.

Intuitively, the closer percentual agreement between shortcut and simulated solvent requirements of Case (ii) with respect to Case (i) should lead to a closer agreement between boilup requirements. Contrarily, Case (ii) features a greater discrepancy between boilups than Case (i). On a closer examination of the column conditions, it is possible to attribute this behaviour to the lower temperatures prevailing in the column of Case (ii), due to the colder conditions in the reboiler at the lower pressure and the colder feed to the column. As a result of the colder temperatures (5 to 10°C lower, based on the simulated column profiles), the absorption of light components is more favourable, thus, a similar absolute solvent flowrate increase may lead to an amplified boilup increase.

In summary, the proposed shortcut model is capable of predicting the solvent feed requirements to the absorber column with moderate accuracy (less than 5% deviation from commercial simulation). The distorted deviations (10-15%) between boilup requirements have been attributed to

the validation strategy whereby solvent and boilup requirements are the simultaneous outputs of the Aspen Plus® simulation. Subsequent discussion has suggested that the actual departure of shortcut boilup from actual boilup is expected to be significantly lower. Confirmation of this probability would require altering the validation strategy to disengage the interdependent boilup and solvent flowrate.

3.6 Conclusions (i) – Absorption and desorption

The first part of this chapter has dealt with modelling at two levels: (1) modelling of the absorber-desorber flowsheet; (2) modelling of the absorber column.

At the flowsheet level, this work has proposed ways to overcome the problems associated with the assembling of the absorber-desorber separation block in the sequence orientated optimisation framework. These issues relate to absorption-desorption falling in the category of Material Separation Agent separation methods. By way of the adjustments proposed at flowsheet level, the absorption-desorption block is assimilated as a black box, which performs a separation task anonymously. The optimisation framework presented in this thesis now features two types of black boxes: the absorption-desorption block and the pure distillation block. Both blocks may be selected independently by the optimisation framework to perform a given separation task in the separation sequence.

At the column level, this chapter reflects the emphasis of this work on the development of highly representative models while keeping the computational overhead to a minimum. The shortcomings of some of the customary absorption shortcut models in the literature have been identified. A proposed improvement to the implementation of the Edmister model has been shown to increase the accuracy of previous implementation approaches. Validation using commercial simulation

software suggests that the proposed shortcut model is suitable for the purpose of preliminary screening of design options.

3.7 Distillation column models

3.7.1 Introduction

Adequate models for distillation column design are required as part of the proposed synthesis framework to enable the representation of distillation columns in the flowsheet, including the desorber of the absorption-desorption separation block.

A key development of the present synthesis methodology allows to achieve an improved prediction of the minimum reflux ratio in comparison with previous synthesis approaches based on the pure Fenske-Underwood-Gilliland method, including the approach of Wang (2004). By means of this correction, the minimum reflux ratio given by the classical Underwood equations (Underwood (1946), (1948)) and originally prescribed to the column pinch point location, becomes a better approximation of the actual minimum reflux at the top of the column.

This correction is advantageous because it allows a more accurate estimate of one of the most decisive variables in the design of distillation columns at undetectable expense in computation time. An immediate consequence of this improvement is that it leads to a more realistic prediction of reboiler and condenser duties. Ultimately, this enables the synthesis framework to compare design options on firmer grounds.

In the proposed synthesis framework, the optimisation algorithm will explore desorber feed qualities generally between 0 and 1, but it may also accept any subintervals of this range. Distillation of sub-cooled or superheated feeds has a lower efficiency due to the feed deviation from saturated conditions that reign inside the tower. Liquid feeds are usually

preferable because of the easy pressure control without need for expensive vapour compression equipment. However, this preference is rarely extensible to gas separations due to the low temperatures at which a liquid feed is encountered.

According to Suphanit (1999) and Yeomans and Grossmann (1999) saturated liquid feeds (i.e. q = 1) tend to result in a reduced minimum reflux ratio in comparison to vapour feeds.

3.7.2 Background

3.7.2 (i) Calculation of minimum reflux

The calculation of minimum reflux is an important initial step in the design of distillation columns. The minimum reflux ratio is a key design parameter and an indicator of the operating cost of the separation. Because minimum reflux can only be achieved at infinite number of stages, the design of practical distillation columns often employs a recommended reflux scale-up factor of 1.1 (Douglas (1988)).

There are various methods for calculating minimum reflux rates in multicomponent distillation, including approximate and rigorous methods. Most of these methods were developed by 1950 but in recent years have been cited among the preferred methods for calculation of the minimum reflux (Perry and Green (1998), Seader and Henley (1998), Smith (2005)). Rigorous methods (Thiele and Geddes (1933), Brown and Holcomb (1940)) are recommended as tools in distillation research or unusual design problems, but are too laborious for most design purposes. Of the approximated methods, the most well-established method is the method introduced by Underwood (1946), (1948). Underwood's theta-function method is valid under the assumptions of constant molar overflows and constant relative volatilities. This method is quite accurate and relatively fast and may be applied to sharp separations between adjacent keys as well as to cases with distributed intermediate components.

For the calculation of minimum reflux, Shiras *et al.* (1950) classified multicomponent systems with respect to the distribution of components at infinite number of stages. Class 1 systems have all components distributed between the top and bottoms, whereas in Class 2 systems, only some components are distributed.

In a section consisting of infinite stages, a pinch point is encountered which is characterised by infinitesimal changes in component concentrations and molar flows between consecutive stages. Class 1 separations feature only one pinch point that occurs at the feed stage. This implies that the liquid leaving the feed tray has the same composition as the liquid leaving the stage above the feed tray and the liquid leaving the stage below the feed tray. This observation is important in the development of minimum reflux equations for Class 1 separations. Binary separations are an example of Class 1 separations.

In class 2 separations two pinch points are encountered and at least one of them occurs away from the feed stage. If neither the distillate nor the bottoms contain all feed components, both pinch points occur away from the feed stage. It is primarily class 2 separations the object of the present work, where it is assumed that all of the lighter than light key components are separated overheads and all of the heavier than heavy key components are separated in the bottoms. In addition, this present work focuses on separations where the light and heavy key components are adjacent in volatility, and therefore no components distribute between the keys.

An overall material balance may be written for the envelope around the rectifying section of Figure 3.11, which could also feature a pinch point situated at the feed as well as away from the feed:

$$V_{\infty} = L_{\infty} + D \tag{3.10}$$

Where V_∞, L_∞ are the vapor and liquid flowrates at the rectifying pinch and D is the distillate rate.

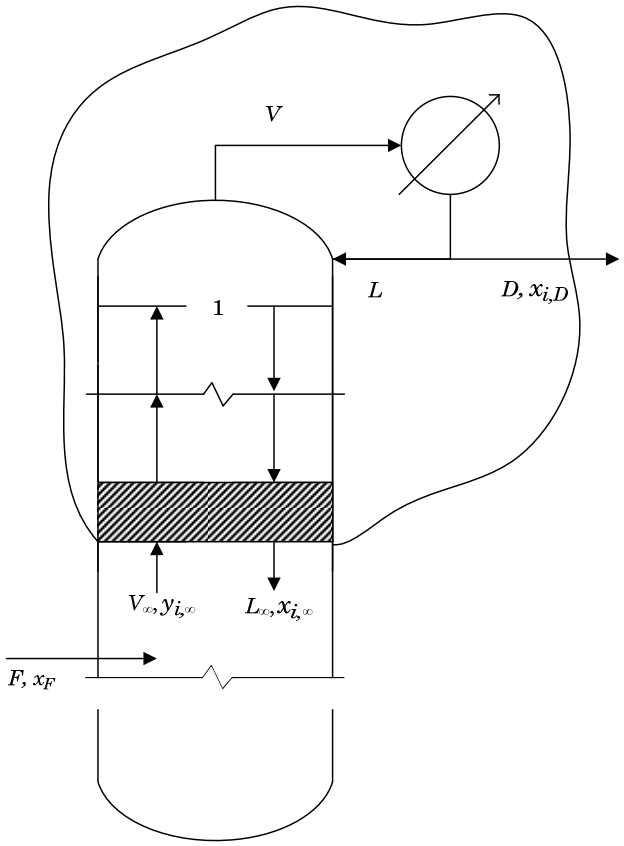

Figure 3.11: Schematics of rectifying section of a distillation column showing rectifying pinch.

For component i, the individual material balance is given by:

$$y_{i,\infty} V_\infty = x_{i,\infty} L_\infty + x_{i,D} D \tag{3.11}$$

Where $y_{i,\infty}$, $x_{i,\infty}$ are the vapour and liquid mole fraction of component i at the rectifying pinch and $x_{i,D}$ is the vapour mole fraction of component i in distillate.

Because the internal liquid and vapour concentrations do not change in the pinch zone, the liquid-vapour equilibrium relationship may be extended to relate $y_{i,\infty}$ to $x_{i,\infty}$:

$$y_{i,\infty} = K_{i,\infty} x_{i,\infty} \tag{3.12}$$

The equations above may be combined to obtain the vapour and liquid compositions at the pinch point of the rectifying section.

$$V_\infty y_{i,\infty} = \frac{x_{i,D} D}{1 - \dfrac{L_\infty}{V_\infty K_{i,\infty}}} \tag{3.13}$$

This equation is attributed to Brown and Martin (1939). A similar procedure may be applied to obtain the pinch compositions at the stripping section.

By applying the above equations to components *i* and *j*, it is possible to eliminate the vapour flowrate entering the pinch zone and the vapour molar fractions. Solving for the internal ratio, L_∞/D, Underwood (1932) showed that:

$$\frac{L_\infty}{D} = \frac{\dfrac{x_{i,D}}{x_{i,\infty}} - \alpha_{ij,\infty} \dfrac{x_{j,D}}{x_{j,\infty}}}{\alpha_{ij,\infty} - 1} \tag{3.14}$$

Where:

$$\alpha_{ij,\infty} = \frac{K_{i,\infty}}{K_{j,\infty}} \tag{3.15}$$

For Class 2 separations, there is not an obvious relationship between the pinch and the feed composition, $x_{i,F}$, unlike for Class 1 separations, where $x_{i,\infty}$ equals $x_{i,F}$.

For this common type of separations, Underwood (1948) devised a method that uses a set of parameters, θ_j, for the rectifying section, which are defined as the roots of the equation:

$$R_{\infty min} + 1 = \sum_{i=1}^{N} \frac{\alpha_{ij,\infty} x_{i,D}}{\alpha_{ij,\infty} - \theta} \tag{3.16}$$

Similarly, for the stripping section, Underwood (1948) defined θ as the root of the equation:

$$-R'_{min} + 1 = \sum_{i=1}^{N} \frac{\alpha'_{ij,\infty} x_{i,B}}{\alpha'_{ij,\infty} - \theta'} \tag{3.17}$$

Where N is the number of components, the prime refers to the stripping section pinch point, $x_{i,B}$ is the bottoms concentration and $R'_{min} = L'_{\infty}/B$, with B representing the bottoms rate.

The assumptions in the derivation of Underwood method are constant volatilities between the two pinch point zones and that there is a constant molar overflow between the feed stage and the rectifying pinch and the feed stage and the stripping pinch. As a result:

$$L'_{\infty,min} - L_{\infty,min} = qF \tag{3.18}$$

Where q represents the feed condition and equals 1 for a saturated liquid feed, and 0 for a saturated vapor feed, and is defined by:

$$q = \frac{heat\ to\ vaporise\ one\ mole\ of\ feed}{molar\ latent\ heat\ of\ vaporisation\ of\ feed} \tag{3.19}$$

It can be shown that equations (3.16) and (3.17) will have some roots in common. If only the two key components defining the separation are present in both products, there will be only one common θ root, if three components distribute, there will be two common roots, etc. These lie between the α-values for those components which distribute between top and bottom products.

Combining equations (3.16) to (3.18) with an overall material balance gives:

$$\sum_{i=1}^{N} \frac{\alpha_{ij} x_{i,F}}{\alpha_{ij} - \theta} = 1 - q \tag{3.20}$$

Where $x_{i,F}$ represents the mole fraction of component i in the feed.

When only the two key components distribute, Equation (3.20) is solved for a theta-root that is located between α_{ij} and 1. Substitution of this root in the initial Equation (3.16), may be used to calculate the minimum reflux.

3.7.2 (ii) Calculation of external reflux via enthalpy correction

The reflux ratio at the top of the column may be found by overall heat balance around the rectifying section shown in Figure 3.11. The calculation of the molar enthalpies of the liquid and vapour at the top pinch, $H_{V\infty}$ and $h_{L\infty}$, requires knowing the vapor and liquid composition at the top pinch.

Underwood (1948) showed that these compositions may be obtained from:

$$x_{i,\infty} = \frac{x_{i,D}}{\frac{L_\infty}{D}\left(\frac{\alpha_{ij}}{\theta} - 1\right)} \tag{3.21}$$

Where θ is the root of the Underwood equation (3.20) which satisfies the inequality: $\alpha_{HNK,HK} < \theta < 1$, where $\alpha_{HNK,HK}$ is the relative volatility of the component below the heavy key.

The mole fraction in the vapor phase may be obtained from Equation (3.11) or directly from:

$$y_{i,\infty} = \frac{x_{i,\infty}\frac{L_\infty}{D} + x_{i,D}}{\frac{L_\infty}{D} + 1} \tag{3.22}$$

An energy balance gives:

$$V_\infty H_{V\infty} = L_\infty h_{L\infty} + Dh_L + Q_{COND} \tag{3.23}$$

Where h_L represents the molar enthalpy of the liquid at the top of the column and Q_{COND} is the heat rejected in the condenser.

The enthalpy balance to the condenser is written as:

$$Q_{COND} = V\left(H_V - H_L\right) \tag{3.24}$$

Where V is the vapor flowrate at the top of the column and H_V represents the molar enthalpy of the vapor at the top of the column.

Also:

$$V = L + D \tag{3.25}$$

Incorporating the condenser enthalpy balance (3.24) into the section enthalpy balance (3.23) and combining with condenser and section mass balances (3.25) and (3.10) gives:

$$\frac{L}{D} = \frac{\frac{L_\infty}{D}\left(H_{V\infty} - H_{L\infty}\right) + H_{V\infty} - H_V}{H_V - H_L} \tag{3.26}$$

Equation (3.26) allows estimating the reflux at the top of the column from the reflux at the pinch zone given by the Underwood method.

This work is the first work of its kind that incorporates the enthalpy correction of the Underwood minimum reflux ratio into separation synthesis in a systematic optimisation framework. Suphanit (1999) discusses the benefit of applying this correction to the design of complex columns, primarily crude refinery columns and uses it within an optimisation methodology for cost minimisation, which was not implemented in a standalone systematic synthesis framework. In addition, the vast majority of existing synthesis approaches relies on more simplified column models. For instance, the disjunctive programming method of Yeomans and Grossmann (1999) for the design of distillation sequences, uses the classical Fenske-Underwood-Gilliland method. Novak *et al.* (1996) simplified distillation calculations even further, using the Underwood binary equation and ideal equilibrium calculations.

3.7.2 (iii) Evaluation of input variables

- Relative volatilities

The adequate α-values for application of the Underwood theta-function are found at an estimated feed stage temperature. In applying the Underwood method to separations involving variable α-values, Smith (2005) recommends to use the α-values based on the feed conditions rather than the average values based on the distillate and bottoms compositions. The reason for this is that the location of the pinches is often close to the feed.

- Feed stage temperature

For finding the feed stage temperature, two recommended methods are proposed by Shiras *et al.* (1950). The first method involves calculating the arithmetic mean of the top stage and reboiler temperatures weighted by the molar amounts of top and bottom product. The second alternative method is applicable to ordinary petroleum feed streams, and presumes

that the feed temperature is the temperature at which the *K-value*s of the two key components are equally distant from unity.

3.7.2 (iv) Calculation of minimum number of theoretical stages and actual theoretical stages

The Fenske method (Fenske (1932)) is used to generate the minimum number of stages from total reflux conditions and to initialise overhead compositions of any non-key components needed as inputs to the Underwood method for calculation of the minimum reflux ratio. Having obtained the minimum number of stages and the minimum reflux ratio, the Gilliland correlation (Gilliland (1940)) may be used to determine the theoretical number of stages. A description of these methods can be found elsewhere (Smith (2005)).

3.7.3 Model validation

3.7.3 (i) General strategy of validation of the minimum reflux calculation

The effect of the enthalpy correction on the prediction of the minimum reflux ratio is presented for a number of examples. For each example, an estimate of the real minimum reflux is derived from Aspen Plus® 2006, which serves as a benchmark for comparing the Underwood pure method and the improvement introduced by the enthalpy correction.

The minimum reflux ratio from an Aspen Plus® RadFrac® column is obtained by increasing the number of stages while maintaining the product specifications on the key components until no appreciable reduction of the reflux ratio is observed. Product specifications are controlled by manipulation of key operating variables in the column, for example, the reflux ratio and the bottoms rate or the boilup ratio and the distillate rate. Reboiler or condenser duties in combination with an external flowrate are suitable variables for controlling product specifications. The feed tray position can be automatically mapped to a location corresponding to the middle height of the column.

The Underwood method and the enthalpy correction may be tested against the minimum reflux ratio derived from Aspen Plus® at different levels of accuracy for the input variables.

For instance, it is expected that the following recipe will bring the Underwood model prediction as close as possible to the Aspen Plus® prediction:

- Relative volatilities are extracted from simulated profile at the feed tray
- q is retrieved from simulated flowrates at feed tray
- Pinch compositions are retrieved from simulated profile
- Relevant θ-root of Underwood equation (3.20) is calculated from simulated profile and used by enthalpy correction

At the opposite pole of accuracy, the simple yet widely applied Underwood model in its standard form is based on the following assumptions:

- Relative volatilities corresponds to feed conditions
- q corresponds to feed conditions
- No allowance for reflux variation along the column is made by omitting the enthalpy correction

Table 3.13 summarises the different paths that the estimation of the different input parameters may follow.

Underwood model inputs	1a	1b
$\alpha_{i,j}$	From simulated column profile at pinch zone	At feed conditions
	2a	**2b**
q	From simulated column profile at pinch zone	At feed conditions
	3a	**3b**
Concentrations at pinch and at column top	From simulated column profile	From Underwood method
	4a	**4b**
θ	From simulated column profile at feed stage, $L\infty/(V\infty K\infty)$	From Underwood method

Table 3.13: Different pathways in the application of Underwood method.

The following examples will illustrate the application of the Underwood method using the alternative pathways shown in Table 3.13. Since the column design model implemented in the proposed synthesis framework will exclusively rely on paths (b), the emphasis of the validation will be placed on the enthalpy-corrected Underwood method using paths (b).

3.7.3 (ii) Distillation column model validation

- Case 1

In the first example, the distillation column feed is a simplified version of a typical rich absorption oil stream, loaded with recovered NGL from natural gas. The distillation column acts as the desorber of the absorption-desorption cycle. Composition for the feed to the distillation column is provided in Table 3.14. Flowrate and pressure are given in Table 3.15, which also contains the temperatures for feed qualities of zero (saturated vapour) and one (saturated liquid).

	Feed concentration mol fraction
Methane	0.0524
Ethane	0.1303
Propane	0.0517
n-Octane	0.7655
Total	1

Table 3.14: Molar concentration of feed to distillation column for desorption.

Flow, kmol/h	3347
Pressure, bar	10
Dew temperature, °C	214.3
Bubble temperature, °C	-19.8

Table 3.15: Distillation feed flowrate, pressure and two-phase temperature range.

Given the feed composition, flowrate and pressure, the feed quality is the last remaining degree of freedom in the problem definition. The phase envelope for the feed given in Table 3.15 and the products is provided for reference in Appendix section 12.2. The enthalpy correction will be tested for q = 0 and q = 1, which denote the operating boundaries of common desorbers. Desorber feeds are predominantly in the two-phase region. In fact, in common solvent regeneration applications, the solvent leaves the bottom of the reboiled absorber at saturate conditions and normally is let down to the lower pressure in the desorber through a valve. This pressure drop usually provokes partial vaporisation of the saturated rich solvent. Additionally, in common industrial absorption-desorption schemes, the rich solvent receives heat from exchange with the hotter regenerated solvent from the desorber bottoms, which will further vaporise the rich solvent feed to the distillation column. The motivation behind feed preheating is that it balances the reboiler duty.

Table 12.1 illustrates the evolution of the column operating variables as the number of stages is increased. Data correspond to vapour feed (q = 0). The number of significant figures has been adjusted to detect small variations in the column operating variables as the number of stages grows. It can be seen that at 25 stages, the reflux ratio is already within 1% tolerance of the minimum reflux ratio of 1.708.

Figure 3.12 shows the evolution of the reflux ratio as the number of stages is extended. The irregularities in the shape of the curve may be attributed to the adjustment of the feed stage in each run. Because the feed stage can only take integer values, it is updated with half the frequency than the total number of stages in the column.

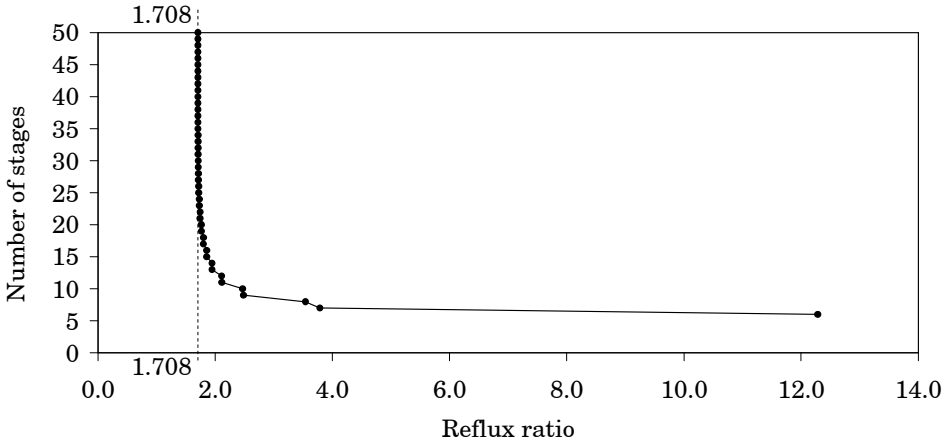

Figure 3.12: Graphical calculation of the minimum reflux ratio from simulation data.

From the simulated profile of a RadFrac® column with large number of stages, thus operating close to minimum reflux, it is possible to populate Table 3.16 with information which is related to the Underwood minimum reflux calculation. This information may then be used to apply the Underwood method and the enthalpy correction in their multiple variations corresponding to the different pathways.

Case 1 Saturated vapour feed		
	1a	**1b**
$\alpha_{1,4}$	24.8	24.9
$\alpha_{2,4}$	13.4	13.4
$\alpha_{3,4}$	8.2	8.2
$\alpha_{4,4}$	1	1
	2a	**2b**
q	0.013	0
	4a	**4b**
θ	0.99908	0.99912
L_{α}/D	**3.630**	
L/D	**1.708**	

	Feed concentration mol%
Methane	5.24
Ethane	13.03
Propane	5.17
n-Octane	76.55
Pressure, bar	10

Table 3.16: Aspen Plus® data for use in different pathways and minimum reflux ratio at the top of the column and at the pinch from Aspen Plus®.

The application of these methods to the calculation of the external reflux ratio is presented in the diagram of Figure 3.13. Each path in the diagram shows a name. Path names and their meaning are provided in Table 3.13. The minimum reflux ratios from Aspen Plus® at the top of the column and at the column pinch are provided in Table 3.16.

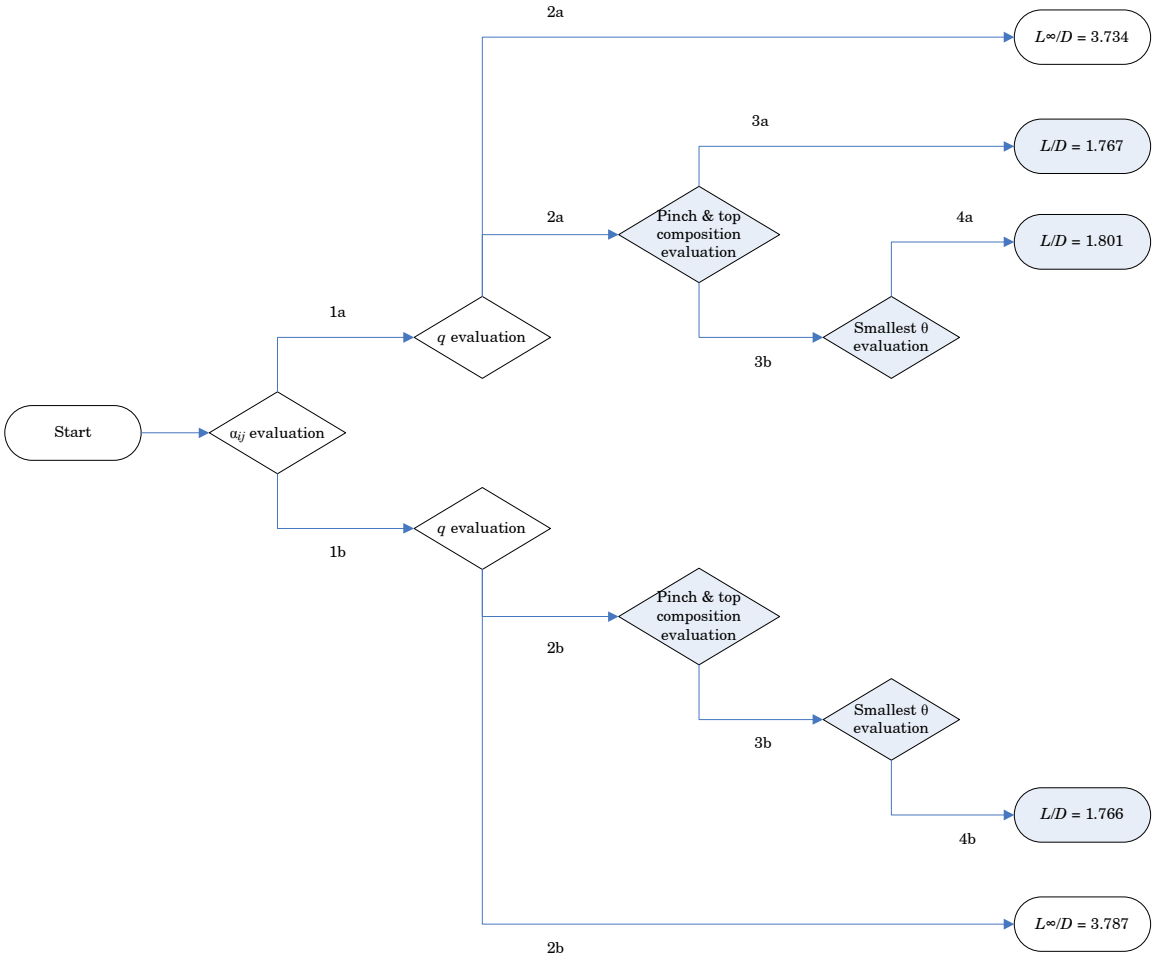

Figure 3.13: Illustration of the application of the various pathways of the Underwood method.

In Figure 3.13, the shaded blocks are part of the enthalpy correction. The pathways of type (a) represent a more accurate approach to the application of the Underwood method than pathways of type (b). Excessive branching was prevented by disallowing most combinations of type (a) and type (b) paths.

In this example, the result of the calculation does not depend significantly on the convention used for retrieval of the relative volatilities. The same conclusion is applicable to the feed stage quality. In fact, the minimum reflux ratio at the pinch location calculated from rigorous inputs is 3.734 (paths 1a & 2a) in comparison to the value obtained from less rigorous inputs of 3.787 (paths 1b & 2b). Both values are in similar degree of

agreement with the corresponding value obtained from the column profile of 3.630.

Similar results for the feed stage relative volatilities and feed quality apply to the pinch compositions and the theta-solution, which are required for the calculation of the reflux ratio at the top of the column. As a result, the various estimates of this latter parameter are within a 2% deviation of the highest estimate, i.e.: 1.767 (paths 1a - 3a) vs. 1.801 (paths 1a & 2a & 3b & 4a) vs. 1.766 (paths 1b - 4b). These values are in good agreement with the corresponding column profile value of 1.708.

This example highlights the importance of incorporating the enthalpy correction in the distillation column model in order to obtain a reasonable approximation of the external reflux ratio.

- Case 2

The difference between Cases 1 and 2 resides in the feed condition. The column feed in Case 2 is a liquid. Feed composition and column conditions remain the same.

The minimum reflux ratios at the column pinch and at the column top from Aspen Plus® simulation are provided in Table 3.17, alongside other data extracted from the simulation for use for illustration of the application of the Underwood method. In this case, a feasibility constraint was encountered during the calculation of the minimum reflux by successively increasing the number of stages of the column, due to insufficient internal column flowrates. Hence, the minimum reflux values in Table 3.17, must be used with caution. By superficial inspection of the data across the columns of Table 3.17, it is anticipated that the various pathways will lead to substantially different estimates of the minimum reflux ratio.

Case 2 Saturated liquid feed		
	1a	**1b**
$\alpha_{1,4}$	653.4	84941
$\alpha_{2,4}$	183.6	9053
$\alpha_{3,4}$	68.6	1635
$\alpha_{4,4}$	1	1
	2a	**2b**
q	1.279	1
	4a	**4b**
θ	0.901	0.75144
L_α/D	**0.036**	
L/D	**0.038**	

	Feed concentration mol%
Methane	5.24
Ethane	13.03
Propane	5.17
n-Octane	76.55
Pressure, bar	10

Table 3.17: Aspen Plus® data for use in different pathways and minimum reflux ratio at the top of the column and at the pinch from Aspen Plus®.

This observation is confirmed by the data in Figure 3.14. While the combination of paths 1a & 2a lead to a prediction of the pinch reflux ratio with is a fraction of the value obtained from the RadFrac® column profile, the combination of paths 1b & 2b, which represents the classical application of the Underwood model, yields a negative result, in the proximities of zero.

Application of the enthalpy correction, represented by the shaded blocks of Figure 3.14, does not result in negative results in any of its variations; however, the predictions are consistently lower than the profile value.

Some insights may, however, be derived from these results regarding the separation feasibility. When considering the magnitude of the relative volatility of the light component with respect to the heavy component (68.6, based on feed conditions), the application of distillation for

separation of the mixture appears questionable. In effect, this separation can be carried out by a standalone stripping section, where the feed enters at the top of the column and is stripped out of the light components by the ascending vapours generated by a reboiler. The redundancy of a rectifying section, and thus of reflux, is consistent with the order of magnitude of the estimates of the minimum reflux, as given in Figure 3.14.

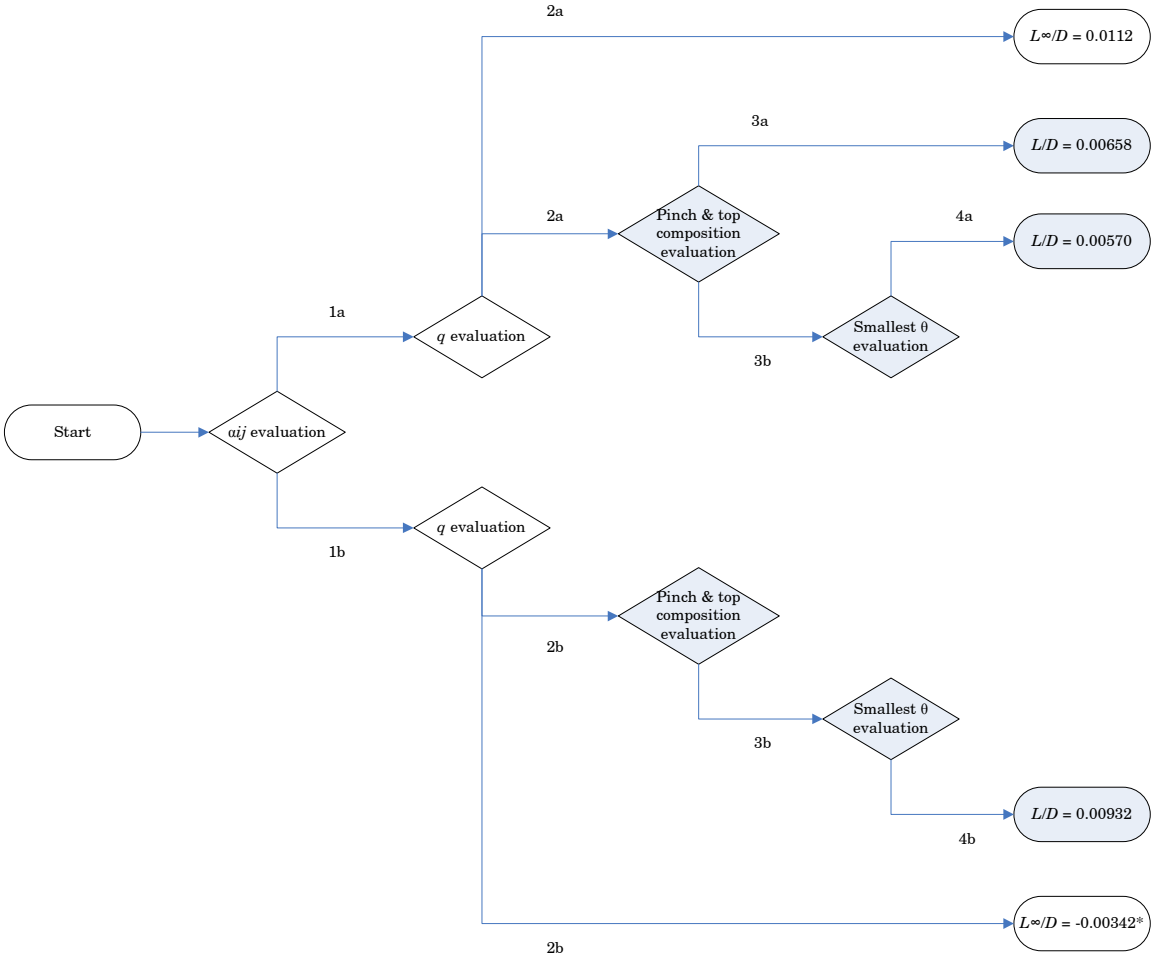

Figure 3.14: Illustration of the application of the various pathways of the Underwood method.

- Case 3

The difference between Cases 2 and 3 resides in the identity of the heavy key component. n-Octane has been replaced with n-hexane, however, the feed conditions remain the same. The aim of Case 3 is to test the

Underwood method application and the enthalpy correction for a liquid feed.

Because the volatility difference between the column key components is not as high as in Case 2, a distillation column may be used to perform the separation. Still, the calculated minimum reflux ratios, included in Table 3.18 are substantially low.

Case 3 Saturated liquid feed		
	1a	**1b**
$\alpha_{1,4}$	591.5	3672
$\alpha_{2,4}$	99.3	353.5
$\alpha_{3,4}$	31.5	82.5
$\alpha_{4,4}$	1	1
	2a	**2b**
q	1.342	1
	4a	**4b**
θ	0.82281	0.77107
$\boldsymbol{L_{\infty}/D}$	**0.026**	
$\boldsymbol{L/D}$	**0.039**	

	Feed concentration mol%
Methane	5.24
Ethane	13.03
Propane	5.17
n-Hexane	76.55
Pressure, bar	10

Table 3.18: Aspen Plus® data for use in different pathways and minimum reflux ratio at the top of the column and at the pinch from Aspen Plus®.

The application of the Underwood method to Case 3 is illustrated in Figure 3.15. With respect to the pinch minimum reflux calculations, the more rigorous form of calculation, characterised by paths 1a & 2a, leads to a remarkably similar value than it is obtained from RadFrac® column profiles. Differently, the standard application of the Underwood method, given by paths 1b and 2b, underestimate the value of the pinch minimum reflux by nearly 50%.

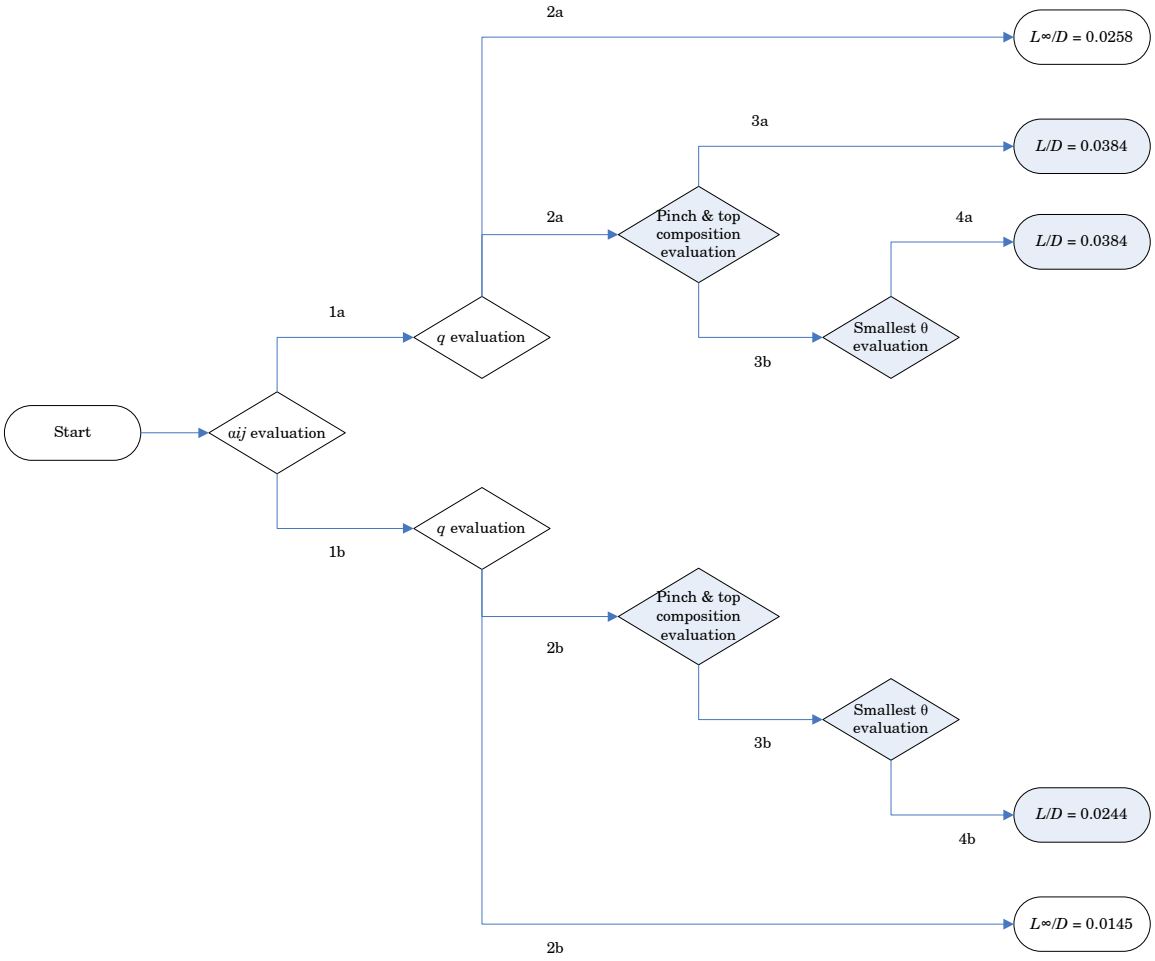

Figure 3.15: Illustration of the application of the various pathways of the Underwood method.

In Case 3, the enthalpy correction, in its more rigorous forms, leads to a consistent prediction of the reported top reflux ratio. The less rigorous form of the enthalpy correction given by paths 1b – 4b do not yield as good agreement with RadFrac® profile data as the other forms. Still, the enthalpy correction offers a better estimate of the top reflux ratio than the standard application of the Underwood method.

3.8 Conclusions (ii) – Distillation

The second part of this chapter has dealt with the modelling of the distillation columns in the developed synthesis framework for

representation of: (1) simple distillation block; (2) desorber of the absorption-desorption block.

The basis of the adopted model is the well-established Fenske-Underwood-Gilliland method. This method is widely accepted as a tool for preliminary distillation column design; however the applicability of these equations relies on the validity of a number of assumptions.

A distinctive feature of this work with respect to existing separation synthesis approaches lies in the incorporation of the existing enthalpy correction of the Underwood minimum reflux ratio into a systematic synthesis and optimisation framework. The resulting improvement of the model accuracy is achieved at insignificant computational expense.

The emphasis of this work on the development of highly representative yet simple models persists in this section. Since the minimum reflux is an effective indicator of the column use of energy, the attention has been placed on the methods for prediction of the minimum reflux. The shortcomings of widely used Underwood method of calculation of the minimum reflux have been identified. The enthalpy correction to the Underwood minimum reflux calculation has been evaluated in a number of examples. The prediction of the top minimum reflux is shown to consistently improve the Underwood prediction across the examples. The sensitivity of the Underwood model to the accuracy of the input parameters has also been investigated. Validation using commercial simulation software suggests that the presented shortcut model is suitable for the purpose of preliminary screening of design options.

3.9 Implementation of absorption-desorption column modelling

The absorption-desorption separation block consists of a reboiled absorber column and a distillation column. This section concentrates on the

practical implementation aspects of the proposed absorption-desorption models in the optimisation framework within COLOM® (©CPI, University of Manchester 1985-2009).

3.9.1 Absorber column design

The objective of the design algorithm is to determine the number of theoretical stages of the absorber, the feed location and to establish key operating variables. Key operating variables include the absorber pressure, the absorber feed and inlet solvent temperatures, the inlet solvent flowrate and the reboiler duty or boilup ratio. Common design inputs are the given absorber feed, inlet solvent composition, and specified component recoveries.

The absorber pressure is a degree of freedom which is treated as an optimisation variable within the proposed optimisation framework. The inlet solvent temperature and the absorber feed temperature or quality (q = 0 for a vapour, 1 for a liquid) are additional optimisation variables.

In the proposed optimisation framework, the reboiled absorber boilup rate acts as an optimisation variable, whilst the absorber inlet solvent flowrate and the number of stages of the absorber sections are calculated from model equations.

The design of the reboiled absorber begins with the design of the top section. The top section of the absorber is designed around the recovery specification of the heavy key. While in this section the absorption of light key component from the vapor feed to the section must be kept to a minimum, corrective action can be taken to compensate for excessive co-absorption. This action is supplied by adequate stripping of the component in the bottom column section. Similarly, the bottom section is designed around the recovery specification of the light key component.

The steps in the design of the top absorber section are illustrated in Figure 12.1 and Figure 12.2.

3.9.1 (i) Initialisation of top absorber section inlets and outlets

A difficulty lies in the estimation of the vapour flowrate feed to the top section, which is a combination of the vapour feed and the vapour from the top of the stripping section. This estimate is needed for the calculation of the minimum solvent inlet flowrate and number of stages of the top section by the method introduced in section 3.5.2 (v).

An initial estimate of the flowrate and composition of the vapour feed to the top section for use in the design of the section can be derived by assuming that the separation objectives for both keys are achieved by this section standalone. In this situation, the absorption of light key component in the upper section is within limits, thus the bottom stripping section is not required. Under this assumption, the vapour feed to the top section coincides with the gas feed to the column.

3.9.1 (ii) Characterisation of terminal stages and estimation of internal profiles

The absorber model presented in section 3.5.2 (v) uses as inputs the conditions prevailing in the absorber. The design of the top section of the reboiled absorber begins with the calculation of temperatures and compositions at the top and the bottom stages. The recovery specifications can be used for estimating the conditions at the top and the bottom stages of the absorber according to the procedure described in section 12.1.3 of the Appendix.

With the complete characterisation of the top and bottom stages, including inlets and outlets, the conditions of the adjacent stages can be derived, i.e. stages 2 and $n - 1$, where stage 1 and stage n represent the top and bottom stages, respectively.

Subsequently, the characterisation of the internal streams can be inferred from the conditions of the terminal streams. The interpolation procedures described in section 3.5.3 may be applied to obtain the internal liquid and vapour flowrates, stage temperatures and key component equilibrium constants from the top and bottom stages. These values allow calculation of the key components stage absorption and desorption factors.

3.9.1 (iii) Solve Edmister model for top section number of stages and solvent feed

Solving the Edmister model equations for the solvent inlet flowrate and the top section number of theoretical stages requires trial and error, since these equations are not explicit on these variables.

The design algorithm for the top section is represented in Figure 12.1. In this algorithm, the solvent flowrate is initialised to a low value. For isothermal absorbers and dilute feeds, Douglas (1988) suggests a solvent rate of $1.4 \cdot K \cdot Feed$ where K is the K-value of the heavy key component and $Feed$ is the gas feed molar flowrate. While this rule may be adequate for scrubbing of components in low concentrations in the gas feed, it may not be suitable for bulk gas separations.

The number of theoretical stages is initially set to four stages but is increased gradually if the desired heavy key recovery is not achieved. If the separation objectives for the heavy key are not achieved in a certain number of theoretical stages (40 is used as reference), then, the solvent flowrate is allowed to increase in steps, generally up to 10% of the gas feed. The process is repeated until the heavy key specifications are met or a maximum number of iterations is reached, in which case, the design of the reboiled absorber for the given operating variables is regarded as infeasible and abandoned.

3.9.1 (iv) Top product specifications check

The molar flow of heavy key in top product is calculated using Edmister's Equation (3.53).

With the specifications for the heavy key component met, the selected design variables, i.e. number of stages and solvent flowrate, are assessed against the specifications of the light key component. The molar flow of the light key in the top product is estimated by applying Equation (3.53) to the light key component.

If the specifications for the two key components in the overhead vapour draw are met, then, the design of the top section of the absorber is complete.

3.9.1 (v) Recalculating feeds to top section and iterating

A calculated light key component recovery that does not satisfy the corresponding recovery specification may be attributed to the selected design variables or to the assumed vapour feed to the top section is insufficient. A deficient light key component rejection is an indicative of a substantial retention of this component by the solvent.

With respect to the selected design variables, there is no control over these to enhance the rejection of light key. Effectively, an increment of the number of stages of the top section will not improve the light key calculated recovery. Contrarily, a greater number of stages would generally deteriorate the rejection of the light key due to improved absorption. Similarly, a higher solvent flowrate is likely to enhance the retention of the light key component. However, modifying the number of stages and the solvent flowrate in the opposite direction is not possible without violating the product specifications of the heavy component.

It follows that significant light key losses to the solvent in the absorber top section can only be handled by allowing for a recalculated vapour feed to the section, which requires a stripping section to provide sufficient desorption of light key from the solvent.

Because the magnitude of this vapour flowrate is related to the liquid leaving from the top section by material balance to the individual column section, the recalculation of vapour flowrates will lead to a larger flowrate of light component in circulation between absorber sections.

At the same time, because the stripper section will desorb some of the heavy key component which was absorbed in the absorber section, it may be necessary to update the vapour to the top section with an estimate of the flowrate of heavy key to the bottom of the top section, as shown in Figure 12.2.

One method to estimate the molar flowrates of the heavier component in-between sections is to use the Fenske equation (Fenske (1932)) to provide the relationship between vapour fractions of key components at the top of the bottom section as a function of the relative volatility, the number of stages of the bottom section and the ratio of concentrations at the reboiler:

$$v_{tx}(HK) = v_{tx}(LK)\frac{x_{Btms}(HK)}{x_{Btms}(LK)}\frac{1}{\alpha_{LK,HK}{}^{N_S}} \tag{3.27}$$

Where N_S denotes the number of stages of the stripping section of the reboiled absorber.

This equation is based on total reflux conditions, where no products are extracted and the interstage liquid and vapour flowrates at a given location are identical. However, the real operation of a reboiled absorber bottom section may be very different from the total reflux ratio due to the main bulk of the solvent stream being extracted from the bottom, which

causes a notable discrepancy between the liquid and the vapour flowrates at any given interstage location. However, this approximation will be replaced with a more accurate estimate following the first pass execution of the design algorithm for the column bottom section.

With the updated flowrates of key components entering the top section, the calculation of the solvent inlet flowrate and number of stages of the absorber top section may be executed again until the top product specifications for the two key components are met (Figure 12.2).

3.9.1 (vi) Bottom stripper section design

The stripping section is needed to strip out the required amount of light key component from the entering solvent. The design method for the stripper section is very similar to the method of the top section with the version of the Edmister equations that accounts for a reboiler (Equation (3.54)). However, the number of stages of this section is now controlled by the specifications of the light key.

If the bottom product heavy key specifications cannot be met with the number of stages necessary by the light key specifications, then the heavy key concentration in the vapour to the top section must be incremented. This new estimate may be more accurate than previous estimates since it is not derived from the Fenske equation. With the new estimate, it is necessary to repeat the design of the top section and bottom section.

Further iterations may be required until the specifications for the key components are met in the top and bottom product.

3.9.2 Regenerator design

The design of the regenerator requires identification of the key components of the desorber column. The light key component is the

heaviest component in the gas feed to the absorption-desorption block, while the heavy key component is the lightest solvent constituent.

The design of the solvent regeneration column begins with the calculation of the minimum reflux ratio according to the modified Underwood model presented in section 3.7.2 (iv).

A predicted value of the minimum reflux rate that is in the vicinity of zero is indicative of the viability of the separation if it was to be carried out in a standalone stripping section. Most often, however, a rectifying section in addition to the stripping section is required to meet the overhead product specifications, thus a complete distillation column is needed to perform the regeneration of the solvent.

The calculated minimum reflux ratio must then be scaled up to allow for a finite number of stages in the column. As a rule of thumb, the optimal reflux ratio is in the vicinity of 1.1 (Douglas (1988)), however, in the optimisation framework, the reflux ratio scale-up factor acts as a degree of freedom, which varies within a specified range.

Condenser and reboiler duties can be calculated from enthalpy balances to the top and the bottom of the column. Liquid and vapour traffic in the column are then checked for consistency.

During the design of the distillation tower, the number of theoretical stages is calculated from the Gilliland equation (Gilliland (1940)). The location of the feed stage to the column is derived from the Kirkbride equation. Theoretical stages are converted to actual stages using the desired Murphree stage efficiency.

Chapter 4. Heat Exchanger Network Design

4.1 Introduction

Opportunities for heat integration between the heat sources and sinks of the separation system may reduce the use of cold and hot utilities. By allowing individual hot process streams to exchange heat with cold process streams, the operating costs can be reduced. Thus, efficient system design must contemplate heat integration opportunities.

Existing approaches targeting at maximum energy recovery exclusively are unable to generate the configuration of the HEN (Heat Exchanger Network). In this work, the proposed HEN design approach overcomes the limitations of existing systematic approaches that ignore capital tradeoffs and generates a feasible HEN's physical configuration.

In the proposed methodology, the design of the overall separation system including the heat recovery system is optimised using a stochastic optimisation algorithm. This methodology is capable of a systematic evaluation of the structural and operating variables in the system and their impact on the cost objective. As a result, this methodology may potentially achieve more cost-effective separation systems than other design approaches that do not allow interaction between the design of the separation and the heat recovery systems.

4.2 Background

Heat integration network design is an important aspect of process design as it is responsible for major economic process improvements. It is a

classical synthesis problem involving a combination of discrete and continuous decisions.

4.2.1 Synthesis of heat integrated separation systems

In the traditional hierarchical approach (Linnhoff and Boland (1982), Douglas (1988), Smith and Linnhoff (1988)), the heat recovery system design is performed in sequence, following the separation system design. In a more effective design approach, the design of the separation system and the heat recovery system is performed simultaneously. Simultaneous design approaches have the potential to exploit more comprehensively the interactions between the separation system and the heat recovery system.

The synthesis of heat integrated separation sequences is a popular topic in the open literature. Existing methods for synthesis of heat integrated separation sequences may be categorised into heuristic methods, MILP (Mixed Integer Linear Programming) methods, MINLP (Mixed Integer Non-Linear Programming) methods and stochastic methods.

Heuristic rules and evolutionary methods have been developed by a number of researchers to reduce the large search space of heat integrated separation processes (Umeda *et al.* (1979), Qian and Lien (1995)). In these approaches, the lack of a systematic framework often leads to conflicting and inferior solutions.

Superstructure based approaches are also common in synthesis of heat integrated separation sequences. Papoulias and Grossmann (1983) showed how HEN transshipment models may be incorporated easily within a MILP approach for synthesising chemical processing systems. Andrecovich and Westerberg (1985) also applied MILP to the synthesis of heat integrated distillation sequences. MILP methods represent an improvement over heuristic methods, but linear programming

implementation relies on a number of simplifications affecting the separation models.

Mixed integer non-linear programming (MINLP) has been widely applied to synthesis of heat-integrated separation sequences (Novak *et al.* (1996), Kravanja and Grossmann (1997), Yeomans and Grossmann (1999)). MINLP can deal with relatively complicated integration problems at the risk of converging to local optimal, due to the non-linear nature of the problem. In these works, shortcut models are used to describe the performance of simple distillation columns.

The robustness of the stochastic methods is advantageous for optimisation of problems involving continuous and discrete variables. The application of stochastic methods to synthesis of heat exchanger networks have been investigated by Lewin (1998), Lewin *et al.* (1998), Lin and Miller (2004).

4.2.2 Algorithmic approach to targeting for HEN design

The solution to the standalone HEN design problem for minimum total annualised cost entails the identification of pairs of hot and cold streams to be matched in heat exchangers, the topology of the network and the size of the heat exchangers. Traditional algorithmic hierarchical approaches consist of two separate steps: (1) the determination of the minimum utility demand and the minimum number of heat exchangers (Papoulias and Grossmann (1983)) ; (2) the determination of the HEN configuration, including the streams matches and the best sequence of the equipment. This hierarchical methodology is based on the assumption that the optimal network features minimum utility cost for a given minimum temperature approach. This rule implies that if the minimum utility cost for a heat exchange problem can be found, then it is justifiable to attribute this cost to the optimal HEN. The rationale for substituting the total annualised HEN costs optimisation problem with the optimisation of the HEN utility costs followed by the optimisation of the number of heat

exchangers is the assumption that the optimal network is the network with the minimum number of heat exchange units among the set of networks with minimum utility cost. A limitation of this approach is that there is not always a direct relationship between the number of heat exchangers and the capital cost of the HEN, since the capital cost also depends on the area of the heat exchangers. Partial solutions to the design of HENs include:

4.2.2 (i) Utility cost targeting

The available methods for utility cost targeting do not systematically generate a HEN configuration.

Design methods based on thermodynamic targets and the pinch concept may be categorised as manual methods, which may be regarded disadvantageous when dealing with large-scale problems.

In the transshipment model of Papoulias and Grossmann (1983), the synthesis problem is represented as a set of temperature intervals based on the inlet temperatures of the hot and cold streams, respecting the minimum temperature approach at the boundaries of each interval. Each temperature interval can be accompanied by the "heat content" of each stream in that interval. When intermediate utilities are present, their inlet temperatures are used to construct the temperature interval diagram.

The minimum utility cost problem is then treated as a transport problem where heat is transferred from sources (hot streams) to intervals and onto sinks (cold streams). Additional variables called residuals are employed to allow for heat transfer between intervals. Heat balances around each interval can be completed using the residuals and the sum of external heating and cooling demands with optional cost factors formulated as the objective function. The resulting minimum utility consumption/cost

problem falls in the category of Linear Programming LP optimisation problems, which can be easily solved manually or automatically.

4.2.2 (ii) Heat exchange units targeting

The algorithmic methods for determination of the minimum number of heat exchangers, can provide a solution that indicates which matches take place and what is the heat duty involved. However, to derive the physical HEN from this information is not usually a trivial task. In addition, these methods cannot discriminate between various solutions with the same number of units but with different capital costs. Therefore, finding a HEN with the minimum number of units is not a guarantee for finding the minimum cost.

In the algorithmic approach of Papoulias and Grossmann (1983), the existence or non-existence of a match between a pair of streams is represented by binary variables. These variables may be employed to formulate a MILP (mixed-integer linear problem) where the objective is to minimise the number of heat exchangers.

The framework for intervals and residuals is inherited from the minimum utility target formulations with an additional lower bound on the number of heat exchangers. This constraint is formulated as a set of inequalities, each of them corresponding to a pair of streams. The binary variables intervene in these inequalities to enable a finite heat transfer for the matches taking place. This set of inequalities places a restriction on the minimum number of heat exchangers. This formulation requires computing the maximum heat that can be exchanged between each pair of streams.

4.3 Key features of the developed heat integration methodology

4.3.1 Interval decomposition and match prioritisation

Heat recovery is severely constrained by not contemplating temperature interval decomposition, as in COLOM® Version 2.2.003 and previous versions (©CPI, University of Manchester 1985-2009). In these elementary heat integration methodologies, feasibility of a match between streams is simply assessed by comparing stream target temperatures, i.e. the match between a hot and cold stream is automatically discarded if the target temperature of the hot stream is lower than the cold stream target temperature.

The above condition is equivalent to the condition of non-existence of a temperature cross in the corresponding heat exchanger, which agrees with the observation that actual counter-current shell and tube heat exchangers cannot achieve a temperature cross in a single shell. By imposing this condition, the above elementary heat integration approaches ignore heat integration matches that do not obey it, but which could be effectively matched in subintervals of the total temperature range.

In this work, the heat integration temperature domain is organised in intervals and heat integration opportunities are considered within each interval and between intervals separated by a greater temperature difference than the desired temperature approach. This allows heat recovery between all streams provided that there is a sufficient driving force for heat transfer. By considering more matches than in previous approaches, the utility requirements can be reduced further.

Following the identification of feasible matches, the selection of the final matches among any alternative matches is required. An algorithm for match allocation has been developed in this work for this purpose, which is described in section 4.4.6. The set of feasible matches is analysed in a

succession that maximises heat recovery within each temperature level and hence, avoids matches between streams of extreme temperature levels. Matches between above- and below-ambient temperature levels are only allowed if the cooling and heating demands in these intervals can otherwise be satisfied by supplementary use of utilities only.

4.3.2 Heat integration between above and below-ambient regions

A key feature of the proposed heat integration methodology resides in allowing heat integration between streams that require heat exchange at opposite sides of the ambient utility temperature. This methodology however, does not ignore the incentives of partitioning the heat exchange problem into above- and below-ambient subproblems; in fact, a mechanism is developed to favour matches that occur strictly in the above-ambient region or in the below-ambient region over cross-ambient matches.

In most heat integrated processes involving above-ambient and sub-ambient operations, there is little integration between the two temperature regions due to the balancing of any sub-ambient heating demands within the sub-ambient region. Most below-ambient processes are characterised by a net cooling demand, which is satisfied by refrigeration. Due to the elevated cost of refrigeration, valuable below-ambient streams demanding heating are primarily reserved for cooling other streams in the below-ambient region, which otherwise would require refrigeration.

By splitting the heat integration problem into above- and below-ambient subproblems, degradation of valuable energy of extreme temperature levels may be reduced by preventing matches between sub-ambient streams with above-ambient streams. However, splitting the heat integration problem may also lead to a reduction in heat recovery and excessive use of utilities if it is not applied carefully.

The following is an example of how the division of the temperature domain may adversely affect process economics by neglecting important heat recovery opportunities. As a result of the division of the temperature domain, any unsatisfied heating demand in the below-ambient domain will be met by additional use of utilities. Equally, any heat surplus in the above-ambient region will be rejected to ambient utility. By preventing cross-ambient matches, this approach incurs inflated costs due to excessive use of utilities. Variations of this partition heat integration methodology are encountered in COLOM® Version 2.2.003 and previous versions (©CPI, University of Manchester 1985-2009).

In this work, the proposed heat integration methodology does not automatically segregate the temperature domain into below- and above-ambient regions.

4.3.3 Partition temperature for solvent cooling in absorber-desorber block

Overall, the proposed heat integration methodology is facilitated by partitioning the solvent cooling total load in smaller intervals: one or more intervals corresponding to above-ambient cooling and a further interval corresponding to below-ambient cooling, hence the three separate solvent coolers in Figure 3.3.

This partition reflects general practice implementation of solvent cooling configurations. The above-ambient cooling temperature interval is generally very ample, ranging from the desorber bottoms temperature to the lowest possible temperature for heat rejection to cooling water. Consequently, it is unusual to shift the total above-ambient cooling load in a single heat exchanger.

Above-ambient cooling is commonly carried out by an available colder process stream, such as the desorber feed or the feed to the reboiler of the reboiled absorber. Subsequent below-ambient cooling is carried out by a

refrigerant in a separate heat exchanger. Additional temperature sub-intervals for above-ambient cooling can be handled by additional partition temperatures.

The implications of employing solvent cooling partition temperatures as additional degrees of freedom in the optimisation framework are various. Firstly, by specifying partly the configuration of the solvent cooling system, the resulting system resembles real systems.

Secondly, despite the reduced variability of the heat exchanger network problem, solvent cooling partitioning does not necessarily make the application of the subsequent heat integration methodology more efficient, due to the abundance of heat sources.

Finally, artificial partitioning may not lead to the optimal capital utilisation, since unnecessary duplication of heat matches between the same streams and adjacent intervals may occur at both sides of the partition temperatures.

4.4 Workflow of proposed HEN design methodology

4.4.1 Stream data collection

The separation scheme proposed by the separation system design methodology exhibits heat sources and heat sinks in a number of locations, as indicated by Figure 4.1 for an example consisting of two distillation columns. The required inputs to the HEN design methodology are the process streams that are linked to condensers, reboilers, intermediate heat exchangers and feed and product heaters and coolers. Intermediate or auxiliary heat exchangers are specific to the absorber-desorber scheme proposed in this work.

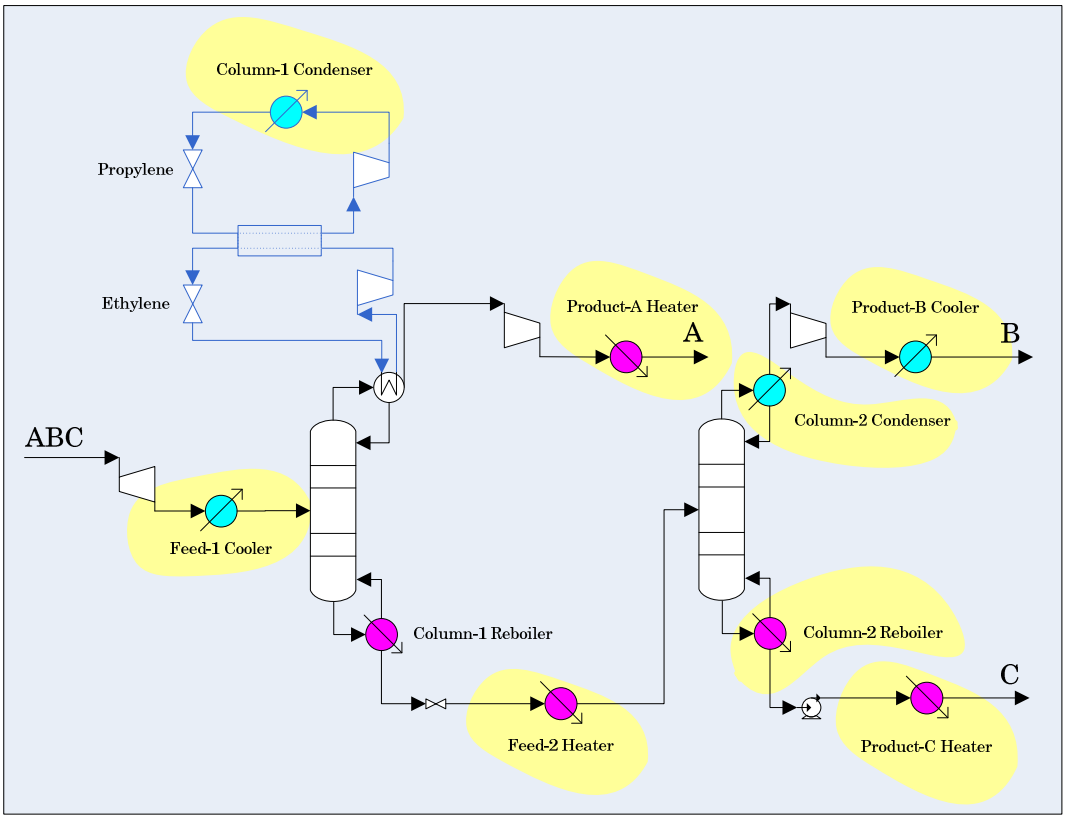

Figure 4.1: Location of heat exchangers in example configuration.

Inlet and outlet temperatures are used to classify all the streams as hot or cold streams. Two respective lists of data for the existing hot and cold streams are generated, which contain the following information:

i. Supply and target temperatures of hot and cold streams

ii. Cooling and heating demands of hot and cold streams

The streams in the above lists are ordered per ascending order of target temperatures, as illustrated in Table 4.1 and Table 4.2 for the process configuration of Figure 4.1 .

ID	Name	Inlet T °C	Outlet T °C	Enthalpy kW
H_1	Column-2 Condenser	-31	-40	1689
H_2	Heat-Pump-1 Condenser	-14	-14	3055
H_3	Feed-1 Cooler	21	0	1002
H_4	Heat-Pump-2 Condenser	11	11	1869
H_5	Product-B Cooler	95	35	495

Table 4.1: List of hot streams in example configuration of Figure 4.1.

ID	Name	Inlet T °C	Outlet T °C	Enthalpy kW
C_1	Column-1 Reboiler	-73	-18	5746
C_2	Feed-2 Heater	-39	7	1869
C_3	Column-2 Reboiler	26	34	876
C_4	Product-A Heater	-37	35	3476
C_5	Product-C Heater	33	35	10

Table 4.2: List of cold streams in example configuration of Figure 4.1.

4.4.2 Utility data collection

The set of available utilities to a given process are classified into hot and cold utilities based on supply and target temperatures. Hot and cold utilities are then listed separately and arranged in temperature ascending order.

Finally, the list of hot utilities is appended to the end of the list of hot streams and the list of cold utilities to the list of cold streams.

4.4.3 Discretisation of temperature domain

The construction of the heat integration framework involves characterising the temperature intervals for heat exchange. The heat exchange temperature intervals are determined from the hot and cold side temperature levels or interval boundaries. These levels are primarily derived from supply streams and utilities temperature levels. This section presents the steps involved in the characterisation of the heat exchange temperature intervals.

Once the temperature intervals are defined, the distribution of duty across the intervals is calculated for each stream.

4.4.3 (i) *Temperature levels based on hot and cold streams and unification of levels*

The temperature levels on the hot side are derived from the hot streams supply temperatures. Figure 4.2 illustrates level generation at the hot side, where H_i represents hot stream i and L_{Hk} represents hot-side temperature level k.

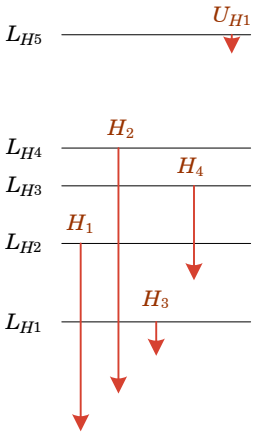

Figure 4.2: Generation of temperature levels based on hot side.

The equivalent procedure is applied on the cold side to generate a separate list of intervals based on the cold streams supply temperature levels. Figure 4.3 illustrates level generation at the cold side, where C_j represents cold stream j and L_{Cl} represents cold-side temperature level l.

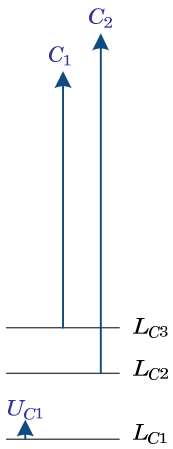

Figure 4.3: Generation of temperature levels based on hot side.

Figure 4.4 illustrates the unification of the cold side and the hot side temperature levels, where the new variable L'_m represents level m in the composite level list. In this figure, cold side temperatures are shifted by ΔT_{min} to allow for horizontal representation of the heat flow from the hot side to the cold side.

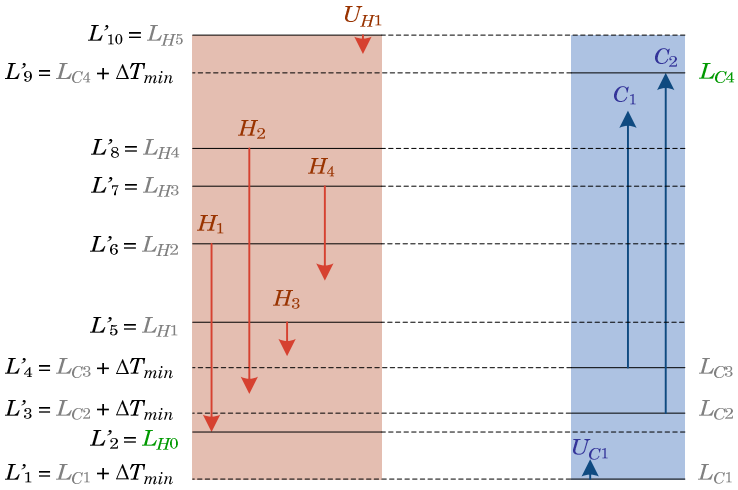

Figure 4.4: Generation of temperature intervals by aligning hot and cold temperature level lists.

Temperature intervals confined between temperature levels in close proximity increase the complexity of the heat integration framework and yet, their consideration adds negligible value to the framework. Therefore, it is desirable to not account for intervals narrower than an arbitrarily

small value, e.g. 1°C. This consideration is reflected in the programming framework by imposing a minimum difference of 1°C between consecutive temperature levels in the level list.

4.4.3 (ii) Temperature levels based on target temperatures on hot/cold side beyond supply temperatures in opposite side

An additional temperature level at the bottom of the list must be incorporated when a hot stream target temperature is lower than the coldest "effective" sink temperature, e.g. stream H_1 in Figure 4.4. The term "effective sink temperature" is employed in this work to refer to sink temperatures that are corrected for the minimum temperature approach; a cold stream with an actual supply temperature of 30°C has an associated effective temperature level of 30°C plus the minimum temperature approach, ΔT_{min}.

In this case it is necessary to incorporate the target temperature of the hot stream in question to the list of temperature levels. Importantly, if there are several hot streams that need cooling below the coldest available cold stream, the lowest of all target temperatures is selected for inclusion. Only one level of this kind must be added to the list of temperature levels due to the construction of temperature intervals relying on supply temperatures.

This class of temperature level may equally occur on the cold side. If a cold stream effective target temperature is higher than the hottest source temperature, e.g. stream C_2 in Figure 4.4, the corresponding temperature level is incorporated to the list of cold side temperature levels.

Figure 4.4 illustrates the inclusion of this class of levels L_{H0} and L_{C4} in the levels list. A minimum difference of 1°C between existing and new levels is imposed.

4.4.3 (iii) Temperature levels for utilities

Hot utility supply temperatures introduce additional temperature levels on the hot side, independently of their position in the temperature range established so far.

Cold utility temperature levels are similarly incorporated to the cold side temperature level list.

Figure 4.4 illustrates the inclusion of this type of levels, L_{H_5} and L_{C_1}, at the hot and the cold sides.

4.4.4 Match feasibility evaluation for streams

A systematic procedure is employed in this work to enumerate all the possible matches between hot and cold streams across the temperature range. A feasibility matrix is generated with the results derived from this procedure, which is summarised by Figure 4.5.

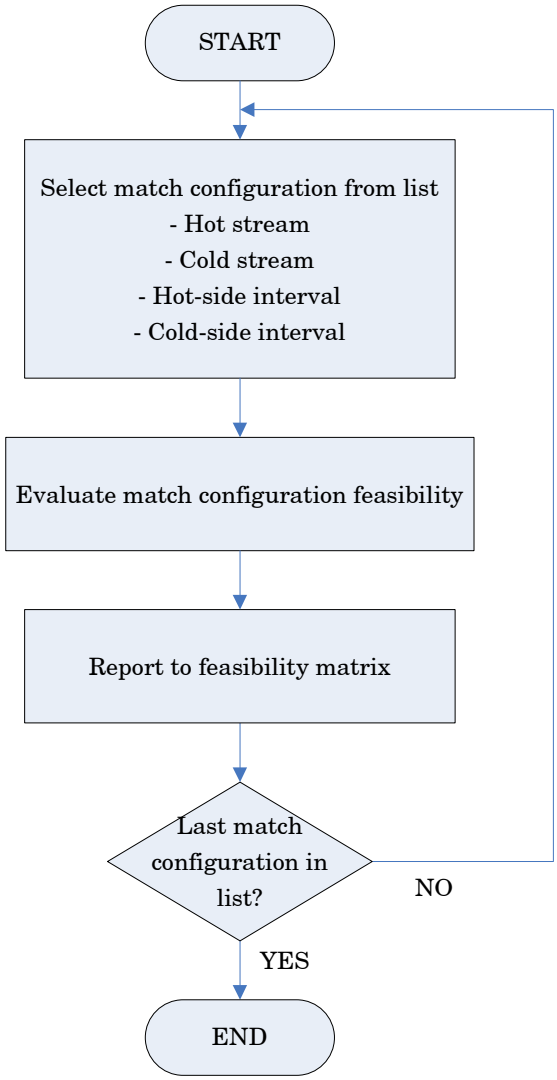

Figure 4.5: Flowchart of computation of the match feasibility matrix.

Heat exchange matches between hot and cold streams are allowed between intervals at the same temperature level or from hot side intervals to colder intervals on the cold side. Therefore, match feasibility between two streams from a hot-side temperature interval to a cold-side temperature interval is decided upon the relative position of the two intervals.

4.4.5 Match feasibility evaluation for streams with utilities

A similar procedure to that for identification of possible matches between streams is applied to identify the possible utility allocations to each hot

and cold stream. The main difference with respect to the procedure introduced in 4.4.4 is that each utility is available for heat exchange at a unique temperature interval. This feature allows this procedure to be a simplified version of the procedure for match identification between streams.

4.4.6 Match selection

The feasible matches identified by steps 4.4.4 and 4.4.5 are systematically investigated before they are accepted or discarded. A matrix of confirmed matches is generated with the results of the match selection procedure summarised by Figure 4.6.

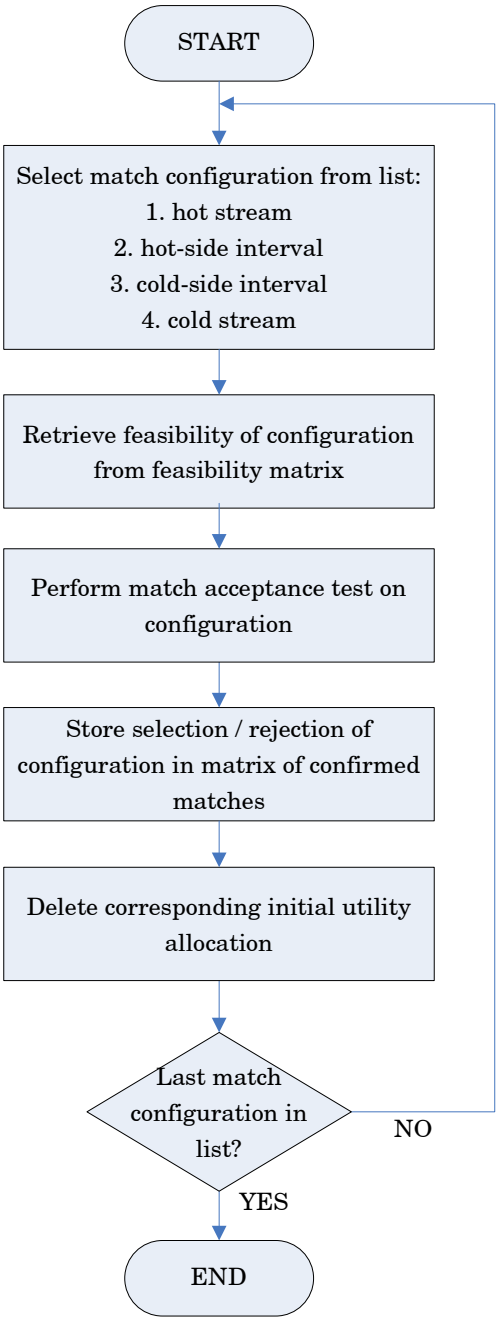

Figure 4.6: Flowchart of computation of the matrix of confirmed matches.

The order in which the evaluation of matches is carried out is central to the heat integration approach employed in this work. This order is designed to maximise heat recovery within temperature intervals and to minimise the degradation of thermal energy due to heat exchange between different temperature levels.

In order to maximise heat recovery within each temperature interval, all stream matches within a temperature interval are prioritised over any alternative matches between different intervals.

With the purpose of minimising utility consumption, matches between streams are prioritised over utilities, and matches with more inexpensive utilities are then prioritised over matches with more expensive utilities.

4.4.6 (i) Hierarchy in the evaluation of feasible matches

The order in which match evaluation is performed is in itself the foundation of the strategy for heat recovery maximisation and utility cost minimisation and the details of it are illustrated by Figure 12.11.

The sequential procedure for evaluation of match configurations is illustrated by Figure 4.7 and begins with the hot stream with the highest target temperature and the lowest temperature interval where this stream exchanges heat. The cold stream with the highest target temperature among the cold streams available in the given interval is identified.

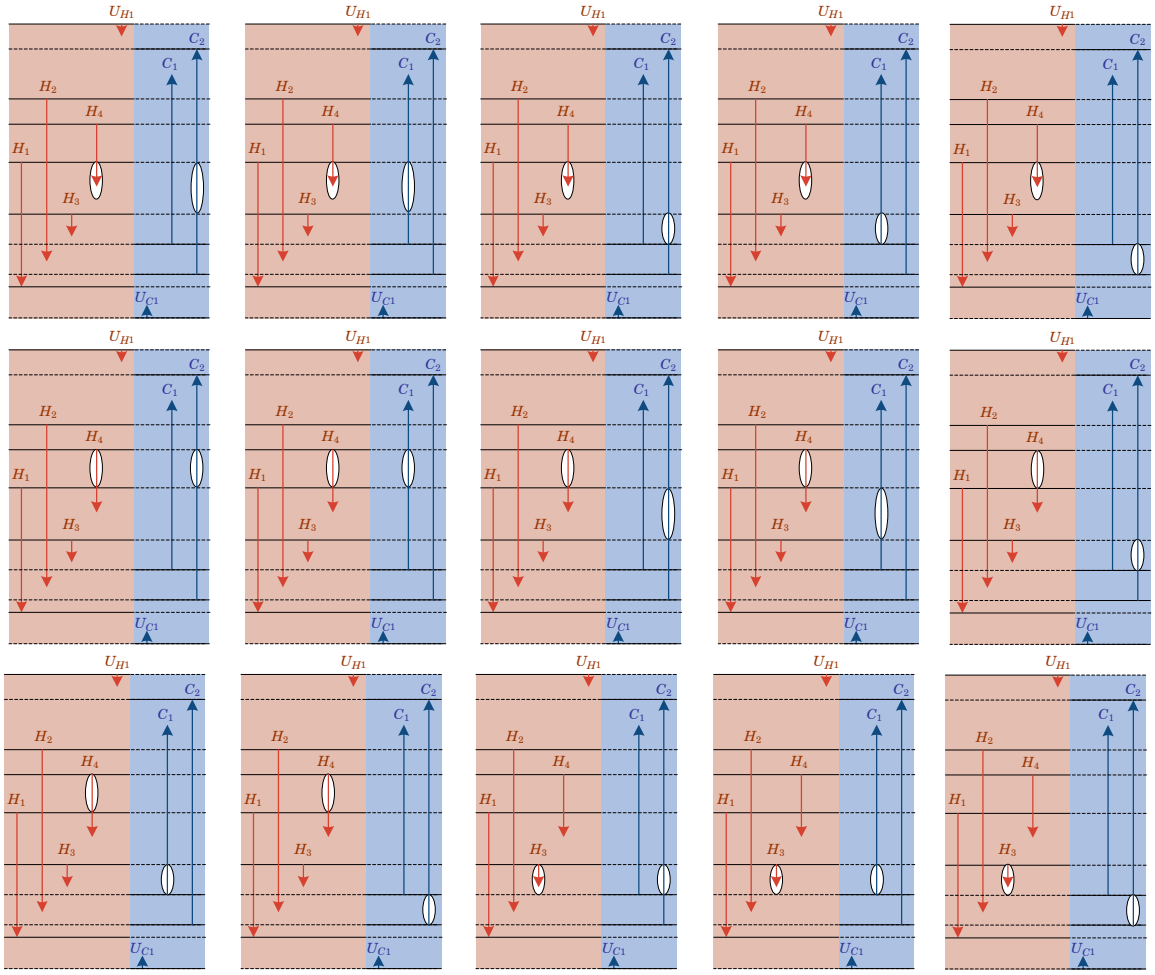

Figure 4.7: Illustration of the 15 first moves (from left to right, then from top to bottom) in the successive match evaluation process for an example.

The selected configuration is then subjected to a match acceptance test, which is explained in greater detail in subsection 4.4.6 (ii). The match acceptance test is successively applied as the different match configurations are selected. The second match configuration in the sequential methodology inherits the selection of hot stream and temperature intervals from the first match configuration but features a different cold stream, which is the next cold stream in the list. The evaluation of this family of matches with common hot stream and temperature intervals continues until all options of cold streams have been exploited.

Because in the proposed heat integration methodology hot streams can transfer heat to cold streams between different intervals, the next step in the match identification procedure consists of shifting the selection of cold side temperature interval to the immediately colder interval. The cold stream selection is reinitialised, however, the selection of the hot stream and the hot side temperature interval are preserved. The match evaluation test is repeated for this group of match configurations until the bottom interval at the cold side is reached.

Following the evaluation of all heat exchange opportunities for the initial hot stream in the initial hot side temperature interval, heat matches for the stream in question at the immediately hotter interval are investigated. The evaluation test is repeated until the upper interval for heat exchange of the given hot stream is reached. By focusing on heat transfer from hotter intervals to colder intervals only, this match identification procedure avoids the unnecessary evaluation of infeasible configurations.

The match evaluation procedure is repeated for the next available hot stream in the list and continues until all existing hot streams have been studied.

The allocation of utilities to streams is performed after the matches between streams have been selected. By performing the allocation of utilities in this order, matches between streams are prioritised over utilities, and only the heating or cooling demands that the process streams are unable to satisfy are then allocated to utilities.

4.4.6 (ii) Match acceptance test

The details of the algorithm for match acceptance/rejection are presented in Figure 12.12.

The acceptance of matches takes into account the number of matching opportunities of each stream by temperature interval. The rules applied for match acceptance are summarised below:

1. Only matches that feature a non-negligible load are retained. For each possible match, the maximum load that can be exchanged is given by the smallest of the individual cooling or heating demands.

2. In order to maximise heat integration in the below-ambient region, any feasible match between any cold stream and a hot stream featuring a below-ambient supply temperature is accepted and assigned a maximum heat load. If two or more matches of this kind are possible for a unique cold stream, the hot stream with the lowest target temperature takes precedence.

3. In order to minimise utility consumption, any feasible match between streams with no additional matching alternative (excluding utilities) is accepted and assigned a maximum heat load.

Except for situations 2 and 3 above, any match opportunity between a hot stream and a cold stream is only accepted with a certain probability. A random number (also called random seed) is then used to generate one in three equally probable scenarios. The significance of each scenario is described below:

A. The potential match is discarded.

B. The potential match is accepted and has an associated heat load totalling the total maximum load.

C. The potential match is accepted and has an associated heat exchange load that is limited to a fraction of the total maximum load available. This implies that neither the heating nor the cooling demand in the

corresponding temperature interval of the two participating streams is fully satisfied. In this scenario, an additional random number is used to establish the fraction of maximum load that is associated to the confirmed match. This number is fractional and can vary between zero and one. Marginal heat loads resulting in impractically small heat exchangers are prevented by rounding this fraction to one if it is greater than 0.95 and to zero if it is below 0.05 or simply by restricting the generation of the random number to these limits. Any unsatisfied cooling demands of the hot stream in question must be met by alternative matches within the same interval, or if these are unavailable, cascaded down to matches with streams in colder intervals or cold utilities.

This range of scenarios are responsible for the variability in the resulting heat exchanger networks and for facilitating the optimisation of the heat integrated separation system within the optimisation framework presented in this work. The random number controlling the selection of matches is responsible for the heat exchanger network perturbation following heat integration moves.

The above scenarios are not applicable to matches of streams with utilities because in absence of utility use constraints, the selection of utility for a particular heating or cooling demand is trivial, since there is no incentive for allowing matches with unnecessarily costly utilities. It is the role of the proposed evaluation methodology to make a biased selection of the most economic utility available for each match. This methodology is founded on the assumption that the price of utility per unit energy increases as the utility supply temperature becomes more extreme. This is a general assumption that is acceptable in most situations and is based on the economy of utilities production fuel (for comparison of steam levels and hot water) and from electric power (for comparison of refrigeration levels).

4.4.7 Consolidation of matches in adjacent temperature intervals for capital cost minimisation

The proposed methodology for selection of matches between hot and cold streams described in previous steps is targeted at maximising energy recovery and minimising the use of utilities. However, the implications of this approach on the capital cost of the network have not yet been addressed.

The proposed heat integration framework, which is based on temperature interval decomposition, allows streams to be matched in different temperature intervals, as well as within the same temperature interval. If each of the matches is paired with a standalone heat exchange equipment item, this approach may result in a heat exchange network that features an impractically large number of heat exchangers and consequently, an elevated network cost.

Alternatively, some of these matches may be merged in a single heat exchanger if the two streams involved exchange heat across adjacent intervals. For this argument to be valid, these streams must maintain constant flowrates along the entire temperature range of the merged matches. This condition is annulled if splitting or bypassing in one or more subsections of the overall temperature range is prescribed by the heat integration methodology.

This combination of adjacent heat exchangers reduces the number of required heat exchangers and the associated cost. This has a direct effect on the cost of the heat exchanger network, which consists of variable and fixed costs. Fixed costs including the installation costs of the individual heat exchangers may be condensed by merging multiple heat exchangers into a single one.

The simplification of the initial HEN by consolidation of adjacent matches is achieved by the procedure summarised in Figure 4.8. The hierarchy of

match evaluation for match-merging is shown with more detail in Figure 12.13.

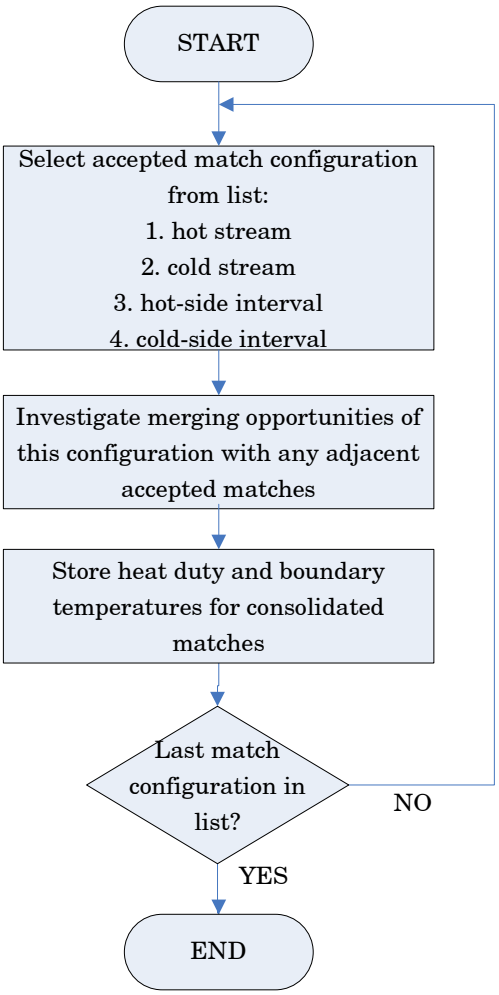

Figure 4.8: Flowchart of match-merging procedure.

This work contemplates three scenarios for merging heat exchangers, each related to the relative position of the confirmed matches in the temperature domain.

i. **Case 1** - Figure 4.9. Heat exchangers A and B between streams H_i and C_j may be merged provided that the following set of conditions is met:

- Hot stream H_i in heat exchanger A exchanges heat with cold stream C_j in hot-side interval I_{Hk}.

- Hot stream H_i in heat exchanger B exchanges heat with cold stream C_j in hot-side interval I_{Hk}.

    - In the initial configuration, H_i is split in two substreams. The ratio of flowrates routed to heat exchangers A and B is directly related to the ratio of loads in these heat exchangers.

- Cold stream C_j in heat exchanger A exchanges heat with hot stream H_i in cold-side interval $I_{Cl} \leq I_{Hk}$.

- Cold stream C_j in heat exchanger A exchanges heat with hot stream H_i in cold-side interval I_{Cl} -1, which is adjacent to I_{Cl}.

- Equal mass flowrate of cold stream C_j passes through heat exchangers A and B.

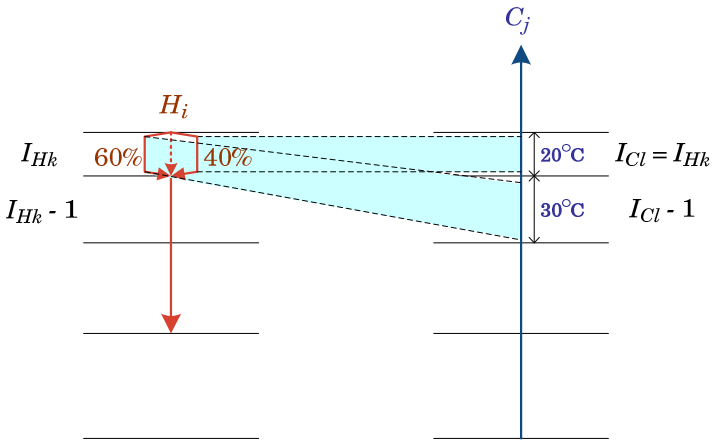

Figure 4.9: An example of adjacent matches contemplated in Case 1.

ii. **Case 2** - Figure 4.10. Heat exchangers A and B between streams H_i and C_j may be merged provided the following set of conditions is met:

- Hot stream H_i in heat exchanger A exchanges heat with cold stream C_j in hot-side interval I_{Hk}.

- Hot stream H_i in heat exchanger B exchanges heat with cold stream C_j in hot-side interval I_{Hk} -1, which is adjacent to I_{Hk}.

- Equal mass flowrate of hot stream H_i passes through heat exchangers A and B.

- Cold stream C_j in heat exchanger A exchanges heat with hot stream H_i in cold-side interval $I_{Cl} \leq I_{Hk}$.

- Cold stream C_j in heat exchanger A exchanges heat with hot stream H_i in cold-side interval I_{Cl} -1, which is adjacent to I_{Cl}.

- Equal mass flowrate of cold stream C_j passes through heat exchangers A and B.

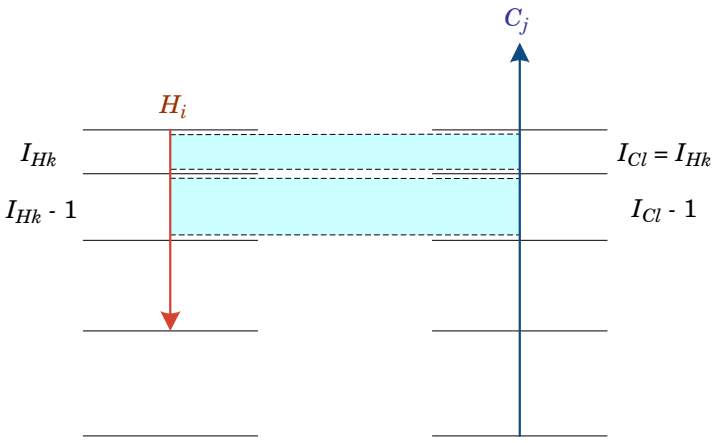

Figure 4.10: An example of adjacent matches contemplated in Case 2.

iii. **Case 3** - Figure 4.11. Heat exchangers A and B between streams H_i and C_j may be merged provided that the following set of conditions is met:

- Hot stream H_i in heat exchanger A exchanges heat with cold stream C_j in hot-side interval I_{Hk}.

- Hot stream H_i in heat exchanger B exchanges heat with cold stream C_j in hot-side interval I_{Hk} +1, which is adjacent to I_{Hk}.

- Equal mass flowrate of stream H_i passes through heat exchangers A and B.

- Cold stream C_j in heat exchanger A exchanges heat with hot stream H_i in cold-side interval $I_{Cl} \leq I_{Hk}$.

- Cold stream C_j in heat exchanger A exchanges heat with hot stream H_i in cold-side interval I_{Cl}.

    - In initial configuration, C_j is split in two substreams. The ratio of flowrates routed to heat exchangers A and B is directly related to the ratio of loads in the heat exchangers.

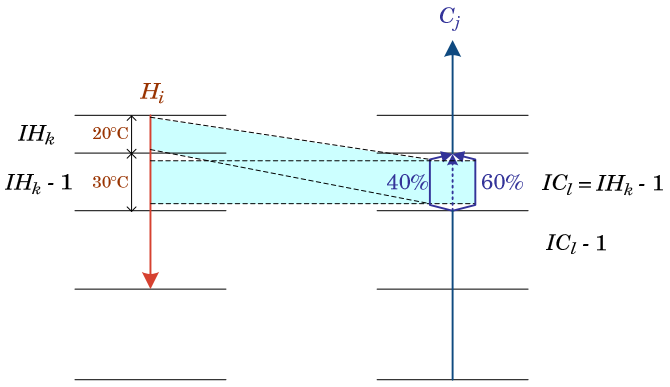

Figure 4.11: An example of adjacent matches contemplated in Case 3.

By relying on the conservation of flowrates across adjacent matches, the proposed match-merging methodology is accurate for streams of constant heat capacity and temperature-dependent heat capacity streams, which include streams changing phase, i.e. vaporisation and condensation.

There is no limit on the number of matches that may be merged into a single heat exchanger, and each confirmed match is investigated for adjacent matches iteratively until all options are exhausted. The formulation of the methodology for merging adjacent matches is complex

because of the examination of the various scenarios and the verification of constant mass flows across adjacent temperature intervals, and is illustrated in Figure 12.14.

By merging adjacent matches, a simplification of the initial network is achieved. The resulting network is also more practical after removing artificial match boundaries; however, the final configuration may feature more than one heat exchanger for a given pair of streams.

Multiple heat exchangers for a specific pair of streams are possible as these two streams can exchange heat in non-adjacent intervals or participate with different flowrates in each heat exchanger. The randomness in the allocation of loads at the matches acceptance step makes the latter occurrence particularly likely.

4.5 Refrigeration system design

Refrigeration is often required to meet the below-ambient cooling requirements of common gas separation process. Below-ambient temperature levels predominate in gas separation processes that exploit differential volatilities, since vapour-liquid equilibrium is only encountered at low temperatures. Condensing duties in distillation columns are usually required at below-ambient temperatures. Similarly, absorption performance is higher at low temperatures, which requires chilling of the lean solvent.

Compression refrigeration cycles are the most common choices to provide the required cooling. The cold refrigerant in the cycle shown in Figure 4.12 extracts heat from the below-ambient heat source and after compression rejects it at a higher temperature to an available heat sink, generally ambient utility. Effectively, heat is pumped from lower temperatures to higher temperatures by means of the work of the compressor, which is necessary to reverse the direction of natural heat flow as given by

thermodynamics. Absorption refrigeration is a relatively infrequent option and therefore has not been considered in this work.

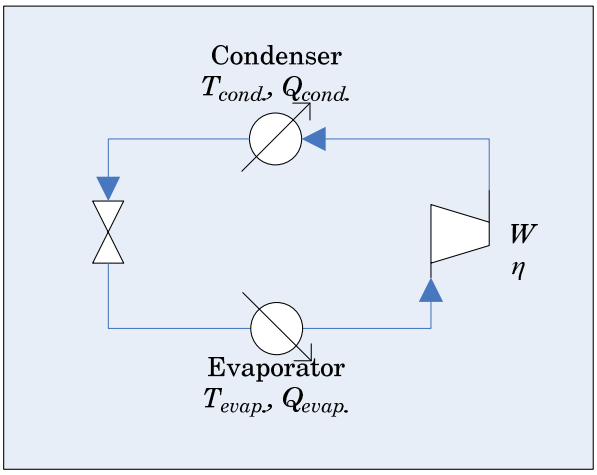

Figure 4.12: Schematics of a simple refrigeration cycle.

This work uses the integrated refrigeration system design approach presented by Wang (2004) and implemented in COLOM® (Version 2.2.003 ©CPI, University of Manchester 1985-2009). This approach integrates the selection of refrigeration configurations with the available process heat sinks and sources.

Integration between heat sinks and sources at below-ambient temperatures via heat pumping has a two-fold economic incentive. On the one hand, it eliminates the need for ambient utility (generally cooling water) to remove heat from the condenser of the refrigeration cycle. On the other hand, it reduces the hot utility process demand by meeting, partially or totally, the heating demands of the stream that acts as the heat sink.

The developed HEN design methodology favours below-ambient process-to-process matches. If the below-ambient cooling requirements cannot be fully satisfied by other process streams, then, the design of refrigeration system is undertaken. The rejection of heat from refrigeration cycles to process streams is subsequently prioritised over cooling water rejection. By virtue of this feature, heat pumping configurations are possible

whereby the heat extracted from the condenser of a column at low temperatures may be heat-pumped and rejected to the reboiler of the same column. These configurations are impractical if the column temperature gradient is pronounced, since a moderate difference between source and sink requires a cascade of refrigeration cycles.

In the adopted design approach, the configuration of a refrigeration cycle is decided upon the temperature difference between a sink and a source. Simple refrigeration cycles are adequate for small temperature difference. If the temperature difference is large, a cascade cycle is recommended. This is consistent with the fact that shaftpower requirements increase with a larger temperature difference between evaporation and condensation in a refrigeration cycle. This fact becomes clear from inspection of the equation that allows estimating the power requirement of a refrigeration cycle:

$$W = \frac{Q_{evap.}}{\eta} \frac{T_{cond.} - T_{evap.}}{T_{evap.}} \tag{4.1}$$

Where $Q_{evap.}$ is the heat absorbed by the refrigerant from the heat source at temperature $T_{evap.}$ in Kelvin, $T_{cond.}$ is the temperature in Kelvin at which the refrigerant condenses, and η is the mechanical efficiency of the compressor.

In the adopted algorithm for refrigeration system design, this observation translates into the prioritisation of heat pumping matches between streams with a minimum temperature difference.

Equation (4.1) also indicates that for the matches with ambient utility at a fixed $T_{cond.}$, a lower $T_{evap.}$ leads to a higher power. This is reflected in the adopted design algorithm by prioritising heat pumping matching for the colder heat sources. In this way, if a below-ambient hotter heat source stays unmatched due to lack of stream sinks, the heat rejection of the

corresponding refrigeration cycle to ambient utility will not be too energy-intensive.

The below-ambient matching algorithm by Wang and Smith (2005) enumerates the available below-ambient sources and sinks in a list in ascending order of temperatures, and the possibility of matching is assessed starting from the top of the list. When the stream at the bottom of the list has been reached, external utilities are employed to meet any unsatisfied the heating / cooling demands.

Thereafter, refrigeration cycles are designed for each heat pumping match. First of all, the decision to use simple or cascade cycles is based on the temperature difference between evaporation and condensation. If the temperature difference is relatively small, a refrigerant that is suitable for the simple cycle temperature levels is selected. Lighter refrigerants, such as ethylene, have a lower boiling point than heavier refrigerants, such as propylene. This makes lighter refrigerants particularly useful for cooling at very low temperatures. Each pure refrigerant has a recommended temperature range of application.

On the other hand, if the temperature difference between evaporation and condensation exceeds the recommended temperature range of each of the available refrigerants, a cascade of refrigerants is selected. In the cascade represented in Figure 4.13, the lower cycle extracts heat from the heat source and rejects it to the next cycle at an intermediate partition temperature. The condenser of the lower cycle and the evaporator of the immediately upper cycle are now combined into a single heat exchanger. The upper cycle refrigerant receives heat at the partition temperature and after compression, rejects it to a higher temperature level. Cascades of two and three refrigerant levels are very common.

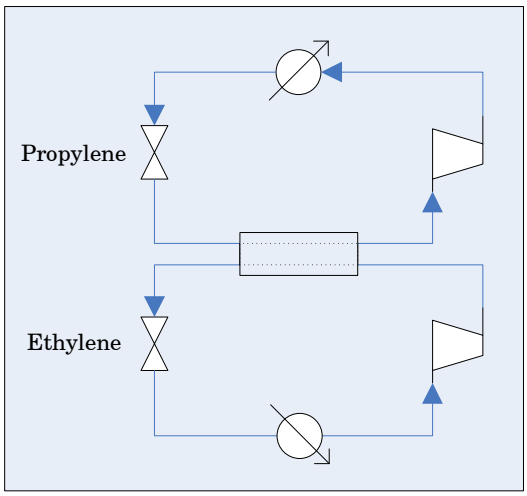

Figure 4.13: Refrigeration cycle in cascade with a lower ethylene cycle rejecting heat to the evaporator of the upper propylene cycle.

The adopted refrigeration system design approach is limited to simple and cascaded refrigeration cycles. In practical design, it is frequent to encounter single refrigerant multistage cycles featuring multiple evaporating stages and a single condensing stage. This type of design is preferred because it simplifies the design of multiple separate simple cycles of the same refrigerant and requires only one heat exchanger that serves as a condenser. According to Wang and Smith (2005), because the shaftpower demand difference between simple cycles and the corresponding multistage cycles is small, the described design methodology restricted to an assembly of simple cycles is useful for the screening of design options on the basis of shaftpower targeting.

The design methodology of Wang (2004) is selected for application in the present work because it is believed that the restriction to simple cycles in conceptual process design is a fair approximation on the basis of not only shaftpower targeting, but also of combined capital and operating cost. Final design of refrigeration cycles must consider additional aspects in detail, such as safety, operability and complexity, which are outside the scope of this work.

4.6 Conclusions

This chapter has presented the key features of the developed HEN design methodology, which supports heat integration in the proposed separation system synthesis framework. This methodology does not rely on algorithmic optimisation approaches, which traditionally have difficulty in generating a HEN physical configuration. Instead, the developed HEN design methodology takes advantage of the stochastic optimisation framework hosting the synthesis methodology to allow for investigation of a large number of feasible HEN design configurations. Secondly, the mechanism for generation of feasible HEN design configurations is supported by rules for preferential match selection which aim at minimising utility consumption. Thirdly, the optimisation of the separation system and the HEN is carried out simultaneously. This is in opposition to traditional hierarchic process design approaches, where the design of the HEN is not undertaken until the separation system has been decided upon. By bringing HEN design to the foreground, the complete system can be optimised as a whole and new heat recovery opportunities may affect the choice of separation system and vice versa.

Finally, the principles for the design of refrigeration cycles in the proposed synthesis methodology are presented. The design of the refrigeration system is fully integrated with the HEN design, and hence, with the design of the separation system.

Chapter 5. Costing considerations

5.1 Introduction

The quantitative synthesis methodology developed in this work uses capital and operating costs to establish a quantitative comparison between design options and to enable the systematic optimisation of the problem.

In this work, operating costs are assumed to be the equivalent of utility costs. The capital cost contribution consists of the annualised capital installed cost of the different pieces of equipment in the flowsheet, which requires equipment sizing and costing correlations.

This methodology accounts for the installed cost of compressors, columns and heat exchangers. Costs of valves and pumps are negligible. To account for the inflation of the final cost due to piping costs and the cost of instrumentation and control systems and of any spare equipment, methodologies are available in the literature to scale up the cost estimates of the bare equipment or purchase cost estimates using various factors.

A number of sources of equipment sizing and capital cost correlations are available in the open literature (Douglas (1988), Peters *et al.* (2003), Coulson *et al.* (1983)). Published capital cost data often derive from heterogeneous sources of different ages. Such data may be brought up to date and expressed on a common basis using cost indexes.

In this work, the sizing and capital cost correlations for columns and heat exchanger compiled by Triantafyllou (1991) are employed throughout. The sizing and purchase cost of compressors is derived from Peters *et al.* (2003), while the compressors installation costs are obtained from Douglas (1988).

In the first half of this chapter, a comparison is established between various existing methods for heat exchanger capital cost estimation and real cost data with the purpose of rationalising the choice of capital costs in the present synthesis framework. The application of these methods is accompanied by the relevant economic indices and currency exchange rates. By way of the above comparison, the challenging problem of capital cost estimation is introduced. The insights from heat exchanger cost estimation are largely extensible to the cost estimation of other types of equipment.

On the second half of this chapter, the problem of utility costs selection is addressed.

5.2 Preliminary sizing and cost estimates of heat exchangers

The HEN design methodology of Chapter 4 culminates in a proposed HEN configuration for the separation system. This configuration is characterised by the pairs of streams participating in the matches, the heat duty of each match and the inlet and outlet temperatures of each match streams.

5.2.1 Heat exchanger preliminary design

The heat exchangers featured in the resulting HEN must be sized and cost-estimated. A preliminary area may be obtained from the heat exchanger load, Q, the inlet and outlet temperatures and an approximate overall heat transfer coefficient, U, using Equation (5.1):

$$A = \frac{Q}{U\Delta T_{LM}} \tag{5.1}$$

Where ΔT_{LM} represents the logarithmic mean temperature of the heat exchanger. For a counterflow heat exchanger, ΔT_{LM} is given by:

$$LMTD = \frac{T_{H,in} - T_{C,out} - \left(T_{H,out} - T_{C,in}\right)}{ln\left(\frac{T_{H,in} - T_{C,out}}{T_{H,out} - T_{C,in}}\right)} \tag{5.2}$$

The following values of U are assumed: 600 W/m^{2}°C (condensers) and 900 W/m^{2}°C (reboilers). For other heat exchangers, U is derived from the individual heat transfer coefficients according to the following equation:

$$\frac{1}{UA} = \frac{1}{h_{tubes} A_{in\ tubes}} + \frac{1}{h_{shell} A_{out\ tubes}} + Wall\ resistance \tag{5.3}$$

Where h_{tubes} and h_{shell} are the heat transfer coefficients for the individual fluids circulating through the tubes and the shell, respectively; $A_{in\ tubes}$ and $A_{out\ tubes}$ (= A) are the inner and the outer area of the tubes, respectively. For preliminary design, these areas may be assumed equal, and the wall resistance may be neglected. A value of 200 W/m^{2}°C for the individual heat transfer coefficients is assumed. The overall heat transfer coefficient is lower if there no change of phase occurs across the heat exchangers.

Equation (5.2) holds for simple counterflow heat exchangers. The area of multiple-pass heat exchangers must be corrected with an additional factor that adjusts the logarithmic mean temperature.

In this work, the choice of heat exchangers is limited to pure counterflow heat exchangers, which are the commonest type in process applications. Heat exchangers with multiple tube passes are useful to achieve an adequate fluid velocity in the tube side. On the other hand, heat exchangers with multiple shells connected in series, are useful to overcome a temperature cross between outlet streams. Because the

proposed design methodology is aimed at conceptual design, establishing details such as the number of tube passes are out of the scope of this work. This methodology does not account for temperature crosses in the formulation of the heat integration framework, therefore multiple shells are also out of the scope of this work.

5.2.2 Heat exchanger cost estimation

The capital cost of a heat exchanger must reflect purchase and installation costs. Costs for foundations, piping, instrumentation and commissioning must also be considered into the equipment capital cost. These latter contributions are generally plant-specific and shared by most heat exchangers in the plant (Smith (2005)), thus, irrespective of the size of the heat exchanger.

The purchase cost of a heat exchanger depends on the operating pressure, temperature, material of construction, type of heat exchanger, type of processing plant and location.

This work discusses three methods for heat exchanger cost estimation.

5.2.2 (i) Method 1

The total heat exchanger cost is derived from the cost guide published by IChemE (1987), and it is given by:

$$HXCost = UnitCost + InstCost \tag{5.4}$$

Where *UnitCost* is the purchase cost and *InstCost* is the installation cost:

$$UnitCost = f_{material} BaseCost \tag{5.5}$$

Where $f_{material}$ is a factor that accounts for the material of construction for the heat exchanger and *BaseCost* is a function of the heat transfer area:

$$BaseCost = f\left(UnitArea\right) \tag{5.6}$$

Often cast steel is the material of reference; hence, the cast steel material factor is one. More expensive materials of construction have an associated higher material factor. The material factor of stainless steel is usually greater than 1.7. The list of material factors of Smith (2005) is incorporated for reference in Method 3.

The calculation of *BaseCost* is split into three intervals depending on the heat transfer area, *UnitArea* in m^2. Interval limits and coefficients are obtained from the cost guide published by IChemE (1987):

UnitArea < 10 m^2: *BaseCost* (£) = 6600

$$10 \leq UnitArea < 1000\ m^2:\ BaseCost\left(£\right) = \sum_{i=1}^{6} C_i A^{i-1} \tag{5.7}$$

The coefficients C_i for the above equation are given in Table 5.1.

UnitArea ≥ 1000 m^2: BaseCost (£) = 82 · UnitArea

C_1	5391
C_2	113.4
C_3	-0.32
C_4	0.0009013
C_4	-0.000001027
C_6	$4.095 \cdot 10^{-10}$

Table 5.1: Coefficients for calculation of *BaseCost*.

The evaluation of the installation cost of a heat exchanger uses the installation subfactors provided in the cost guide published by IChemE IChemE (1987). The installation cost, in £, is a function of the purchase cost and it is given by the following equation:

$$InstCost = UnitCost\left(F_{ER} + F_P + F_I + F_{EL} + F_C + F_{SB} + F_L\right) \tag{5.8}$$

Coefficients F_{ER}, F_P, F_I, F_{EL}, F_C, F_{SB} and F_L are provided for three different ranges of *UnitCost* in Table 5.2:

	UnitCost < 1800	1800 ≤ *UnitCost* < 180000	UnitCost ≥ 180000
F_{ER}	0.38	Use (5.9) with coefficients in Table 12.2	0.05
F_P	1.76		0.16
F_I	1		0.09
F_{EL}	0.19		0.03
F_C	0.35		0.08
F_{SB}	0.08		0.012
F_L	0.38		0.03

Table 5.2: Coefficients for calculation of *InstCost*.

$$Factor\left(e.g.\ F_{ER}, F_P, F_I, F_{EL}, F_C, F_{SB}, F_L\right) = C_1 + \left(C_2 - C_3\right)\frac{UnitCost - C_4}{C_5 - C_6} \qquad (5.9)$$

The coefficients for the calculation of F_{ER}, F_P, F_I, F_{EL}, F_C, F_{SB} and F_L in the intermediate range of *UnitCost* are broken down further into intervals and are shown in Table 12.2 of Appendix section 12.3.

5.2.2 (ii) Method 2

Method 2 uses the installation subfactors of a Private Communication of the Centre for Process Integration of the University of Manchester with ICI Engineering Department in 1990.

Methods 1 and 2 share identical purchase cost calculation but feature a different evaluation of installation costs. Thus, Equations (5.4) to (5.6) are applicable to Methods 1 and 2.

The installation cost, in £, is related to the purchase cost by the following equation:

$$InstCost = UnitCost\ F_{total} \qquad (5.10)$$

Where F_{total} is a function of *UnitCost* for most cases and it is given by Table 5.3:

	UnitCost < £6300	£6300 ≤ *UnitCost* < £158200	*UnitCost* ≥ £158200
F_{total}	0.38	Use (5.11) with coefficients in Table 12.3	0.05

Table 5.3: Coefficient F_{total} for calculation of *InstCost*.

$$F_{total} = Y_1 + (Y_3 - Y_1)\frac{UnitCost - X_1}{X_3 - X_1} \tag{5.11}$$

The coefficients of Equation (5.11) are shown in Table 12.3 of Appendix section 12.3.

5.2.2 (iii) Method 3

This cost evaluation method of Method 3 is extracted from Smith (2005). This method is slightly more complete than the previous methods as it accounts for more factors in the total heat exchanger cost.

Area must be comprised between certain limits for this method to be applicable. If this condition is met, the heat exchanger purchase cost is given by:

$$BaseCost = \frac{C_B}{Q_B^M} UnitArea^M \tag{5.12}$$

The parameters in the above equation are given in Table 5.4.

Q_B	80
C_B	32800
Minimum Area	80
Maximum Area	4000
M	0.68

Table 5.4: Parameters for estimation of shell and tubes heat exchangers purchase costs.

The total cost of the heat exchanger is given by a series of multipliers of the initial purchase cost:

$$Cost = F_{material}F_{pressure}F_{temperature}F_{location}\left(1+f_{pip}\right)BaseCost$$
$$+F_{location}\left(f_{er}+f_{inst}+f_{elec}+f_{util}+f_{os}+f_{build}+f_{sp}+f_{dec}+f_{cont}+f_{wc}\right)BaseCost \quad (5.13)$$

Where: Equipment erection is f_{er}, Piping (installed) is f_{pip}, Instrumentation & controls (installed) is f_{inst}, Electrical (installed) is f_{elec}, Utilities is f_{util}, Off-sites is f_{os}, Buildings (including services) is f_{build}, Site preparation is f_{sp}..

Material, pressure, temperature and location factors are provided by Table 12.4, Table 12.5, Table 12.6 and Table 12.7 of Appendix section 12.3, respectively. The cost of a new plant may differ significantly between different locations, even within the same country. Costs in certain areas of USA may be as high as 1.5 times the costs in US Gulf Coast (Smith (2005)). The remaining factors for direct and indirect cost and working capital, are shown in Table 12.8 of Appendix section 12.3.

5.2.2 (iv) Bringing capital costs up-to-date

The capital cost estimates for heat exchangers given by each method were applicable at the time of the method's release. In order to obtain current cost estimates, it is necessary to update the original estimates with the adequate economic indexes. This is essential in being able to establish a comparison between methods of a different timeline. This relationship is given by Equation (5.14):

$$HXCost_{current\ time} = \frac{CostIndex_{current\ time}}{CostIndex_{reference\ time}} HXCost_{reference\ time} \quad (5.14)$$

Typical economic indexes for the chemical process industries include the Chemical Engineering Plant Cost Index, published monthly in *Chemical Engineering* magazine, or its variation for plant equipment or heat exchangers and tanks. Traditional economic indexes for refinery construction include the Nelson Farrar Inflation Index, published

quarterly in *Oil and Gas Journal*, which also features a version of this index for miscellaneous equipment and for heat exchangers. The Marshall & Swift Economic Index is also of general use for equipment costing and is also published by *Chemical Engineering* magazine.

In this work, data have been compiled from the cited sources for the Chemical Engineering Plant Cost indexes and the Nelson Farrar indexes and are shown in Figure 5.1, Figure 5.2 and Figure 5.3.

Data for the CEPCI of Equipment and Heat Exchangers and Tanks was only available from year 2000. As a result, Figure 5.1 displays historic data from 1950 only for the general Chemical Engineering Plant Cost Index. Because plant economic indexes are related to global economy trade-offs, it was expected that all indices would show a similar trend. However, at the top right corner of Figure 5.1, an inversion of the relative position of the CEPCI indexes is observed. This is shown more clearly by Figure 5.2. In 2004, the CEPCI Index for heat exchangers and tanks rises above the general CEPCI. The January 2002 issue of *Chemical Engineering* magazine reported a modification in the definition of some of the CEPCI versions, however, the 2004 change in the relative position between CEPCI indexes cannot be attributed to the 2002 modification.

From Figure 5.1 and Figure 5.2, it may be concluded that if a correlation for heat exchanger costs that is dated prior to 2004 is applied to generate a current cost estimate, the incorporation of the standard CEPCI for cost correction would predict an cost up to 40% lower (using year 2001 as reference) than the result of using the CEPCI for Heat Exchangers and Tanks.

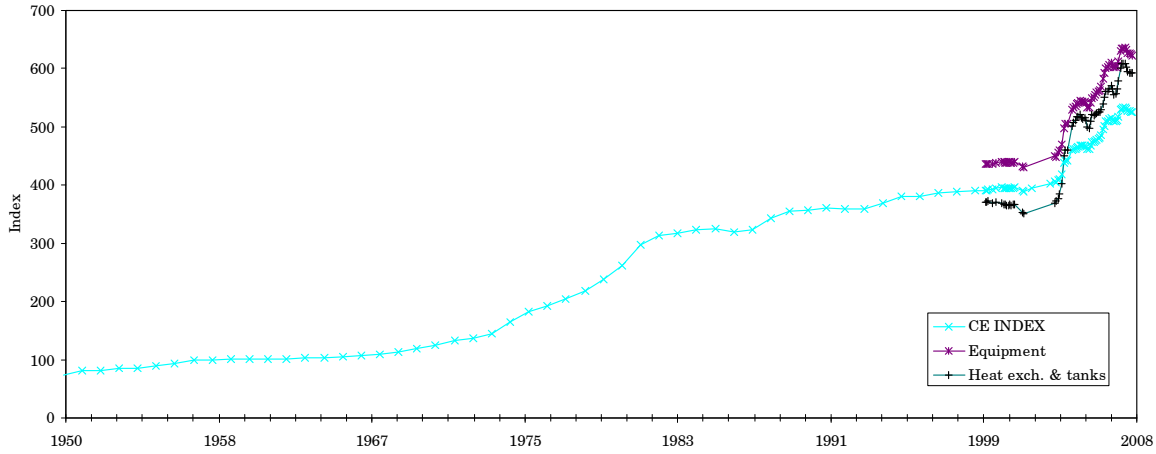

Figure 5.1: Chemical Engineering plant cost indexes for 1950 – 2008.

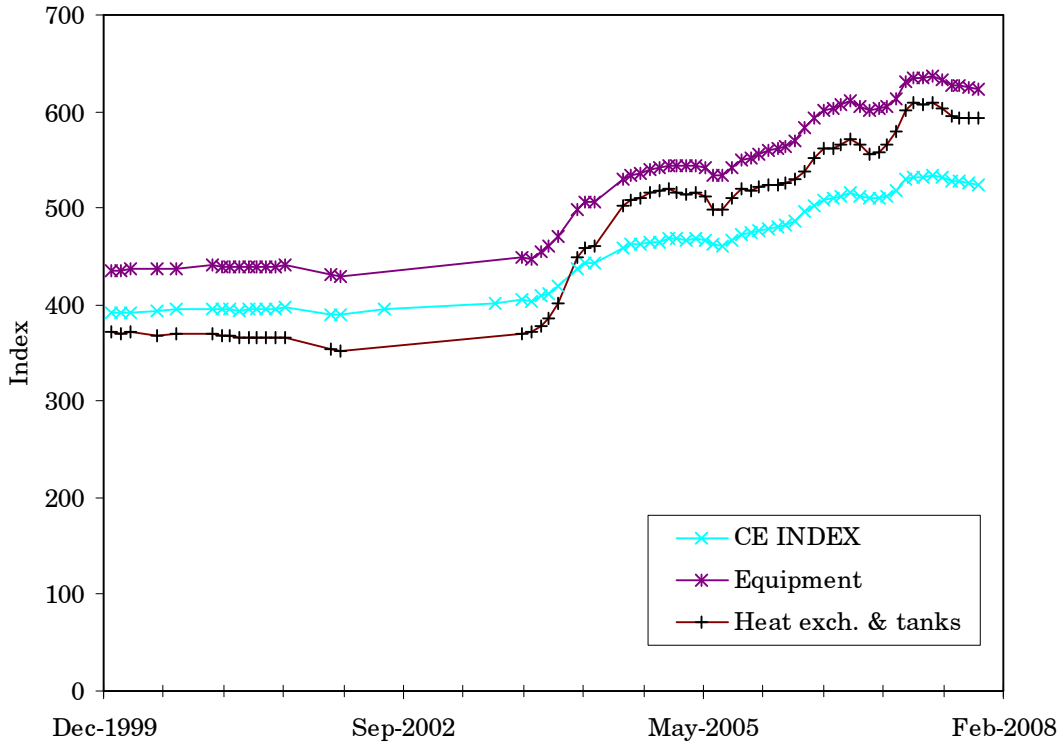

Figure 5.2: Chemical Engineering plant cost indexes for 1999 – 2008.

Figure 5.3 is a compilation of the Nelson-Farrar Refinery Construction Index and its variations for miscellaneous equipment and heat exchangers. The historical data of the heat exchanger index is less dense than that of the other two indexes. Similarly to the CEPCI historic data,

the historic data for the NF Index for Heat Exchangers features an irregular trend over the past two decades, which could possibly result in a notable discrepancy (up to ± 30%, using year 1983 as reference) between the capital cost estimates given by the various NF indexes.

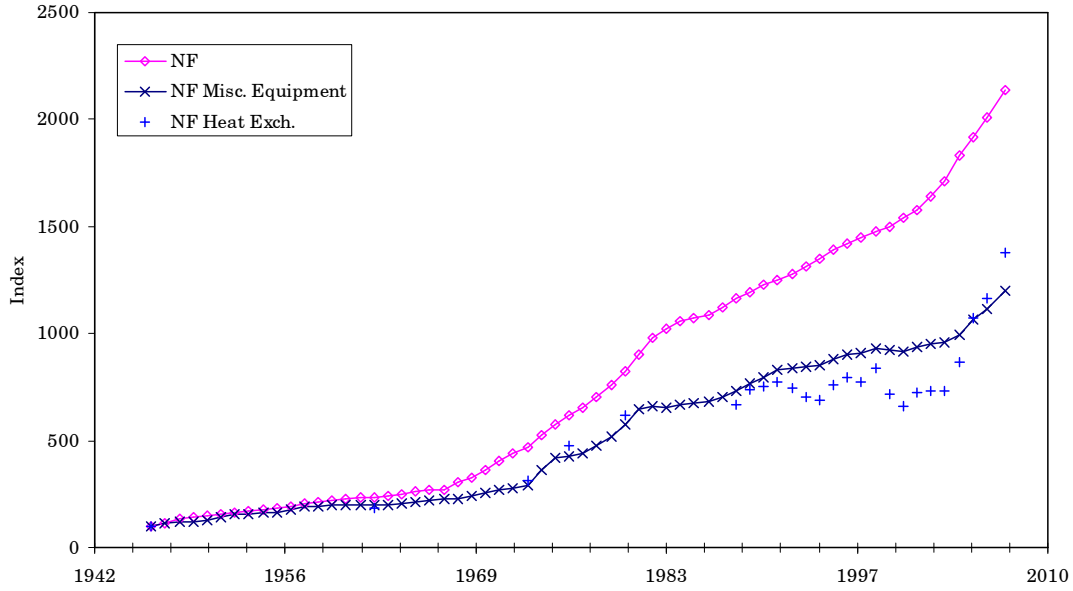

Figure 5.3: Nelson-Farrar Refinery Construction indexes for 1950 to 2008.

An example is used to illustrate how the choice of economic index affects correlation-based capital cost estimates. For this purpose, the publication date of each of the costing methods is required. Additionally, actual capital costs of a limited number of heat exchangers from a private industrial communication were used as a reference. These need to be brought up to date too. Table 5.5 provides dates for each method.

Method 1	1987
Method 2	1990
Method 3	2005
Reference industry costs	2002

Table 5.5: Date of reference of heat exchanger costing correlations.

Before proceeding with the example, another issue that arises when trying to evaluate different costing methods is the different currencies employed by them. Method 3 and the reference costs are given in US Dollar,

however, the output cost estimates of Method 1 and Method 2 are in GBP. In order to achieve currency consistency, it is necessary to convert the cost estimates to a single currency.

The fluctuation of currency exchange rates is a key challenge for capital cost estimation, in particular, the fluctuating exchange rate between US Dollar and GBP. It is difficult to establish a convention for conversion rate retrieval, i.e. conversion rate at the time of the costing method release vs. conversion rate at the present time. Because the economic indexes are global parameters, Equation (5.14) could yield different results depending on the timeline convention for application of the conversion rate. In fact, if the exchange rate at the time of the costing method's release is applied to the initial estimate, and the converted cost is then brought up to date using the chosen economic index, the result differs from the cost obtained by taking these two steps in the different order, because of the exchange rate volatility. The comparison between different costing methods could benefit from location-specific cost indexes.

Figure 5.4 shows the historic exchange rate from 1971 based on data from the US Federal Reserve provided by the Institute of Chartered Accountants of England and Wales. The average exchange rates for 1987, 1990 and 2008 are 1.64, 1.78 and 1.87 $/£. The following examples use the 1.87 $/£ value.

Figure 5.4. Historical rate of exchange between US$ and GBP.

5.2.2 (v) Heat exchanger costing method comparison

Table 5.6 is an example of the capital cost predictions using the various methods described in a previous section. The results are corrected with the CEPCI corresponding ratios.

	Data from industry (updated from 2002, US)	IChemE (purchase + inst.)	IChemE (purchase)+ ICI (inst.)	Smith, 2005
HExch Costing Method		1	2	3
Total Area (m^2)	931	931	931	931
Shells No.	1	1	1	1
Design Pressure (bar)	1			1
Material	CS&CS	CS	CS	CS&CS
Design Date	01-Jan-09	01-Jan-09	01-Jan-09	01-Jan-09
Cost Index Type	CEPCI	CEPCI	CEPCI	CEPCI
Design Temperature (°C)	50			50
HExch Type	S&T			S&T
Location	US			US Gulf Coast
HX Installed Cost ($)	$680,000	$449,027	$714,859	$1,117,151

Table 5.6: Heat exchanger real capital cost and capital cost predictions using different methods.

The effect of the choice of economic index conversion factor on the cost estimates is investigated in Figure 5.5. The data-points corresponding to CEPCI of Equipment and CEPCI of Heat Exchangers are missing from the

graph for Methods 1 and 2 (IChemE based methods). The reason for this is that these indexes were not available at the methods' release date.

This representation shows that each economic index may have a different effect on each cost estimation method. This is due to the different timelines and consequently, to the distinct index ratios for each of the methods.

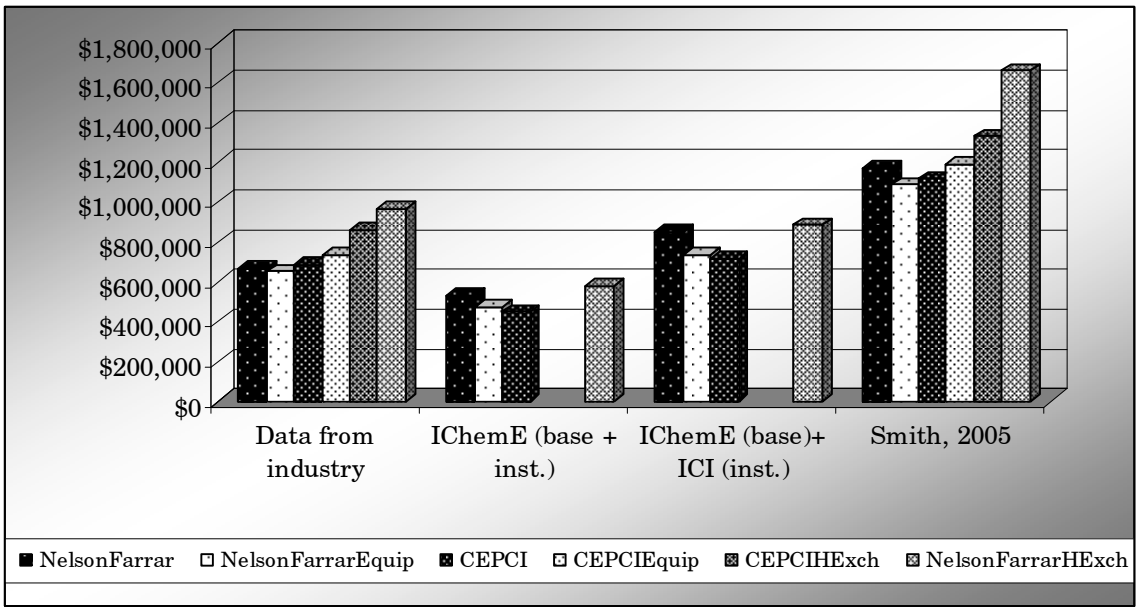

Figure 5.5: Effect of the choice of economic index on corrected cost estimates of methods of different age.

Another conclusion that may be drawn from Figure 5.5 is that the original date of the method presented by Smith (2005) and industry data are the most sensitive to the choice of Cost Index.

Following this analysis of a single heat exchanger, a similar analysis is conducted for a number of heat exchangers of different heat transfer areas using only the CEPCI. The points in Figure 5.6 are strongly correlated to the area because all other heat exchanger design parameters, e.g. design pressure, number of shells and tube passes, were kept constant for every heat exchanger. The slope of the representation in Figure 5.6 only changes from areas greater than 1400 m^2 due to multiple shells being specified for

larger heat exchangers. Industry reference capital estimates were first regressed with respect to the area in order to eliminate the effect of different design parameters for various heat exchangers.

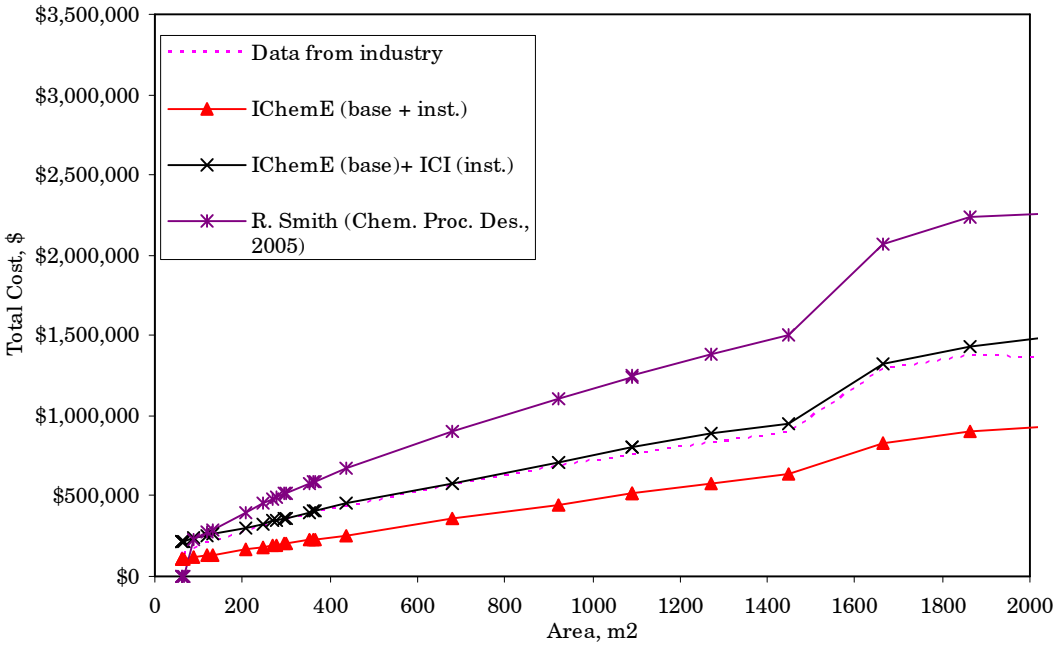

Figure 5.6: Application of heat exchanger capital cost estimation methods for a range of design areas.

In Figure 5.6, Method 2 and industry reference capital estimates appear noticeably proximate. This result could also be appreciated in Figure 5.5 and suggests the adoption of Method 2 and CEPCI ratios in the proposed synthesis framework.

5.2.2 (vi) Costing assumption for multiple heat exchangers between one pair of streams

Subsection 4.4.7 illustrated the possibility of the resulting HEN of having multiple heat exchangers for certain pairs of streams after the merging step. Mathematically, each heat match in the HEN requires an individual physical heat exchanger. However, the presence of multiple heat exchangers for single pairs of streams may lead to a disproportionate HEN capital cost, due to the accumulation of individual fixed costs.

In practice, multiple matches for a given pair of streams could be amalgamated into a complex heat exchanger, which is capable of accommodating intermediate draws and bypassing, thus mitigating the multiplication of individual installation costs. In this case, the cost of the corresponding equipment only requires a single installation cost contribution to the total heat exchanger fixed costs.

This result may be incorporated into the proposed heat exchanger costing methodology by accounting for a single fixed capital cost contribution per pair of matched streams. The heat transfer area and the purchase cost for each individual match are estimated as if the various matches between the given pair of streams were physically unconnected. This approximation could lead to inaccurate purchase cost estimation of the combined heat exchanger. On the one hand, the increased manufacturing complexity of multi-stream heat transfer equipment, which could enable merging of non-adjacent matches between the same pair of streams, would probably incur a higher heat exchanger purchase cost. On the other hand, by putting together various heat transfer units into a single heat exchanger, the resulting device may be more compact and require a smaller quantity of construction materials, which could potentially result in lower purchase costs than corresponds to the equivalent separate heat exchangers. In this work, it is assumed that these opposed effects are offset and it is justifiable to employ the same purchase cost estimation method for individual matches of a pair of streams as for the rest of heat exchangers in the HEN.

5.3 Conclusions (i) – Capital costs

In this section, the numerous contributions to heat exchanger capital costs are introduced along with three methods for capital cost estimation.

Quantitative analysis of these methods has provided the rational grounds for selection of the costing method, while revealing key discrepancies

between methods. Historic and economic factors distorting capital cost estimates are investigated.

In summary, the significant differences between heat exchanger capital cost predictions for the various costing methods may be attributed to the difficulty in accounting for:

- Installation factors and location specific trade-offs
- Different currency and cost correlations timelines
- Currency exchange rate fluctuations
- Heterogeneous cost index trends

These conclusions may be extended to capital cost estimation of other pieces of equipment, such as columns and compressors.

According to Smith (2005), the estimate of bulk costs (civil engineering, labour, etc.) are accurate within a ±30% deviation, but a ±50% deviation is not unusual. Greater accuracy would demand an exhaustive examination of all details of the investment, which is not appropriate in the context of conceptual system design.

It is expected that the implications of the inaccuracies of capital cost estimates are less severe in preliminary process design because any errors tend to manifest consistently across the design options (Smith (2005)). It follows that, since design options are usually compared on a common basis, the errors do not generally alter the relative priority of the different options.

5.4 Utility Costs

Utility prices play an important role in separation synthesis by projecting important energy trade-offs onto the synthesis process. Effectively, the relative weights of the various utilities have a direct effect on the solution to the synthesis problem. The sensitivity of the synthesis outcome to the utility costs relationships is a key challenge for process synthesis.

This section introduces the factors underpinning the cost of the most frequent utilities and discusses various estimates of general utility costs with the aim of rationalising the selection of the cost basis for the proposed separation synthesis methodology.

5.4.1 Factors affecting utility costs

The selection of the cost of utilities is a difficult task due to the volatility of energy costs and utility tariffs being determined on individual plant basis. The economics of process utilities as well as commodities are plant specific and depend on the balance between availability and demand and the possibility of exports or imports.

Steam prices may be related to the unit cost of fuel which is consumed in a boiler to generate the steam (Smith and Varbanov (2005)). Fuel costs must be scaled up with the boiler efficiency to account for heat losses and combustion inefficiency. Boilers can produce a steam of a fixed pressure. Steam costs of medium and low pressure levels depend upon the path that the steam follows from the point of generation to the point of use. Low-pressure steam that is produced by pressure letdown through a pressure-reducing valve is superheated and is often subsequently de-superheated. Low-pressure steam generation through a pressure-reducing valve is inefficient. Kumana and Associates (2003) recommend expanding the steam through a backpressure steam turbine for steam flows over 23 t/h ($50 \cdot 10^3$ lb/h), to recuperate power as a more cost effective way of letting

down the high pressure steam. If electricity is recovered by expansion through a turbine, the low pressure steam is assigned a lower cost than corresponds to high pressure stream. Smith (2005) provides an illustration of how steam prices may be estimated from fuel price, fuel heat content, boiler efficiency, price of electricity and driver mechanical efficiency.

It is not uncommon in industry to assign a unified price to different steam pressure levels due to the incapacity of recovering valuable energy from higher pressure levels to lower pressure levels. In certain processes, including ethylene cracking and refining, steam may be generated with the heat recovered from exothermic reactors and furnaces. Steam frequently appears as a reactant in such processes. In these cases, a different steam costing basis must be established.

Fuel costs are subject to oil price variations and vary widely from one location to another because of cost of transportation. Each fuel type has characteristic uses and a price per unit of energy, mass or volume. For example, the heating oil, also known as No. 2 fuel oil, is used to fuel building furnaces or boilers. Heating oil prices by NYMEX (New York Mercantile Exchange, Inc., the world's largest physical commodity futures exchange) escalated from 1.47 $/gallon in January 2007 to 2.25 $/gallon in September 2007.

Electricity tariffs for industrial users differ from the tariffs for domestic users and generally follow the global patterns of energy prices due to the major fossil fuel component to the grid conglomerate: 86% of the world's energy production is derived from fossil fuels, with petroleum, coal and natural gas accounting for 36.8%, 26.6% and 22.9% of the total, respectively (United States Energy Information Administration (2006)).

Cooling water costs are related to the pumping costs of water through the exchangers and to and from the cooling tower. The cooling water flowrate is given by the temperature rise across the heat exchangers. A 5-degree

temperature rise is commonly accepted for the design of heat exchangers involving cooling water. Higher temperature rises on the cooling water side are also possible, which limits the flowrate of cooling water through the exchanger but also the heat exchanger temperature approach, therefore requiring a larger heat exchange area.

Hot oil and hot water costs per unit of energy are generally linked to the cost of the fuel feed to a furnace, e.g. liquid fuel or natural gas. The furnace efficiency, which is related to the excess of air and the temperature of the stack, may be calculated from empirical correlations to refine the initial cost estimate based on the fuel combustion only.

5.4.2 Background

The Department for Business, Enterprise and Regulatory Reform, BERR, (previously part of the former UK Department of Trade and Industry) provides quarterly average fuel and electricity purchasing prices for UK industrial users. This database is however, limited to electricity and various fuels, including natural gas, but will be of use in a later discussion.

Ulrich and Vasudevan (2006) present a method to estimate utility costs based on empirical correlations. According to this method, the cost of any utility may be correlated to the cost of oil through an equation of the form:

$$C_{uty} = a\ PCI + b\ C_{fuel} \tag{5.1}$$

Where C_{fuel} is the price of fuel in \$/GJ, PCI is the Chemical Engineering Plant Cost Index and coefficients a and b are functions of certain utility specific variables. Coefficients a and b were derived by Ulrich and Vasudevan (2006) using manufacturing cost analysis (Vatavuk (2005)).

The results of applying Equation (5.1) to different types of steam are displayed in Table 5.7. The input values for the fuel cost and the Plant Cost Index are provided in Table 5.8.

Basis	m_s	a	P	b	C_{uty}	ΔH	$\boldsymbol{C_{uty}}$
	kg/s	\$/kg	bar	\$/kg	\$/kg	kJ/kg	\$/kWyr
Process module	0.06	$3.40 \cdot 10^{-4}$	2	$3.40 \cdot 10^{-3}$	0.231	2201	3313
	0.06	$3.40 \cdot 10^{-4}$	10	$3.79 \cdot 10^{-3}$	0.237	2014	3715
	0.06	$3.40 \cdot 10^{-4}$	30	$4.02 \cdot 10^{-3}$	0.241	1795	4231
	0.06	$3.40 \cdot 10^{-4}$	45	$4.11 \cdot 10^{-3}$	0.242	1676	4555
	1	$2.70 \cdot 10^{-5}$	2	$3.40 \cdot 10^{-3}$	0.066	2201	948
	1	$2.70 \cdot 10^{-5}$	10	$3.79 \cdot 10^{-3}$	0.072	2014	1130
	1	$2.70 \cdot 10^{-5}$	30	$4.02 \cdot 10^{-3}$	0.076	1795	1329
	1	$2.70 \cdot 10^{-5}$	45	$4.11 \cdot 10^{-3}$	0.077	1676	1448
	40	$9.76 \cdot 10^{-7}$	2	$3.40 \cdot 10^{-3}$	0.052	2201	751
	40	$9.76 \cdot 10^{-7}$	10	$3.79 \cdot 10^{-3}$	0.058	2014	915
	40	$9.76 \cdot 10^{-7}$	30	$4.02 \cdot 10^{-3}$	0.062	1795	1088
	40	$9.76 \cdot 10^{-7}$	45	$4.11 \cdot 10^{-3}$	0.063	1676	1189
Grass-roots plant	0.06	$2.89 \cdot 10^{-4}$	2	$3.40 \cdot 10^{-3}$	0.205	2201	2933
	0.06	$2.89 \cdot 10^{-4}$	10	$3.79 \cdot 10^{-3}$	0.211	2014	3299
	0.06	$2.89 \cdot 10^{-4}$	30	$4.02 \cdot 10^{-3}$	0.214	1795	3764
	0.06	$2.89 \cdot 10^{-4}$	45	$4.11 \cdot 10^{-3}$	0.216	1676	4055
	1	$2.30 \cdot 10^{-5}$	2	$3.40 \cdot 10^{-3}$	0.064	2201	917
	1	$2.30 \cdot 10^{-5}$	10	$3.79 \cdot 10^{-3}$	0.070	2014	1097
	1	$2.30 \cdot 10^{-5}$	30	$4.02 \cdot 10^{-3}$	0.074	1795	1292
	1	$2.30 \cdot 10^{-5}$	45	$4.11 \cdot 10^{-3}$	0.075	1676	1408
	40	$8.32 \cdot 10^{-7}$	2	$3.40 \cdot 10^{-3}$	0.052	2201	750
	40	$8.32 \cdot 10^{-7}$	10	$3.79 \cdot 10^{-3}$	0.058	2014	914
	40	$8.32 \cdot 10^{-7}$	30	$4.02 \cdot 10^{-3}$	0.062	1795	1086
	40	$8.32 \cdot 10^{-7}$	45	$4.11 \cdot 10^{-3}$	0.063	1676	1188

Table 5.7: Calculation of steam prices using the method of Ulrich and Vasudevan (2006)

Where:

m_s: Total auxiliary boiler steam capacity; P: pressure of steam; a, b: parameters in steam cost correlation, as given by Equations (5.2) - (5.4):

$$a = 0.000027\ m_s^{-0.9} \text{ (for process module)} \tag{5.2}$$

$$a = 0.000023\ m_s^{-0.9} \text{ (for grass-roots)} \tag{5.3}$$

$$b = 0.0034\ P^{0.05} \tag{5.4}$$

Steam cost correlation is recommended for $2 < P < 47$ bar and $0.06 < m_s < 40$ kg/s.

C_{fuel}, \$/gallon	2.2379	Nymex Heating Oil, September 2007
Higher Heating Value, GJ/m^3	38.739	Equivalent of 139000 Btu/gal corresponding to a No. 2 fuel oil of 33 A.P.I. and 1% sulphur, from Perry and Green (1998)
C_{fuel}, \$/GJ	15.3	
PCI	528.2	From Chemical Engineering Magazine, September 2007

Table 5.8: Fuel data and Plant Cost Index for Equation (5.1).

Table 5.9 and Table 5.10 contain the results of applying Equation (5.1) to calculate electricity and cooling water costs, respectively.

Basis	a	b	C_{uty}	$\boldsymbol{C_{uty}}$
	\$/kWh	\$/kWh	\$/kWh	\$/kWyr
Purchased from outside	$1.3 \cdot 10^{-04}$	0.010	0.221	1938
Onsite power (charged to module plant)	$1.4 \cdot 10^{-04}$	0.011	0.242	2118
Onsite power (charged to grass-roots plant)	$1.1 \cdot 10^{-04}$	0.011	0.226	1979

Table 5.9: Calculation of electricity prices using the method of Ulrich and Vasudevan (2006)

Basis	q	a	b	C_{uty}	$\boldsymbol{C_{uty}}$
	m^3/s	\$/m^3	\$/m^3	\$/m^3	\$/kWyr
Process module	0.01	$3.10 \cdot 10^{-03}$	0.003	1.683	2540
	1	$1.30 \cdot 10^{-04}$	0.003	0.114	173
	10	$1.03 \cdot 10^{-04}$	0.003	0.100	151
Grass-roots plant	0.01	$2.57 \cdot 10^{-03}$	0.003	1.403	2117
	1	$9.50 \cdot 10^{-05}$	0.003	0.096	145
	10	$7.25 \cdot 10^{-05}$	0.003	0.084	127

Table 5.10: Calculation of cooling water prices using the method of Ulrich and Vasudevan (2006).

Where:

q: Total water capacity; ΔT in cooling water: 5°C; a is calculated from Equations (5.5) and (5.6):

$$a = 0.0001 + 3.0 \,.\, 10^{-5} q^{-1} \text{ (for process module)} \tag{5.5}$$

$$a = 0.00007 + 2.5 \,.\, 10^{-5} q^{-1} \text{ (for grass-roots)} \tag{5.6}$$

The cooling water costing equation is recommended for use in the range $0.01 < q < 10$ m^3/s.

5.4.3 Utility cost selection

The cost estimates generated by the approach of Ulrich and Vasudevan (2006) are compared with data from various sources, including two industrial examples in Table 5.11.

	Source A			Source B		Source C	
	Ulrich and Vasudevan (2006) for 2007 grass-roots plant	Basis		2008 Asia/Pacific Plant	Basis	1995 UK Plant	Basis
Steam	Cost, GBP/t	m_s, kg/s	P, bar	Cost, GBP/t		Cost, GBP/t	P, bar
	25.56	40	2	20.27	LS (4.5 kg/cm^2, 690 kcal/kg)	8.7	4.5
	28.51	40	10	20.76	MS (11.5 kg/cm^2, 720 kcal/kg)	9.6	15
	30.21	40	30	22.37	HS (43.5 kg/cm^2, 760 kcal/kg)		
	30.84	40	45	23.92	XS (101 kg/cm^2, 800 kcal/kg)	10.2	40
Electricity	Cost, pence/kWh			Cost, pence/kWh		Cost, pence/kWh	
	11.04			3.22*		1.65* – 3.5**	
Cooling water	Cost, pence/t	q, m^3/s		Cost, pence/t		Cost, pence/t	
	4.11	10		3.22		0.97*** – 3.1***	

Notes: (*) Based on the availability of a combined heat and power system for power generation. (**) Cost of external electricity in 1995. (***) Cooling water price is highly dependent on the scale of the process.

Table 5.11: Different sources of operating costs for comparison.

Because of the different time and location of the data in Table 5.11, it is difficult to compare cost estimates across the columns of the table. However, relative ratios between data in the same column may be used as a valid basis for comparison between costing methods. The first observation from Table 5.11 is that the steam costs for Source A are 20-30% higher than those for Source B. Secondly, the steam costs of Source A are more strongly correlated to pressure levels than in Source B. This latter observation reflects stronger economics of electricity recovery between pressure levels in A than in B. Also, steam costs in Source A correlate to those in Source C by a factor of approximately three. The most notorious discrepancy between the various sources in Table 5.11 is observed for electricity costs, where Source A predicts an onsite power price (charged to grass-roots plant) which is mostly unrelated to the values in the other sources. The purchase power cost derived from Source A is

10.81 pence/kWh. Regarding cooling water costs, it is not clear how to derive any insights from this table.

In the following, the above observations are scrutinised against the BERR database. According to survey data of industrial users from BERR, the price of electricity in the 4th quarter of 2007 for large industrial users is of 5.17 pence/kWh and 4.47 pence/kWh for extra large users. These values are prices or electricity purchased by manufacturing industry in UK excluding the Climate Change Levy. Electricity prices for the 4th quarter of 2007 are at the same level as in 2005. According to the same source, the prices of electricity for the same 2007 period have increased by a factor of 1.445 with respect to the level in 1995. This takes the 1995 average electricity price for industrial consumers to 3.58 pence/kWh for large industrial users and 3.09 pence/kWh for extra large users, which is consistent with the electricity purchase cost of 3.5 pence/kWh in the far right column in Table 5.11 for a UK plant in 1995. Because cooling water costs may be related to electricity costs, the historic growth factor for electricity may be used to bring up to date cooling water cost past estimates. Electricity and cooling water cost estimates used in the case studies of Chapter 7 are not aligned with current electricity costs as the assumption is made that cheaper electricity is available internally from steam turbines. The prices applied to the case studies of Chapter 7 are given in Table 5.12.

In the same period (1995 to 2007, 4th quarter), the prices of coal, heavy fuel oil have grown by a factor of 1.313 and 3.134 respectively, based on a survey of the prices (excluding VAT) of fuels delivered to industrial consumers in UK. The price of gas based on the average unit value of sales to industrial customers (excluding VAT) doubled from 1995 to 2007. Because high pressure steam costs may be related to the prices of fuel, the fastest escalation of steam prices in comparison to electricity and cooling water may be explained by the higher rate of increase of fuels prices than of electricity prices. Medium and low pressure steam levels are often made

available through expansion of the high pressure steam through steam turbines. If this is the case, medium and low pressure steam costs depend on the cost of electricity. The steam prices selected in the case studies of Chapter 7 are shown in Table 5.12. The high pressure steam cost estimate from the heating oil combustion and a minimum boiler efficiency of 0.7 is relatively small (18.26 GBP/t) when compared to the values in Table 5.11. The values in Table 5.12 are favoured over the estimate from the boiler model. Hot water cost is estimated simply from a fuel calculation since additional heating is required to supply the required sensible heat to bring the utilised hot water to saturated conditions in the boiler.

	Cost, GBP/t	Cost, GBP/(kW.yr)	Source temperature, °C	Target temperature, °C
Hot water	0.31	233.0	100	90
LP steam (4.8 bar)	18.9	282.0	150	149
MP steam (15.5 bar)	19.4	315.0	200	199
HP steam (39.8 bar)	20.7	381.0	250	249
	Cost, pence/kWh	Cost, GBP/(kW.yr)		
Electricity	3.12	273.6		
	Cost, pence/t	Cost, GBP/(kW.yr)	Source temperature, °C	Target temperature, °C
Cooling water	1.56	23.6	25	30

Table 5.12: General utility costs for the case studies of Chapter 7.

5.5 Conclusions (ii) – Utility costs

A rational framework for selection of utility costs has been presented. The aim is to select meaningful utility costs for use in the case studies of Chapter 7, rather than to propose a holistic approach to the estimation of utility costs. Such an effort would be in vain due to the vast number of factors affecting utility costs.

Disparity between the various consulted sources has been systematically reconciled by mediation of fuel and electricity purchasing prices for UK industrial users as published by BERR. Finally, a set of utility costs and supply temperatures have been proposed for use in the case studies of Chapter 7.

An important feature of the proposed synthesis methodology lies in that it offers a systematic and quantitative framework to investigate the effect of the changes in the utility prices on the optimal process selection. In addition to assisting with the synthesis of the complete gas separation systems, also offers the operational advantage of optimising key operating variables for a fixed process configuration and updated input costs. Demonstration of these features will not be undertaken by the studies of Chapter 7.

Chapter 6. Optimisation framework

6.1 Introduction

The optimisation framework that supports the proposed synthesis methodology is presented in this chapter.

The background section of this chapter provides a review of some of the commonest optimisation methods utilised by existing synthesis approaches with emphasis on the principles of Simulated Annealing, SA. The grounds for selection of SA as the optimisation method for the present methodology work are then discussed. Finally, the adaptation of SA to the proposed synthesis framework is presented.

The proposed optimisation framework has been implemented in an alpha version (not released) of COLOM® (©CPI, University of Manchester 1985-2009). COLOM® is a software package for analysing distillation-based separation problems including column sequencing, column profiles, azeotropic distillation, dividing wall initialisation and steam stripping.

By virtue of this work, the capabilities of COLOM® are enhanced at various levels: (1) incorporation of absorption-desorption schemes to the synthesis framework; (2) improved distillation column modelling; (3) new heat integration framework based on interval decomposition; (4) extended SA to enable optimisation of sequences of absorption-desorption systems and distillation columns. The accommodation of these enhancements was the result of an extensive renovation of the Fortran77 platform that constitutes the foundations of COLOM®.

6.1.1 Optimisation problem statement

The separation synthesis problem may be formulated as an optimisation problem in which the objective function reflects the economy of the process.

In the proposed synthesis framework, the objective function may be selected from a set of options: (1) annualised capital costs; (2) annual operating costs; (3) total shaftpower; (4) total annual costs. Clearly, optimising for different objectives will generally lead to different designs. Additionally, distributing the capital cost over a longer or shorter period of time, imposed by the annualisation factor, will generally lead to different designs. In the case studies of Chapter 7, the total annual cost is employed as objective function.

The optimisation problem may be stated as follows:

Minimise:

Total Annualised Cost = Annualised Capital Cost + Annual Operating Cost

Subject to:

- Design specifications (recoveries)
- Conservation equations (material and enthalpy balances around the columns and the sequence)
- Equipment design equations

6.1.2 Degrees of freedom of separation system - Optimisation variables

The purpose of optimisation is to find the combination of optimisation variables that result in the minimum cost objective. These variables coincide with the design variables of the separation system and include: (1) parametric or discrete variables, such as the choice of sequence and the choice of separation technologies to perform each separation task; (2) continuous variables, such as the operating conditions in each of the separating columns, solvent flowrate and temperature.

Table 6.1 lists the variables involved, their types (continuous, discrete) and the levels of the flowsheet hierarchy where they apply. Table 6.1 shows, for example, that the primary column pressure is a variable that intervenes at column level and may apply to: (1) the distillation column of a distillation-based separation task; (2) the absorber column of an absorption-desorption separation task. The absorber boilup-to-feed ratio also intervenes at column level, but on the other hand, it is restricted to the absorber column of an absorption-desorption separation task.

	Sequence	Task		Column		
		Distil.	Abs. Des.	Distil.	Abs.	Des.
Sequence configuration (D)	x					
Separation type (D)		x	x			
Heat integration variable (C)	x					
Condenser type (D)				x		x
Reflux ratio scale-up factor (C)				x		x
Primary column pressure (C)				x	x	
Secondary column pressure (C)						x
Primary column feed quality (C)		x	x			
Secondary column feed quality (C)						x
Absorber boilup-to-feed ratio (C)					x	
Inlet solvent temperature (C)					x	
Solvent cooling partition temperature (C)			x			

Key: (D) = Discrete variable; (C) = Continuous variable.

Table 6.1: Flowsheet levels and task restrictions for optimisation variables in synthesis framework.

6.2 Background - Optimisation techniques

Optimisation-based methods provide a systematic framework for a variety of process synthesis problems. While significant progress has been made in optimisation in areas such as nonlinear and mixed-integer optimisation, difficulties arise with large problem sizes. Floudas *et al.* (2005) reports on the recent progress in global optimisation.

6.2.1 (i) Deterministic methods

Of all deterministic or algorithmic methods, Mixed Integer Non-Linear Programming (MINLP) is suited to common synthesis problems because it explicitly accounts for non-linearities in models equations and can handle discrete variables related to the topology of the process. Candidate synthesis problems are characterised by the implementation of logical decisions via binary variables, which appear in the model equations. Only linear terms are allowed for the binary variables within the formulation of the MINLP problem. MINLP formulations, however, may include non-linear model equations of continuous variables, such as mass and heat balances and equipment sizing equations.

Typical methods for solving MINLP problems include the Branch and Bound method, more common of the Mixed Integer Linear Programming (MILP) problems, with the added difficulty of a less efficient solution strategy than for MILP problems, due to the presence of non-linear equations (Grossmann and Kravanja (1995)). MINLP problems may also be approached by standard methods such as Outer-Approximation, Generalised Benders, and Extended Cutting Plane (Biegler and Grossmann (2004)). These methods are based on the decomposition of the MINLP problem into Non Linear Programming (NLP) and MILP sub-problems, which are solved iteratively, as shown in Figure 6.1.

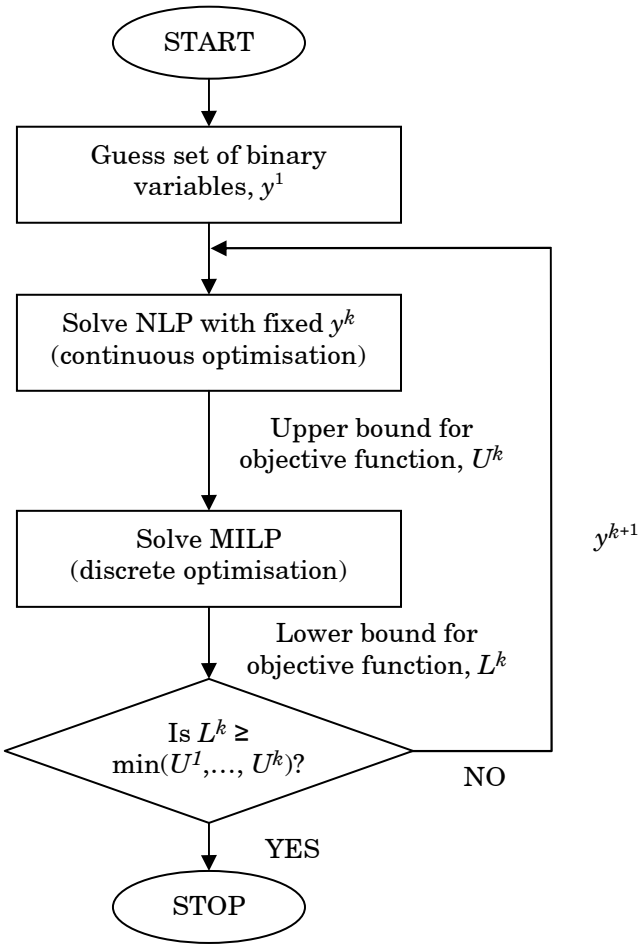

Figure 6.1 MINLP solution procedure by decomposition methods for minimisation problems.

As these methods rely on solving consecutive NLP problems, and these partial solutions are based on gradient information, if the problem is non-convex, then the convergence to the global optimum is not guaranteed.

Conventional MINLP methods are slow and calculation intensive, as for every NLP subproblem solution, a linear approximation must be formulated and solved as a MILP subproblem. The complexity of the problems escalate with the number of binary and continuous variables.

Generalised Disjunctive Programming (Türkay and Grossmann (1996)) was introduced as an improvement over MINLP models for representing discrete/continuous optimisation problems. Barnicki and Siirola (2004) refer to Generalised Disjunctive Programming as a major advance in the resolution of the superstructure optimisation problem.

6.2.1 (ii) Stochastic methods

Stochastic optimisation methods were devised as an alternative to conventional MINLP methods to overcome non-convergence issues, reduce mathematical complexity and offer flexibility for optimisation of a wider range of optimisation problems.

Stochastic methods rely on statistics to randomly explore the solution space; therefore, local information in the form of mathematical gradients for the problem of interest is not required. In effect, stochastic methods perceive the optimisation problem as a black box with inputs and outputs. The search mechanism is supported by the values of the objective function at different points of the search space. Consequently, discontinuous or non-differentiable problem formulations, impenetrable by mathematical programming approaches, can be tackled by stochastic methods. The black box feature allows total independence between the optimiser and the problem under optimisation. As a result, large and complex simulation models can be solved without affecting the optimisation robustness.

Importantly, most stochastic algorithms incorporate control mechanisms in the form of logical conditions to avoid converging to local optima, making these methods ideal for optimising nonconvex problems. An advantage of stochastic methods over deterministic methods is that the performance of the search is independent of the starting point. Stochastic methods, however, do not offer a guarantee of finding the global solution.

Common stochastic methods include Hill-Climbing, Genetic Algorithms (GA) and Simulated Annealing (SA). This categorisation is provided by Michalewicz (1994).

Hill-Climbing, also known as *greedy* Descent algorithms, generally fail to find the globally optimal solution, because they usually do not operate exhaustively on the entire optimisation space. They commit to certain choices too early, which prevent them from finding the best overall solution as the algorithm progresses.

GA methods are a class of evolutionary optimisation methods that use techniques inspired by evolutionary biology such as inheritance, mutation, selection, and crossover. GA methods are based on population-based approaches, governed by the principle of evolution or survival of the fittest. While hill-climbing and SA generate new candidate points in the neighbourhood of the latest solution, GA allow the examination of points in the neighbourhood of two or more solutions. GA is robust and efficient in large-scale parallel search in large and irregular search spaces.

Simulated Annealing (SA) is a popular stochastic optimisation algorithm due to its ease of implementation and to its robustness. SA is suited to diverse problem types, where the conventional mathematical approaches generally fail. SA has been applied to various problems related to synthesis and optimisation of process systems (Rodriguez (2005), Marcoulaki and Kokossis (1996), Marcoulaki and Kokossis (1998), Dolan *et al.* (1989)). As with other stochastic optimisation methods, SA does not

guarantee finding the global solution. However, it may be proved that SA will converge to a globally optimal solution given infinitely large number of iterations and a temperature schedule that converges to zero sufficiently slowly (Hajek (1988)).

The SA algorithm is relatively easy to implement in a systematic optimisation framework in comparison to other optimisation methods. Its greater flexibility with respect to the number and type of optimisation variables, including continuous and discrete variables, is linked with minimal modifications to the optimisation framework under circumstances that recommend changes to the models, objective function or the number of optimisation parameters.

6.2.2 Simulated Annealing

SA is named after the metallurgic process of metal annealing it resembles. In this process, a metal is subjected to high temperatures, and once it has melted it is then allowed to cool very slowly. In the melted state, the system is characterised by total disorder, with the metal atoms distributed randomly. As cooling takes place, the entropy of the system decreases and the system becomes more ordered. If cooling is carried out so slowly that the process is reversible, the metal will finally crystallise into a stable minimum energy structure. However, if cooling does not take place slowly enough or if the initial temperature is not high enough, then the metal forms a glass-like metastable structure with higher energy than the crystalline state. The analogies between the cooling process and the mathematical optimisation become obvious when the undesirable metastable state and the minimum energy structure are interpreted as a local and global minimum, respectively. These analogies were first observed by Kirkpatrick *et al.* (1983), who then proposed the application of the simulated annealing procedure in large optimisation problems.

Metropolis *et al.* (1953) developed a method to determine stable equilibrium configurations of groups of atoms at given conditions. Starting at the initial melting temperature, the basic step of the Metropolis algorithm is performed by perturbing the current configuration of the system and computing the change in the energy of the system, ΔE. If the change in energy is negative, the new configuration is accepted and used as starting point for the next step. However, if the change in energy is positive, it is accepted with a probability given by Equation (6.1), which is analogous to the Boltzmann equation.

$$P = exp\left(\frac{-\Delta E}{T_a}\right) \tag{6.1}$$

Where T_a is the annealing temperature of the system.

It becomes apparent from Equation (6.1) that the probability of accepting any positive change decreases with the temperature of the system, and small positive changes are more likely to be accepted than large changes. The temperature of the system then decreases according to a particular cooling schedule and new perturbations are evaluated during the cooling process. The algorithm terminates when the temperature of the system reaches the temperature of the solid state.

The Metropolis algorithm may be directly incorporated into the SA method for optimisation of combinatorial problems, by establishing the following analogies. The current state of the thermodynamic system corresponds to the current values of the optimisation variables and the energy of the system corresponds to the objective function. The Metropolis algorithm was employed by Kirkpatrick *et al.* (1983) when they first devised the use of SA as an optimisation strategy. Very much like its physical equivalent, a number of factors govern the progress of the SA, including the initial and final annealing temperatures and the cooling schedule. SA inherits the nomenclature of the equivalent parameters from the physical

annealing process. An adequate, high initial value of the annealing temperature, T_a, is a key SA input parameter.

The optimisation process starts with an initial feasible location in the optimisation space. The next solution is then selected from the optimisation space by a random change, or move, from the current solution. The calculated objective function of the new solution is compared with the objective function of the current trial solution and accepted or rejected depending on the magnitude of the change and the current temperature in the cooling schedule. The Metropolis acceptance criterion may be used for this purpose. A number of trial solutions will usually be explored and accepted or rejected, before the annealing temperature is reduced, in order to obtain the best solution at each point of the cooling schedule. The exploration of the optimisation space then continues at a lower annealing temperature by the process already described. The algorithm stops when a certain termination condition is met. The termination and acceptance criteria may be adapted to different problems. Types of termination and acceptance criteria are presented in 6.2.2 (i).

The initial and final annealing temperatures, the cooling schedule and the number of iterations performed at each temperature have also an important affect on the performance of SA. Similarly to its physical equivalent, a simulated annealing procedure may end prematurely at a suboptimal solution if the initial temperature is not high enough or it is reduced too quickly. Insufficient number of perturbations at each point of the cooling process may also lead to an inferior solution. On the other hand, an excessively high initial temperature or a cooling process that takes place too slowly may result in unnecessarily high computation time. Criteria for the selection of a suitable annealing schedule are discussed in more detail in 6.2.2 (i).

An important feature of SA with Metropolis acceptance criterion is that it helps to prevent local optimum convergence by occasionally accepting

moves that do not improve the objective function, known as uphill moves in minimisation problems. In accordance to Equation (6.1), a small deterioration of the objective function increases the chances of uphill moves being accepted. Downhill moves are always accepted. In addition, the probability of accepting uphill moves is greater at the start of the optimisation, when the annealing temperature is high; the method accepts most of the moves and behaves as a pure random search. In contrast, as the annealing temperature approaches its final value, very few uphill moves are accepted and the algorithm behaves as a *greedy* Descent method (also known as Hill-Climbing method in maximisation problems). The performance of the SA algorithm may be improved by comparing each new solution to the best solution found so far.

6.2.2 (i) Annealing schedule parameters

The annealing schedule is characterised by the initial annealing temperature, the acceptance criteria, the cooling schedule, the Markov chain length and the termination criteria. The performance of the SA algorithm is greatly affected by the selection of these parameters, which is targeted at balancing solution quality with optimisation time. In the following, some guidelines for annealing parameter selection are provided.

- *Initial annealing temperature*

The optimal initial annealing temperature depends on the nature of the problem and the scale of the objective function. Excessively high temperatures will unnecessarily elongate optimisation times. However, in accordance with Equation (6.1), excessively low temperatures will restrict the number of accepted uphill moves, thus limiting the ability of the method to escape from local optima.

Van Laarhoven and Aarts (1987) propose an approach to selecting initial annealing temperatures:

$$T_{a0} = -\frac{\Delta f_{avg.}}{ln\, p_0} \tag{6.2}$$

Where $\Delta f_{avg.}$ and p_0 represent, respectively, the average deterioration of the objective function for uphill moves in a run where all the uphill moves are accepted and the desired initial acceptance probability. An initial acceptance probability of around 0.8 is recommended.

Another criterion consists in setting initial annealing temperature to ten times the maximum change in the value of the objective function between any two consecutive configuration moves (Athier *et al.* (1997)).

- *Acceptance criterion*

Acceptance criteria control the acceptance or rejection of trial moves. Among the most popular acceptance criteria of the literature are the Metropolis criterion (6.2.2), the Glauber criterion (Glauber (1963)) and the Threshold Accepting criterion; however there is no sufficient evidence to suggest the superiority of one criterion over the others. In this work, the original Metropolis acceptance criterion is used.

The Glauber criterion is characterised by not accepting all the downhill moves. Both uphill and downhill moves are accepted with the probability function given by Equation (6.3).

$$P = \frac{exp\left(\frac{-\Delta E}{T_a}\right)}{1 + exp\left(\frac{-\Delta E}{T_a}\right)} \tag{6.3}$$

For high annealing temperatures, the Glauber criterion accepts downhill and uphill moves with approximately the same probability. The reduction of the annealing temperature drives the probability of uphill and downhill moves in opposite directions.

The Threshold Accepting algorithm was introduced by Dueck (1990) as an alternative version of the SA algorithm that do not feature the annealing temperature parameter. Acceptance of uphill moves is confirmed by the deterioration of the objective function being confined within a specified threshold, which decreases as the search proceeds.

- *Cooling schedule*

The cooling schedule controls the reduction of the annealing temperature. The speed of the cooling process must be adequate to preserve the algorithm's ability to escape local minima while preventing the optimisation time from escalating unnecessarily.

In the exponential schedule of Kirkpatrick *et al.* (1983), the annealing temperature is reduced by a constant percentage in each step. Typical reduction percentages range from 5% to 20%.

Van Laarhoven and Aarts (1987) propose a cooling schedule whereby the annealing temperature at a given time, $T_{a,j+1}$ is related to the value of the previous iteration, $T_{a,j}$, by Equation (6.4):

$$T_{a,j+1} = \frac{T_{a,j}}{1 + \frac{T_{a,j}\, ln(1+\theta)}{3\sigma}} \tag{6.4}$$

Where θ is a cooling parameter, which is indicative of the cooling speed and is typically selected in the range of 0 to 0.05; σ represents the standard deviation of the values of the objective function achieved at temperature $T_{a,j}$.

- *Markov chain length*

In the SA algorithm, the set of moves executed at each temperature corresponds to a Markov Chain and the number of these moves is known as the Markov Chain Length.

The length of the Markov must be adequate to explore the search space sufficiently without leading to an excessive solution time.

The optimal Markov chain length depends on the type and dimensionality of the problem being solved. The Markov chain length is commonly chosen to be a multiple of the dimensionality of the problem.

An additional condition may be imposed with the purpose of limiting the number of moves performed at each temperature level by overriding the Markov chain length. This condition instigates the decay of the annealing temperature when the number of accepted configurations reaches a fraction of the Markov chain length, typically half of it. This condition has a minimum impact on the method's performance.

- *Termination criteria*

These criteria are employed to detect convergence of the algorithm and to control the completion of the optimisation. Commonly, interruption is triggered when the annealing temperature reaches the specified final annealing temperature, or when no moves are accepted after a given number of temperature iterations, typically ten.

6.3 Choice of optimisation method

The occurrence of non-linear terms in the modelling equations (polynomial, exponential and logarithmic terms) and the logical decisions embedded into discrete optimisation variables contribute to the high complexity of the optimisation problem that supports the proposed synthesis framework.

In the present synthesis problem, under certain ranges of optimisation variables, model equations may fail to reconcile column design with the material balances around the separation. This is direct consequence of separation infeasibility. In optimisation terms, it is a case of violation of the equalities representing the column models. Separation infeasibility causes the optimisation space of the present synthesis problem to be discontinuous.

Traditional deterministic optimisation methods have shortcomings that render them unsuitable for the proposed synthesis framework. Deterministic methods are restricted to problems where the equations in the mathematical formulation of the problem are continuous and differentiable. Additionally, because deterministic optimisation is gradient based, convergence of non-convex problems to a global optimum may not be achieved.

In contrast, SA, the optimisation adopted in this work, is less prone to converging to suboptimal solutions by not relying on local gradient information. The robustness of this method makes it appropriate to deal with the highly non-convex model equations and the irregular optimisation domain.

6.4 Implementation of the SA

6.4.1 SA moves and probabilities

The SA implementation requires defining the optimisation variables and the probabilities associated with perturbing each variable. For each variable in the optimisation space, continuous and discrete, an SA "move" is proposed. Each move has an allocated parameter which represents the probability of the SA perturbing the variable associated with the move at every point during annealing. Figure 6.2 illustrates the transition between two consecutive states during SA. The probabilities of the moves in the

optimisation framework add up to one. In every iteration, a random number is generated, which is then translated into a corresponding move.

Move probabilities relates to the exhaustivity of the search algorithm across the associated variable range. Since the sum of the probabilities is the unity, increasing one move's probability demands a reduction of the other moves probabilities. Qualitatively, low probability in a move constrains the search in the associated variable range, and makes it more difficult to explore the trade-offs where this variable is involved. It is then justifiable to select a small probability for those variables to which the objective function is less sensitive. To a large extent, the effect of lowering the probability of one or more moves, may be compensated by a less pronounced cooling schedule or a higher initial temperature.

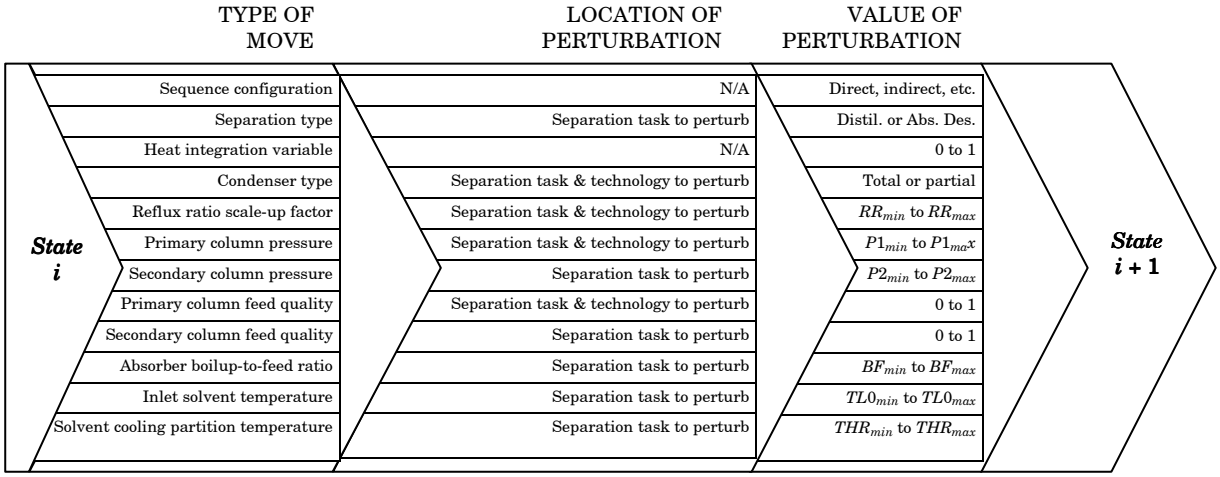

Figure 6.2: Perturbation of state *i* during SA leading to state *i* + 1.

6.4.2 SA parameter tuning

With reference to the SA principles introduced in section 6.2.2, the customisation of the annealing algorithm involves the selection of an annealing schedule, which has been introduced in section 6.2.2 (i). The selection of adequate annealing parameters, such as the initial and final annealing temperatures, the length of the Markov chain and the cooling

parameters, is problem-specific and needs to be carried out by trial and error.

The annealing history is a graphical representation of the objective function versus the logarithm of the annealing temperature (Figure 6.3) and provides useful feedback for selection of annealing parameters.

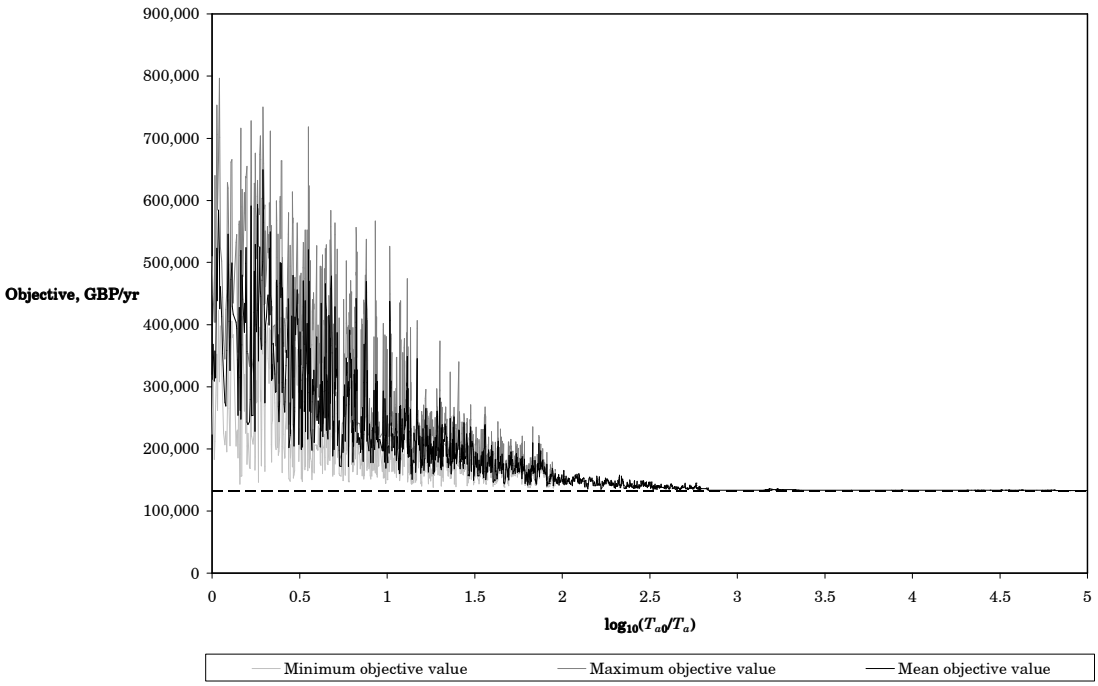

Figure 6.3: Example of SA annealing history.

Important fluctuations of the objective function are usually registered in the beginning of the SA, where the vast majority of moves is accepted. This behaviour may be observed in Figure 6.3. As the SA progresses, any move that incurs in a deterioration of the objective function is rejected with a greater probability, as a result of which the curve tends to settle towards the optimum objective value achieved so far. Near the end of the SA, only the moves that improve the objective function are accepted, which resembles the behaviour of *greedy* algorithms.

Different annealing strategies are required to acquire confidence in the global optimality of the solution. A low initial annealing temperature

coupled with a fast cooling schedule may sometimes be sufficient to enable a superficial investigation of the sensitivity of the objective function to the different variables, which may be used to readjust the probabilities of the moves accordingly. For general multivariable problems, however, the range of options explored at the end of a fast SA run represents just a small fraction of the total optimisation space. Starting with a fast annealing schedule, the trial and error procedure for SA parameter tuning involves adjusting SA parameters iteratively and evaluating the resulting SA annealing history. The adequate set of parameters is such that results in a smooth sigmoid curve, which is characteristic of an adequately converged SA run.

The effect of the annealing strategy on the annealing history is illustrated by the case study in section 8.2.4 (i).

6.5 Conclusions

This chapter has presented the key features of the developed framework that supports the proposed synthesis methodology. The challenging nature of the synthesis problem, which involves continuous and discrete of variables and complex models, make SA, a stochastic method, the ideal candidate to solve this problem. Design and implementation issues of the SA algorithm to the current synthesis framework have been discussed. Despite the existing recommendations for SA parameter selection, the tailoring of the SA to a particular optimisation problem requires trial and error.

Chapter 7. Flowsheet design methodology

This section briefly summarises the features of the implemented structure of the developed flowsheet design methodology in the optimisation framework within COLOM® (©CPI, University of Manchester 1985-2009).

It is important to highlight that the methodology for flowsheet design developed in this work is hierarchical. The different levels in the methodology operate in sequence to generate the design of a flowsheet configuration that achieves the required separation objectives. The steps of this methodology are shown in Figure 7.1.

Being this methodology hierarchical is not in conflict with the simultaneous optimisation of all levels of the separation system. This may be better understood by recalling that the hierarchy of flowsheet design is executed once in each iteration of the optimisation for the given set of design variables imposed by the optimiser.

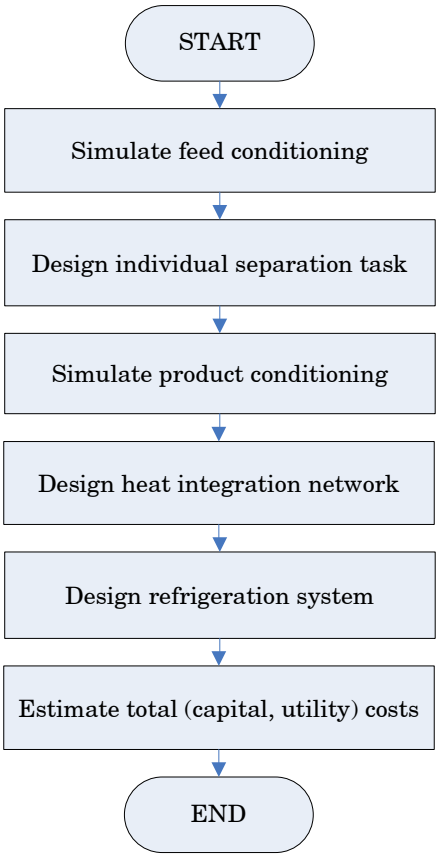

Figure 7.1: Architecture of flowsheet design methodology within the optimisation framework

7.1 Feed and product conditioning

The sequence level of the design methodology is concerned with the accommodation of each proposed separation task in the separation sequence. The articulation of the connections between adjacent separation tasks in the sequence is achieved by adjustment of the task feed and product conditions.

Column feeds pressures are adjusted to the column pressure by allowing for pressure changers (pumps, valves, compressors, expanders) to prevent flashing in the column. No allowance is made for pressure drop within the column.

In this methodology, electricity is always recovered from gas expansion, regardless of the quantity of recoverable energy. A more flexible approach would allow the option to recover electricity or to not recover it, i.e. by letting the vapour down through a throttle valve, due to the trade-off between electricity production and the high capital cost of turbines.

7.2 Modelling of separation tasks

This level accomplishes the design of the separation columns in the sequence, including distillation and absorption-desorption blocks. The model of the distillation column is described in section 3.7. Absorption-desorption require the multilevel design methodology of section 3.4 for characterisation of internal block streams. Column design within absorption-desorption blocks is carried out in accordance with the modelling strategy presented in section 3.9. Heat exchanger information, including duties, temperatures and pressures are also generated at this level.

7.3 Heat integration

The heat integration methodology is executed according to the principles described in section 4.4.

A partition temperature representing the limit for above-ambient cooling will be used throughout.

7.4 Refrigeration system design

The shortcut design of the refrigeration system is carried out in accordance to the principles introduced in 4.5.

7.5 Flowsheet cost evaluation

The cost of the separation sequence, including the capital and operating costs of the separation tasks and the feed/product conditioning is calculated in compliance with the basis presented in Chapter 5.

7.6 Physical and thermodynamic property prediction

The retrieval of physical and thermodynamic properties during the execution of the flowsheet design methodology takes place during most phases of the methodology, including: Feed and product conditioning, modelling of separation tasks and refrigeration system design. This is illustrated in Figure 7.2.

The Fortran77 platform hosting the developed synthesis methodology communicates during optimisation with the physical property engine of Aspen Properties© through an Aspen Properties Definition file (extension appdf.). This file contains a list of the chemical species relevant to the problem (including the solvent but excluding the refrigerants, if other than the components in the feed). It also contains the choice of property method or property package for flash calculations and thermodynamic functions calculations. The flow of information is bidirectional: Fortran sends a query to the property calculation engine and this sends a response back to Fortran. A separate file is required that contains the identity of the available candidate refrigerants in the problem and the selection of the refrigerant property method.

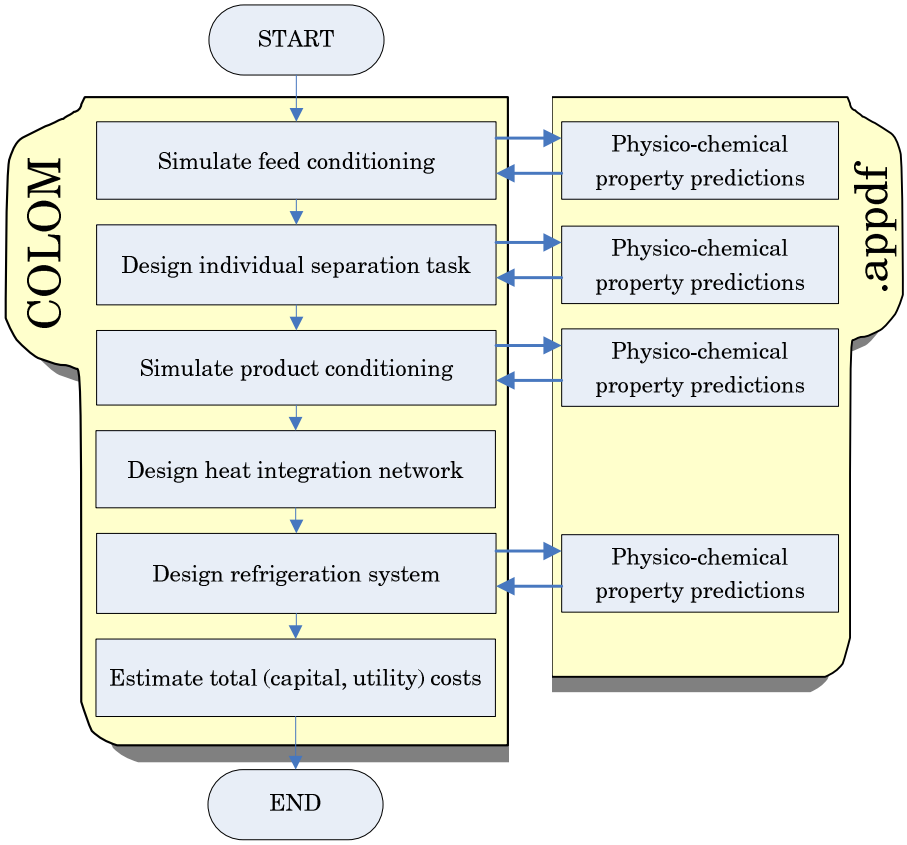

Figure 7.2: Architecture of the interaction between the design methodology in Colom® and the external property calculations in Aspen Properties©

Chapter 8. Case Studies

8.1 Introduction

The proposed synthesis methodology provides a quantitative framework for evaluation of preliminary separation flowsheet configurations and key operating variables. The use of the presented methodology is illustrated through the examples in this chapter.

In the first example, the synthesis methodology is applied to a natural gas feed that is split into three products. Optimisation of the two-split separation sequence is performed. In the second example, the synthesis methodology is applied to the separation of a refinery gas stream into two products. The case studies are structured into various sections, which are summarised below.

8.1.1 (i) Fixing feed and product conditions

To compare design options on a consistent basis, it is necessary to define the process boundaries, including the conditions of the feed and products. This allows for quantitative evaluation of design options against the cost of transforming a given feed into a unique product set.

In some cases, fixing the temperature and pressure of a product stream is an artificial constraint that is not forced on the real process. If these artificial constraints are not chosen carefully, they may incur in an inflated operating cost for the separation system, which may distort the comparison between the options. This is due to the destruction of integration opportunities within the process, which leads to excessive utility requirements.

8.1.1 (ii) Validation of results

This part involves validating the integrity of the annealing history of the converged optimisation solution and that of the flowsheet solution.

Firstly, the validity of the annealing history is assessed against the criteria presented in section 6.4. However, the optimality of the solution does not admit rigorous validation by the current available process synthesis tools. The relative position of the best solutions in the optimisation results is difficult to validate due to the lack of standarised capital cost estimation methods, as discussed in Chapter 5. The low level of detail of the generated flowsheet solutions contribute to the relativity of capital costs. However, the energy demands of the flowsheet solution may be validated using commercial process simulation software. The validation of the separation models was accomplished in Chapter 3.

8.1.1 (iii) Analysis of results

The optimisation framework has the capacity of storing and reporting the best configuration and a set of sub-optimal separation configurations ranked by the scale of the objective function. For instance, for a 3-product optimisation problem, a maximum set of eight best separation configurations is stored. In this chapter, the different solutions are compared on the basis of energy demands and total costs. The distribution between the various cost components (e.g. capital versus operating, compressors versus columns, etc.) is discussed. Emphasis is placed on the analysis of key variables, trade-offs and differences between the various configurations.

8.2 Case 1: NGL recovery from natural gas

As stated in Chapter 1, natural gas primarily consists of methane but it additionally contains NGL components including ethane, propane, butanes and C5+.

Historically, there has been an economic incentive to recover NGL from the natural gas, due to the higher value of the recovered NGL components as feedstock over their fuel value as natural gas components. The main market for ethane is ethylene production, where ethane feeds are traditionally the most cost-effective due to the generation of fewer byproducts in comparison to naphtha feeds (Farry (1998)). On the other hand, there is an ample field of application of C3+ LPG as a valuable feedstock for petrochemicals production. These economic incentives motivate the installation of NGL recovery units.

8.2.1 Background

A preliminary study for the incorporation of a new NGL recovery unit in a Saudi gas plant was conducted by Mehra (2001). The natural gas feed to this site contains 10-12% of C2+ NGL, which differentiates it from the generally leaner gas being produced in North America and the North Sea. This latter natural gas contains a maximum of 8% of C2+ NGL for associated gas that coexists with crude oil in the natural gas deposits. According to Mehra (2001), at high C2+ concentrations absorption-desorption is a more competitive separation option and may be more cost-effective than cryogenic distillation following turboexpansion.

Mehra (2001) investigates two licensed process technologies based on cryogenic distillation and absorption, respectively. While this paper provides a qualitative discussion on the configuration of the considered LPG recovery processes and on the flexibility of these to operate under various scenarios, the quantitative evaluation of the interactions between capital and operating costs is very limited.

8.2.2 Aims

This case study aims at the design of an optimised NGL recovery system by application of the proposed synthesis methodology. This application needs to establish the optimal configuration and operating conditions of

the fractionation sequence including demethanisation at 97.5% of methane recovery and 86% of ethane extraction. The LPG recovery unit operates at a 98% propane recovery in the heavy product.

8.2.3 Problem inputs

The feed composition for Case Study 1 is presented in Table 8.1. Heavier components than butane are artificially eliminated from the feed in order to conform to the limitations of the developed methodology. These limitations are relative to the selected solvent for any featured absorption-desorption separation tasks. The choice of solvent for Case Study 1 is pure n-pentane. Additionally, carbon dioxide is ignored due to the complications introduced by the presence of a component situated between the key components in the scale of volatility.

The recovery specifications are provided in Table 8.2. The feed is available as a vapour at the pressure of 31.03 bar and temperature of 25°C. Table 8.3 provides the specified feed and product conditions.

The Peng-Robinson property prediction method in Aspen Properties® is applied throughout. This equation-of-state property method is selected on the basis of low to moderate pressure gas processing.

	Actual gas feed composition, mol%, Mehra (2001)	Modified composition for optimisation, mol%
Nitrogen	6.23	6.37
Methane	80.86	82.64
Carbon Dioxide	1.71	0.00
Ethane	6.98	7.13
Propane	2.61	2.67
Isobutane	0.43	1.20
n-Butane	0.74	0.00
Isopentane	0.18	0.00
n-Pentane	0.15	0.00
n-Hexane	0.06	0.00
n-Heptane	0.05	0.00
Total	100	100
Flow, kmol/h	4109	4109

Table 8.1: Original gas feed composition and manipulated composition for case study.

	Component recovery in products		
	A	B	C (DE)
Nitrogen	1	0	0
Methane	0.975	0.025	0
Ethane	0.14	0.835	0.025
Propane	0	0.02	0.98
Isobutane	0	0	1
n-Pentane	-	-	-

Table 8.2: Recovery specifications for 3-product separation problem.

	Feed	Products		
	ABC (DE)	A	B	C (DE)
Temperature,°C	25	35	35	35
Pressure, bar	31.026	72.395	72.395	72.395

Table 8.3: Specified temperature and pressure of feed and products.

The specified values of the various design constants employed by the synthesis framework are compiled in Table 8.4.

Economic constants	Annualisation factor	3 yr
	Rate of interest	0
	Number of operating hours	8600 hr/yr
	Cost correction factor (CEPCI)	1.4678
Column design constants	Tray space	0.46 m
	Top space	2 m
	Bottom space	2 m
	Tray efficiency	0.7
Compression efficiency	Compressor isentropic efficiency	0.8
	Pump mechanical efficiency	0.9
	Carnot cycle efficiency	0.4
Temperature approaches	Above ambient	10°C
	Refrigeration (evaporators)	3°C
	Refrigeration (condensers)	4°C
	Refrigeration (cascade partition)	4°C

Table 8.4: Design constants for case study.

Table 8.5 and Table 8.6 present the assigned probabilities to the different optimisation moves and the imposed optimisation boundaries for each move. For low-temperature distillation columns, the lowest pressure specification is generally imposed by the coldest available refrigeration level, as when the pressure decreases, a lower temperature is needed to condense the overhead vapours into a reflux. Information on typical refrigeration levels and temperatures can be found elsewhere (Wang (2004)).

	Minimum	Maximum	Default	Move probability
Heat integration variable	0	1	0	0.1248
Reflux ratio scale-up factor	1.1	5	1.1	0.0633
Primary column pressure	10	29	12	0.1248
Secondary column pressure	10	29	10	0.1248
Primary column feed quality	0	1	0	0.0316
Secondary column feed quality	0	1	1	0.1248
Absorber boilup-to-feed ratio	0.2	2	1.4	0.1248
Inlet solvent temperature	-30	-15	-16.638	0.1248
Solvent cooling partition temperature	45	190	70	0.0000

Table 8.5: Optimisation range of continuous variables and move probabilities.

	Mode 1	Mode 2	Default	Move probability
Sequence configuration	Direct	Indirect	Indirect	0.0000
Separation type	Distil.	Abs. Des.	Distil.	0.1248
Condenser type	Partial	Total	Partial	0.0316

Table 8.6: Optimisation range of discrete variables and move probabilities.

The probability of the move representing the sequence configuration is zero, as shown in Table 8.6. This implies that the sequence configuration was kept fixed during optimisation. To allow for exploration of the two different sequence configurations, two separate optimisation runs were executed, each one of them featuring a different fixed sequence configuration.

Because below ambient cooling generally requires external refrigeration, it may be advantageous to set a solvent partition temperature upfront. The solvent cooling partition temperature is given by:

$$T_{solvent\ cooling\ partition} = T_{CW} + \Delta T_{min} \tag{8.1}$$

Where T_{CW} is the cooling water supply temperature and ΔT_{min} is the minimum temperature approach for above-ambient heat matches.

Since the heat integration methodology employed by the optimisation framework is robust and handles successfully wide temperature ranges, it is not necessary to optimise the partition temperatures, which could increase optimisation time, hence the zero probability of the partition temperature in Table 8.5.

8.2.4 Results and discussion

8.2.4 (i) SA parameter tuning

The principles of selection of an adequate set of Simulated Annealing parameters are introduced in section 6.4.2. The strategy for tuning of SA parameters is applied to this case study with the purpose of achieving a satisfactory exploration of the search space that endorses the optimality of the solution.

Starting with a fast annealing schedule, the different SA parameters are systematically adjusted to improve the annealing history. Table 8.7 displays information on the tests conducted for optimisation of the direct sequence and the key SA termination results. In all cases, optimisation terminates ahead of the final annealing temperature due to consistent move rejection over the final Markov chains.

	Test (i)	Test (ii)	Test (iii)	Test (iv)	Test (v)
Initial temperature	$5{\cdot}10^5$	**$5{\cdot}10^6$**	$5{\cdot}10^5$	$5{\cdot}10^5$	$5{\cdot}10^5$
Final temperature	0.02	0.02	0.02	0.02	0.02
Cooling parameter	0.05	0.05	**$5{\cdot}10^{-3}$**	**$5{\cdot}10^{-3}$**	**$5{\cdot}10^{-3}$**
Markov chain length	20	20	20	**30**	**40**
Maximum no. of failed chains	10	10	10	**30**	**20**
Termination cause	*Maximum number of failed chains reached*				
Termination temperature	12.43	35.73	8.63	4.16	0.83
Run time (hh:mm:ss)	00:42:16	00:50:42	04:26:37	06:18:26	19:13:11
Optimal objective	7,692,077	7,703,292	7,667,276	7,665,753	7,665,600

Table 8.7: Trial and error SA parameter tuning for case study 1.

As the speed of the cooling schedule is reduced and initial annealing temperature is increased, the SA is capable of exploring a larger number of trial solutions in a wider region of the optimisation problem, thus, the probability of finding a solution near the global optimum increases.

The annealing history offers valuable insights regarding SA convergence. Typical annealing history plots display the progression of the optimisation objective during the cooling schedule in a logarithmic scale. To orientate the annealing history along the positive x-axis, the decimal logarithm of the annealing temperature is replaced with the logarithm of the ratio of

the initial annealing temperature to the local annealing temperature. Figure 8.1 displays the annealing history of Test (i). Only one point per Markov chain is shown in the annealing history. For clarity, these points have been connected with straight lines. The different trends shown in Figure 8.1 represent the average, the maximum and the minimum of the accepted moves within the consecutive Markov chains.

Figure 8.1 suggests that the optimisation problem may not have been sufficiently explored due to the scarcity of the history datapoints. The irregular shape of the trend is an indicative of a premature annealing completion.

In Test (ii), the initial annealing temperature was increased by a factor of ten, while the other parameters remained at their values of Test (i). However, this had an insignificant effect on the execution time as per Table 8.7; hence, the higher initial temperature does not lead to a substantially improved exploration of the optimisation problem. This result also transpires from Figure 8.2. The above comments regarding the shape of the trend of Figure 8.1 extend to Figure 8.2. Contrary to expectations, the final objective value achieved in Test (ii) is marginally higher than that of Test (i), as shown in Table 8.7. Because of the random nature of the SA algorithm, the set of trial solutions of any given test is unique. Hence, longer optimisation times do not necessarily lead to solution improvements.

Test (iii) subsequently investigates the reduction of the cooling parameter by one order of magnitude, and thus, of the consequent cooling deceleration with respect to the annealing schedule of Test (i). The slowing of the annealing schedule multiplies the computation time by a factor of six. The corresponding annealing history, as shown in Figure 8.3, starts resembling the typical pattern of robust annealing strategies. With regards to the objective function, despite the important scalation of computation time, Test (iii) only achieves a 0.3% solution improvement

with respect to Test (i). It appears that Test (i) and Test (ii) were progressing towards the same optimum than Test (iii) is pointing to. It is not always the case that inadequate annealing schedules lead to a solution in the proximities of the global optimum. Often these schedules converge to local optima.

Test (iv) consequently investigates a 50% increase in the length of the Markov chain, with respect to the annealing schedule of Test (iii). Larger Markov chains contribute to a more comprehensive exploration of the optimisation problem than previous tests. This results in a computation time increase in the vicinity of 50%, as shown in Table 8.7, leading to a steadier convergence than previous tests, as shown in Figure 8.4. Generally, the annealing history of Test (iv) may be regarded as acceptable for SA tuning.

A final test, Test (v), is conducted with a 33% increased length of the Markov chain. The achieved SA annealing history of Figure 8.5 is smooth and regular at the expense of a dilated optimisation time. Final objective of Test (v) is marginally improved with respect to Test (iv).

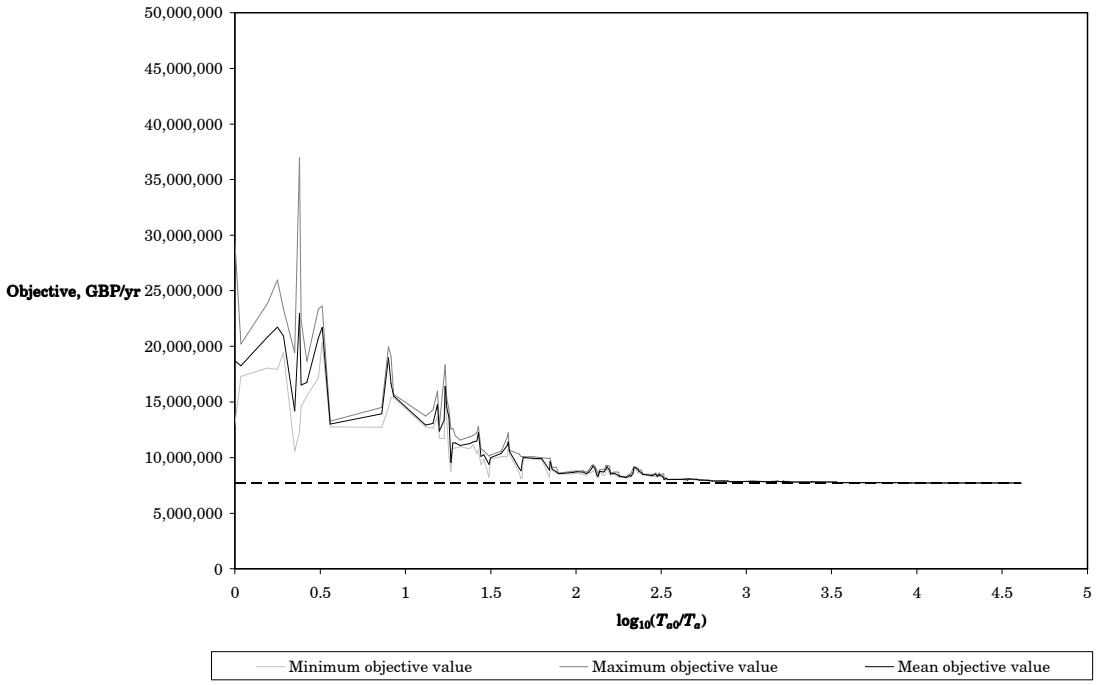

Figure 8.1: Annealing history of Test (i).

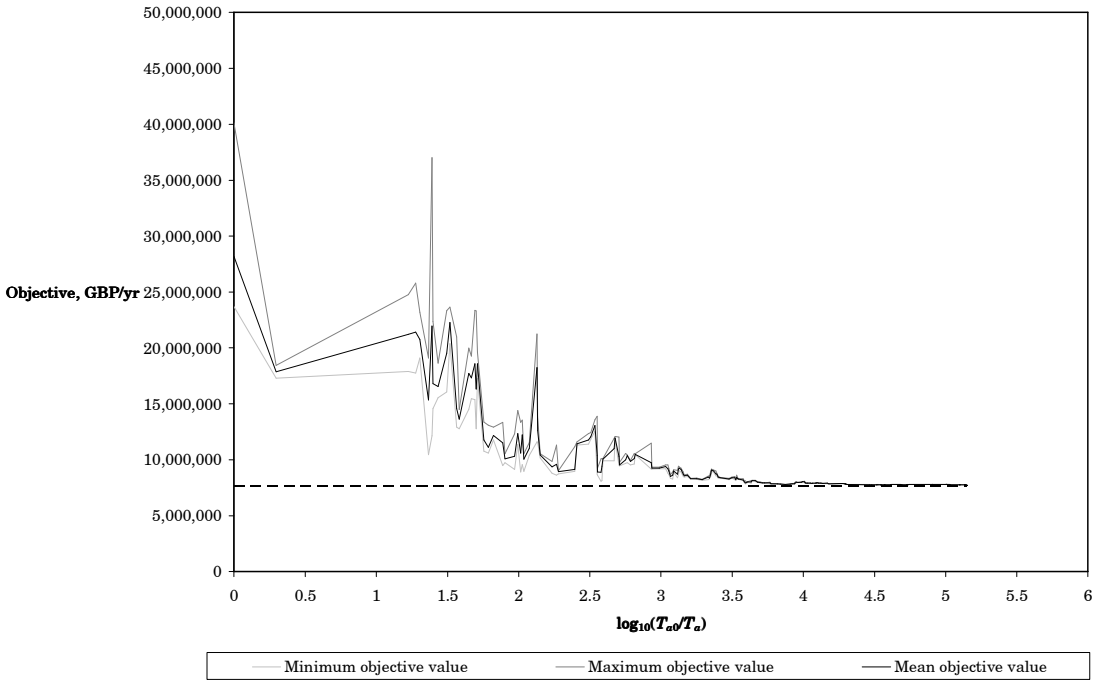

Figure 8.2: Annealing history of Test (ii).

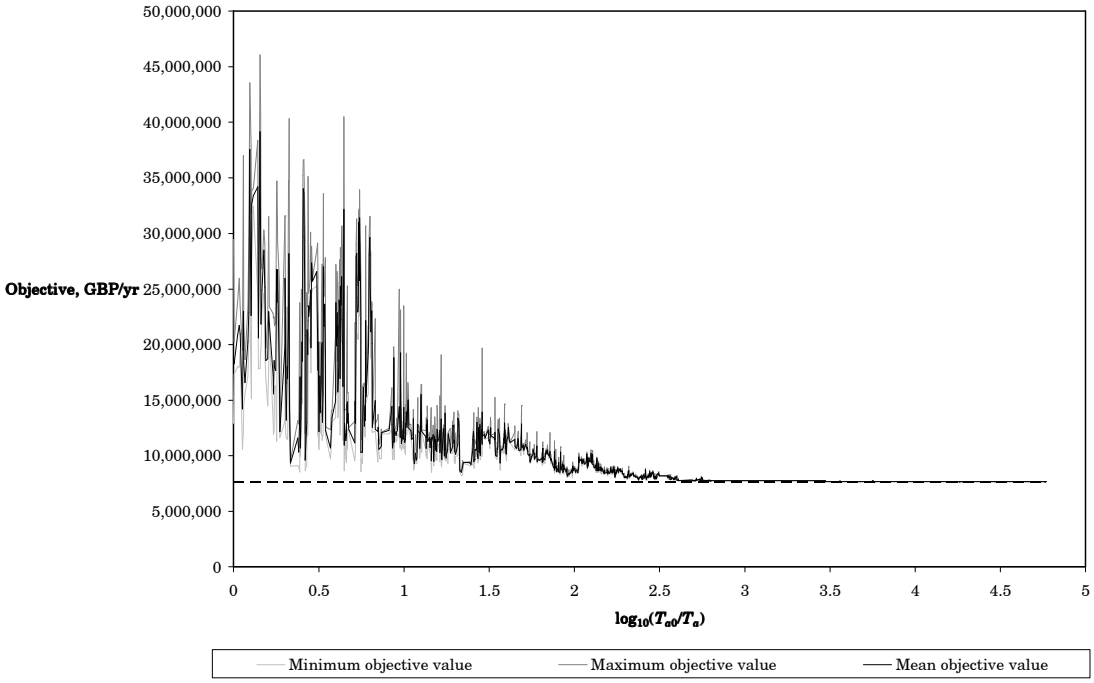

Figure 8.3: Annealing history of Test (iii).

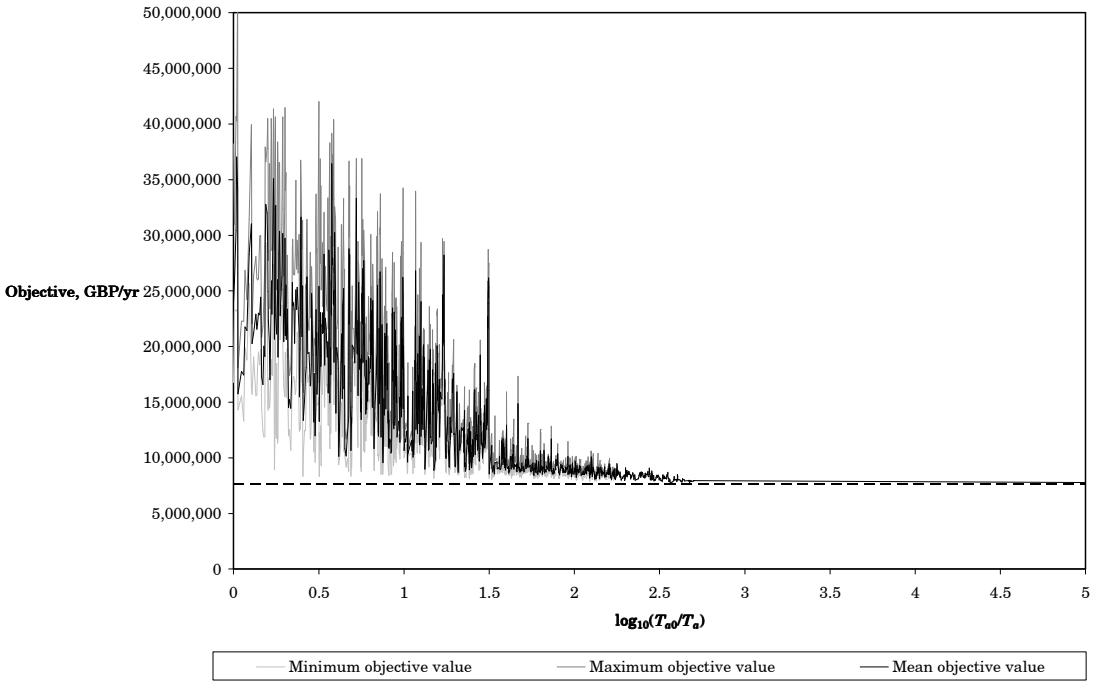

Figure 8.4: Annealing history of Test (iv).

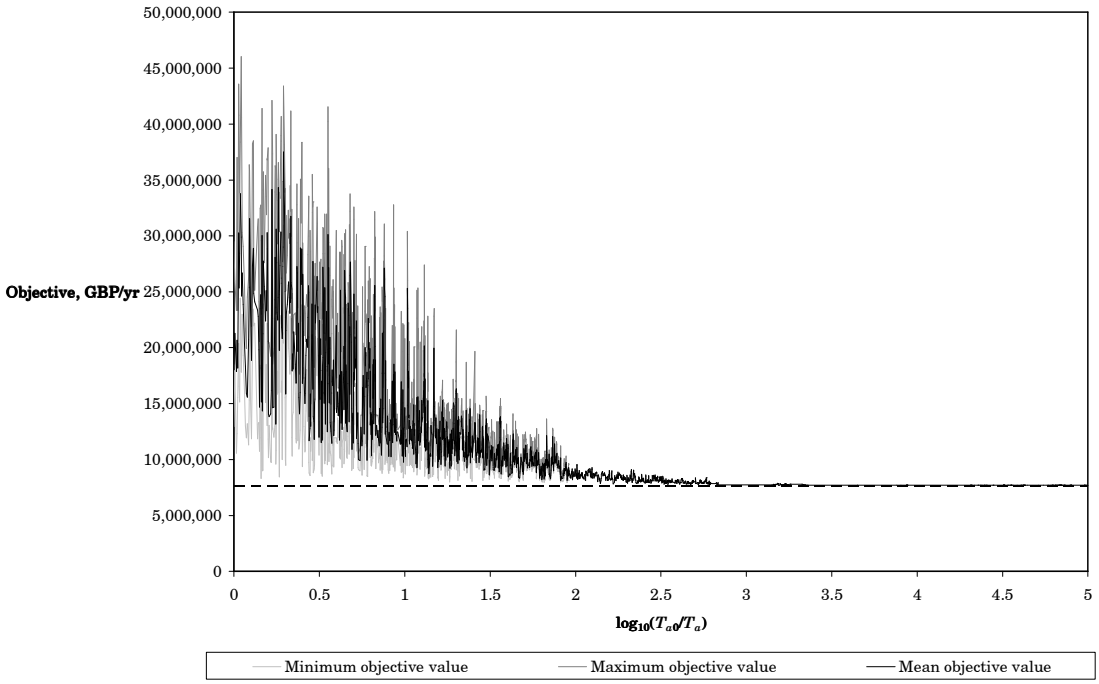

Figure 8.5: Annealing history of Test (v).

8.2.4 (ii) Assembly of process configurations

In the direct sequence, Figure 8.6a, the lighter component group as given by product specifications is separated from the feed in the initial separation task. In the indirect sequence, Figure 8.6b, the heavier component group according to product specifications is separated from the feed in the initial separation task. Since the specifications of this problem concern to three products, direct and indirect sequences are the only possible configurations.

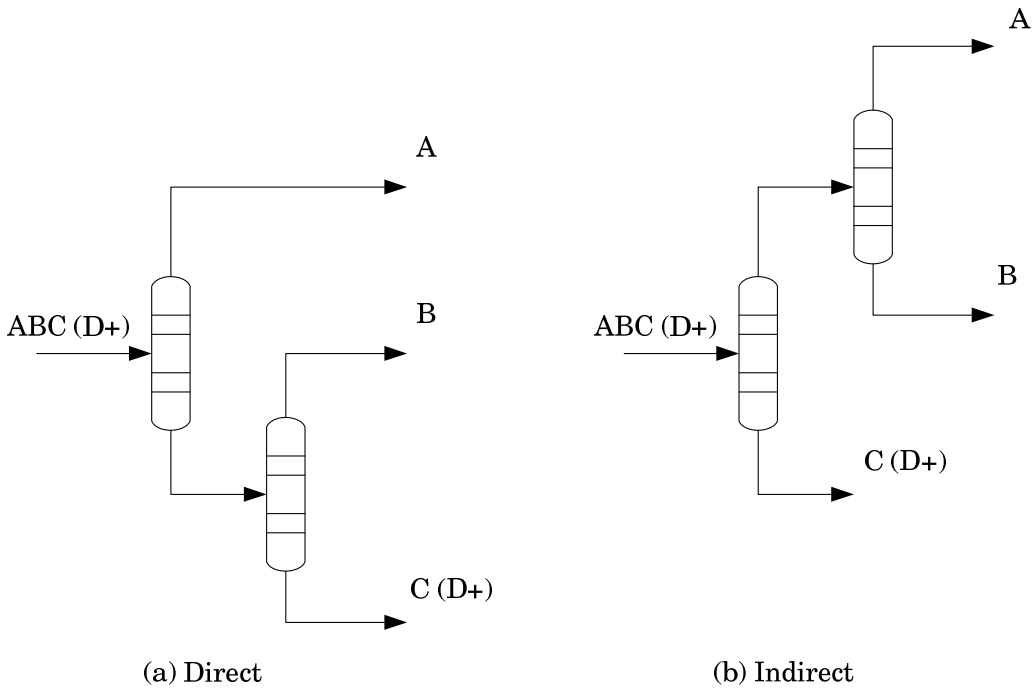

Figure 8.6: Direct vs. indirect sequences for a three-product separation problem.

The material balance around the sequence is solved internally by the synthesis framework to determine feed and product compositions of the individual separation tasks, as well as the recoveries relative to individual separation tasks. Because direct and indirect sequences are possible, the characterisation of streams must be obtained to each sequence arrangement.

For clarity, the result of applying the material balance to the initial split (A/BC) in the direct sequence is presented in Table 12.9. The balance around the second split in the direct sequence results in the stream data and recoveries provided in Table 12.10. Table 12.11 and Table 12.12 contain the equivalent results for the indirect sequence. For intermediate or final separation tasks in the separation sequence, the respective recoveries may be defined with respect to the individual feed to the task or with respect to the overall feed to the flowsheet, as Table 12.10 and Table 12.12 demonstrate.

8.2.4 (iii) Problem solution and discussion

Figure 8.7 presents a summary of the optimisation solution to the synthesis problem for total cost optimisation. Total costs and the capital and operating contributions to the total cost of each best sequence are provided.

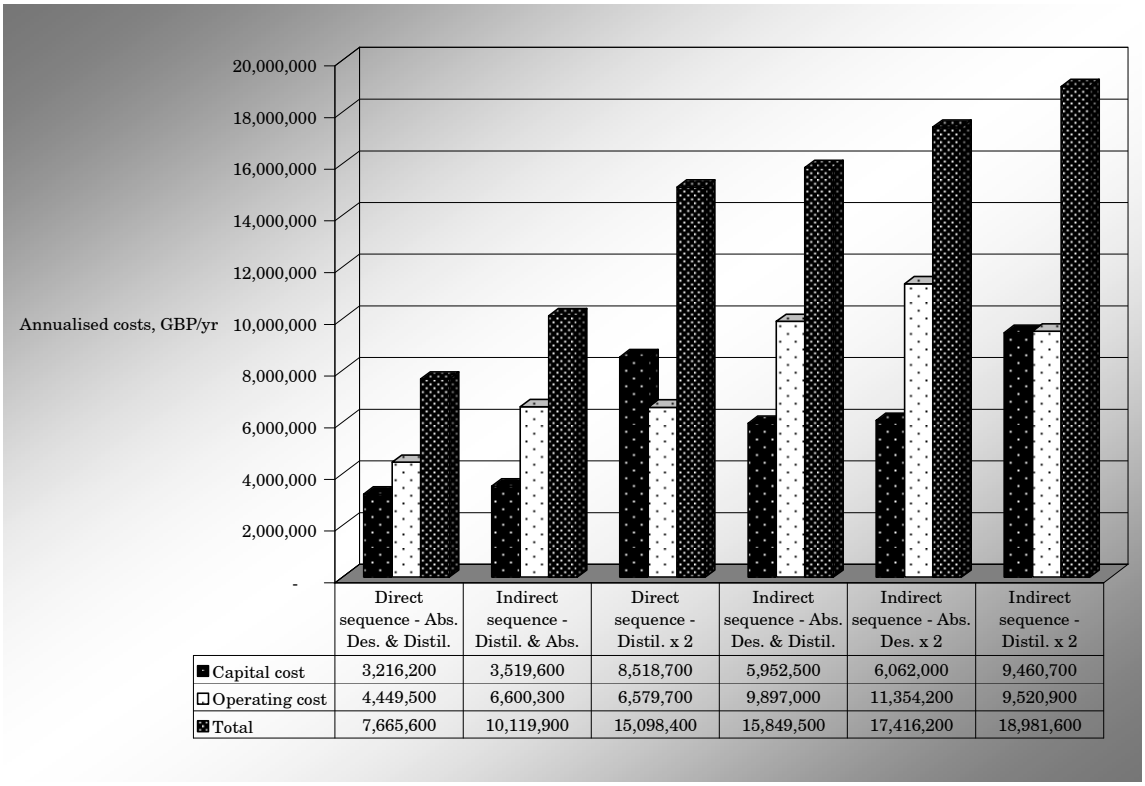

	Direct sequence - Abs. Des. & Distil.	Indirect sequence - Distil. & Abs.	Direct sequence - Distil. x 2	Indirect sequence - Abs. Des. & Distil.	Indirect sequence - Abs. Des. x 2	Indirect sequence - Distil. x 2
Capital cost	3,216,200	3,519,600	8,518,700	5,952,500	6,062,000	9,460,700
Operating cost	4,449,500	6,600,300	6,579,700	9,897,000	11,354,200	9,520,900
Total	7,665,600	10,119,900	15,098,400	15,849,500	17,416,200	18,981,600

Figure 8.7: Summary of best sequences with minimum total cost.

The set of best configurations includes six configurations and not eight, which is the maximum number of different configurations for a three-product separation system, two possible task sequences (direct and indirect) and two possible separation technologies (absorption-desorption and distillation). The reason for this is that for the current problem, no feasible configuration is achieved that consists of an absorption-desorption block performing the split B/C in the direct sequence. This causes the following configurations to be infeasible: (1) absorption-desorption followed

by absorption-desorption in direct sequence; (2) distillation followed by absorption-desorption in direct sequence.

Each proposed configuration will be discussed in this section. Figure 8.7 indicates that the operating costs generally dominate the total costs of the configurations; on average, annualised capital costs are 25% lower than the operating costs. This is clearly related, to a large extent, to the choice of the annualised factor. For instance, if the annualisation factor is reduced from three to two years, the resulting annualised costs of the given configurations are multiplied by 3/2. A simple calculation shows that this factor would alter the order of best sequences; in particular, configurations 3 and 4 would exchange positions. Most importantly, these configurations may not be the optimal for the new annualisation factor and optimisation is required to obtain the new set of optimal solutions.

Despite the utility costs predominating generally, the exception to this rule are the schemes of Figure 8.7 that consist of two standalone distillation columns. In the direct sequence consisting of pure distillation blocks, annualised capital costs exceed operating costs by 30%, while in the distillation-based indirect sequence, capital costs and operating costs are comparable. This result will be investigated later.

It is expected that the costs of all configurations are penalised to a different extent by the specified product delivery pressure which is over 30 bar greater than the feed pressure. This effect will also be studied in this section.

Table 8.8 and Table 8.9 summarise the utility utilisation by the different configurations of the separation system according to: (a) the type of utility - hot utilities, cold utilities and electricity; (b) the type of user, including reboilers, condensers, heaters and coolers within the solvent loop, feed conditioning (temperature and pressure adjustment to the desired column

feed conditions) and product conditioning (temperature and pressure adjustment to the product specifications).

Table 8.10 and Table 8.11 present a visual comparison of the various contributions to the total annualised capital cost of each of the configurations of the separation system.

	Breakdown by utility type	Breakdown by user type
1	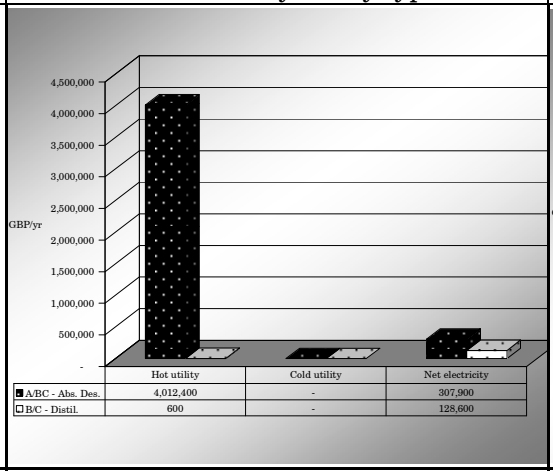 Hot utility / Cold utility / Net electricity A/BC - Abs. Des.: 4,012,400 / - / 307,900 B/C - Distil.: 600 / - / 128,600	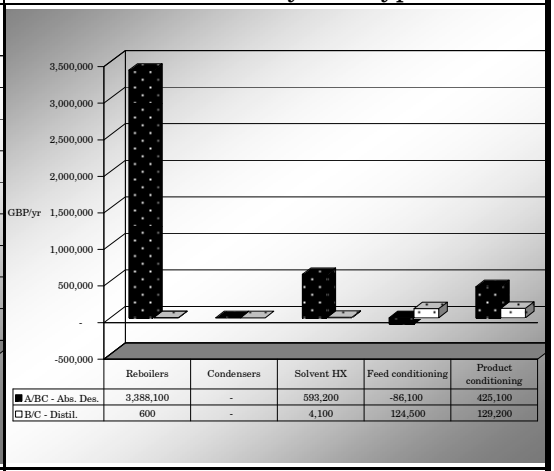 Reboilers / Condensers / Solvent HX / Feed conditioning / Product conditioning A/BC - Abs. Des.: 3,388,100 / - / 593,200 / -86,100 / 425,100 B/C - Distil.: 600 / - / 4,100 / 124,500 / 129,200
2	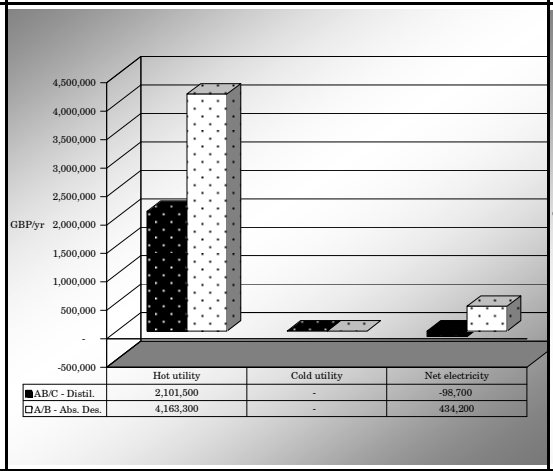 Hot utility / Cold utility / Net electricity AB/C - Distil.: 2,101,500 / - / -98,700 A/B - Abs. Des.: 4,163,300 / - / 434,200	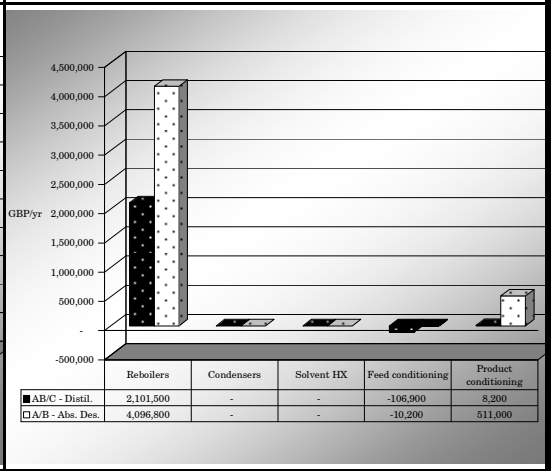 Reboilers / Condensers / Solvent HX / Feed conditioning / Product conditioning AB/C - Distil.: 2,101,500 / - / - / -106,900 / 8,200 A/B - Abs. Des.: 4,096,800 / - / - / -10,200 / 511,000
3	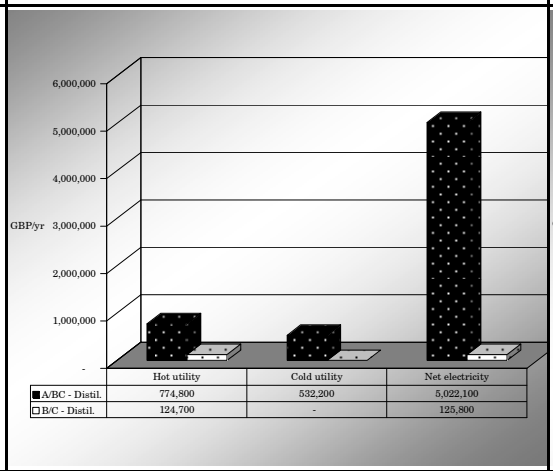 Hot utility / Cold utility / Net electricity A/BC - Distil.: 774,800 / 532,200 / 5,022,100 B/C - Distil.: 124,700 / - / 125,800	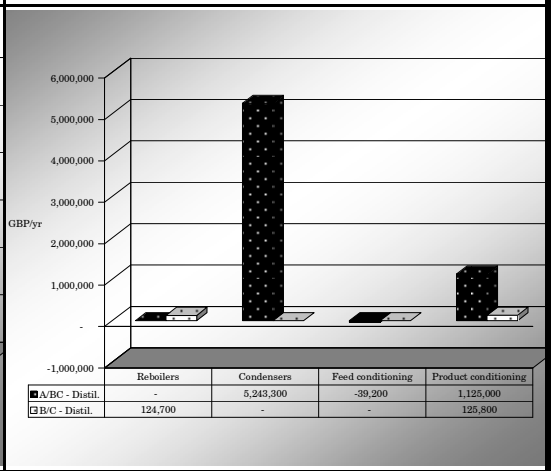 Reboilers / Condensers / Feed conditioning / Product conditioning A/BC - Distil.: - / 5,243,300 / -39,200 / 1,125,000 B/C - Distil.: 124,700 / - / - / 125,800
	Key:	
	1	**Direct sequence – Abs. Des. & Distil**
	2	**Indirect sequence – Distil. & Abs. Des.**
	3	**Direct sequence – Distil. x 2**

Table 8.8 – Annual utility cost breakdowns for top design configurations in Case Study 1

	Breakdown by utility type	Breakdown by user type
4	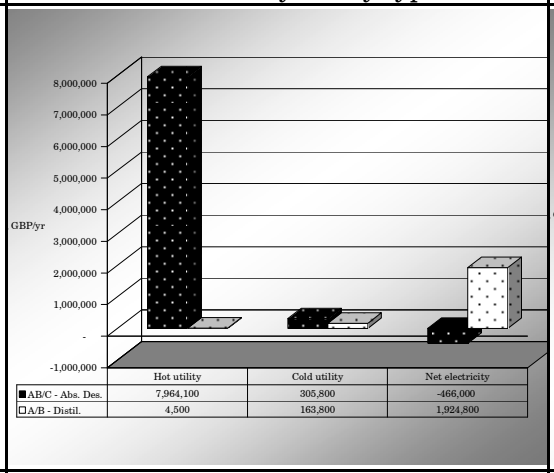 Hot utility / Cold utility / Net electricity ■AB/C - Abs. Des.: 7,964,100 / 305,800 / -466,000 □A/B - Distil.: 4,500 / 163,800 / 1,924,800	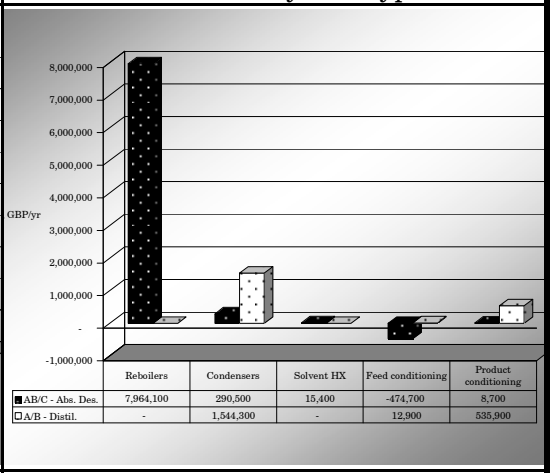 Reboilers / Condensers / Solvent HX / Feed conditioning / Product conditioning ■AB/C - Abs. Des.: 7,964,100 / 290,500 / 15,400 / -474,700 / 8,700 □A/B - Distil.: - / 1,544,300 / - / 12,900 / 535,900
5	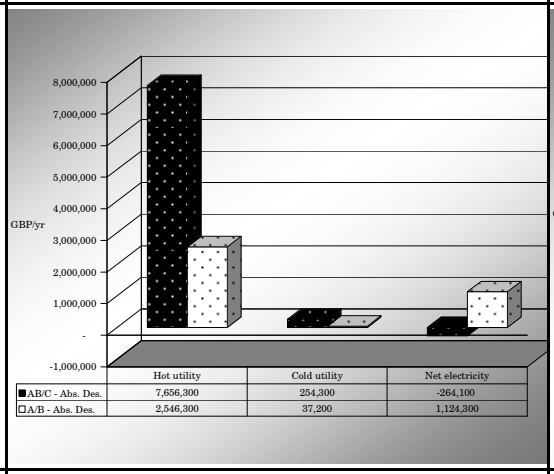 Hot utility / Cold utility / Net electricity ■AB/C - Abs. Des.: 7,656,300 / 254,300 / -264,100 □A/B - Abs. Des.: 2,546,300 / 37,200 / 1,124,300	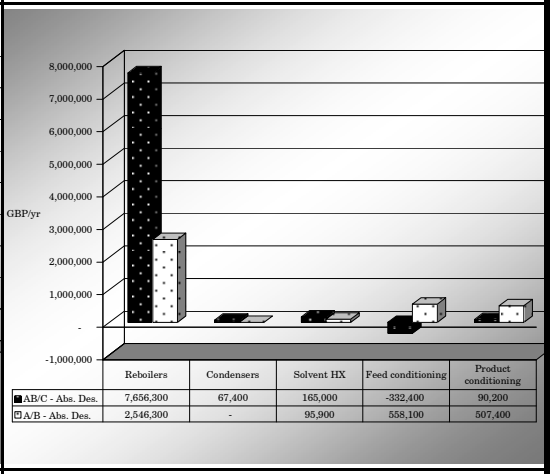 Reboilers / Condensers / Solvent HX / Feed conditioning / Product conditioning ■AB/C - Abs. Des.: 7,656,300 / 67,400 / 165,000 / -332,400 / 90,200 □A/B - Abs. Des.: 2,546,300 / - / 95,900 / 558,100 / 507,400
6	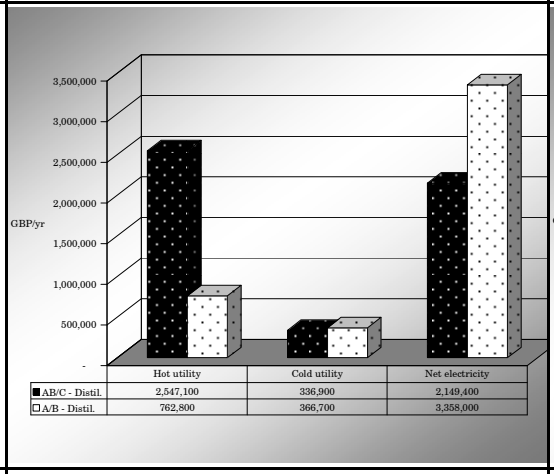 Hot utility / Cold utility / Net electricity ■AB/C - Distil.: 2,547,100 / 336,900 / 2,149,400 □A/B - Distil.: 762,800 / 366,700 / 3,358,000	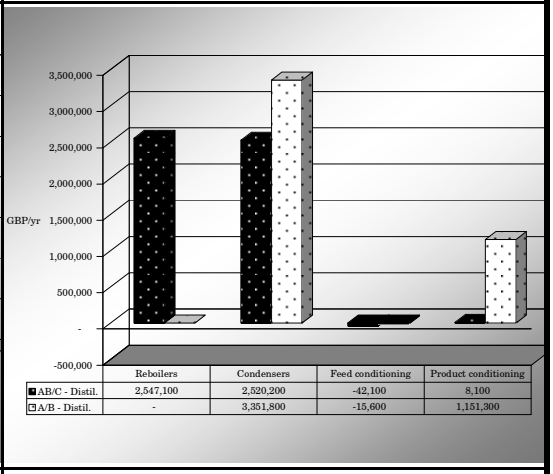 Reboilers / Condensers / Feed conditioning / Product conditioning ■AB/C - Distil.: 2,547,100 / 2,520,200 / -42,100 / 8,100 □A/B - Distil.: - / 3,351,800 / -15,600 / 1,151,300
	Key:	
	4	**Indirect sequence – Abs. Des. & Distil.**
	5	**Indirect sequence –Abs. Des. x 2**
	6	**Indirect sequence – Distil. x 2**

Table 8.9 – Annual utility cost breakdowns for top design configurations in Case Study 1 (continued)

	Capital cost contributions
1 **Direct sequence – Abs. Des. & Distil**	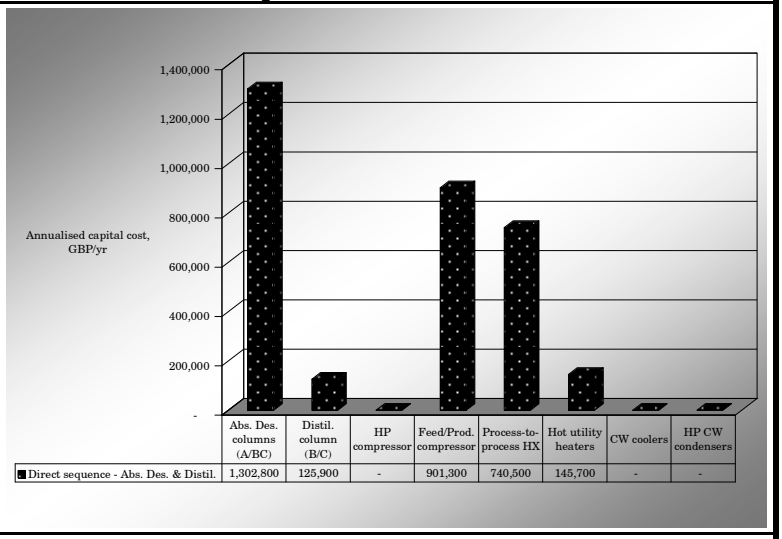
2 **Indirect sequence – Distil. & Abs. Des.**	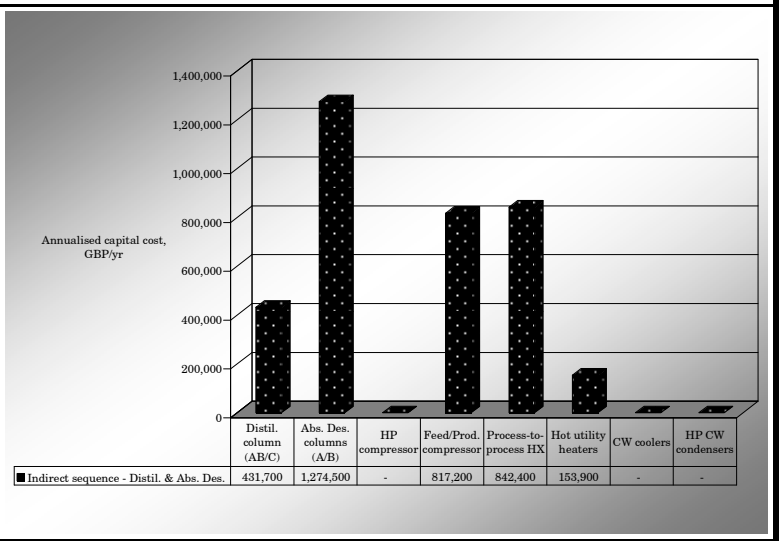
3 **Direct sequence – Distil. x 2**	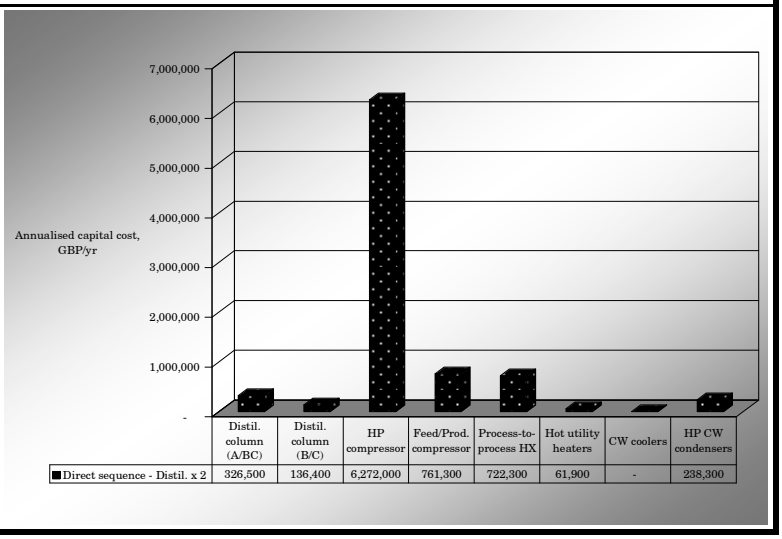

Table 8.10 – Annualised capital cost breakdown for top design configurations in Case Study 1

	Capital cost contributions
4 **Indirect sequence – Abs. Des. & Distil.**	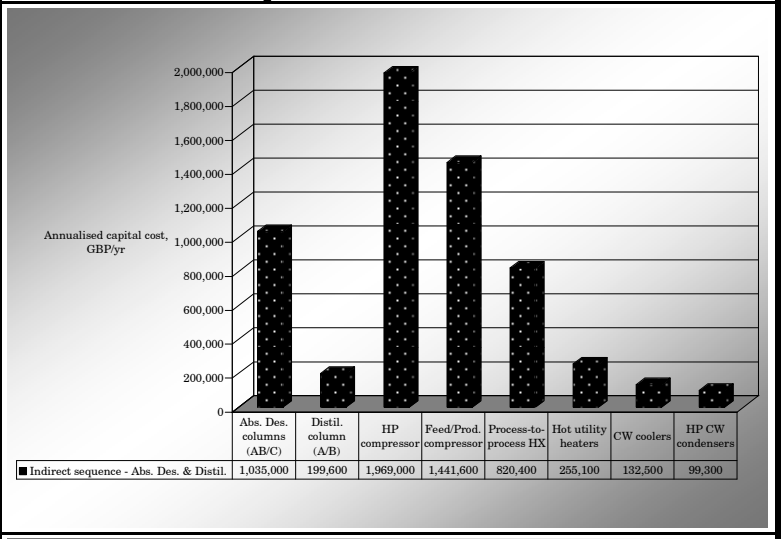
5 **Indirect sequence –Abs. Des. x 2**	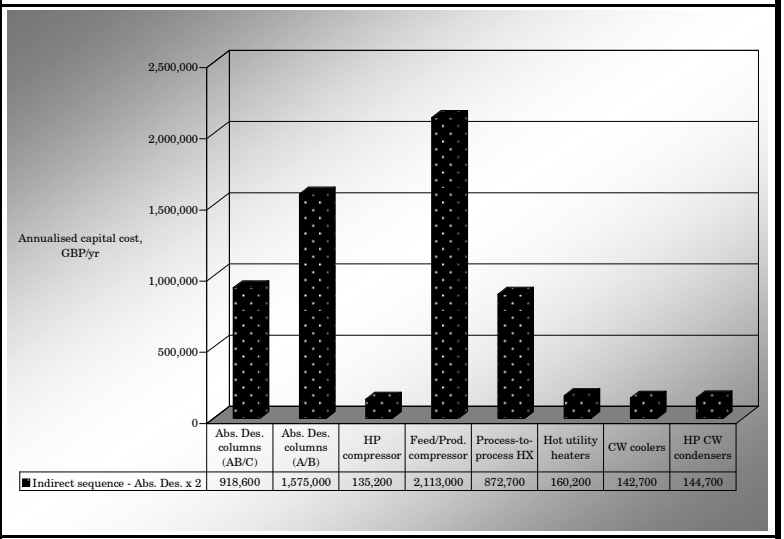
6 **Indirect sequence – Distil. x 2**	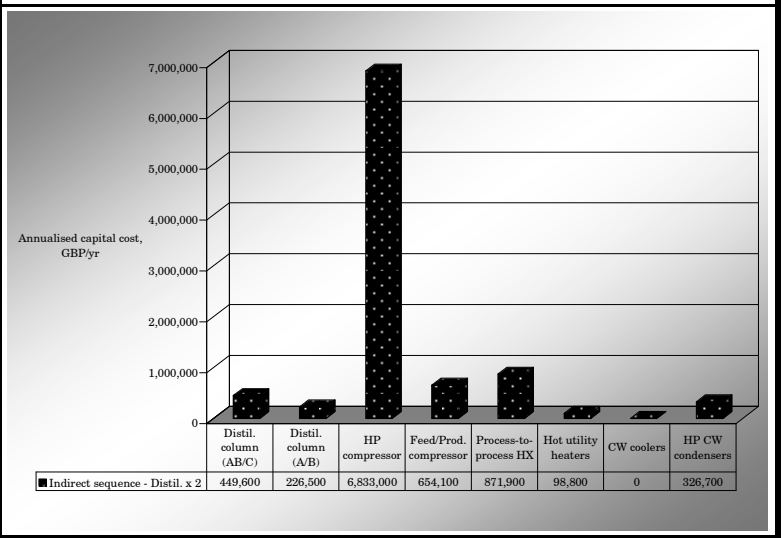

Table 8.11 – Annualised capital cost breakdown for top design configurations in Case Study 1 (continued)

Configuration No. 1: Absorption-Desorption & Distillation in Direct Sequence

The layout and key operating variables of the proposed configuration are shown in Figure 8.8.

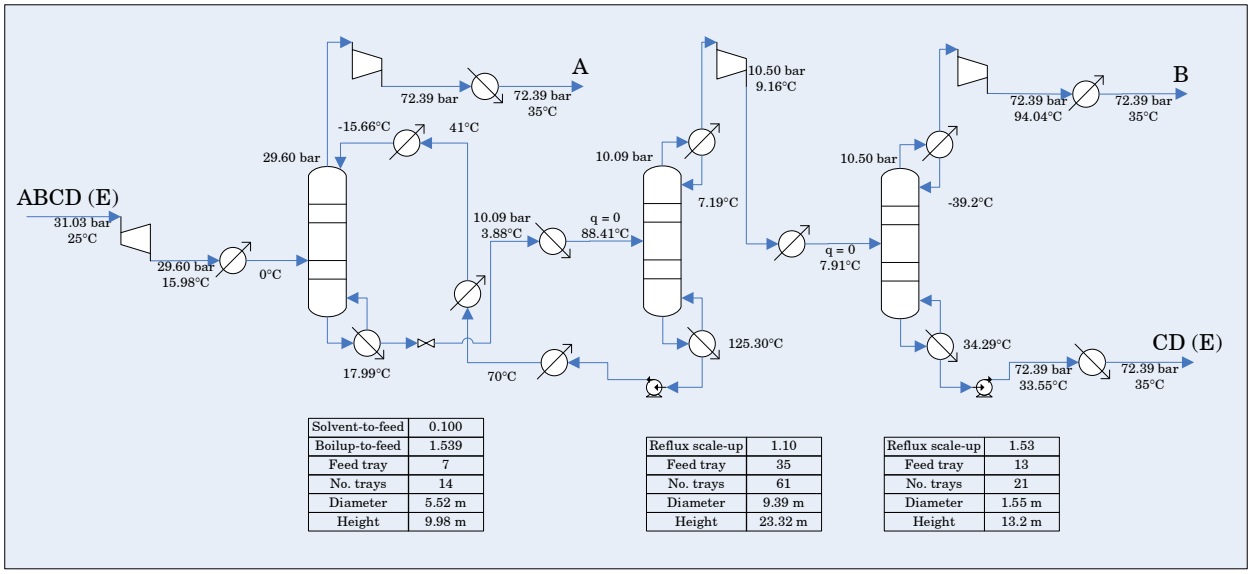

Figure 8.8: Config. No. 1 (Direct sequence – Abs. Des. & Distil.) Key design and operating variables.

- ***Operating costs of Configuration No.* 1**

The process utility demands that correspond to the first and second separations in the sequence are reported in Table 8.12 and Table 8.13, respectively. These tables summarise the process total utility demands before and after heat integration and refrigeration system design.

Table 8.8 highlights the importance of reboiler hot utility contribution to the total utility cost.

			Utility Demand prior to Heat Integration kW	Utility Savings kW	Net Utility Demand kW	**Utility Cost** GBP/yr
Reboilers		Hot utility	37936	20418	17518	£3,388,100
Condensers		Cold utility	22516	22516	0	£0
		HP shaftpower			0	£0
		CW for HP rejection			0	£0
Solvent heat exchangers	Heaters	Hot utility	6033	3928	2105	£593,200
	Coolers	Cold utility	2867	2867	0	£0
Feed conditioning	Heaters	Hot utility	0	0	0	£0
	Coolers	Cold utility	758	758	0	£0
	Expanders	Expansion shaftpower	-315		-315	-£86,100
Product conditioning	Heaters	Hot utility	3239	3105	40	£31,100
	Coolers	Cold utility	0	0	0	£0
	Compressors	Compression shaftpower	1440	0	1440	£394,000
	Pumps	Electricity	0	0	0	£0
Total						£4,320,200

Table 8.12: Config. No. 1 (Direct sequence – Abs. Des. & Distil.): Abs. Des – A/BC. Utility requirements before and after heat integration and final utility costs.

			Utility Demand prior to Heat Integration kW	Utility Savings kW	Net Utility Demand kW	**Utility Cost** GBP/yr
Reboilers		Hot utility	1555	1554	1	£100
Condensers		Cold utility	2370	2370	0	£0
		HP shaftpower			0	£0
		CW for HP rejection			0	£0
Feed conditioning	Heaters	Hot utility	0	0	0	£0
	Coolers	Cold utility	10	10	0	£0
	Compressors	Compressor shaftpower	15		15	£4,100
Product conditioning	Heaters	Hot utility	6	6	0	£0
	Coolers	Cold utility	491	491	0	£0
	Compressors	Compression shaftpower	423	0	423	£115,700
	Pumps	Electricity	32	0	32	£8,700
Total						£128,700

Table 8.13: Config. No. 1 (Direct sequence – Abs. Des. & Distil.): Distillation - B/C. Utility requirements before and after heat integration and final utility costs.

The following messages derive from Table 8.12 and Table 8.13:

1. Energy-intensity of reboiled-absorption for A/BC is much higher than that of distillation for B/C.

The small magnitude of the solvent flowrate needed to meet the relatively relaxed 86%-specification on ethane reduces methane co-absorption. However, due to the low-temperature operation of the absorber, a large boilup-to-feed ratio is required to strip the methane that is retained by the solvent.

The fact that the first separation task in the sequence is much more energy-intensive than the second separation task may be qualitatively attributed to the different feed flowrates to each separation task. In order to establish an approximate mathematical relationship between feed or product flowrates and the utility weights, the following is considered.

For distillation columns, the following proportionality relationships between utility consumption and the mass balance are acceptable approximations:

$$Reboiler\ duty \propto D-(1-q)F \tag{8.2}$$

$$Condenser\ duty \propto Reflux \tag{8.3}$$

Where F, D and q represent the column feed flowrate, the distillate flowrate, and the feed quality (0 for a vapour feed, 1 for a liquid feed). Relationship (8.2) is not applicable for $q \leq 0$, since it leads to a negative reboiler duty.

As a result of proportionality relationships (8.2) and (8.3), in a sequence of distillation columns of liquid column feeds and uniform reflux ratios, the utility costs associated with each column is directly proportional to the overhead vapour flowrate. If these conditions prevailed in the present design configuration, then, the utility demand of the first column would be 10.9 times that of the second column, using the vapour flowrates of Table 12.13 for the direct sequence.

In this case study, this rule is not directly applicable due to the sequence involving absorption-desorption. The results from Table 8.12 and Table 8.13 indicate that the first separation task is 15.4 times more energy-intensive than the second separation task, before heat integration. While this result may be an indication of distillation being less energy-intensive than absorption-desorption for the first separation task, it will be later shown that absorption-desorption offers a greater potential for heat

integration with the rest of the process than distillation, thus leading to an overall reduced cost.

2. The process has zero demands of cold utility as a result of effective heat integration within the process.

The second message from Table 8.12 and Table 8.13 is that this process configuration has zero demands of refrigeration or cooling water. This is the consequence of the process cooling demands being satisfied internally by other process streams, obviating any additional cooling.

Within the absorber-desorber block, these cooling demands include: desorber condenser, 22516 kW; lean solvent cooling, 2867 kW; feed cooling, 758 kW. Within the pure distillation block, these cooling demands include: distillation condenser, 2370 kW; product cooling, 491 kW; feed cooling, 10 kW.

The sinks for these heat sources consist primarily of the absorber reboiler, and the pure distillation reboiler, which operate at low temperatures. The absorber reboiler takes up entirely the pure distillation condenser below-ambient load of 2370 kW. The ocurrence of this match will be discussed later.

Other streams being utilised as heat sinks by the process heat sources are the intermediate rich solvent heater and the overhead absorber product, which absorb 3928 kW and 3105 kW of heating, respectively. The bottom distillation product attracts a negligible amount of 6 kW of heating.

3. Utility costs are dominated by the hot utility use by the desorber reboiler and recommended external refrigeration requirements are small in comparison.

The ocurrence of the match between the absorber reboiler and the pure distillation condenser was not anticipated, since the condenser of the distillation column of the second separation task operates at the very low temperature of -39.2°C.

The calculated below-zero reboiler feed temperature is the direct result of the prevailing very large boilup rate. The rich solvent mixture is a very light mixture, due to the heavy dilution of solvent at the actual operating conditions, with a bubble point of approximately 18°C at the absorber operating pressure in the proximities of 30 bar. The temperature of the reboiler feed is the bubble temperature corresponding to a certain composition which is imposed by material balance around the reboiler. Hence, the reboiler feed temperature is entirely determined by the combination of the reboiler draw and the specified boilup rate.

Since the predicted value of the bottoms temperature may be objectionable, so is the match between the reboiler of the absorber and the condenser of the distillation column of the second split. Refrigeration would be required to satisfy the process cooling demands otherwise, with an estimated shaftwork of 940kW (the approximation of a single cycle is implied) and an associated electricity cost of 257,000 GBP/yr. With an estimated maximum 20% of additional cooling water costs for waste heat rejection, the estimated impact on the operating costs is roughly 300,000 GBP/yr. This represents just under a 7% increase over the operating costs of the present configuration, which is governed by the hot utility consumption of the reboiler of the desorber. Other factors should be taken into account to establish the impact that objecting to the predicted reboiler feed temperature would have on the ranking of the process configurations of Figure 8.7.

- *Capital costs of Configuration No.* 1

From the column dimensions in Figure 8.8, it becomes apparent that the desorber is the largest column in the system. The reboiled absorber column is half the diameter and half the length of the desorber column. This is due to the higher molar volume of the vapour in the desorber, which operates at higher temperatures and a much lower pressure than the reboiled absorber. The distillation column performing the second separation task is slightly taller than the reboiled absorber column but features a much smaller diameter due to the reduced feed flowrate. This feed is mostly free of methane and artificially free of solvent, according to the solvent-free approach adopted in this work and presented in section 3.4.2.

Among the capital cost contributions illustrated in Table 8.10, the contribution associated with the cost of the columns has the largest weight of the total capital cost.

Table 8.10 also offers an indication of the extent of heat integration within the system, which is not provided by the utility plots. This indication is given by the significance of the capital cost of the process-to-process heat exchangers.

Importantly, despite the small contribution to the total energy utilisation of the process that is attributed to compressors (2% of the total process energy use before heat integration), the capital cost of compressors amounts to 28% of the total capital costs.

On a final note, marginally lower total costs could potentially be achieved if the pressure of the desorber and the downstream distillation column were equalised, so the compressor of the feed of the distillation column would be unnecessary. If the favourable economics of this scenario could

be confirmed, then a longer optimisation run should be able to locate this solution.

Configuration No. 2: Distillation & Absorption-Desorption in Indirect Sequence

The layout and key operating variables of the proposed configuration are shown in Figure 8.9. In this configuration, because of the total condenser of the desorber, product B is a liquid. Liquid pumping to the pressure specification of 72.39 bar is less expensive than vapour compression. Total condensers operate at lower temperature than partial condensers, however in the proposed configuration this lower temperature is achieved by complete integration with the absorber reboiler.

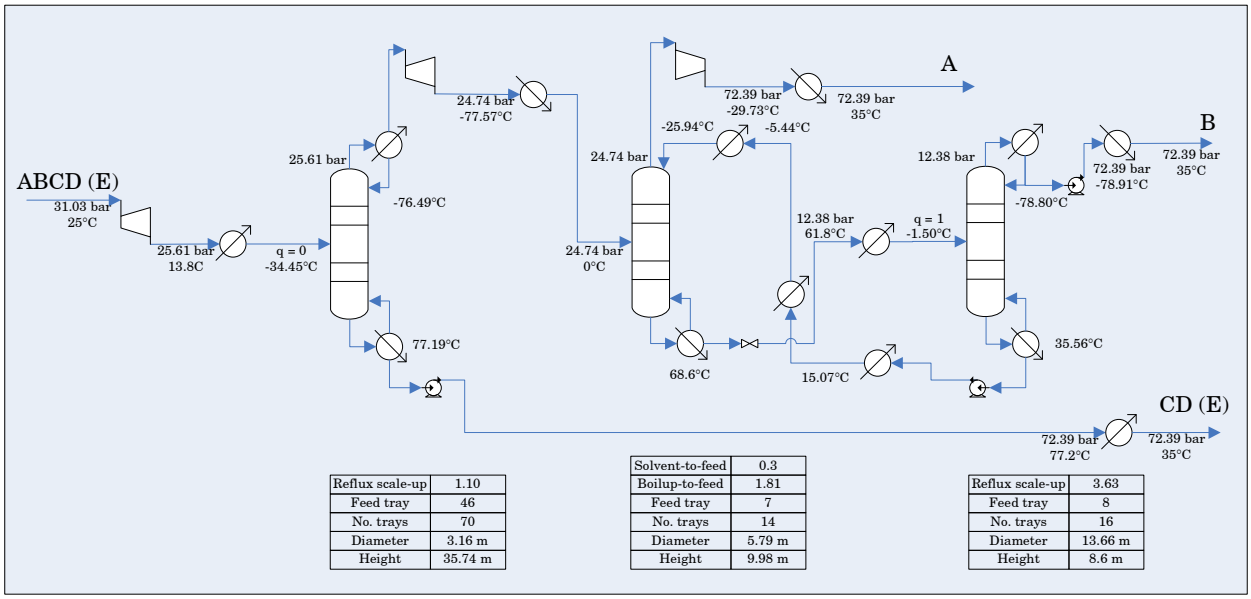

Figure 8.9 Config. No. 2 (Indirect sequence – Distil. & Abs. Des.) Key design and operating variables.

- ***Operating costs of Configuration No. 2***

Table 8.14 and Table 8.15 summarise the process total utility demands of each separation task before and after heat integration and refrigeration system design.

			Utility Demand prior to Heat Integration kW	Utility Savings kW	Net Utility Demand kW	**Utility Cost** GBP/yr
Reboilers		Hot utility	9036	0	9036	£2,101,500
Condensers		Cold utility	10973	10973	0	£0
		HP shaftpower			0	£0
		CW for HP rejection			0	£0
Feed conditioning	Heaters	Hot utility	0	0	0	£0
	Coolers	Cold utility	2295	2295	0	£0
	Expanders	Expansion shaftpower	-391		-391	-£106,900
Product conditioning	Heaters	Hot utility	0	0	0	£0
	Coolers	Cold utility	293	293	0	£0
	Compressors	Compression shaftpower	0	0	0	£0
	Pumps	Electricity	30	0	30	£8,200
Total						£2,002,800

Table 8.14: Config. No. 2 (Indirect sequence – Distil. & Abs. Des.): Distillation – AB/C. Utility requirements before and after heat integration and final utility costs.

			Utility Demand prior to Heat Integration kW	Utility Savings kW	Net Utility Demand kW	**Utility Cost** GBP/yr
Reboilers		Hot utility	34909	15993	18916	£4,096,800
Condensers		Cold utility	1963	1963	0	£0
		HP shaftpower	0	0	0	£0
		CW for HP rejection			0	£0
Solvent heat exchangers	Heaters	Hot utility	0	0	0	£0
	Coolers	Cold utility	19851	19851	0	£0
Feed conditioning	Heaters	Hot utility	3520	2374	1146	£0
	Coolers	Cold utility	0	0	0	£0
	Expanders	Expansion shaftpower	-37		-37	-£10,200
Product conditioning	Heaters	Hot utility	4196	3909	286	£66,500
	Coolers	Cold utility	0	0	0	£0
	Compressors	Compression shaftpower	1590	0	1590	£435,000
	Pumps	Electricity	35	0	35	£9,400
Total						£4,597,500

Table 8.15: Config. No. 2 (Indirect sequence – Distil. & Abs. Des.): Abs. Des. – A/B. Utility requirements before and after heat integration and final utility costs.

This configuration is analogous to Configuration No. 1 in that it does not require external refrigeration or cooling utilities, since all the cooling demands are satisfied by internal process streams. The process operating cost is dominated by the cost of hot utilities, as seen in Table 8.8. In accordance with the proposed heat integration arrangements, the demand for hot utilities (hot water) includes the reboiler of the distillation task (9036 kW) and the reboiler of the desorber (17616 kW after 174 kW of integration with product A). Table 8.8 affirms the predominant contribution of the reboilers to the total utility costs.

Because the feed to the separation blocks is a vapour and the present configuration comprises one absorption-desorption block, is it is not possible to explain the utility cost contribution of each block to the total utility cost on the basis presented previously (relationships (8.2) and (8.3)). The second separation task is 1.84 times more energy-intensive than the first column.

- *Capital costs of Configuration No.* 2

The distillation column for the AB/C split is moderately tall, with 70 calculated real trays. A large number of trays is needed to achieve a high separation between B and C with recoveries of ethane and propane of 0.975 (in top product) and 0.98 (in bottom product), respectively. The larger dimensions of the distillation column of this configuration in relation to the distillation column of Configuration No. 1, are responsible for the increase of the capital cost that is attributed to distillation columns in the sequence (excluding the desorber), which may be observed in Table 8.10.

The desorber column (reboiler: 18936 kW; condenser: 1963 kW) is more energy-intensive than the reboiled absorber column (15973 kW) because of the high reboiler and condenser duty and the elevated reflux (3.63 times the minimum reflux ratio). A high vapour-liquid traffic in the desorber column is associated with a greater column diameter.

The relative weights of feed and product compressor capital costs, process-to-process heat exchangers capital costs and hot utility heaters capital costs are similar to those of Configuration No. 1.

Configuration No. 3: Distillation x 2 in Direct Sequence

The layout and key operating variables of the proposed configuration are shown in Figure 12.15. The proposed refrigeration system configuration is

shown in Figure 8.11. All refrigeration duties are provided by refrigeration cycles of propylene and ethylene in cascade.

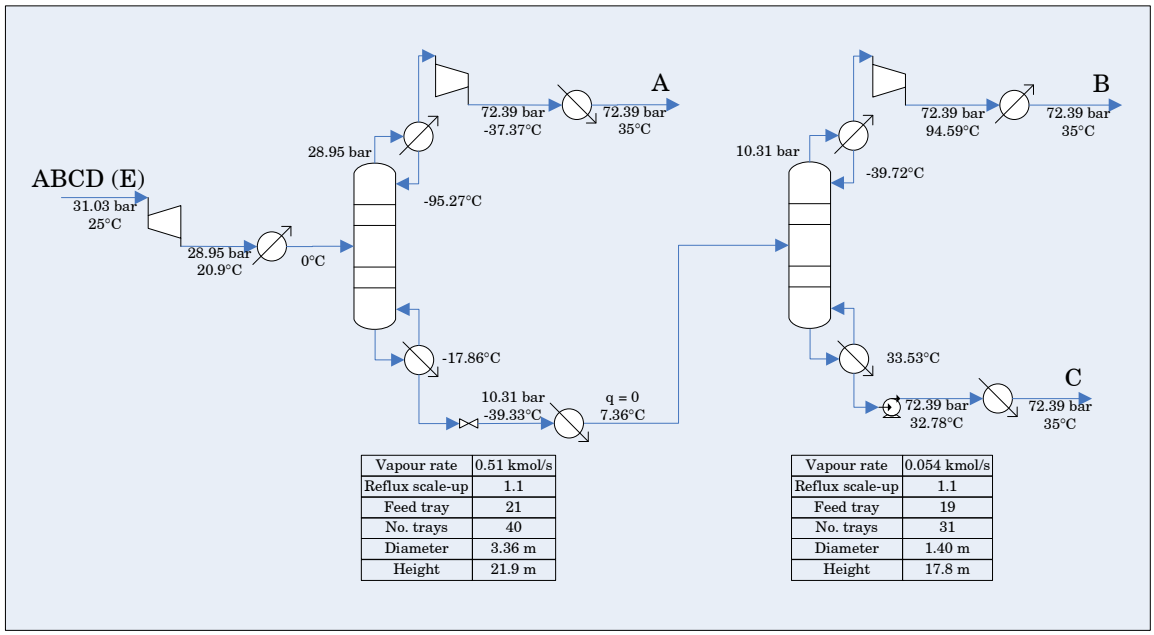

Figure 8.10: Config. No. 3 (Direct sequence – Distil. x 2): Distillation. Key design and operating variables.

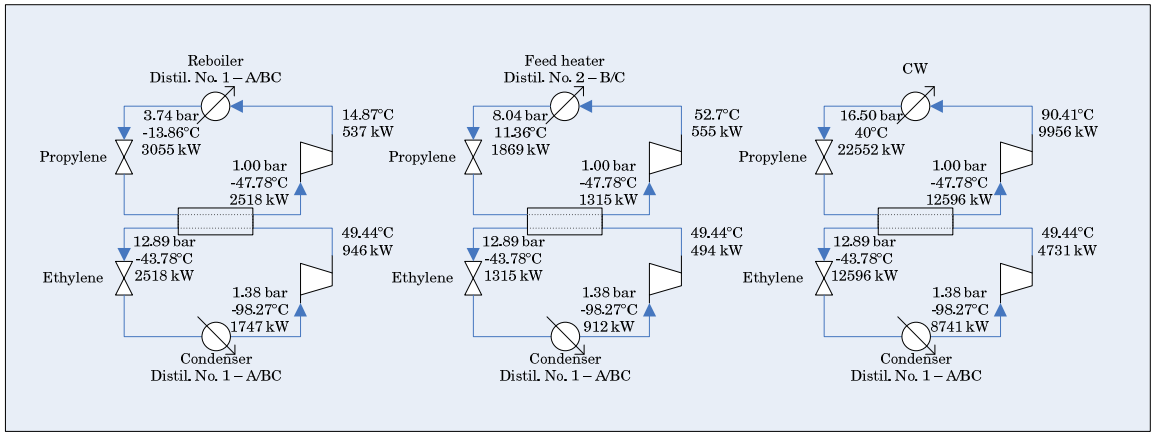

Figure 8.11: Config. No. 3 (Direct sequence – Distil. x 2): Refrigeration system.

Due to the reduced extent of heat integration in comparison to Configuration Nos. 1 and 2 and the reduced number of matches, the proposed heat exchanger is relatively simple. Figure 12.15 shows the proposed heat integration network, which was depicted using HX-Net® 2006. This network excludes the refrigeration matches of the condenser of

the first column but includes the matches of below-ambient heat rejection (referred to as HPCond1 and HPCond2 in Figure 12.15) to process streams.

The network is efficient because all the cooling demands of the process (excluding refrigeration demands) are met internally. The unsatisfied heating demands equal the minimum utility requirements given by the composite curve of Figure 12.16. In this figure, the flat segments on the hot curve correspond to the heat rejection by refrigerants.

- ***Operating costs of Configuration No.* 3**

Table 8.16 and Table 8.17 summarise the process total utility demands of each separation task before and after heat integration and refrigeration system design.

			Utility Demand prior to Heat Integration kW	Utility Savings kW	Net Utility Demand kW	**Utility Cost** GBP/yr
Reboilers		Hot utility	5746	5746	0	£0
Condensers		Cold utility	11401	0	0	£0
		HP shaftpower			17219	£4,711,100
		CW for HP rejection			22552	£532,200
Feed conditioning	Heaters	Hot utility	0	0	0	£0
	Coolers	Cold utility	1002	1002	0	£0
	Expanders	Expansion shaftpower	-143		-143	-£39,200
Product conditioning	Heaters	Hot utility	3476	145	3331	£774,800
	Coolers	Cold utility	0	0	0	£0
	Compressors	Compression shaftpower	1280	0	1280	£350,200
	Pumps	Electricity	0	0	0	£0
Total						£6,329,100

Table 8.16: Config. No. 3 (Direct sequence – Distil. x 2): Distillation - A/BC. Utility requirements before and after heat integration and final utility costs.

			Utility Demand prior to Heat Integration kW	Utility Savings kW	Net Utility Demand kW	**Utility Cost** GBP/yr
Reboilers		Hot utility	876	340	536	£124,700
Condensers		Cold utility	1689	1689	0	£0
		HP shaftpower			0	£0
		CW for HP rejection			0	£0
Feed conditioning	Heaters	Hot utility	1869	1869	0	£0
	Coolers	Cold utility	0	0	0	£0
	Comp./Exp.	Expansion shaftpower	0			£0
Product conditioning	Heaters	Hot utility	10	10	0	£0
	Coolers	Cold utility	495	495	0	£0
	Compressors	Compression shaftpower	428	0	428	£117,100
	Pumps	Electricity	32	0	32	£8,700
Total						£250,500

Table 8.17: Config. No. 3 (Direct sequence – Distil. x 2): Distillation – B/C. Utility requirements before and after heat integration and final utility costs.

The distribution of operating costs in this configuration features some key differences with respect to Configuration Nos. 1 and 2. This configuration is greatly dominated by refrigeration costs, as shown in Table 8.8. This is a characteristic of typical gas separation systems by distillation.

This feature is a direct consequence of less intensive heat integration in this configuration than in Configuration Nos. 1 and 2. In this configuration, the energy saved due to heat integration is 42.5% (11296 kW out of the initial 26564 kW, excluding compression and expansion of feed and products). In Configuration No. 1, the savings amount to 74.6% (58023 kW out of the initial 77780 kW), while in Configuration No. 2, savings are 66.2% (57653 kW out of the initial 87036 kW).

The absorption-desorption-based processes of Configuration Nos. 1 and 2 have significantly higher heating and cooling demands than the process of Configuration No. 3, but offer additional opportunities for heat integration, and in particular, for partial or total elimination of external refrigeration demands. As a result of this, the absorption-desorption-based processes of Configuration Nos. 1 and 2 feature an inferior external energy demand (21258 kW, and 30610 kW, respectively) than Configuration No. 3 (45235 kW). These external energy demands include refrigeration cycles and compression and expansion of feed and products.

- *Capital costs of Configuration No.* 3

The scale of the corresponding capital cost plot in Table 8.10 is larger than in previous capital cost figures to accommodate the dominating heat pumping compressor costs. The cost of the compressors within the refrigeration cycles is distinctively prominent.

No substantial decrease is observed of the process-to-process heat exchangers costs with respect to Configuration Nos. 1 and 2 (722,300 £/yr for Configuration No. 3 vs. 740,500 £/yr and 842,400 £/yr for Configuration Nos. 1 and 2, respectively). This result is not inconsistent with the comparatively less intensive heat integration, since the costs of the evaporators of the refrigeration system are included in the process-to-process heat exchangers costs by convention of this work. Any refrigerant condensers rejecting heat to a process stream and not to cooling water are also included in the sum of process-to-process heat exchangers costs.

Finally, because of the infeasibility of the configuration consisting of a distillation separation task followed by an absorption-desorption separation task in direct sequence, the distillation column performing separation task A/BC in Configuration No. 3 cannot be compared with the equivalent distillation column of such hybrid scheme involving distillation and absorption-desorption. However, the capital cost of 136,400 £/yr corresponding to the distillation column performing separation task B/C is of similar magnitude to the cost of 125,900 £/yr for the equivalent distillation column in the direct sequence of Configuration No. 1.

Configuration No. 4: Absorption-Desorption & Distillation in Indirect Sequence

The layout and key operating variables of the proposed configuration are shown in Figure 8.12. The boilup ratio that is needed to remove the bulk of

the absorbed A and B from the solvent is low, which is related to the high temperatures at the bottom of the column.

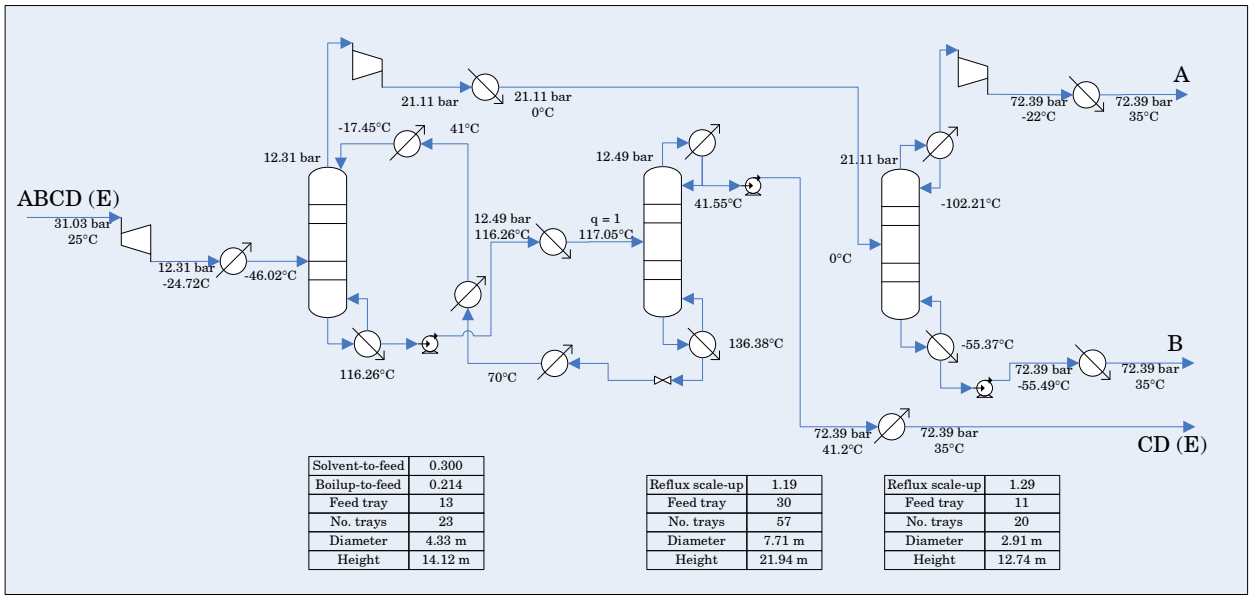

Figure 8.12: Config. No. 4 (Indirect sequence – Abs. Des. & Distil.) Key design and operating variables.

- ***Operating costs of Configuration No. 4***

Table 8.18 and Table 8.19 summarise the process total utility demands of each separation task before and after heat integration and refrigeration system design.

			Utility Demand prior to Heat Integration kW	Utility Savings kW	Net Utility Demand kW	**Utility Cost** GBP/yr
Reboilers		Hot utility	28261		28261	£7,964,100
Condensers		Cold utility	18266	5959	12307	£290,500
		HP shaftpower	0	0	0	£0
		CW for HP rejection			0	£0
Solvent heat exchangers	Heaters	Hot utility	65	0	65	£0
	Coolers	Cold utility	9541	8889	652	£15,400
Feed conditioning	Heaters	Hot utility	0	0.00	0	£0
	Coolers	Cold utility	936	936	0	£0
	Expanders	Expansion shaftpower	-1735		-1735	-£474,700
Product conditioning	Heaters	Hot utility	0	0	0	£0
	Coolers	Cold utility	41	41	0	£0
	Compressors	Compression shaftpower	0	0	0	£0
	Pumps	Electricity	32	0	32	£8,700
Total						£7,803,900

Table 8.18: Config. No. 4 (Indirect sequence – Abs. Des. & Distil.): Abs. Des – AB/C. Utility requirements before and after heat integration and final utility costs.

			Utility Demand prior to Heat Integration kW	Utility Savings kW	Net Utility Demand kW	**Utility Cost** GBP/yr
Reboilers		Hot utility	4303	4303	0	£0
Condensers		Cold utility	7202	4418	2785	£0
		HP shaftpower	0	0	5046	£1,380,500
		CW for HP rejection			6940	£163,800
Feed conditioning	Heaters	Hot utility	12741	12741	0	£0
	Coolers	Cold utility	0	0	0	£0
	Compressors	Compression shaftpower	47		47	£12,900
Product conditioning	Heaters	Hot utility	3623	3600	20	£4,500
	Coolers	Cold utility	0	0	0	£0
	Compressors	Compression shaftpower	1910	0	1910	£522,600
	Pumps	Electricity	32	0	32	£8,800
Total						£2,093,200

Table 8.19: Config. No. 4 (Indirect sequence – Abs. Des. & Distil.): Distillation - A/B. Utility requirements before and after heat integration and final utility costs.

This configuration includes a refrigeration system, which is employed to provide below-ambient cooling to the condenser of the second separation task. However, hot utility costs or reboiler costs in Table 8.9 dominate operating costs due to the low refrigeration requirements.

- ***Capital costs of Configuration No. 4***

As seen in Table 8.11, compressors costs dominate capital costs, but to a lower degree than in Configuration No. 3.

Configuration No. 5: Absorption-Desorption x 2 in Indirect Sequence

This is the first configuration where an absorber-desorber block requires a certain degree of refrigeration. Differently to previous instances of absorber-desorbers blocks, a small amount of external refrigeration is required for lean solvent chilling and product cooling for separation block 2. The corresponding demands for separation block 1 are met internally by other process streams.

The layout and key operating variables of the proposed configuration are shown in Figure 8.13.

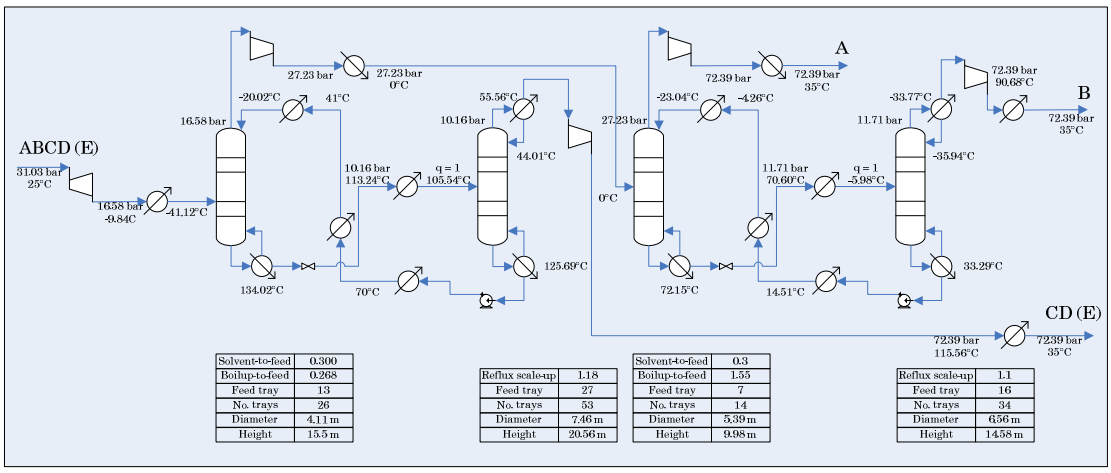

Figure 8.13: Config. No. 5 (Indirect sequence – Abs. Des. x 2): Key design and operating variables.

- ***Operating costs of Configuration No.* 5**

Table 8.20 and Table 8.21 summarise the process total utility demands of each separation task before and after heat integration and refrigeration system design.

			Utility Demand prior to Heat Integration kW	Utility Savings kW	Net Utility Demand kW	**Utility Cost** GBP/yr
Reboilers		Hot utility	27169	0	27169	£7,656,300
Condensers		Cold utility	15720	12866	2854	£67,400
		HP shaftpower	0	0	0	£0
		CW for HP rejection			0	£0
Solvent heat exchangers	Heaters	Hot utility	0	0	0	£0
	Coolers	Cold utility	11211	4267	6944	£163,700
		HP shaftpower	0	0	4	£1,100
		CW for HP rejection			12	£300
Feed conditioning	Heaters	Hot utility	0	0	0	£0
	Coolers	Cold utility	1413	1413	0	£0
	Expanders	Expansion shaftpower	-1215		-1215	-£332,400
Product conditioning	Heaters	Hot utility	0	0	0	£0
	Coolers	Cold utility	936	0	936	£0
		HP shaftpower	0	0	35	£9,600
		CW for HP rejection			971	£22,900
	Compressors	Compression shaftpower	211	0	211	£57,700
	Pumps	Electricity	0	0	0	£0
Total						£7,646,400

Table 8.20: Config. No. 5 (Indirect sequence – Abs. Des. x 2: Abs. Des.) – AB/C. Utility requirements before and after heat integration and final utility costs.

			Utility Demand prior to Heat Integration kW	Utility Savings kW	Net Utility Demand kW	**Utility Cost** GBP/yr
Reboilers		Hot utility	31982	21033	10949	£2,546,300
Condensers		Cold utility	197	197	0	£0
		HP shaftpower	0	0	0	£0
		CW for HP rejection			0	£0
Solvent heat exchangers	Heaters	Hot utility	0	0	0	£0
	Coolers	Cold utility	7675	6841	833	£0
		HP shaftpower	0	0	257	£70,200
		CW for HP rejection			1090	£25,700
Feed conditioning	Heaters	Hot utility	1247	1247	0	£0
	Coolers	Cold utility	0	0	0	£0
	Compressors	Comopression shaftpower	2040		2040	£558,100
Product conditioning	Heaters	Hot utility	3303	3303	0	£0
	Coolers	Cold utility	468	0	468	£0
		HP shaftpower	0	0	17	£4,800
		CW for HP rejection			486	£11,500
	Compressors	Compression shaftpower	1795	0	1795	£491,100
	Pumps	Electricity	0	0	0	£0
Total						£3,707,800

Table 8.21: Config. No. 5 (Indirect sequence – Abs. Des. x 2: Abs. Des.) – A/B. Utility requirements before and after heat integration and final utility costs.

The most important contributor to the total operating costs is the consumption of hot utility in each of the absorber-desorber blocks (27169 kW for separation task AB/C and 10949 kW -after integration of 21033 kW- for separation task A/B). The total hot utility reboiler consumption of the absorber-desorber block performing separation AB/C in the configuration of Configuration No. 5 is 27169 kW, while that of the

equivalent separation block in Configuration No. 4 is 28261 kW. In conclusion, the reboiling hot utility requirements for the process of Configuration No. 5 are arguably close to those of the configuration where absorption-desorption is combined with distillation.

Operating costs of first separation in the sequence are higher than those of the second separation. This result may be appreciated in Table 8.9.

- *Capital costs of Configuration No.* 5

Table 8.11 shows that the capital costs attributed to refrigeration are a very small fraction of the total capital costs. This is related to the smaller refrigeration requirements than those of other process configurations, due to refrigeration being only required for solvent and product chilling rather than for providing condensation duties.

Configuration No. 6: Distillation x 2 in Indirect Sequence

The layout and key operating variables of the proposed configuration are shown in Figure 8.14. Figure 8.15 and Figure 8.16 show the schematics of the proposed refrigeration cycles for the condensers of distillation column 1 and 2, respectively.

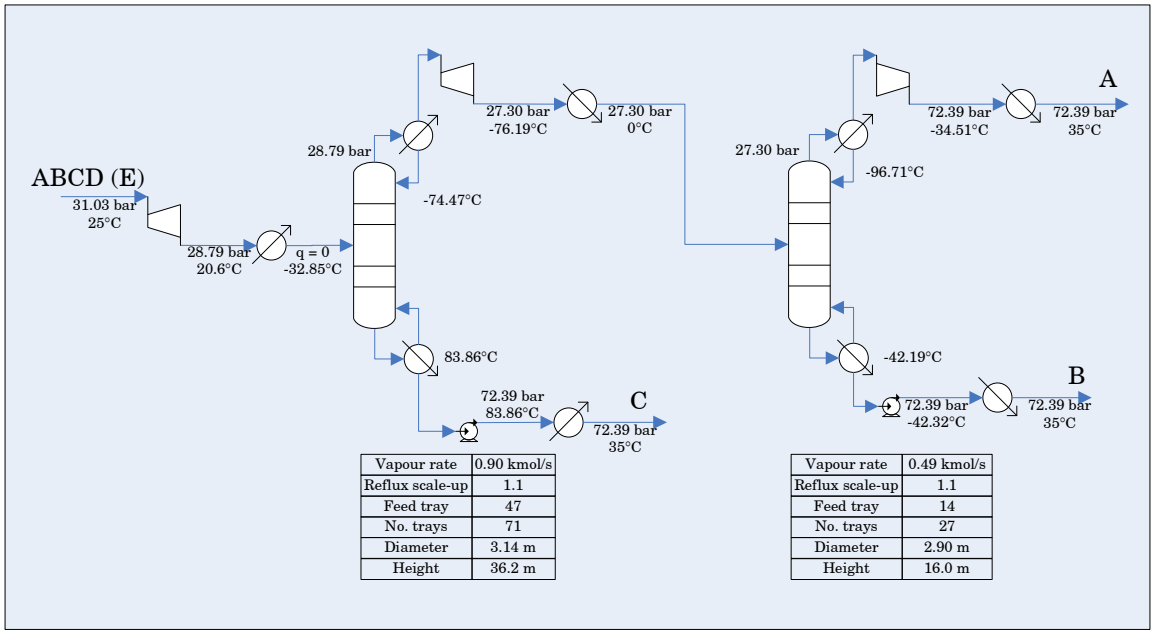

Figure 8.14: Config. No. 6 (Indirect sequence – Distil. x 2): Distillation. Key design and operating variables.

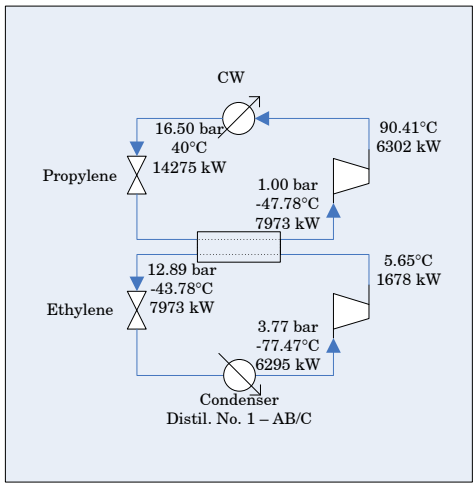

Figure 8.15: Config. No. 6 (Indirect sequence – Distil. x 2): Distillation. Refrigeration matches for condenser of distillation column No. 1.

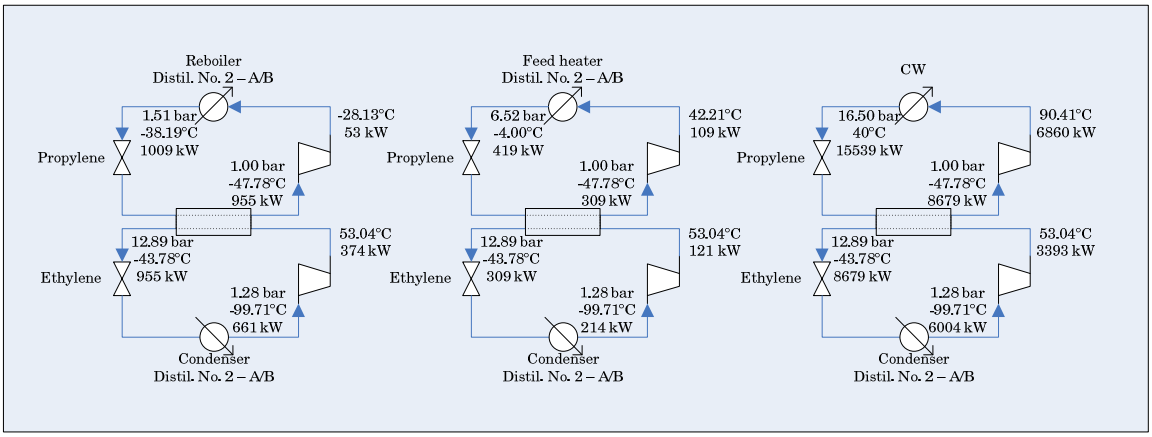

Figure 8.16: Config. No. 6 (Indirect sequence – Distil. x 2): Distillation. Refrigeration matches for condenser of distillation column No. 2.

- ***Operating costs of Configuration No. 6***

Table 8.22 and Table 8.23 summarise the process total utility demands of each separation task before and after heat integration and refrigeration system design.

			Utility Demand prior to Heat Integration kW	Utility Savings kW	Net Utility Demand kW	**Utility Cost** GBP/yr
Reboilers		Hot utility	9039	0	9039	£2,547,100
Condensers		Cold utility	10906	4611	0	£0
		HP shaftpower			7980	£2,183,300
		CW for HP rejection			14275	£336,900
Feed conditioning	Heaters	Hot utility	0	0	0	£0
	Coolers	Cold utility	2586	2586	0	£0
	Expanders	Expansion shaftpower	-154		-154	-£42,100
Product conditioning	Heaters	Hot utility	0	0	0	£0
	Coolers	Cold utility	348	348	0	£0
	Compressors	Compression shaftpower	30	0	30	£8,100
	Pumps	Electricity	0	0	0	£0
Total						£5,033,400

Table 8.22: Config. No. 6 (Indirect sequence – Distil. x 2): Distillation – AB/C. Utility requirements before and after heat integration and final utility costs.

			Utility Demand prior to Heat Integration kW	Utility Savings kW	Net Utility Demand kW	**Utility Cost** GBP/yr
Reboilers		Hot utility	4494	4494	0	£0
Condensers		Cold utility	6879	0	0	£0
		HP shaftpower			10910	£2,985,100
		CW for HP rejection			15539	£366,700
Feed conditioning	Heaters	Hot utility	3560	3560	0	£0
	Coolers	Cold utility	2586	2586	0	£0
	Expanders	Expansion shaftpower	-57		-57	-£15,600
Product conditioning	Heaters	Hot utility	4198	918	3280	£762,800
	Coolers	Cold utility	0	0	0	£0
	Compressors	Compression shaftpower	1390	0	1390	£380,300
	Pumps	Electricity	30	0	30	£8,200
Total						£4,487,500

Table 8.23: Config. No. 6 (Indirect sequence – Distil. x 2): Distillation - A/B. Utility requirements before and after heat integration and final utility costs.

The key utility users of the separation system include the reboiler of column 1 and the condensers of the two columns. Utility costs associated to each of these, accounting for the refrigeration costs, are comparatively close, as seen in Table 8.9.

- *Capital costs of Configuration No. 6*

Capital costs presented in Table 8.11 are governed by the cost of the product refrigeration compressors, which is common of low-temperature distillation systems.

The capital cost of 449,600 £/yr corresponding to the distillation column performing separation task AB/C is comparatively close to the cost of 431,700 £/yr for the distillation column performing the same separation task in the indirect sequence of Configuration No. 2. These columns have a number of features in common: (1) both operate in the same pressure range and at the same minimum reflux scale-up factor; (2) both feature a vapour feed.

Equally, the capital cost of 226,500 £/yr corresponding to the distillation column performing separation task A/B is comparatively close to the cost of 199,600 £/yr for the distillation column performing the same separation

task in the indirect sequence of Configuration No. 4. These columns have identical feed conditions and the difference in pressures and reflux ratios is translated into a difference of seven column stages, which is accountable for the capital cost difference between the two columns, since these columns have the same diameter.

In summary, Configuration No. 6 may be interpreted as a nearly perfect assembly of features of previous configurations, whereby the total costs exceed the sum of the individuals. The absorption-desorption blocks of Configuration Nos. 2 and 4 work in synergy with the corresponding distillation blocks by granting additional opportunities for heat integration.

8.3 Case 2: LPG recovery from refinery off-gases

Refinery net gas is a stream rich in hydrogen containing also methane, ethane and C3+ LPG. To recover value from the net gas, an LPG recovery unit may be employed to maximise LPG recovery and increase the hydrogen purity of the net gas for subsequent hydrotreating use.

8.3.1 Background

Al-Shahrani and Mehra (2007) describe the incorporation of an LPG recovery unit at Yanbu' Refinery in Saudi Arabia. The choice of technology is a licensed enhanced absorption process. This process was selected based on licensor process specifications, specifically, the capacity to effectively achieve high propane recoveries (96%+) from off-gases at relatively low pressure (starting at 11 bar), which do not require compression.

The initial process concept, a pure Mehra process, is subsequently modified to work in synergy with the existing process. By using an existing operating debutaniser column as the regenerator of the new absorption cycle, the project investment may be minimised.

According to Al-Shahrani and Mehra (2007), a C5+ solvent is ideal because of the adequate solvent flow rate (due to the low molecular weight) and solvent losses (due to the low vapour pressure). This observation makes the bottoms of the existing debutaniser column a potential lean solvent for the absorption process. However, this choice of solvent was discarded on the basis that achieving the 96% recovery specification on C3 would require a solvent circulation rate in excess of the allowable by the existing debutaniser diameter.

This limit was overcome by applying a further modification to the initial licensed process, consisting on a split-flow arrangement, which allows achieving the desired recovery in the existing equipment. Essentially, in

the split flow arrangement, the absorber column solvent demand is supplied by two solvent fractions, the leaner debutaniser bottoms feeding the top of the absorber, and a lighter stream entering the absorber at an intermediate height. In typical split-flow absorption-desorption schemes, the lighter stream is a liquid side draw from the regenerator column, which therefore has been only partially regenerated. In this situation, however, there is an available separate stream saturated with propane and butanes which is selected as the intermediate solvent.

The third modification to the original licensed process replaces the initial reboiled absorber with a simple absorber without reboiler. This configuration will not achieve the ethane specification on the LPG product. However, the excess of ethane in the solvent and subsequently in the debutaniser overhead condensate is handled by the existing deethaniser column situated downstream of the debutaniser. The C3-C4 product from the deethaniser is further fractionated to produce propane and mixed butanes products.

Finally, various alterations to the existing process are described that enable the accommodation of the new process in the plant, including the addition of heat transfer area of existing heat exchangers and replacement of pumps. A new closed loop three-stage propane refrigeration cycle was required along with the new absorber. -33°C propane refrigerant is needed to provide the chilling of the solvent streams and the gas feed to -29°C.

The commissioned LPG process recovery at the Yanbu' Refinery as described by Al-Shahrani and Mehra (2007) incorporates further energy efficiency enhancements, such as a presaturator at the top of the absorber, economisers in the refrigeration cycle and heat recovery options in the overall process.

Feed compositions and recoveries are presented in Table 8.24. Co-absorbed hydrogen, methane and ethane do not appear in the product liquid fractions as they are removed by the deethaniser.

	Combined gas feed to absorber, mol%	Product gas to hydrotreater, mol%	Recovery in absorber gas product	Recovery in liquid products from fractionation
Hydrogen	73.62	88.63	99.9%	- *
Methane	3.63	4.26	97.4%	- *
Ethane	8.32	6.78	67.6%	- *
Propane	8.13	0.14	1.4%	98.6%
Isobutane	1.77	0.01	0.5%	99.5%
n-Butane	2.11	0.03	1.2%	98.8%
Isopentane	0.78	0.09	9.6%	90.4%
n-Pentane	0.43	0.03	5.8%	94.2%
C6+	1.20	0.03	2.1%	97.9%
Total	100	100		
Flow, kmol/h	2948	2446		

Table 8.24: Recovery achieved at Yanbu' Refinery by the LPG absorption unit.

8.3.2 Aims

The investigation of absorption and distillation options may be approached systematically using the proposed synthesis and optimisation methodology developed in this work. This methodology is applied to this case study with the aim of establishing the optimal configuration and operating conditions of a separation process operating at a 99.5% rejection of ethane and 98.6% recovery of propane. A comparison will be drawn between the yearly economics of the optimal absorption-desorption process and the equivalent pure distillation process.

8.3.3 Problem inputs

Prior to the application of the developed optimisation methodology to Case Study 2, heavier components than C4 are artificially removed from the feed and the composition is normalised to conform to the framework limitations. The feed composition is shown in Table 8.25.

	Actual gas feed composition, mol%	Modified composition for optimisation, mol%
Hydrogen	73.62	76.61
Methane	3.63	3.78
Ethane	8.32	8.66
Propane	8.13	7.42
Isobutane	1.77	3.54
n-Butane	2.11	0.00
Isopentane	0.78	0.00
n-Pentane	0.43	0.00
C6+	1.20	0.00
Total	100	100
Flow, kmol/h	2948	2948

Table 8.25: Original gas feed composition and manipulated composition for illustration of optimisation methodology.

The selected solvent is pure n-pentane and the Peng-Robinson property prediction method in Aspen Properties® is applied throughout. This equation-of-state property method is selected on the basis of low to moderate pressure and refinery gas processing. The hydrogen presence makes some other property methods fail. Some property methods applied to this example may predict inaccurately the relative volatilities of components and invalidate the recovery specification requirements.

It is assumed that the feed is available at saturated vapour conditions at the pressure of 12 bar. The corresponding feed temperature is -21.7°C. The specifications on product conditions are 12 bar and 35°C.

8.3.4 Results and discussion

8.3.4 (i) SA parameter tuning

Similar SA parameters to those employed in Case Study 1 lead to an acceptable annealing history in Case Study 2, as shown in Figure 8.17.

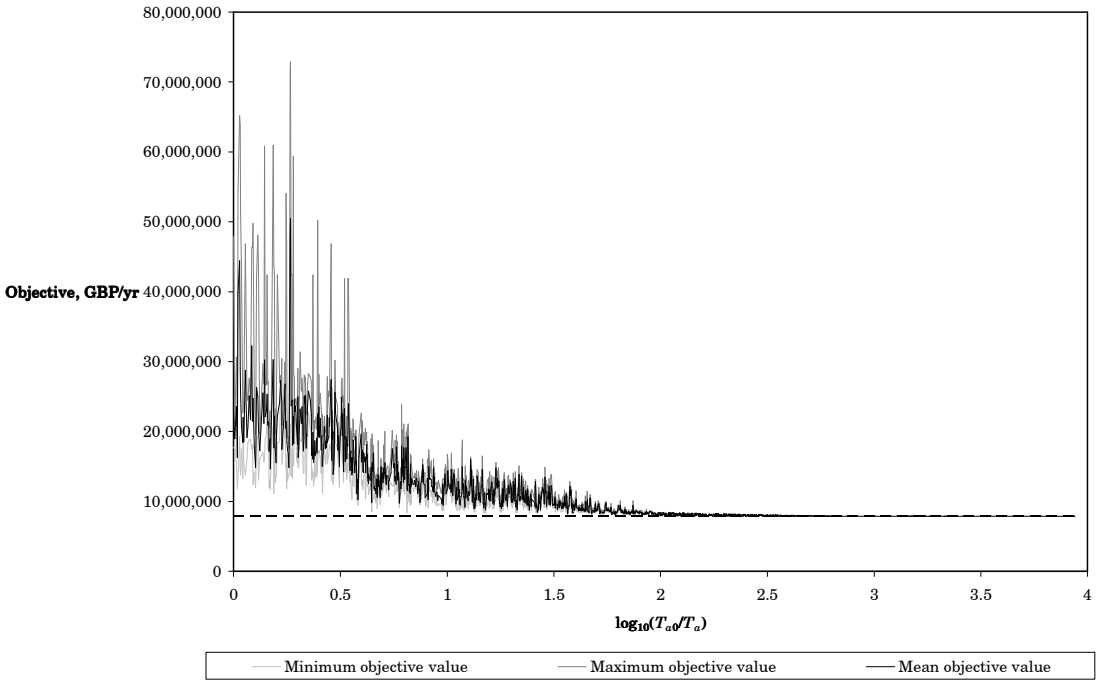

Figure 8.17: Annealing history of Case Study 2.

8.3.4 (ii) Validation of results

The separation system generated by optimisation along with its key design and operating variables is shown in Figure 8.18. An Aspen Plus® simulation has been set up to demonstrate the validity of the separation system optimised by the proposed synthesis framework. The selected column models are of the RadFrac® type.

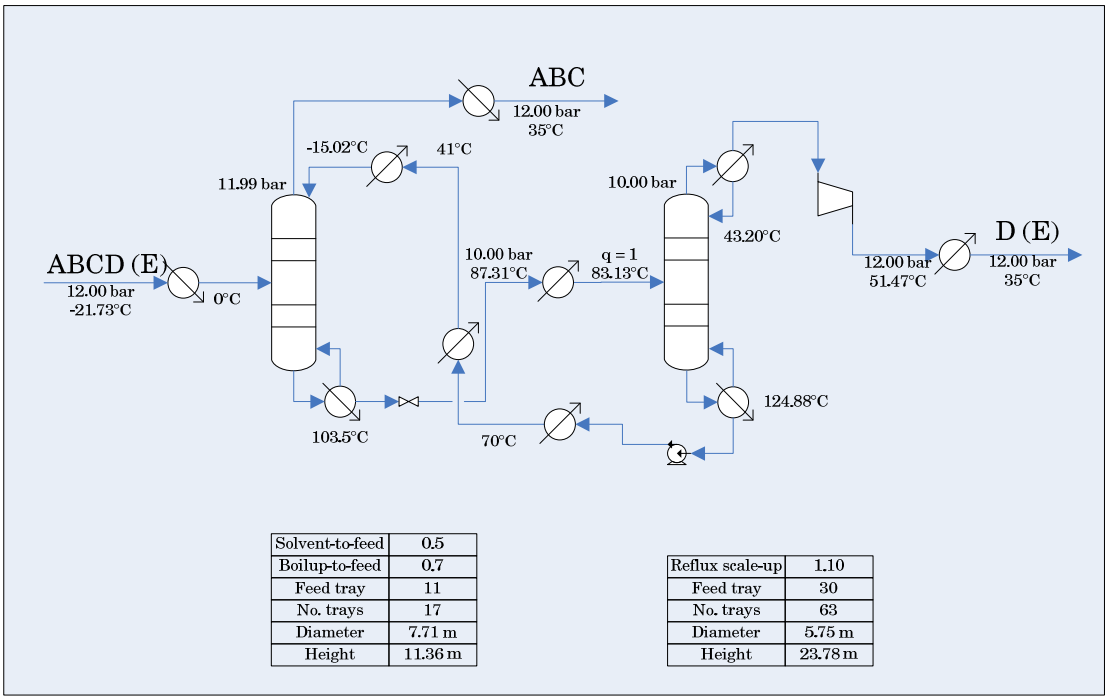

Figure 8.18: Config. No. 1 (Abs. Des.) – Key design variables and operating conditions.

Aspen Plus® simulation tools known as “design specifications” are employed along the setup of the simulation in order to obtain a reboiled absorber column design that meets the desired recovery specifications. For the number of stages and feed location featured in the optimised separation system, the resulting design configuration is characterised by the operating variables provided in Figure 8.19. In Figure 8.19, the reboiled absorber column has been conveniently modelled as an assembly of two RadFrac® columns to facilitate the analysis of the tray distribution, which will be explained later in this section.

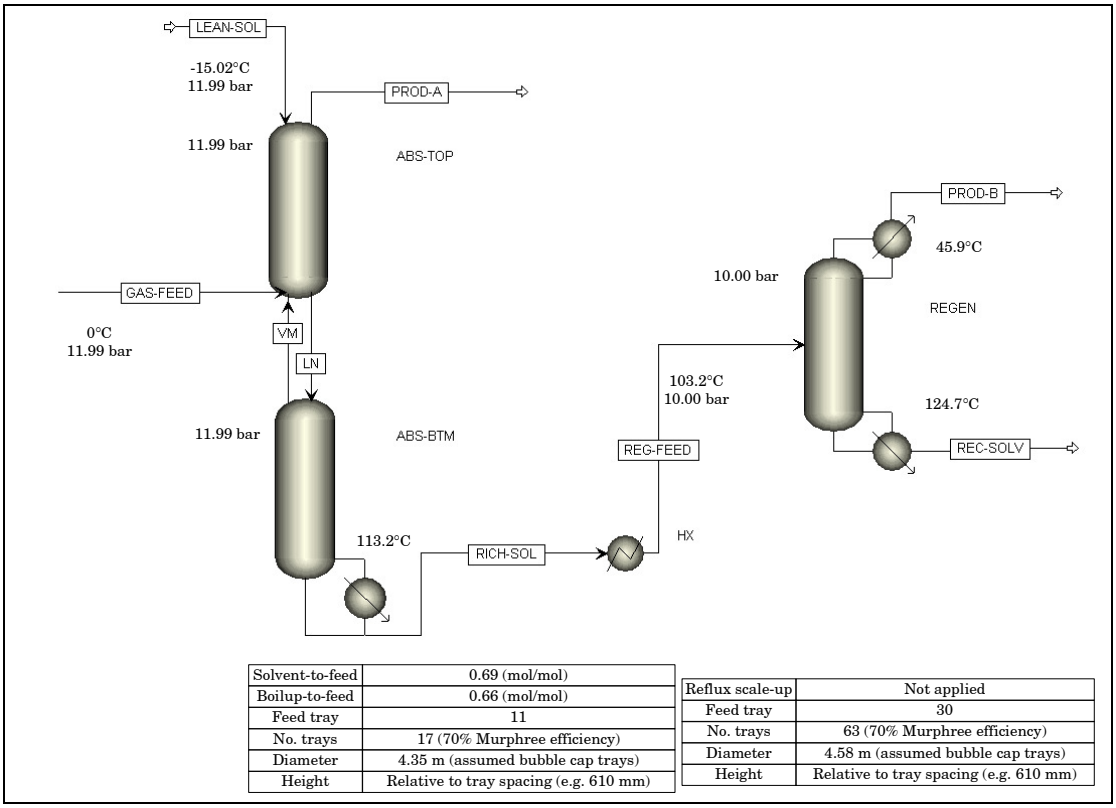

Solvent-to-feed	0.69 (mol/mol)
Boilup-to-feed	0.66 (mol/mol)
Feed tray	11
No. trays	17 (70% Murphree efficiency)
Diameter	4.35 m (assumed bubble cap trays)
Height	Relative to tray spacing (e.g. 610 mm)

Reflux scale-up	Not applied
Feed tray	30
No. trays	63 (70% Murphree efficiency)
Diameter	4.58 m (assumed bubble cap trays)
Height	Relative to tray spacing (e.g. 610 mm)

Figure 8.19: Aspen Plus® simulation results for Config. No. 1 of Case Study 2.

Any major differences between the shortcut and the Aspen Plus® column duties can distort the true energy utilisation of the optimised system. Evaluation of Figure 8.18 in conjuction with Figure 8.19 indicates that the solvent and reboiling requirements of the reboiled absorber column are comparable but not identical. A distortion of this kind tends to affect most separation system alternatives in a similar way, which results in an attenuated impact of model inaccuracies on the relative evaluation of process configurations during optimisation.

For the current example, little responsibility of the above distortion can be attributed to an inaccurate column stage distribution. A sensitivity analysis has been carried out which shows the limited effect on the number of the stages of each column section on the solvent and boilup requirements. The results of this analysis are provided in Table 12.14.

A tray sizing tool which is available to the Aspen Plus® column models has been used to generate an estimate of the column diameter. Vapour traffic in the bottom of the absorber is higher than in the top of the absorber. As a result, the reboiled absorber column diameter is controlled by the bottom section of the absorber.

The two estimates of the regenerator column diameter coincide more strictly than those of the reboiled absorber column diameter. Also, if a typical scale-up reflux ratio factor was applied to the simulated regenerator column, an even closer agreement could be obtained. The Aspen Plus® prediction of the reboiled absorber column is significantly lower than the shortcut prediction possibly due to the reduced vapour flowrate in the RadFrac® column.

8.3.4 (iii) Problem solution and discussion

The set of best configurations found through optimisation includes two configurations, which correspond to absorption-desorption and distillation. Each proposed configuration will be discussed in this section.

Figure 8.20 presents a summary of the results of the optimisation problem for total cost minimisation. The capital and operating contributions to the total cost of each best solution are provided.

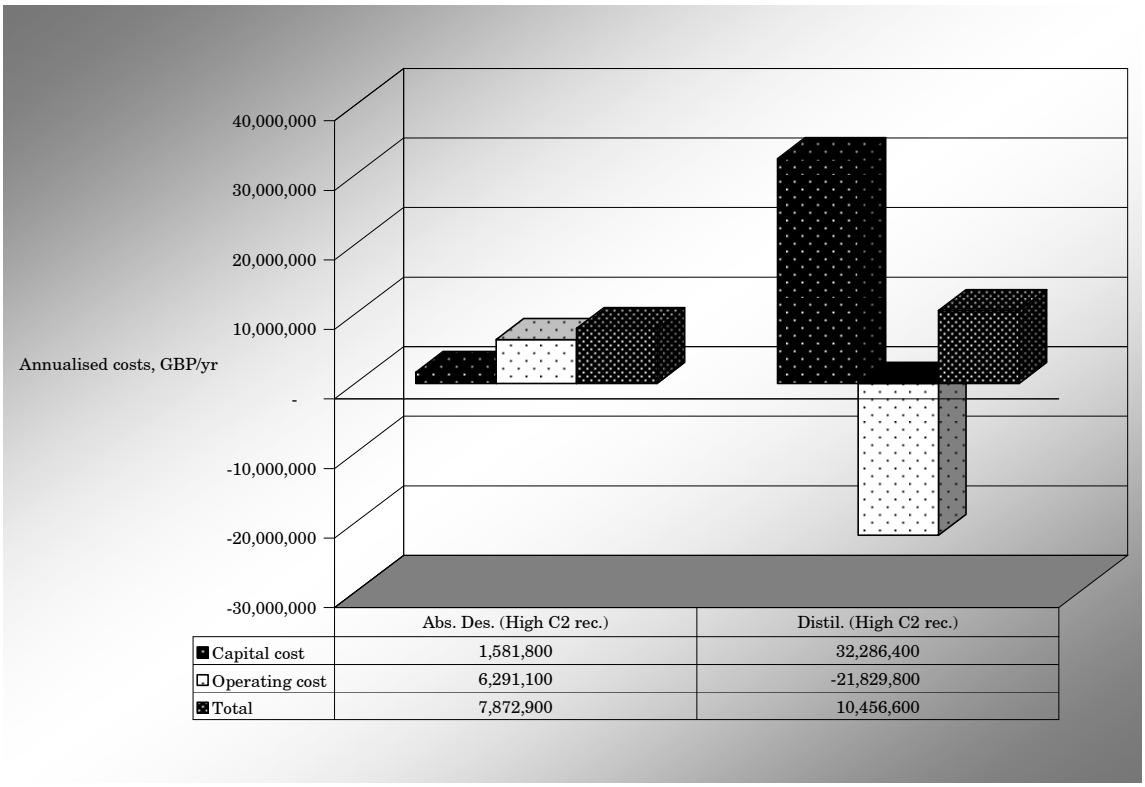

	Abs. Des. (High C2 rec.)	Distil. (High C2 rec.)
Capital cost	1,581,800	32,286,400
Operating cost	6,291,100	-21,829,800
Total	7,872,900	10,456,600

Figure 8.20: Summary of best configurations with minimum total cost.

The fundamental differences observed in Figure 8.20 between absorption-desorption and distillation in the distribution of capital and operating costs are discussed in this section.

Configuration No. 1: Absorption-Desorption

- ***Operating costs of Configuration No.*** **1**

Table 8.26 summarises the process total utility demands before and after heat integration and refrigeration system design.

			Utility Demand prior to Heat Integration kW	Utility Savings kW	Net Utility Demand kW	**Utility Cost** GBP/yr
Reboilers		Hot utility	24422	2979	21442	£6,042,400
Condensers		Cold utility	7888	0	7888	£186,200
		HP shaftpower	0	0	0	£0
		CW for HP rejection			0	£0
Solvent heat exchangers	Heaters	Hot utility	0	0	0	£0
	Coolers	Cold utility	6763	5148	1615	£38,100
Feed conditioning	Heaters	Hot utility	641	641	0	£0
	Coolers	Cold utility	0	0	0	£0
	Expanders	Expansion shaftpower	0		0	£0
Product conditioning	Heaters	Hot utility	2712	2712	0	£0
	Coolers	Cold utility	1525	1185	340	£0
		HP shaftpower	0	0	13	£3,500
		CW for HP rejection			353	£8,300
	Compressors	Compression shaftpower	46	0	46	£12,600
	Pumps	Electricity	0	0	0	£0
Total						£6,291,100

Table 8.26: Config. No. 1 (Abs. Des.) Utility requirements before and after heat integration and final utility costs.

This configuration is characterised by relatively large reboiler duties, which are mainly provided by external utilities, as shown in Figure 8.21 and Figure 8.22. The system is highly heat-integrated. Most of the total cooling demands of the solvent circulation system are satisfied internally by other process streams. Similarly, feed and product conditioning demands are fully integrated, with the exception of the bottom product, which, in addition to heat integration, requires a small amount of refrigeration to meet the imposed product delivery temperature. The shaftpower demands of this refrigeration cycle are as low as 22% of the total flowsheet shaftpower requirements.

Key operating variables and column dimensions are shown in Figure 8.18. The pressure of the desorber column allows condensation on cooling water, thus avoiding refrigeration. It appears from Figure 8.18 that the absorber column pressure is 11.99 bar, which optimisation does not distinguish from 12.00 bar by neglecting any pressure changers on the feed or on the light product. This makes this solution particularly favourable by cutting down on vapour compression capital and operating

costs.

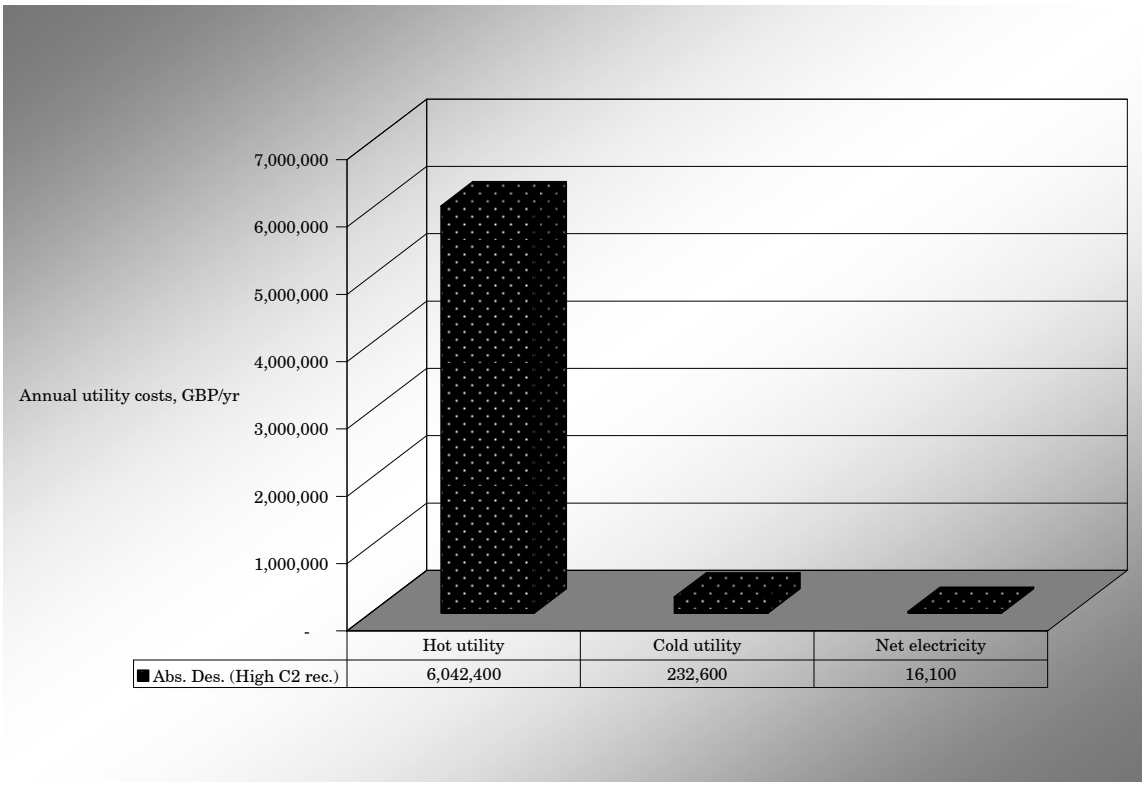

Figure 8.21: Config. No. 1 (Abs. Des.) – Consumption of utilities.

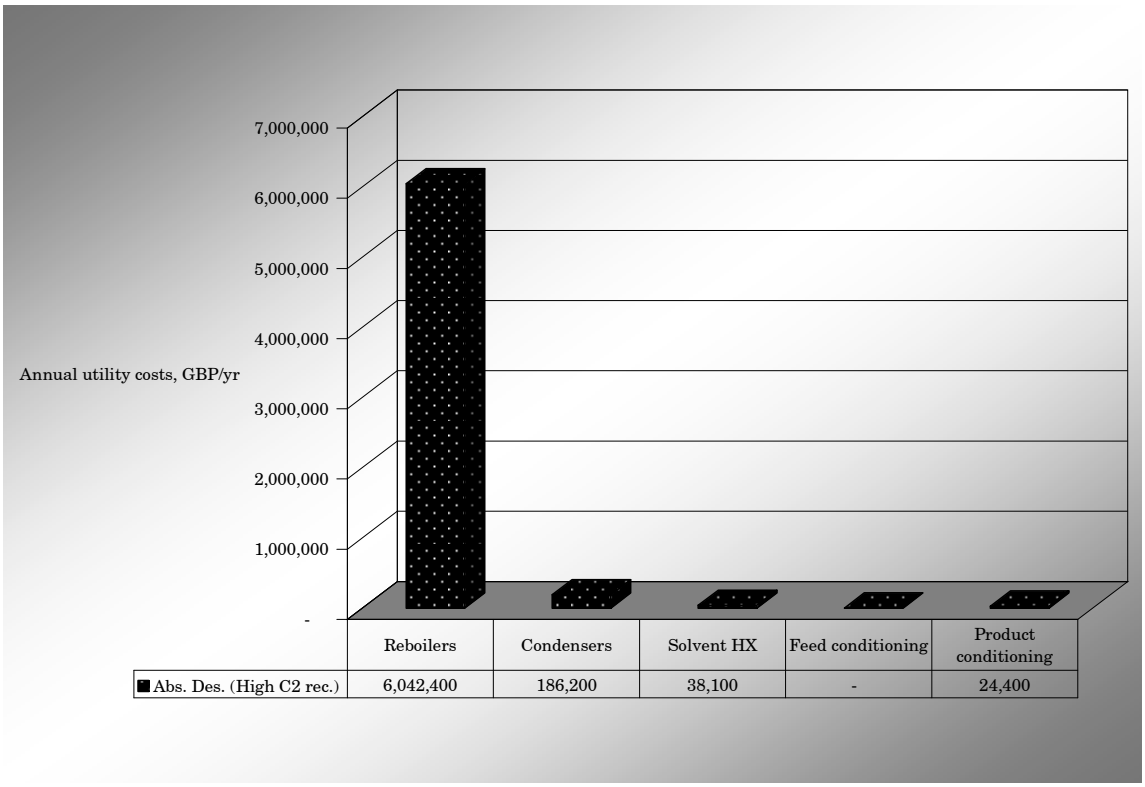

Figure 8.22: Config. No. 1 (Abs. Des.) – Breakdown of utility costs.

- ***Capital costs of Configuration No.*** **1**

The most important single contribution to the total annualised costs is the cost of the columns, as shown in Figure 8.23. The relative scale of the compressor capital costs with respect to the costs of heat exchangers suggests that the capital cost correlation for compressors may be underestimating capital costs at the small end of shaftpower. The present optimisation framework, however, can easily accommodate different capital cost estimation methods as desired.

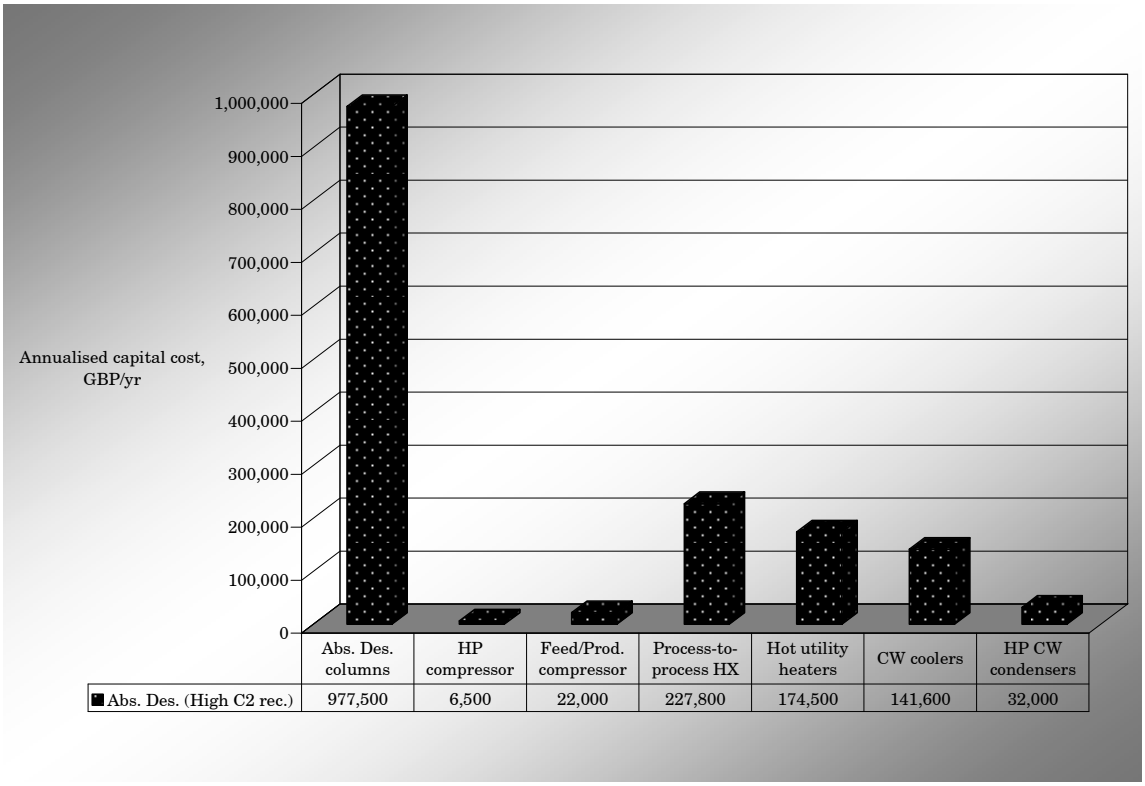

Figure 8.23: Config. No. 1 (Abs. Des.) – Breakdown of capital costs.

Configuration No. 2: Distillation

- ***Operating costs of Configuration No.* 2**

Table 8.27 summarises the process total utility demands before and after heat integration and refrigeration system design.

This configuration is characterised by the generation of energy through feed letdown, which outweighs the utility consumption of the process, resulting into a net export of electricity which manifests as a negative overall energy cost. This result must be observed with caution, since different input electricity unit costs could alter the economics of the process. Additionally, the capital investment associated with the gas turbine may be regarded as prohibitive. Capital costs are shown in Figure 8.26.

The 12 bar feed expands through the inlet gas turbine to the column pressure of 1.31 bar, as shown in Figure 8.24.

The condenser duty is fully integrated with the gas feed. This match accounts for most of the heat integration in the separation system. However, the duty involved is a small portion of the gas feed requirements to achieve the featured column feed temperature. By convention of this work, hot utility has not been allocated to the heating of the cryogenic feed, because in real practice, heat sinks of this kind are useful to other parts of the process, and thus, hot utility is not needed.

			Utility Demand prior to Heat Integration kW	Utility Savings kW	Net Utility Demand kW	**Utility Cost** GBP/yr
Reboilers		Hot utility	8334	0	8334	£0
Condensers		Cold utility	11341	11341	0	£0
		HP shaftpower	0	0	0	£0
		CW for HP rejection			0	£0
Feed conditioning	Heaters	Hot utility	82672	11341	71331	£0
	Coolers	Cold utility	0	0	0	£0
	Expanders	Expansion shaftpower	-83810		-83810	-£22,930,400
Product conditioning	Heaters	Hot utility	747	272	474	£110,300
	Coolers	Cold utility	272	272	0	£0
	Compressors	Compression shaftpower	3610	0	3610	£987,700
	Pumps	Electricity	9	0	9	£2,600
Total						-£21,829,800

Table 8.27: Config. No. 2 (Distil.) Utility requirements before and after heat integration and final utility costs.

Key operating variables and column dimensions are shown in Figure 8.24. The near-atmospheric pressure of the distillation column allows generation of very cold gas feeds through expansion from 12 bar.

The calculated column diameter of 14.5 m from in Figure 8.24 is an indicative of multiple parallel columns being recommended. The predominant contribution of electricity generation during feed conditioning may be appreciated in Figure 8.25 and Figure 8.26.

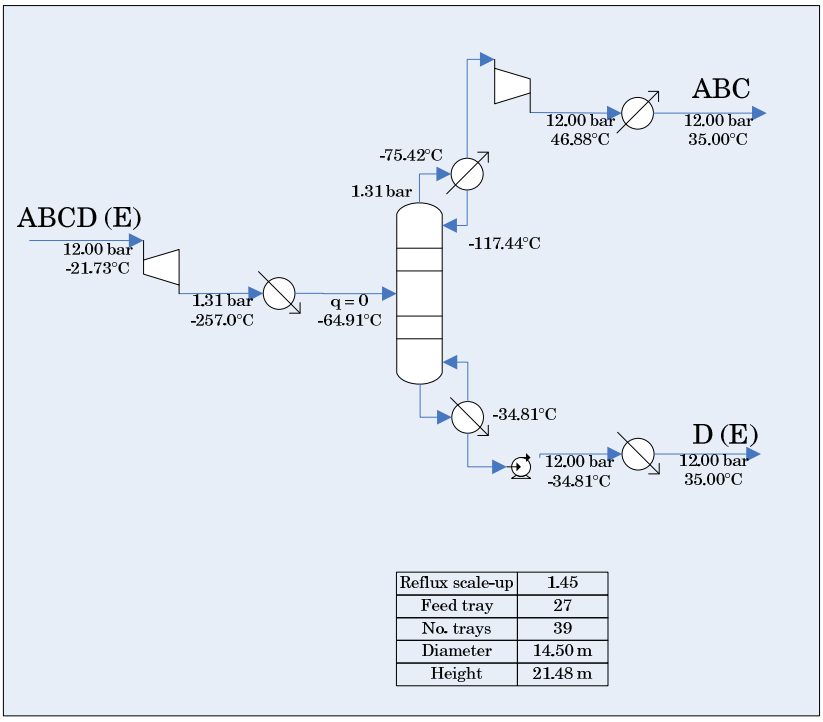

Figure 8.24: Config. No. 2 (Distil.) – Key design variables and operating conditions.

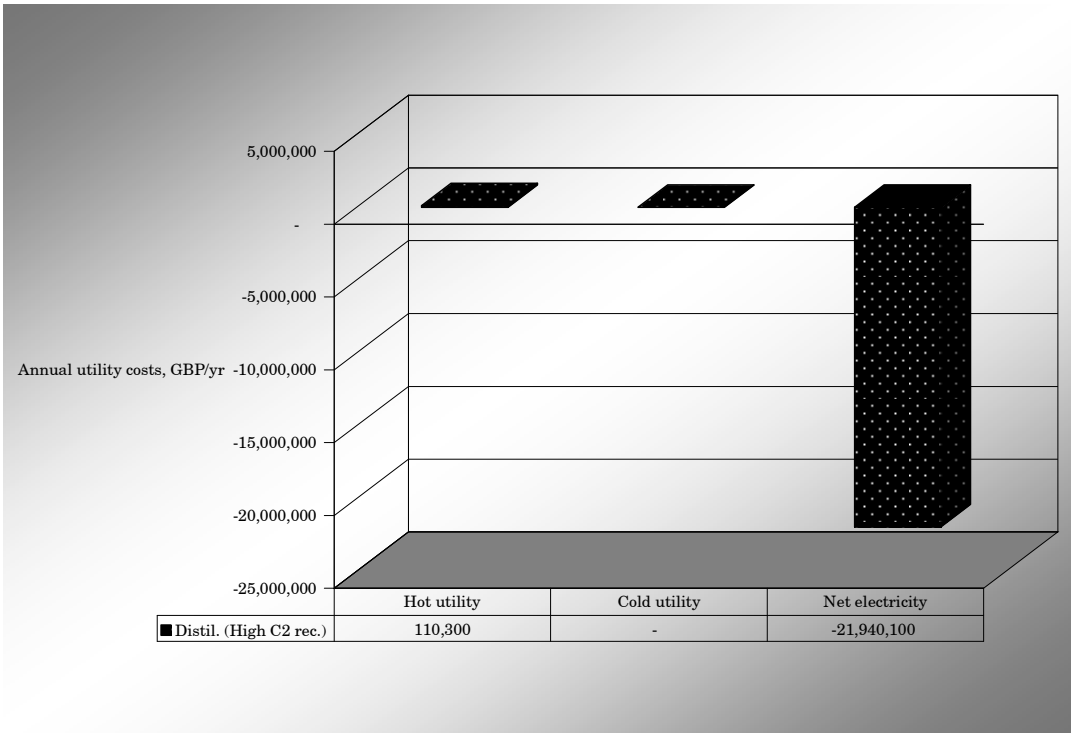

Figure 8.25: Config. No. 2 (Distil.) – Consumption of utilities.

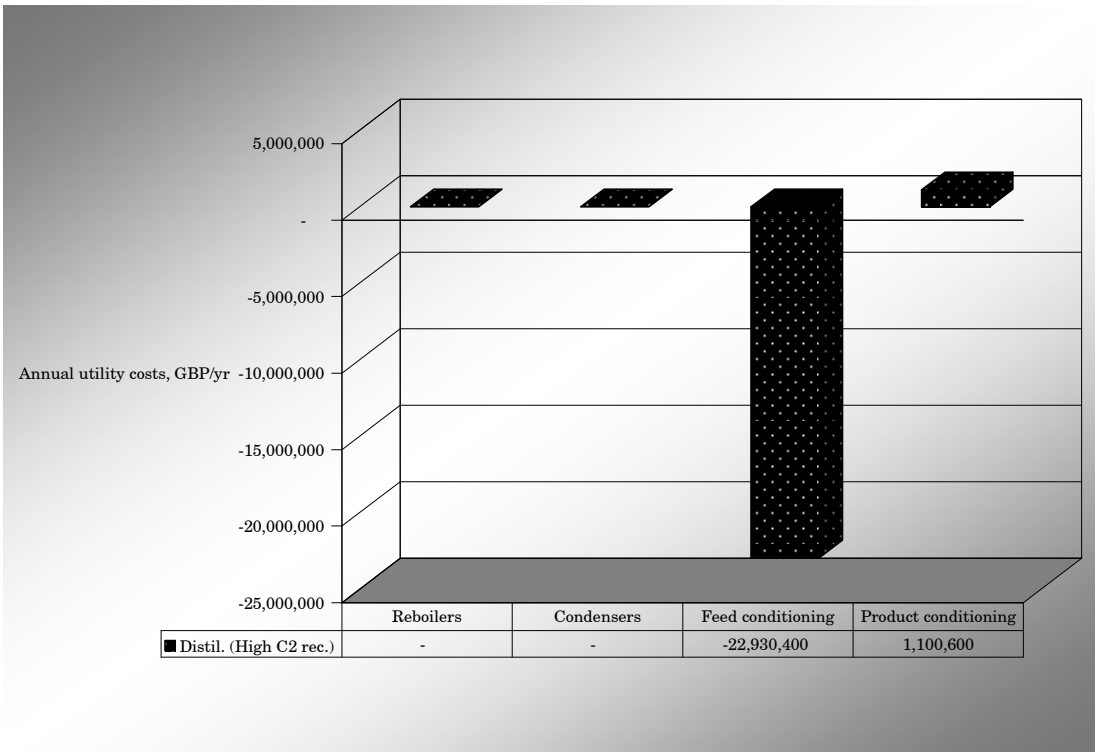

Figure 8.26: Config. No. 2 (Distil.) – Breakdown of utility costs.

- ***Capital costs of Configuration No. 2***

Siimilarly to Figure 8.25 and Figure 8.26 for operating costs, the capital costs shown in Figure 8.27 feature a very distinctive contribution associated with the costs of the feed gas turbo-expander, which will allow for energy recovery from the feed. This cost is in the vicinity of £31M, which offsets the £22M of electricity export profits.

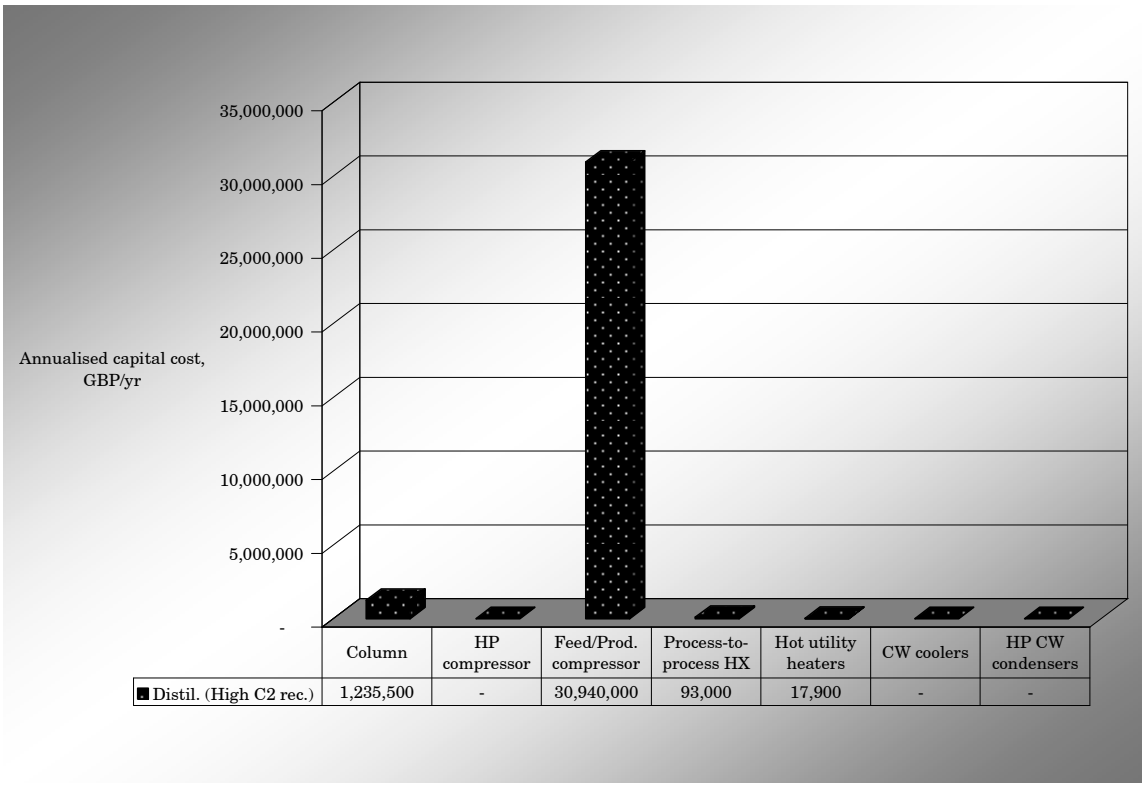

Figure 8.27: Config. No. 2 (Distil.) – Breakdown of capital costs.

In summary, the operating costs of the distillation flowsheet alternative are more favourable than those of the absorber-desorber option due to energy recovery through expansion. Nonetheless, because of the large scale of the capital investment of the gas expander of the distillation flowsheet, in the specified two-year payback time, the distillation flowsheet is less cost-effective overall than the absorber-desorber option.

8.4 Conclusions

In this section, the proposed synthesis methodology has been applied to gas separation examples of high industrial relevance, namely the recovery of LPG and ethane from natural gas and the recovery of LPG from refinery net gas. Optimisation of structural and operating issues has been approached simultaneously to recommend a subset of process configurations capable of achieving the design specifications, in accordance with the separation models used. The developed synthesis framework

equips each configuration with an efficient heat recovery system and an integrated refrigeration system.

This work yields a quantitative frame for discussion of the numerous trade-offs within each configuration and for comparison of the various configurations. Emphasis is placed on identifying the key contributors to the total capital and operating costs and on analysing the causes of these. A plausible explanation to key results and trade-offs has been identified in the majority of the cases.

The results of this Case Study 1 suggest that effective and simultaneous heat exchanger network design and separation system design can successfully exploit the synergism of combining absorption-desorption with distillation to discover potentially superior alternatives to the conventional low-temperature distillation schemes.

Case Study 2 illustrates the capability of the developed separation design methodology to represent simple cryogenic turboexpanders schemes as well as absorption-desorption and pure distillation.

Because the methodology offers complete control over the optimisation variables, the case study may be tailored to investigate specific optimisation variables by adjusting the move probabilities. External variables may also be investigated by conducting parametric studies, which require successive optimisation runs. For instance, the developed optimisation framework enables:

- To study different recovery and feed composition scenarios
- To draw comparisons between sequence optimisation and optimisation of individual separations
- To evaluate the effect of scale on process selection

- To evaluate the effect of objective function type on process selection

- To evaluate the effect of solvent composition and solvent purity on the process selection

The resulting optimisation solutions may be employed as a benchmark for exploration of ranges of operating variables. For example, sensitivity analyses may be conducted over the suggested best configuration to evaluate operational changes.

On a final note, the preliminary design configurations of this case study require detailed design analysis to arrive at more accurate cost estimates. This process may alter the preliminary ranking of the top configurations on total cost basis. Other considerations more appropriate of detailed design, such as process flexibility, operability and complexity, may dictate final process recommendations.

Chapter 9. Conclusions

This chapter summarises the main developments achieved by this work. Firstly, this work proposes to contribute to the area of process synthesis for gas separation systems by way of an optimisation methodology that is capable of evaluating alternative process options and exploring ranges of operating conditions on total cost basis. In actual synthesis practice, there is a demand for tools that assist with process synthesis, which is reflected by the adherence of the vast majority of newly built industrial processes to existing process concepts. Existing optimisation-based synthesis methodologies presented in Chapter 2, Literature review, are heavily constrained by one or more of the following factors: (1) a limited tractable problem size; (2) highly limiting process configuration restrictions; (3) an overly simplified representation of the separations; (4) an incomprehensive basis for cost evaluation; (5) no allowed interaction between the design of the separation system and the heat integration network and the refrigeration system. This work is an exercise of careful consideration and resolution of each of these aspects. Great emphasis is placed on the accuracy, the robustness and the exhaustivity of the proposed synthesis methodology.

Secondly, this work proposes to contribute to process advancement and innovation by way of the proposed synthesis methodology. Through systematic evaluation of alternative sequences of distillation and absorption-desorption separations, this methodology offers the potential of improving existing process concepts, which are largely dominated by low-temperature distillation. This work is believed to be the first of its kind that allows for optimisation-based synthesis of systems consisting of absorption-desorption as well as distillation.

Finally, the milestones of this work are summarised in the following:

i. Evidence has been provided on the proven application of the separation technologies that are the object of this investigation. These technologies are central to the gas processing industry.

ii. Literature review has revealed the limitations of the existing separation synthesis design approaches and the incentives to develop a synthesis methodology that overcomes these shortcomings and in addition, is capable of quantitatively selecting between absorption-desorption and distillation options.

iii. An existing distillation orientated framework for sequence optimisation (COLOM®, © Centre for Process Integration, University of Manchester) has been modified to allow for a seamless accommodation of absorption-desorption separation options. The transition between solvent-based separation blocks and the rest of the separation sequence has been managed successfully.

iv. Separation models have been developed, which are more representative than existing shortcut models and do not compromise computation time. The reboiled absorber column model allows for variation of the internal column overflows and temperature. The column profiles of these variables are estimated using established rules of physical significance.

v. A new strategy for heat integration network design has been developed, which is supported by the adopted optimisation framework. Unlike typical approaches based on minimum utility / minimum number of heat exchange units, the developed methodology is able to propose a heat exchanger network configuration. The optimisation of the separation system, the HEN and the refrigeration system is executed simultaneously, with the

potential of leading to superior solutions than conventional segregated approaches.

vi. A Simulated Annealing (SA) framework for optimisation of the synthesis framework has been proposed. This framework achieves optimisation of structural or discrete and operating or continuous variables at the following levels: sequence level, block level and column level, including variables which are specific of absorption-desorption. This framework has proven to achieve a successful exploration of the present large scale optimisation problem if the adequate paremeters are used.

vii. Some of the available methodologies for capital and utility cost estimation have been analysed and recommendations have been made on the basis for cost estimation with the aim of improving the reliability of the solutions. Previous cost-based optimisation approaches have not generally questioned the validity of available cost estimates.

viii. Case studies have been presented to illustrate the capabilities of the proposed methodology for a number of problems. The application of the methodology to these problems reinforces the argument that this methodology may be used as a powerful tool for consistent and quantitative process evaluation. It also highlights the potential of combining distillation and absorption-desorption for improved economics of the separation system.

More detailed conclusions on the developments of this work are provided at the end of each chapter of this thesis.

Chapter 10. Future work

As the severity of environmental regulations increases, industries will prioritise environmental objectives including energy efficiency, carbon and emissions minimisation.

The capability of the proposed synthesis methodology to identify highly energy efficient process configurations has been illustrated in Chapter 7. However, this synthesis methodology has focused on gas separations that can be carried out by physical absorption-desorption as well as distillation. While this type of gas separations is perhaps the most frequent, there are many other important gas separation applications. The impact factor of the developed synthesis methodology would increase greatly if the optimisation of the synthesis of chemical absorption-desorption systems was accounted for, because the removal of acid gases, including CO_2, H_2S and NO_x from waste gases or processing gas streams is an application that appeals to a much wider range of industries.

Secondly, the synthesis methodology developed in this work would be enhanced by accommodation of additional separation configurations for distillation and absorption-desorption. The developed methodology is restricted to two separation blocks: pure distillation and an absorption-desorption block that consists of a reboiled absorber and a distillation column for solvent regeneration. Additional separation configurations include new absorption-desorption configurations, complex distillation options and proprietary process configurations.

Another interesting area of future work is the extension of the proposed framework to other gas separation technologies, such as membrane separations, adsorption and catalytic conversion. Typically these

separation technologies are best suited to purification applications. Incorporation of these technologies to the developed methodology would enable the optimisation of a wide range of gas separations.

In addition to economic efficiency (capital investment and energy consumption), it would be interesting to reflect other practical objectives on the separation system design. These objectives include system flexibility, controllability, ease of construction and maintainability. However, quantification of these factors for incorporation in an optimisation framework is difficult.

A final recommendation for future work is the incorporation of a solvent design methodology to the synthesis framework, which would enable the optimisation of the composition of the solvent in the absorption-desorption block. The incorporation of molecular design algorighms in the existing separation system methodology is, however, beyond the scope of future work.

Next, these areas for future work are discussed in some more detail.

10.1 Chemical absorption processes

Chemical or reactive absorption is a very important separation process. It is commonly applied to those separations where typical physical solvents cannot retain a significant quantity of gas components, yet some of the gas components can react with a reactant added to the solvent. The reaction shifts the absorption equilibrium to make absorption more favourable. The reaction may be reversible or irreversible. The reversible reactions allow the gas components to be recovered during solvent regeneration and the solvent to be recycled to the absorber. Typical reversible reactions in the gas-processing, refining and petrochemical industries include gas sweetening, i.e. the removal of hydrogen sulphide with ethanolamines and carbon dioxide with an alkaline solution, and also some flue gas

desulphurisation processes. If the reactions are irreversible, the reaction products must be removed from the bulk of the solvent. In some cases these products are valuable products, such as ammonium sulphate.

The complexity of the design of chemical absorption processes is associated with the occurrence of chemical reactions and the associated mass transport of the absorbable components to the liquid phase.

The absorption model presented in this work is founded on the Edmister model, which relies on the only assumption of equilibrium being achieved at each stage. However, because of the presence of chemical reactions in reactive absorption, this assumption may be inacceptable. In addition, the proposed interpolation method for prediction of the internal profiles of absorption factors may be inadequate due to the highly non-ideal vapour-liquid equilibrium relationships.

The absorption model employed in this work has been shown to predict satisfactorily absorption performance under low to moderate heat effects, which are typical of physical absorption processes. Further adaptation of the model may be required to achieve an adequate representation of chemical absorption processes.

10.2 Extended range of process configurations

10.2.1 Additional absorption-desorption configurations

As presented in Chapter 3, a separation system that relies on absorption-desorption to achieve a sharp separation between two groups of feed components will generally require a mechanism to remove the co-absorbed light key component in the absorber. For this reason, in this work, a reboiled absorber has been favoured over a simple absorber. The reboiled absorber features a section where the co-absorbed light key components

are predominantly desorbed by the ascending vapour produced by the reboiler.

There are other mechanisms that provide the required extent of light key desorption. One of these mechanisms consists of using a stripping gas or vapour to achieve the desired desorption, instead of the vapour of the reboiler. This mechanism replaces the need for reboiling the rich solvent, which is usually an important energy user. Depending on the choice of stripping gas selection, this option may introduce an external or inert gas in the system, which is undesirable. Alternatively, an internal component existing in the feed may be used for providing the required stripping action. This vapour may come from a series of flashes downstream of the absorber, as in Figure 1.6. It may also from another part of the process. In principle, it is not desirable to obtain this vapour from a unit that operates at a lower pressure than the absorber to prevent elevated compression costs. However, because of the savings in reboiler duty there are tradeoffs that are susceptible of analysis within the proposed optimisation framework.

In addition to these alternative configurations, the developed synthesis framework could benefit from energy-saving process architectures, such as the split-flow arrangement of Towler and Shetna (1997) and presaturation scheme of Mehra (1987). These configurations may potentially result in reduced solvent flowrates and process duties, and their optimisation will require incorporating additional optimisation variables, thus resulting in an added problem complexity.

In the synthesis methodology of this work, the solvent employed may well be present in the feed, but the assumption is made that the concentration of the solvent components and heavier feed components is negligible. In practice, the solvent is often recovered from the feed itself. Dealing with this situation would require relatively relatively minor alterations to the proposed optimisation framework.

10.2.2 Complex distillation

The software platform that supports the proposed optimisation framework (COLOM) has been adjusted by Wang (2004) to accommodate complex distillation separation alternatives, also known as task representations. These are usable by the present optimisation framework, however, further work is needed to standarise the level of the modelling detail for these task representations with that of the improved models presented in this work.

10.2.3 Proprietary processes

Most of the separations in industry are accomplished in standard flowsheet pattern configurations. This would motivate the replication of some of the well-established process configurations and incorporate them as black boxes or templates to the optimisation framework. For example, NGL is unusually recovered by a simple distillation column. Instead, improved commercial processes such as the Ortloff system introduced in section 1.3.2 are encountered in real gas processing facilities. These processes for NGL/LPG recovery from natural gas include Ortloff's Gas Subcooled Process (GSP) and OverHead Recycle Process (OHR). Latest process modifications by Hudson *et al.* (2001), which achieve higher recoveries, efficiency and carbon dioxide tolerance involve CRR (Cold Residue Reflux), RSV (Recycle Split-Vapour), RSVE (Recycle Split-Vapour with Enrichmend process), SFR (Split-Flow Reflux) and SCORE (Single Column Overhead Recycle).

There is scope for future work on modelling these and other highly complex systems, which feature turboexpanders, recycles, multiple feed columns, columns of changing diameter, etc.

10.3 Extension of framework to other separation technologies

Less established separation methods for bulk separations as opposed to purification separations, such as Pressure Swing Adsorption (PSA), membrane permeation and catalytic conversion, are increasingly being compared favourably with distillation and absorption-desorption. The incorporation of these separation technologies in the proposed synthesis framework requires understanding of the key design variables and model development to allow systematic comparison of different technologies. This is an important area for future work.

10.4 Review of performance criteria for separation design

In addition to economic efficiency (reduction of capital investment and energy consumption), practical criteria for design selection include health and safety, environmental performance, controllability, flexibility, ease of construction and maintainability. In recent times, more factors are becoming decisive, such as raw material and energy availability, sustainability and life cycle impact. The relative importance of competing factors in many cases cannot be rationalised and quantified. Incorporation of these criteria in a systematic synthesis framework is complicated by the lack of methods of estimation of these factors. Multiobjective optimisation is a challenging topic that offers scope for future work.

10.5 Simultaneous approach to process and solvent synthesis

In this work the composition of the solvent needs to be specified beforehand. However, it would be useful if the developed synthesis methodology could optimise the solvent composition for a given set of solvent constituents or synthesise a solvent molecule from existing chemical groups. According to Grossmann (2004), traditional process

design is expanding to include molecular product design using the computer-aided molecular design (CAMD) approach. CAMD uses property and performance predictions (Joback and Stephanopoulos, 1995) for synthesis of molecular structures that meet predefined objectives. In some examples, these objectives are environmental, as in the case of design of a solvent that offers selectivity while being environmentally friendly. Notable studies on the search of potential solvents for separation systems have been carried out by Pistikopoulos and Stefanis (1998) and Marcoulaki and Kokossis (2000). According to Grossmann (2004), these optimisation methodologies require more accurate capabilities for prediction of properties of compounds.

The incorporation of the CAMD approach to the developed process synthesis methodology is a highly challenging task because of the additional computational overhead.

Chapter 11. References

Al-Shahrani, S. M. and Mehra, Y. R. (2007). "Saudi Aramco installs new LPG recovery unit at Yanbú refinery." *Oil and Gas Journal* **105**(21).

Andrecovich, M. J. and Westerberg, A. W. (1985). "SIMPLE SYNTHESIS METHOD BASED ON UTILITY BOUNDING FOR HEAT-INTEGRATED DISTILLATION SEQUENCES." *AIChE Journal* **31**(3): 363-375.

Athier, G., Floquet, P., Pibouleau, L. and Domenech, S. (1997). "Synthesis of Heat-Exchanger Network by Simulated Annealing and NLP Procedures." *AIChE Journal* **43**(11): 3007-3020.

Barnicki, S. D. and Fair, J. R. (1990). "Separation system synthesis: A knowledge-based approach. 1. Liquid mixture separations." *Industrial and Engineering Chemistry Research* **29**(3): 421-432.

Barnicki, S. D. and Fair, J. R. (1992). "Separation system synthesis: A knowledge-based approach. 2. Gas/vapor mixtures." *Industrial & Engineering Chemistry Research* **31**(7): 1679-1694.

Barnicki, S. D. and Siirola, J. J. (2001). Systematic chemical process synthesis. Formal Engineering Design Synthesis, Cambridge University Press: 362 – 390.

Barnicki, S. D. and Siirola, J. J. (2004). "Process synthesis prospective." *Computers & Chemical Engineering* **28**(4): 441-446.

Patent US 5520724, Becker, H. and Bauer, H. (1996). "Process for the recovery of low molecular weight C2+ hydrocarbons from a cracking gas."

Bek-Pedersen, E., Gani, R. and Levaux, O. (2000). "Determination of optimal energy efficient separation schemes based on driving forces." *Computers and Chemical Engineering* **24**(2-7): 253-259.

Biegler, L. T. and Grossmann, I. E. (2004). "Retrospective on optimization." *Computers and Chemical Engineering* **28**(8): 1169-1192.

Bloch, H. P. and Soares, C. (2001). Turboexpanders and Process Applications.

Brown, G. G. and Holcomb, D. E. (1940). *Petroleum Engr.* **11**: 27-30.

Brown, G. G. and Martin, H. Z. (1939). *Trans Aich E* **35**: 679.

Caballero, J. A. and Grossmann, I. E. (2001). "Generalized disjunctive programming model for the optimal synthesis of thermally linked distillation columns." *Industrial and Engineering Chemistry Research* **40**(10): 2260-2274.

Caballero, J. A. and Grossmann, I. E. (2006). "Structural considerations and modeling in the synthesis of heat-integrated-thermally coupled distillation sequences." *Industrial and Engineering Chemistry Research* **45**(25): 8454-8474.

Constantinou, L., Bagherpour, K., Gani, R., Klein, J. A. and Wu, D. T. (1996). "Computer aided product design: Problem formulations, methodology and applications." *Computers and Chemical Engineering* **20**(6-7): 685-702.

Coulson, J. M., Richardson, J. F. and Sinnot, R. K. (1983). Chemical engineering. Design, Pergamon Press. **6**.

Dolan, W. B., Cummings, P. T. and LeVan, M. D. (1989). "Process optimization via simulated annealing: Application to network design." *AIChE Journal* **35**(5): 725-736.

Douglas, J. M. (1988). Conceptual Design of Chemical Processes, McGraw-Hill.

Douglas, J. M. (1995). "Synthesis of separation system flowsheets." *AIChE Journal* **41**(12): 2522-2536.

Douglas, J. M. and Stephanopoulos, G. (1995). "Hierarchical approaches in conceptuel process design: Framework and computer-aided implementation." *AIChE Symposium Series* **304**: 183-197.

Dueck, G. (1990). "Threshold accepting: A general purpose optimization algorithm appearing superior to simulated annealing." *Journal of Computational Physics* **90**(1): 161-175.

Edmister, W. C. (1943). "Design for Hydrocarbon Absorption and Stripping." *Industrial & Engineering Chemistry* **35**(8): 837-839.

Edmister, W. C. (1957). "Absorption and Stripping-factor Functions for Distillation Calculations by Manual and Digital-computer Methods." *AIChE J.* **3**(2): 165-171.

El-Halwagi, M. M. and Manousiouthakis, V. (1989). "Synthesis of mass exchange networks." *AIChE Journal* **35**(8): 1233-1244.

England, C. (1986). "GAS SOLUBILITIES IN PHYSICAL SOLVENTS." *Chemical Engineering (New York)* **93**(8): 63-66.

Farry, M. (1998). "Ethane from associated gas still the most economical." *Oil and Gas Journal* **96**(23): 115-117.

Fenske, F. R. (1932). *Ind. Eng. Chem.* **24**: 482-485.

Floudas, C. A., Akrotirianakis, I. G., Caratzoulas, S., Meyer, C. A. and Kallrath, J. (2005). "Global optimization in the 21st century: Advances and challenges." *Computers and Chemical Engineering* **29**(6 SPEC. ISS.): 1185-1202.

Gani, R., Nielsen, B. and Fredenslund, A. (1991). "Group contribution approach to computer-aided molecular design." *AIChE Journal* **37**(9): 1318-1332.

Patent EP1792131, Gaskin, T. K. (2009). "COMBINED USE OF EXTERNAL AND INTERNAL SOLVENTS IN PROCESSING GASES CONTAINING LIGHT MEDIUM AND HEAVY COMPONENTS."

Gilliland, E. R. (1940). "Estimation of the number of theoretical plates as a function of the reflux ratio." *Ind. Eng. Chem.* **32**(9): 1220-1223.

Glauber, R. J. (1963). "Time-dependent statistics of the Ising model." *Journal of Mathematical Physics* **4**(2): 294-307.

Grossmann, I. E. and Kravanja, Z. (1995). "Mixed-integer nonlinear programming techniques for process systems engineering." *Computers and Chemical Engineering* **19**(SUPPL. 1): 189-204.

Hajek, B. (1988). "COOLING SCHEDULES FOR OPTIMAL ANNEALING." *Mathematics of Operations Research* **13**(2): 311-329.

Harper, P. M., Gani, R., Kolar, P. and Ishikawa, T. (1999). "Computer-aided molecular design with combined molecular modeling and group contribution." *Fluid Phase Equilibria* **158-160**: 337-347.

Horton, G. and Franklin, W. B. (1940). "Calculation of Absorber Performance and Design." *Industrial & Engineering Chemistry* **32**(10): 1384-1388.

Hostrup, M., Gani, R., Kravanja, Z., Sorsak, A. and Grossmann, I. (2001). "Integration of thermodynamic insights and MINLP optimization for the synthesis, design and analysis of process flowsheets." *Computers and Chemical Engineering* **25**(1): 73-83.

Hudson, H. M., Wilkinson, J. D., Lynch, J. T., Pitman, R. N. and Pierce, M. C. (2001). Reducing treating requirements for cryogenic NGL recovery plants. 80th Annual Convention of the Gas Processors Association, San Antonio, Texas.

IChemE (1987). A Guide to Capital Cost Estimation. 3rd.

Jaksland, C. and Gani, R. (1996). "An integrated approach to process/product design and synthesis based on properties-process relationship." *Computers and Chemical Engineering* **20**(SUPPL.1).

Jaksland, C. A., Gani, R. and Lien, K. M. (1995). "Separation process design and synthesis based on thermodynamic insights." *Chemical Engineering Science* **50**(3): 511-530.

Kheawhom, S. and Hirao, M. (2004). "Environmentally benign separation process synthesis." *Journal of Chemical Engineering of Japan* **37**(2): 243-252.

King, C. J. (1980). Separation Processes, McGraw-Hill.

Kirkpatrick, S., Gelatt Jr, C. D. and Vecchi, M. P. (1983). "Optimization by simulated annealing." *Science* **220**(4598): 671-680.

Kister, H. Z. (1992). Distillation design, McGraw-Hill Professional.

Kookos, I. K. (2002). "A targeting approach to the synthesis of membrane networks for gas separations." *Journal of Membrane Science* **208**(1-2): 193-202.

Kookos, I. K. (2003). "Optimal design of membrane/distillation column hybrid processes." *Industrial and Engineering Chemistry Research* **42**(8): 1731-1738.

Koolen, J. L. A. (2001). Design of simple and robust process plants, Wiley-VCH.

Kravanja, Z. and Grossmann, I. E. (1997). "Multilevel-hierarchical MINLP synthesis of process flowsheets." *Computers and Chemical Engineering* **21**(SUPPL.1).

Kremser, A. (1930). *Natl. Petroleum News* **22**(21).

Kumana, J. D. and Associates (2003). "How To Calculate The True Cost of Steam." *Industrial Technologies Program Energy Efficiency and Renewable Energy* **U.S. Department of Energy** (DOE/GO-102003-1736).

Lewin, D. R. (1998). "A generalized method for HEN synthesis using stochastic optimization - II. The synthesis of cost-optimal networks." *Computers and Chemical Engineering* **22**(10): 1387-1405.

Lewin, D. R., Wang, H. and Shalev, O. (1998). "A generalized method for HEN synthesis using stochastic optimization - I. General framework and MER optimal synthesis." *Computers and Chemical Engineering* **22**(10): 1503-1513.

Li, X. and Kraslawski, A. (2004). "Conceptual process synthesis: Past and current trends." *Chemical Engineering and Processing* **43**(5): 589-600.

Lin, B. and Miller, D. C. (2004). "Solving heat exchanger network synthesis problems with Tabu Search." *Computers and Chemical Engineering* **28**(8): 1451-1464.

Linke, P. and Kokossis, A. (2003). "Attainable reaction and separation processes from a superstructure-based method." *AIChE Journal* **49**(6): 1451-1470.

Linnhoff, B. and Boland, D. (1982). A user guide on process integration for the efficient use of energy, The Institution of Chemical Engineers, Rugby, UK.

Marcoulaki, E. and Kokossis, A. (1996). "Stochastic optimisation of complex reaction systems." *Computers & Chemical Engineering* **20**(Supplement 1): S231-S236.

Marcoulaki, E. C. and Kokossis, A. C. (1998). "Molecular design synthesis using stochastic optimisation as a tool for scoping and screening." *Computers and Chemical Engineering* **22**(SUPPL.1): S11-S18.

Marcoulaki, E. C. and Kokossis, A. C. (2000). "On the development of novel chemicals using a systematic optimisation approach. Part II. Solvent design." *Chemical Engineering Science* **55**(13): 2547-2561.

Mehra, Y. R. (1987). "NEW PROCESS FLEXIBILITY IMPROVES GAS PROCESSING MARGINS." *Energy progress* **7**(3): 150-156.

Mehra, Y. R. (2001). "Saudi gas plant site for study of NGL-recovery processes." *Oil and Gas Journal* **99**(44): 56-60.

Mehra, Y. R. (2002). "Which technology for recovering NGL value?" *Saudi Aramco Journal of Technology*(SPRING): 50-56.

Mehra, Y. R. (2009) Advanced Extraction Technologies, Inc. homepage. 22 February 2009, from URL: http://www.aet.com/technology.

Mehra, Y. R. and Gaskin, T. K. (1999). "Guidelines offered for choosing cryogenics or absorption for gas processing." *Oil and Gas Journal* **97**(9): 62-69.

Metropolis, N., Rosenbluth, A. W., Rosenbluth, M. N., Teller, A. H. and Teller, E. (1953). "Equation of state calculations by fast computing machines." *The Journal of Chemical Physics* **21**(6): 1087-1092.

Meyer, E. (1998). Chemistry of Hazardous Materials, Prentice Hall. Third Edition.

Michalewicz, Z. (1994). Genetic Algorithms + Data Structures = Evolution Programs. Berlin, Springer-Velag.

Novak, Z., Kravanja, Z. and Grossmann, I. E. (1996). "Simultaneous synthesis of distillation sequences in overall process schemes using an improved MINLP approach." *Computers and Chemical Engineering* **20**(12): 1425-1440.

O'Young, L., Natori, Y., Pressly, T. G. and Ng, K. M. (1997). "A physical limitation based framework for separations synthesis." *Computers and Chemical Engineering* **21**(SUPPL.1).

Papoulias, S. A. and Grossmann, I. E. (1983). "A structural optimization approach in process synthesis-II. Heat recovery networks." *Computers and Chemical Engineering* **7**(6): 707-721.

Perry, R. H. and Green, D. W. (1998). *Perry's Chemical Engineers Handbook, 7th Ed.*: 372.

Peters, M. S., Timmerhaus, K. D. and West, R. E. (2003). Plant Design and Economics for Chemical Engineers. New York, McGraw-Hill. 5th.

Qian, Y. and Lien, K. M. (1995). "Rule based synthesis of separation systems by predictive best first search with rules represented as trapezoidal numbers." *Computers and Chemical Engineering* **19**(11): 1185-1205.

Rodriguez, C. (2005). Fouling Mitigation Strategies for Heat Exchanger Networks. PhD Thesis, University of Manchester, UK.

Sadhukhan, J. (2002). A Novel Value Analysis Method for Process Network Optimisation. PhD Thesis, University of Manchester, UK.

Schutt, H. C. and Zdonik, S. B. (1956). *Oil and Gas Journal*: 171-174.

Seader, J. D. and Henley, E. J. (1998). *Separation Process Principles*: 499.

Seuranen, T., Hurme, M. and Pajula, E. (2005). "Synthesis of separation processes by case-based reasoning." *Computers and Chemical Engineering* **29**(6 SPEC. ISS.): 1473-1482.

Shiras, R. N., Hanson, D. N. and Gibson, C. H. (1950). "Calculation of Minimum Reflux in Distillation Columns." *Industrial & Engineering Chemistry* **42**(5): 871-876.

Siirola, J. J. (1996). "Strategic process synthesis: Advances in the hierarchical approach." *Computers and Chemical Engineering* **20**(SUPPL.2).

Smith, R. (2005). "Chemical Process Design and Integration." *John Wiley&Sons Ltd*.

Smith, R. and Linnhoff, B. (1988). "The design of separators in the context of overall processes." *CHEM. ENGNG. RES. & DES. (ICHEME)* **66**: 195-228.

Smith, R. and Varbanov, P. (2005). "What's the price of steam?" *Chemical Engineering Progress* **101**(7): 29-33.

Suphanit, B. (1999). Design of Complex Distillation System. PhD Thesis, University of Manchester, UK.

Thiele, E. W. and Geddes, R. L. (1933). "Computation of distillation apparatus for hydrocarbon mixtures." *Ind Eng Chem Res* **25**: 289-295.

Towler, G. P. and Shetna, H. K. (1997). New Processes for Gas Absorption to Ultra-Low Concentrations. Distillation and absorption '97.

Triantafyllou, C. (1991). The Design Optimisation and Integration of Dividing Wall Distillation Columns. PhD Thesis, University of Manchester, UK.

Türkay, M. and Grossmann, I. E. (1996). "Logic-based MINLP algorithms for the optimal synthesis of process networks." *Computers and Chemical Engineering* **20**(8): 959-978.

Ulrich, G. D. and Vasudevan, P. T. (2006). "How to estimate utility costs." *Chemical Engineering* **113**(4): 66-69.

Umeda, T. (2004). "A conceptual framework for the process system synthesis and design congruent with corporate strategy." *Industrial and Engineering Chemistry Research* **43**(14): 3827-3837.

Umeda, T., Harada, T. and Shiroko, K. (1979). "A thermodynamic approach to the synthesis of heat integration systems in chemical processes." *Computers and Chemical Engineering* **3**(1-4): 273-282.

Underwood, A. J. V. (1932). *Trans. Inst. Chem. Engrs. (London)* **10**: 112-158.

Underwood, A. J. V. (1946). "Fractional distillation of multicomponent mixtures - Calculation of minimum reflux ratio." *J. Inst. Pet.* **32**: 614-626.

Underwood, A. J. V. (1948). "Fractional Distillation of Multi-Component Mixtures." *Chemical Engineering Progress* **44**(8): 1948.

Uppaluri, R. V. S., Smith, R., Linke, P. and Kokossis, A. C. (2006). "On the simultaneous optimization of pressure and layout for gas permeation membrane systems." *Journal of Membrane Science* **280**(1-2): 832-848.

Van Laarhoven, P. J. M. and Aarts, E. H. L. (1987). Simulated Annealing: Theory and Applications, Reidel Publishing.

Vatavuk, W. M. (2005). "How to estimate operating costs." *Chemical Engineering* **112**(7): 33-37.

Wang, J. (2004). Synthesis and Optimisation of Low Temperature Separation Processes. PhD Thesis, University of Manchester, UK.

Wang, J. and Smith, R. (2005). "Synthesis and optimization of low-temperature gas separation processes." *Industrial and Engineering Chemistry Research* **44**(8): 2856-2870.

Wang, S. I., Nicholas, D. M. and DiMartino, S. P. (1984). "ANALYSIS DICTATES H//2 PURIFICATION PROCESS." *Oil and Gas Journal* **82**(6): 111-117.

Yeomans, H. and Grossmann, I. E. (1999). "Nonlinear disjunctive programming models for the synthesis of heat integrated distillation sequences." *Computers and Chemical Engineering* **23**(9): 1135-1151.

Yeomans, H. and Grossmann, I. E. (1999). "A systematic modeling framework of superstructure optimization in process synthesis." *Computers and Chemical Engineering* **23**(6): 709-731.

Chapter 12. Appendices

12.1 Appendix I: Implementation of absorption-desorption column modelling

12.1.1 Nomenclature

$count$	=	iteration counter of algorithm of Figure 12.3
$Diff$	=	departure from enthalpy balance to absorber stage 1
$Draw$	=	vapour draw from absorber stage 1
F	=	sum of molar flowrates leaving stage 1
$Factor$	=	interpolation constant
$Feed$	=	solvent feed to absorber stage 1
H_{Draw}	=	molar enthalpy of vapour draw from absorber stage 1
h_{Feed}	=	molar enthalpy of solvent feed to absorber stage 1
h_j	=	molar enthalpy of liquid from stage j
H_j	=	molar enthalpy of vapour from stage j
L_{1New}	=	corrected liquid molar flowrate from stage 1
L_j	=	liquid molar flowrate from stage j
L_m	=	liquid molar flowrate from stage m
n	=	number of components in system
T_{1New}	=	corrected temperature on stage 1
T_{Draw}	=	temperature of vapour draw from absorber stage 1
T_j	=	temperature on stage j
T_m	=	temperature on bottom stage m
V_{1New}	=	corrected vapour molar flowrate from stage 1
V_j	=	vapour molar flowrate from stage j
$x_F(i)$	=	overall molar fraction of component i on combined stream F
$x_{Feed}(i)$	=	molar fraction of component i in solvent feed to absorber stage 1
$x_j(i)$	=	liquid phase molar fraction of component i on stage j
X_{Solv}	=	cumulative molar fraction of solvent components on stage 1 liquid
$y_{Draw}(i)$	=	molar fraction of component i in vapour draw from absorber stage 1
$y_j(i)$	=	vapour phase molar fraction of component i on stage j
Y_{Solv}	=	cumulative molar fraction of solvent components on stage 1 vapour

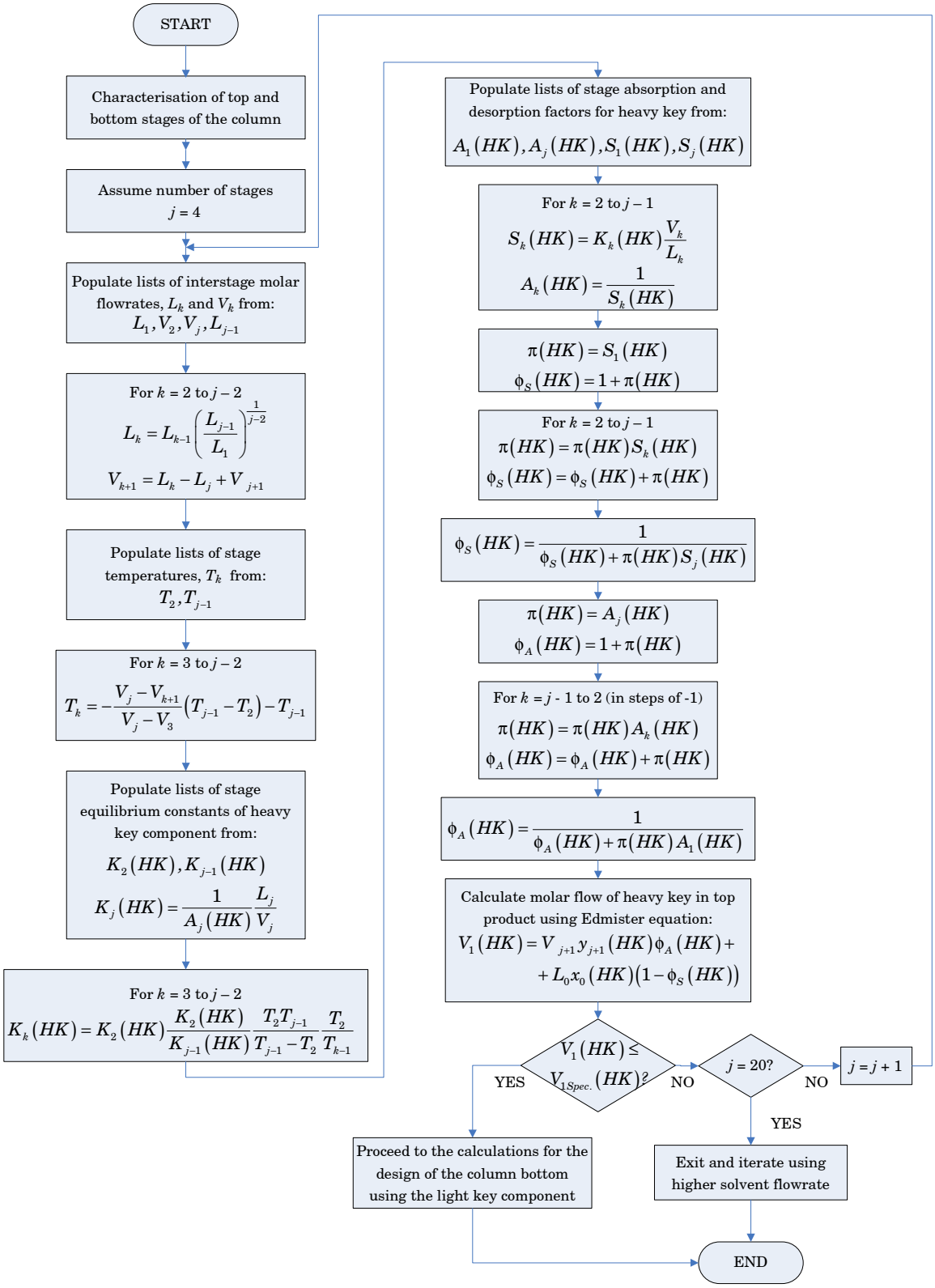

Figure 12.1: Flowchart representing steps 3.9.1 (i) to 3.9.1 (iv) of the absorber design algorithm.

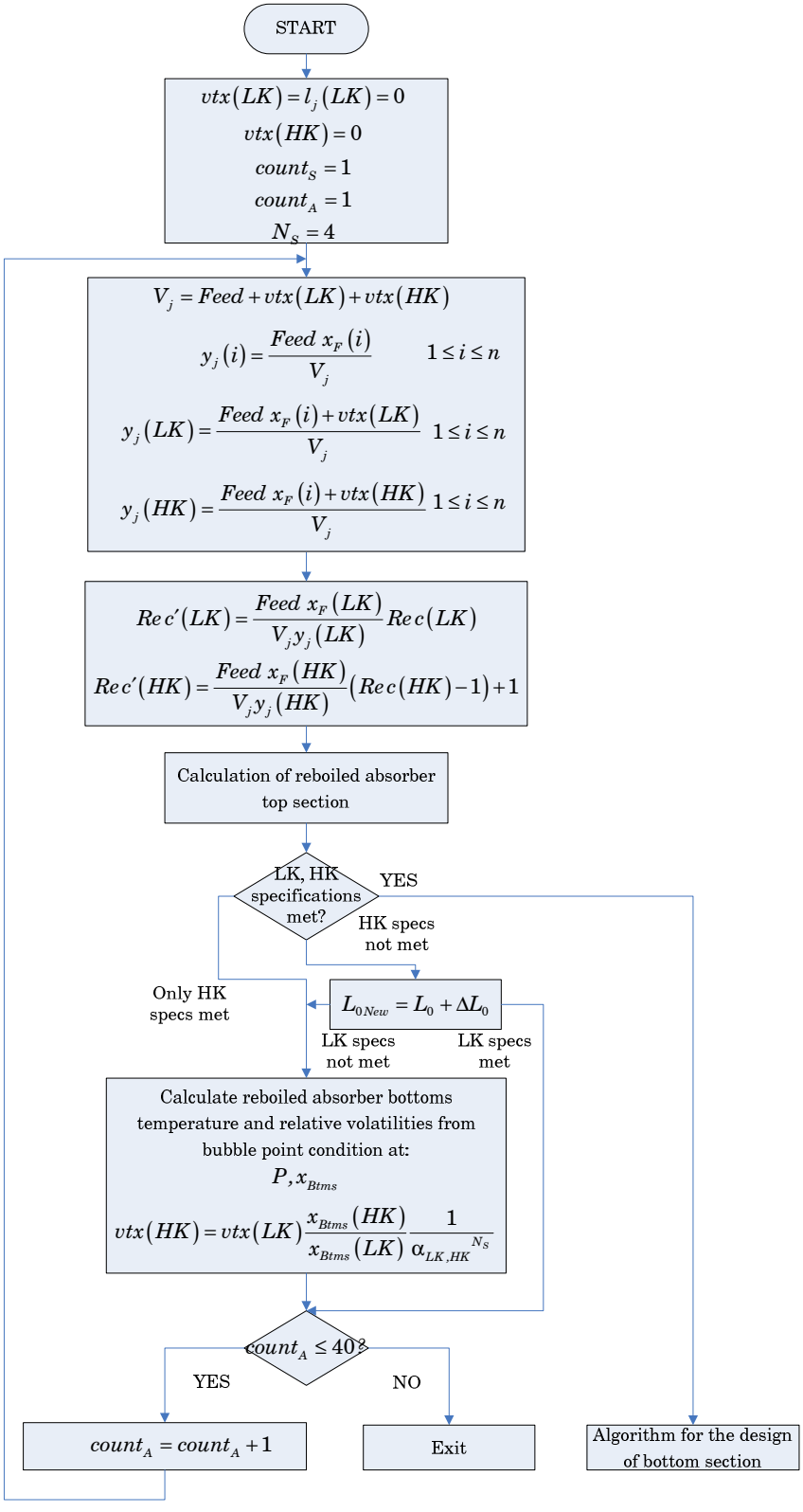

Figure 12.2: Flowchart representing steps 3.9.1 (iv) and 3.9.1 (v) of the absorber design algorithm.

12.1.2 Characterisation of terminal streams

This procedure forms part of the implementation of the absorption-desorption models in the developed synthesis framework. For illustration of this procedure, the top of the absorber is used for reference.

Assuming that the absorber consists of equilibrium stages, the streams leaving a given stage are saturated with each other. Therefore, the vapour effluent from the top of the column is at dew conditions. Knowing the vapour concentration and the stage pressure, the dew condition may be imposed to determine the stage temperature and liquid composition.

Product specifications may then be used to estimate the vapour draw composition. However, because common product specifications are relative to the light and heavy key components, no information regarding the concentration of solvent components is readily available. For most purposes, it is reasonable to assume that the concentration of solvent components in the vapour draw is negligible. This is particularly true for absorption applications that use heavy absorption oils as solvents. However, the presence of heavy components in minimal concentration in the vapour draw may have a large impact on the prediction of the dew conditions. Therefore, the characterisation of the top stage conditions requires an estimate of the vapour composition that allows for minimal losses of solvent to the overhead vapour.

The proposed method to estimate the composition of the vapour effluent consists of the following steps:

i. Initialise the top stage temperature with the solvent inlet temperature. The vapour entering the top stage is expected to be relatively exhausted of absorbable components, which results in limited absorption at the top stage. Intuitively, this implies a small amount of heat of vaporisation going into the solvent with the

dissolved gases, which is largely accountable for the solvent temperature rise.

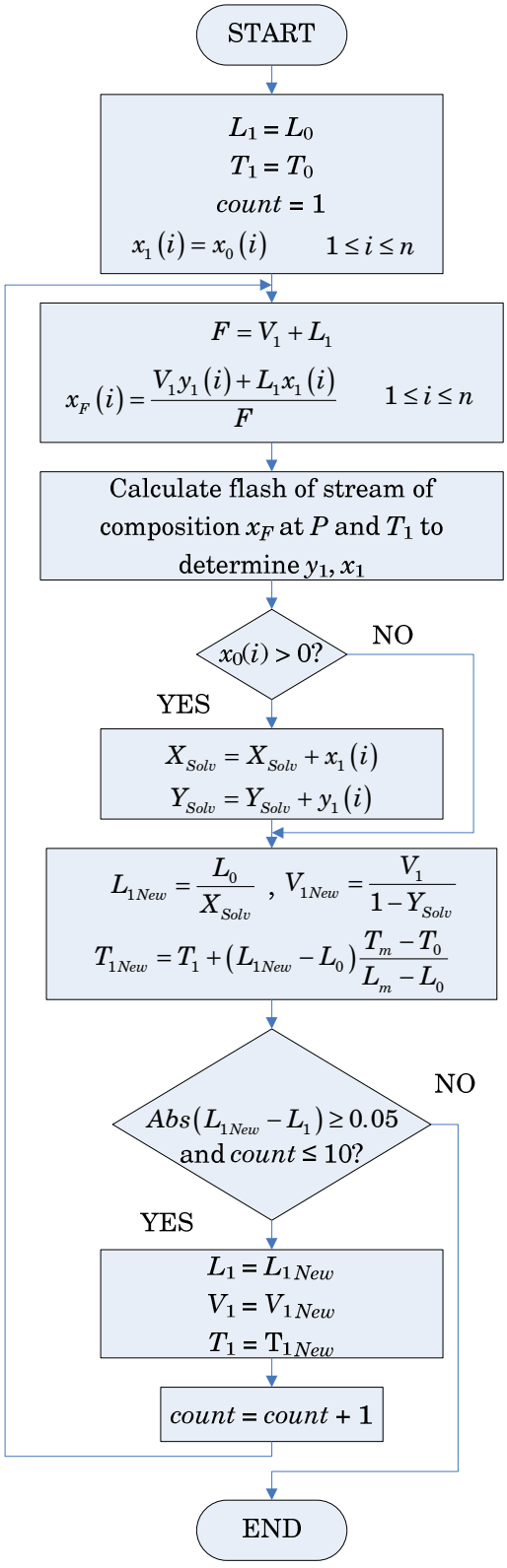

Figure 12.3: Flowchart representation of the method of estimation of the vapour effluent composition

ii. Obtain the vapour composition from a flash calculation of a hypothetical combined stream. This stream consists of the sum of the solvent-free vapour draw plus all of the solvent feed. This combined stream is hypothetical because it does not have a physical equivalent in the column. Flowrate and compositions of this stream are given by the following equations:

$$F = V_1 + L_0 \tag{10.1}$$

$$x_F(i) = \frac{V_1 y_1(i) + L_0 x_0(i)}{F} \tag{10.2}$$

The closest match of this stream is the combined stage 1 outlet, which consists of the real vapour draw plus the liquid stream flowing from the top stage, or by mass balance, of the sum of the solvent feed plus the vapour accessing stage 1 from stage 2. The result of this initial approximation will generally overestimate the solvent concentration in the vapour draw.

iii. Generate estimates of the top stage outlets by correcting the solvent-free vapour draw and inlet solvent with the estimated combined fraction of solvent components in each phase. This correction allows the vapour draw to contain a certain amount of solvent in addition to the calculated flowrate of feed components from recovery specifications. For the internal liquid, this correction allows this stream to consist of the bulk of the inlet solvent plus a certain amount of absorbed components. The estimated combined fraction of solvent components in each phase are calculated with the following relationships:

$$X_{Solv} = \sum_{i \in Solvent} x_1(i) \tag{10.3}$$

$$Y_{Solv} = \sum_{i \in Solvent} y_1(i) \tag{10.4}$$

The outlet flowrates from the top stage are subsequently derived from the following equations:

$$L_{1New} = \frac{L_0}{X_{Solv}} \tag{10.5}$$

$$V_{1New} = \frac{V_1}{1 - Y_{Solv}} \tag{10.6}$$

iv. Generate a new approximation of the top stage temperature from the molar liquid flow increment through the first stage. This increment may be related to the expected absorber's overall liquid flow and temperature increments by the following equation:

$$T_{1New} = T_1 + \left(L_{1New} - L_0\right)\frac{T_m - T_0}{L_m - L_0} \tag{10.7}$$

The variation of temperature is assumed to be directly proportional to the variation in molar flow, although in reality, as the composition of the phases change along the column, the rate of change of temperature per unit of gas absorbed varies.

v. Steps (ii) to (iv) are repeated using the latest combined feed composition to the stage and the estimated stage temperature for a maximum number of times until the estimate of the liquid flowrate according to Equation (10.5) does not vary appreciably between iterations.

12.1.3 Enthalpy balance for characterisation of terminal streams

The top of the absorber is employed for reference throughout this section; however, the enthalpy balance proposed is equally applied to the bottom of the absorber section and the top and bottom of the stripper section.

An enthalpy balance around the top stage of the absorber is formulated to refine the initial estimates and to derive the prevailing conditions and the phases compositions at stages 1 and 2.

Heat losses to the surroundings may be neglected if adiabatic operation is assumed. The expression for the enthalpy balance is given by:

$$0 = Feed\ h_{Feed} + V_2 H_2 - Draw\ H_{Draw} - L_1 h_1 \qquad (10.8)$$

The enthalpy of the vapour draw and the solvent feed are determined by their composition, the pressure and the temperature. The outstanding terms in the enthalpy balance are the molar flowrate and the molar enthalpy of the internal vapour entering the top stage and the liquid from the top stage.

The enthalpy balance is solved by iterating on the liquid flowrate from stage 1 and the vapour flowrate from stage 2. The calculated estimates of the vapour effluent composition, the liquid phase in equilibrium with the vapour and the temperature of the top stage may be used for initialisation.

12.1.3 (i) Limits on liquid flowrate from stage 1

The following procedure is shown in Figure 12.4.

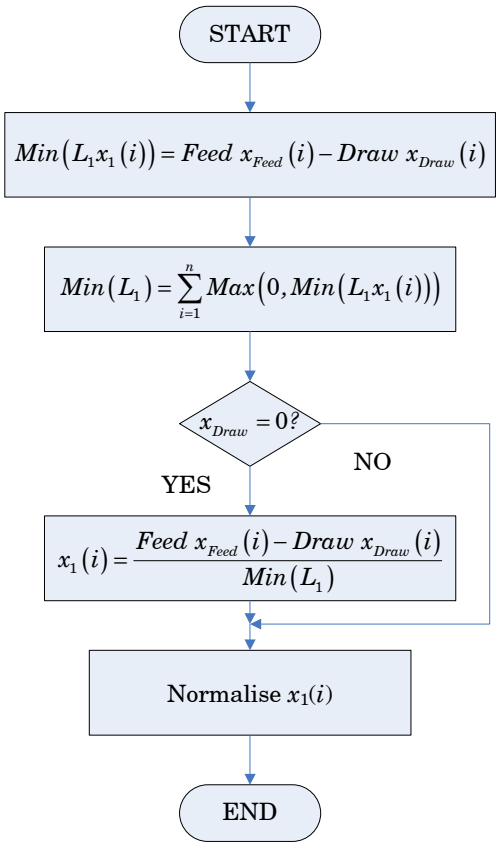

Figure 12.4: Flowchart representation of the method of estimation of minimum stage 1 liquid based on material balance boundaries.

A lower bound for this magnitude is encountered at a nil flowrate of incoming vapour. Similarly, for each component, the minimum individual molar flow in the liquid phase from stage 1 is given by the following equation:

$$Min\left(L_1 x_1(i)\right) = Feed\ x_{Feed}(i) - Draw\ x_{Draw}(i) \qquad (10.9)$$

It is obvious that for most of the components in the gas feed, the result of this calculation is a negative number. Negative values resulting from Equation (10.9) do not contribute to the lower bound for the stage 1 liquid flowrate, which is estimated as the sum of the individual minimum flowrates:

$$Min\left(L_1\right) = \sum_{i=1}^{n} Max\left(0, Min\left(L_1 x_1\left(i\right)\right)\right) \tag{10.10}$$

Combining Equations (10.9) and (10.10) an estimate of the stage 1 liquid concentration for solvent-exclusive components is obtained:

$$x_1\left(i\right) = \frac{Feed\ x_{Feed}\left(i\right) - Draw\ x_{Draw}\left(i\right)}{Min\left(L_1\right)} \tag{10.11}$$

The concentration given by Equation (10.11) replaces the existing concentration estimates for solvent components, which is then subjected to normalisation.

Finally, the updated liquid composition may be used to calculate the top stage temperature and the enthalpy of the liquid from the top stage from a bubble point calculation.

12.1.3 (ii) Limits on vapour flowrate from stage 2

This procedure is illustrated by Figure 12.5.

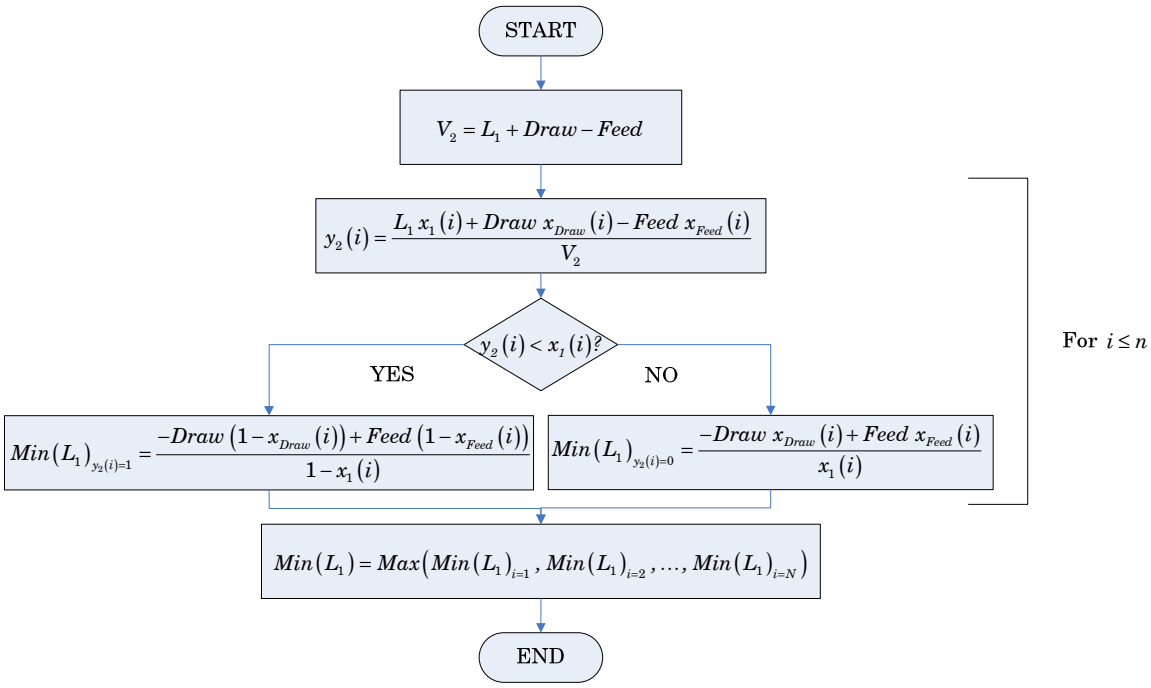

Figure 12.5: Flowchart representation of the method of estimation of the minimum stage 1 liquid based on vapour concentration boundaries.

With the estimated value of the liquid flowrate from stage 1, an estimate for the vapour flow from stage 2 may be obtained from a material balance around stage 1:

$$V_2 = L_1 + Draw - Feed \tag{10.12}$$

The individual vapour concentrations may be estimated from individual molar balance:

$$y_2(i) = \frac{L_1 x_1(i) + Draw\, x_{Draw}(i) - Feed\, x_{Feed}(i)}{V_2} \tag{10.13}$$

A material balance may be formulated for the complete set of components excluding i:

$$1 - y_2(i) = \frac{L_1\left(1 - x_1(i)\right) + Draw\left(1 - x_{Draw}(i)\right) - Feed\left(1 - x_{Feed}(i)\right)}{V_2} \tag{10.14}$$

Equations (10.13) and (10.14) may be used to obtain a revised lower bound for the stage 1 liquid flowrate. It is obvious that the stage 1 liquid flowrate given by Equation (10.13) is minimum when $y_2(i)$ = 0. Similarly, in Equation (10.14), the liquid flowrate is minimum when 1 - $y_2(i)$ = 0 or $y_2(i)$ = 1. For any values of y_2 between these limits, the liquid flowrate is greater than these boundaries.

The new boundaries of the stage 1 liquid flowrate based on terminal individual vapour concentrations are given by the following equations. The minimum liquid flowrate based on $y_2(i)$ = 0 is:

$$Min\left(L_1\right)_{y_2(i)=0} = \frac{-Draw\ x_{Draw}\left(i\right) + Feed\ x_{Feed}\left(i\right)}{x_1\left(i\right)} \qquad (10.15)$$

Similarly, the minimum liquid flowrate based on $y_2(i)$ = 1 is:

$$Min\left(L_1\right)_{y_2(i)=1} = \frac{-Draw\left(1 - x_{Draw}\left(i\right)\right) + Feed\left(1 - x_{Feed}\left(i\right)\right)}{1 - x_1\left(i\right)} \qquad (10.16)$$

It may be shown that Equation (10.15) yields a higher lower bound than the second estimate if $y_2(i)$ is greater than $x_1(i)$. Similarly, for $y_2(i)$ being less than $x_1(i)$, Equation (10.16) will provide the greatest lower bound.

The highest upper bound for the liquid from the top stage may be then identified from the corresponding values for all the components:

$$Min\left(L_1\right) = Max\left(Min\left(L_1\right)_{i=1}, Min\left(L_1\right)_{i=2}, \ldots, Min\left(L_1\right)_{i=N}\right) \qquad (10.17)$$

12.1.3 (iii) Enthalpy balance solution

With the calculated stage 2 vapour concentration, the temperature at stage 2 may be estimated from the dew point calculation. It is possible to establish the molar enthalpy of this vapour from this temperature. The data for enthalpies and molar flowrates may be then used to assess the

deviation from the enthalpy balance at the top stage, according to the following equation:

$$Diff = Feed\ h_{Feed} + V_2 H_2 - Draw\ H_{Draw} - L_1 h_1 \qquad (10.18)$$

This procedure is illustrated in Figure 12.6.

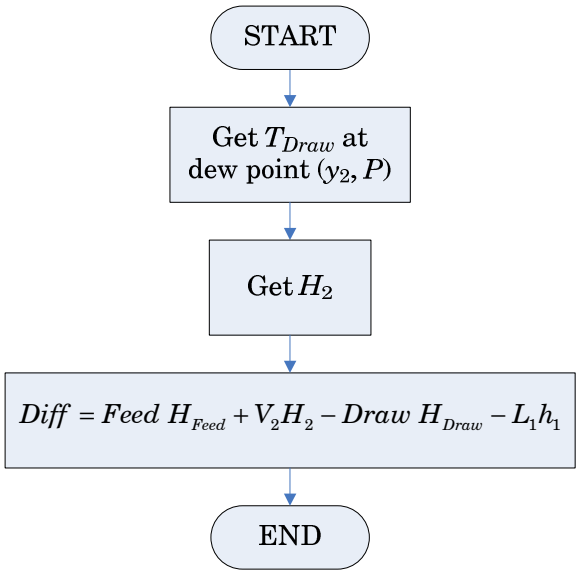

Figure 12.6: Flowchart representation of the method of evaluation of the enthalpy balance around the top stage.

The next step deals with establishing an upper and a lower bound for the location of the stage 1 liquid that fulfils the enthalpy balance around stage 1. This procedure is illustrated in Figure 12.7.

For this purpose, the enthalpy balance deviation is assessed at the lower and and upper bound for the stage 1 liquid. This upper bound may be initialised to a 50% increase over the lower bound and be lifted if it is not sufficient. The departures from the enthalpy balance are given by the following equations:

$$Diff_1 = Feed\ h_{Feed} + V_2 H_2 - Draw\ H_{Draw} - Min(L_1) h_1 \qquad (10.19)$$

$$Diff_2 = Feed\ h_{Feed} + V_2 H_2 - Draw\ H_{Draw} - Max(L_1) h_1 \qquad (10.20)$$

Where sub-indexes 1 and 2 denote the conditions at the lower and upper boundaries of the stage 1 liquid, respectively.

With the purpose of bracketing the solution of the enthalpy balance, the sign and the magnitude of the departures given by Equations (10.19) and (10.20) are compared:

$$Diff_1 Diff_2 \geq 0? \tag{10.21}$$

If the given departures are of different signs, then, the solution to the enthalpy balance will be confined between the liquid estimates corresponding to each departure. The solution to the enthalpy balance may be located by an algorithm for one dimensional optimisation. The Brent's method is selected for this purpose.

The flowrate and composition of the vapour from stage 2 is consequently calculated from the liquid flowrate that is the solution of the enthalpy balance:

$$V_2 = -Feed + Draw + L_1 \tag{10.22}$$

$$y_2(i) = \frac{-Feed\ x_{Feed}(i) + Draw\ x_{Draw}(i) + L_1 x_1(i)}{-Feed + Draw + L_1} \tag{10.23}$$

However, if both departures are of the same sign, as shown by (10.21), then, the magnitudes of the departures must be evaluated.

$$Abs(Diff_1) > Abs(Diff_2)? \tag{10.24}$$

If the magnitude of the departure decays from the lower to the upper boundary of the stage 1 liquid, as given by (10.24), then, this indicates that the initial upper bound need to be extended in order to contain the solution. An updated upper bound may be obtained using the following relationship.

$$New\left(Max\left(L_1\right)\right) = Max\left(L_1\right) + Factor\left(Max\left(L_1\right) - Min\left(L_1\right)\right) \tag{10.25}$$

On the contrary, if (10.24) is not met, this indicates that the enthalpy balance cannot be met without altering the design variables of the problem, in particular, the solvent feed.

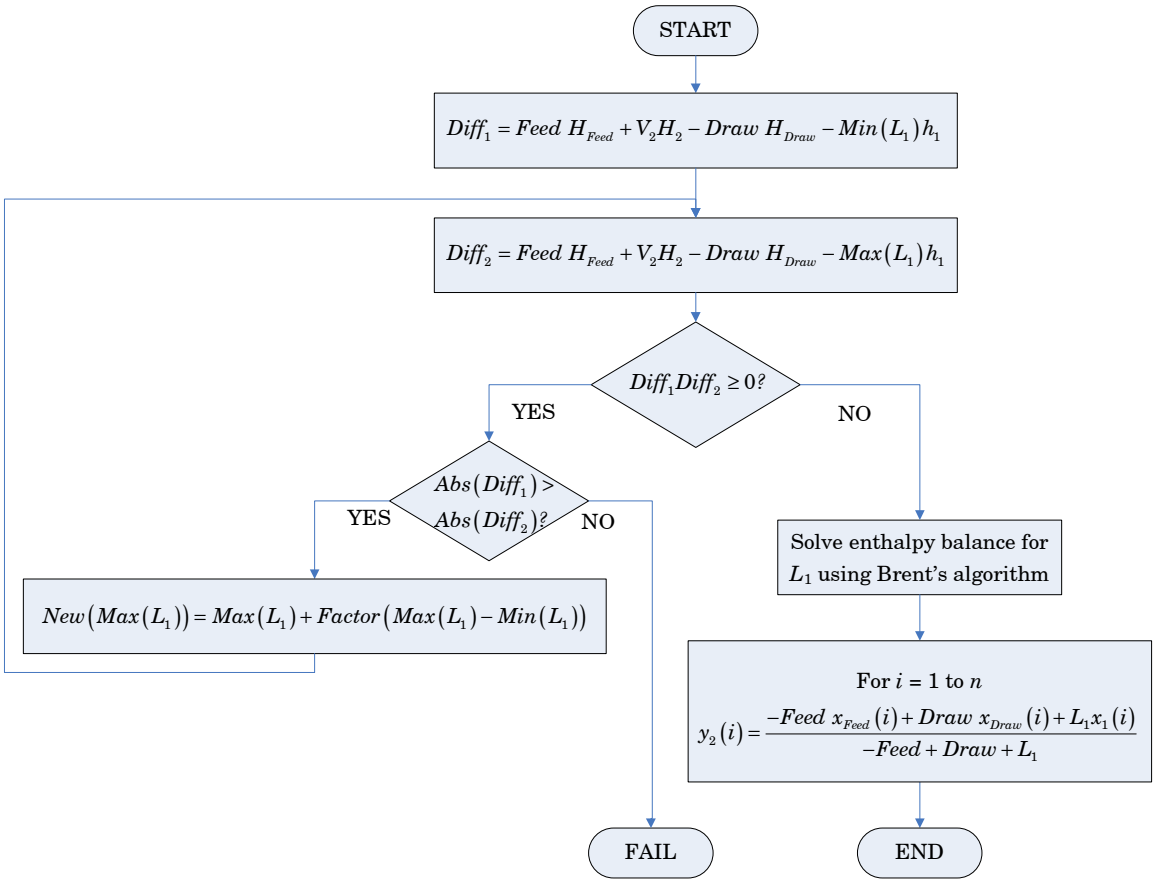

Figure 12.7: Flowchart representation of the bracketing method for resolution of the enthalpy balance around the top stage of the absorber column.

12.2 Appendix II: Distillation column model validation

Number of stages	Feed stage	Reflux ratio	Reboiler temperature C	Reboiler duty MW	Condenser temperature C	Condenser duty MW
5	4	1209.1	233.6	16324	41.1	16339
6	5	12.3	233.6	146	32.5	162
7	5	3.8	233.6	34	32.5	50
8	6	3.5	233.6	31	32.5	47
9	6	2.5	233.6	17	32.5	33
10	7	2.470	233.6	16.8	32.5	32.7
11	7	2.114	233.6	12.2	32.6	28.0
12	8	2.113	233.6	12.2	32.6	28.0
13	8	1.947	233.7	10.0	32.5	25.8
14	9	1.947	233.7	10.0	32.6	25.8
15	9	1.855	233.7	8.8	32.6	24.6
16	10	1.855	233.7	8.8	32.6	24.6
17	10	1.800	233.7	8.1	32.6	23.9
18	11	1.801	233.66	8.08	32.43	23.93
19	11	1.766	233.66	7.62	32.45	23.47
20	12	1.765	233.66	7.62	32.61	23.47
21	12	1.743	233.66	7.33	32.61	23.18
22	13	1.744	233.66	7.33	32.41	23.18
23	13	1.729	233.66	7.15	32.53	23.00
24	14	1.729	233.66	7.15	32.51	23.00
25	14	1.720	233.66	7.04	32.54	22.88
26	15	1.720	233.66	7.04	32.53	22.88
27	15	1.715	233.66	6.97	32.50	22.82
28	16	1.715	233.66	6.97	32.50	22.81
29	16	1.712	233.66	6.93	32.58	22.78
30	17	1.712	233.66	6.93	32.58	22.77
31	17	1.711	233.66	6.91	32.50	22.75
32	18	1.710	233.66	6.91	32.50	22.75
33	18	1.709	233.66	6.89	32.59	22.74
34	19	1.709	233.66	6.89	32.60	22.75
35	19	1.709	233.66	6.89	32.52	22.73
36	20	1.709	233.658	6.888	32.514	22.734
37	20	1.709	233.658	6.884	32.542	22.731
38	21	1.709	233.658	6.884	32.545	22.732
39	21	1.709	233.658	6.882	32.450	22.730
40	22	1.709	233.658	6.883	32.444	22.725
41	22	1.708	233.658	6.881	32.523	22.728
42	23	1.708	233.658	6.881	32.525	22.728
43	23	1.708	233.658	6.881	32.509	22.728
44	24	1.708	233.658	6.881	32.508	22.727
45	24	1.708	233.658	6.880	32.501	22.727
46	25	1.708	233.658	6.881	32.500	22.726
47	25	1.709	233.658	6.880	32.488	22.728
48	26	1.708	233.658	6.880	32.486	22.725
49	26	1.709	233.658	6.880	32.466	22.728
50	27	1.708	233.658	6.880	32.463	22.724

Table 12.1: Determination of minimum reflux ratio from Aspen Plus® simulation data by successively increasing the stages the column.

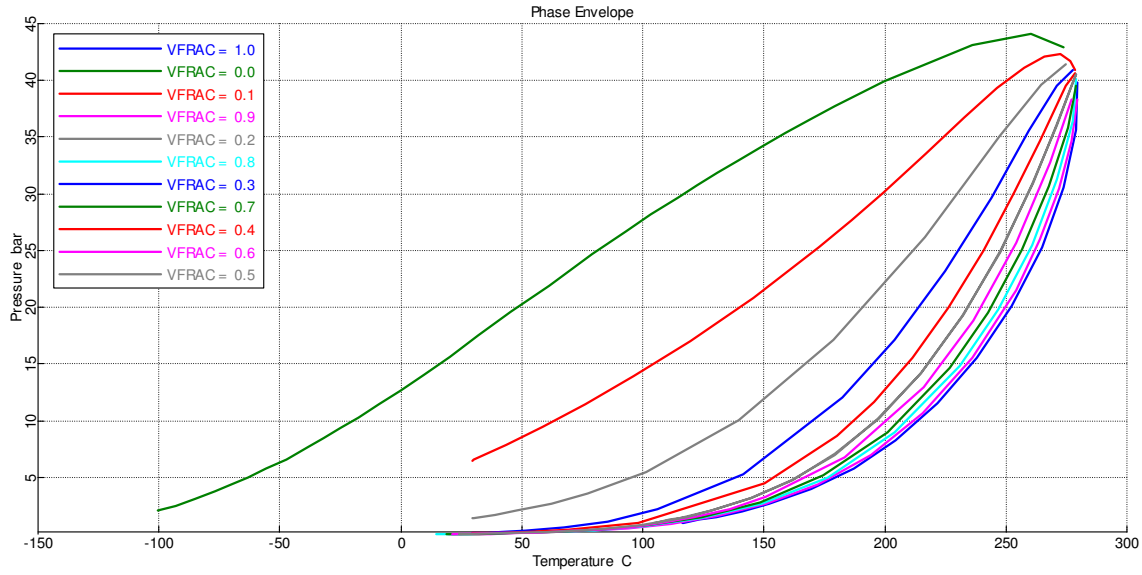

Figure 12.8: Phase envelope from Aspen Plus of feed to distillation column of Example 3.7.3 (ii) – Case 1.

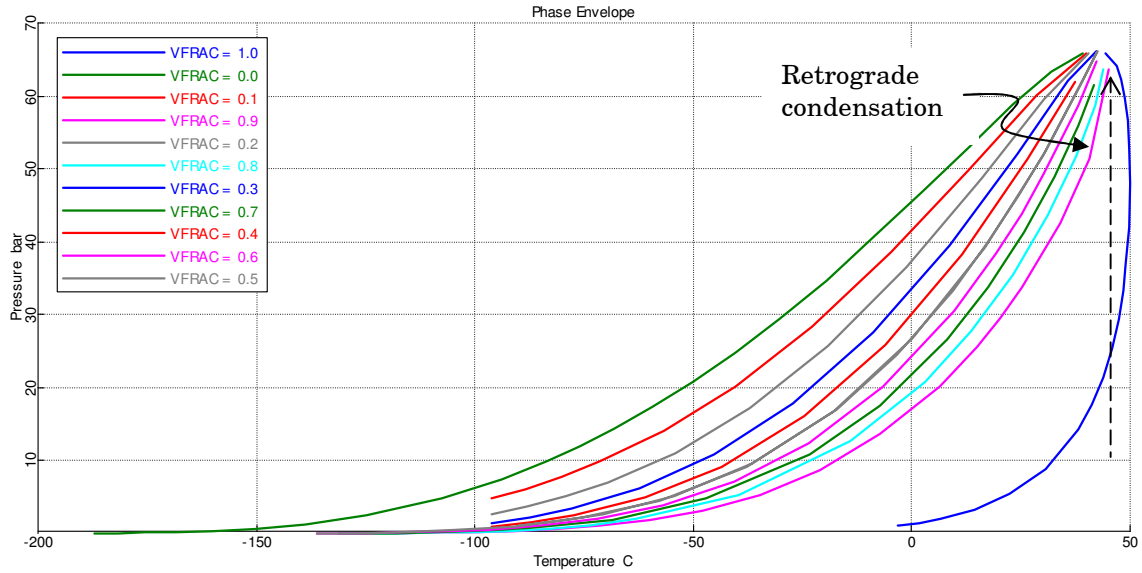

Figure 12.9: Phase envelope from Aspen Plus of vapour feed to condenser of distillation column of Example 3.7.3 (ii) – Case 1, which features retrograde condensation at temperatures above the critical.

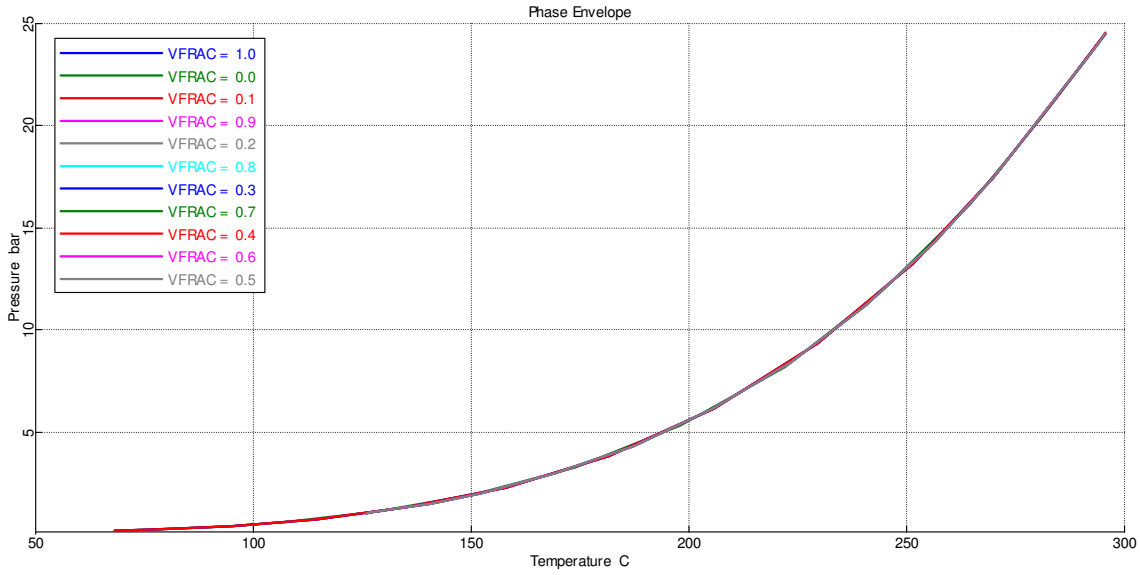

Figure 12.10: Phase envelope from Aspen Plus of liquid feed to reboiler of distillation column of Example 3.7.3 (ii) – Case 1.

12.3 Appendix III: Heat exchanger network design

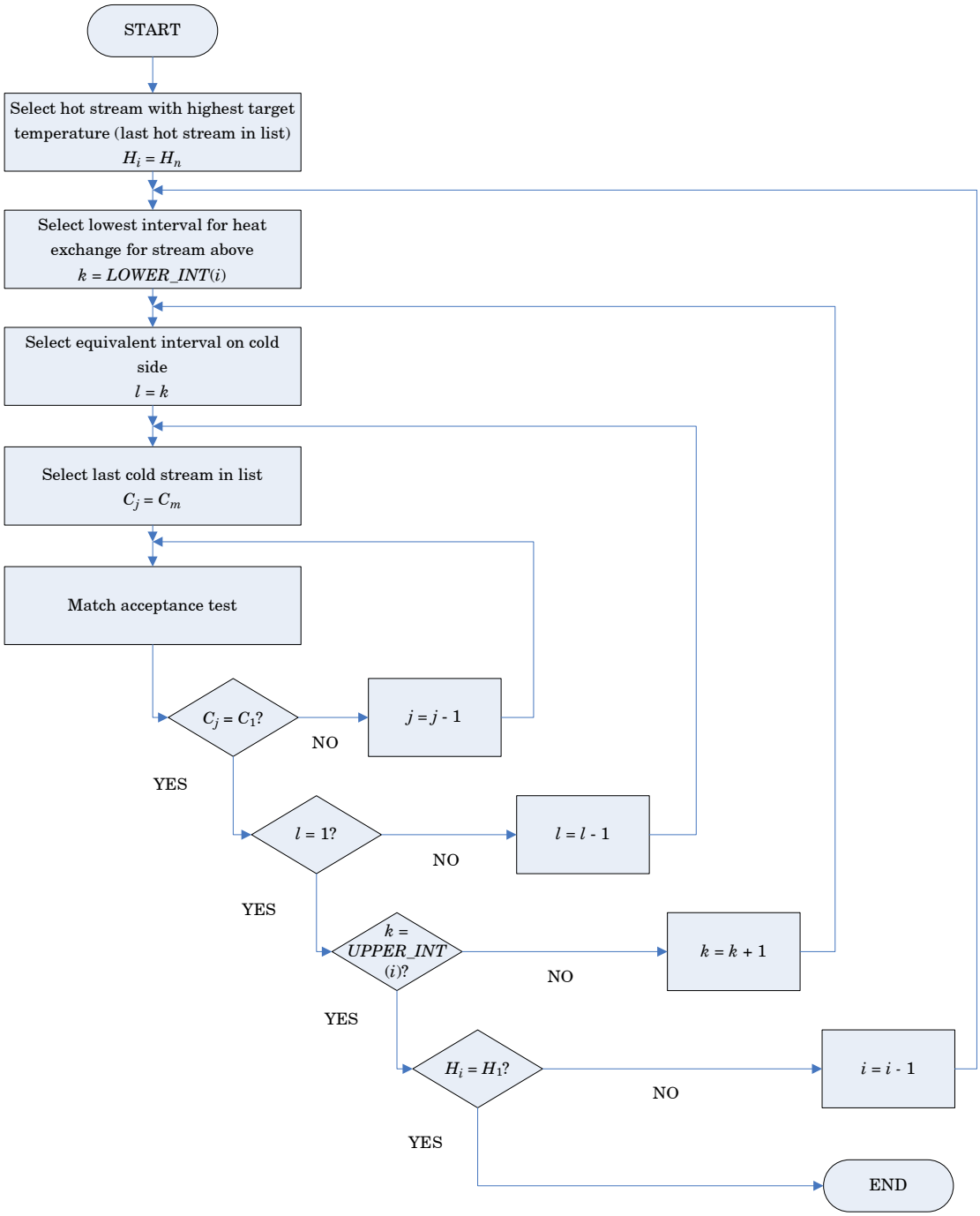

Figure 12.11: Schematics of the sequence of the match acceptance/rejection procedure.

Figure 12.11 uses the following variables:

$LOWER\_INT(i)$	=	Coldest interval for heat exchange of stream i
$UPPER\_INT(i)$	=	Hottest interval for heat exchange of stream i

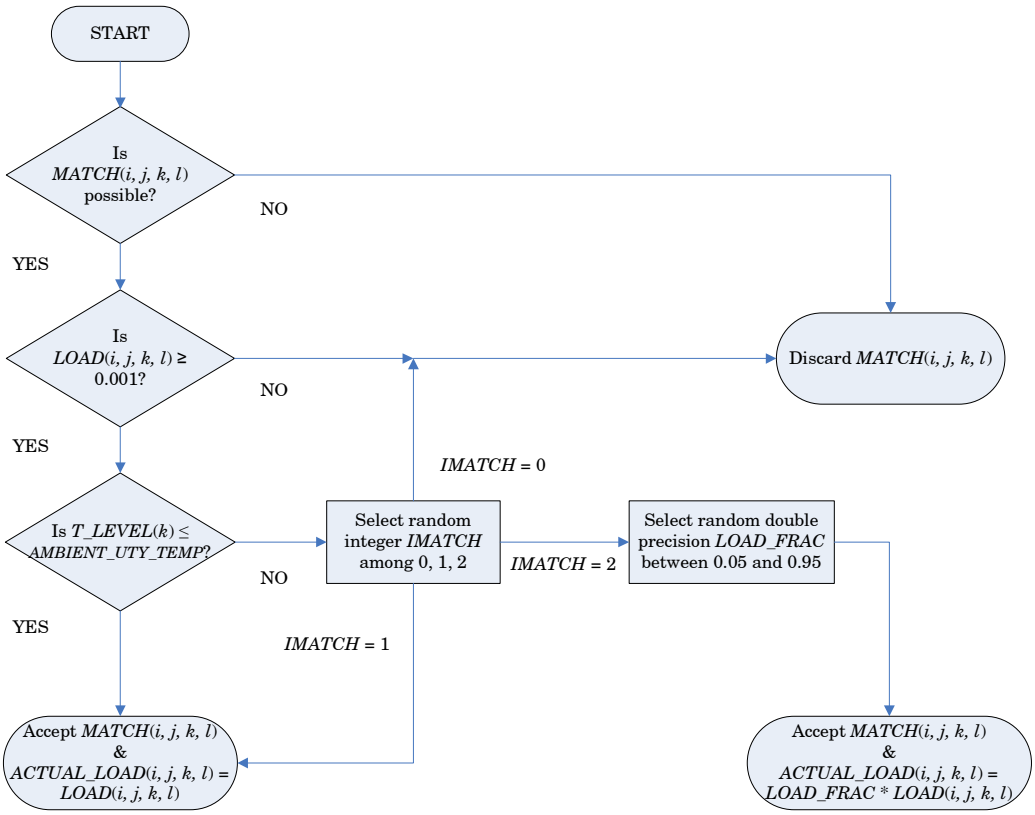

Figure 12.12: Schematics of the algorithm responsible for the match acceptance/rejection test.

Figure 12.12 uses the following variables:

ACTUAL_LOAD(*i*, *j*, *k*, *l*)	=	Selected heat duty between streams H_i and C_j from hot-side interval k to cold-side interval l.
AMBIENT_UTY_TEMP	=	Temperature of ambient utility
IMATCH	=	Integer variable representing the scenarios for heat match selection
LOAD(*i*, *j*, *k*, *l*)	=	Maximum heat duty exchangeable between streams H_i and C_j from hot-side interval k to cold-side interval l.
LOAD_FRAC	=	Fraction of the maximum heat duty exchangeable that is selected
LOWER_INT(*i*)	=	Coldest interval for heat exchange of stream i
MATCH(*i*, *j*, *k*, *l*)	=	Boolean variable representing the existence or inexistence of match between streams H_i and C_j from hot-side interval k to cold-side interval l
T_LEVEL(*k*)	=	Hot-side temperature level k
UPPER_INT(*i*)	=	Hottest interval for heat exchange of stream i

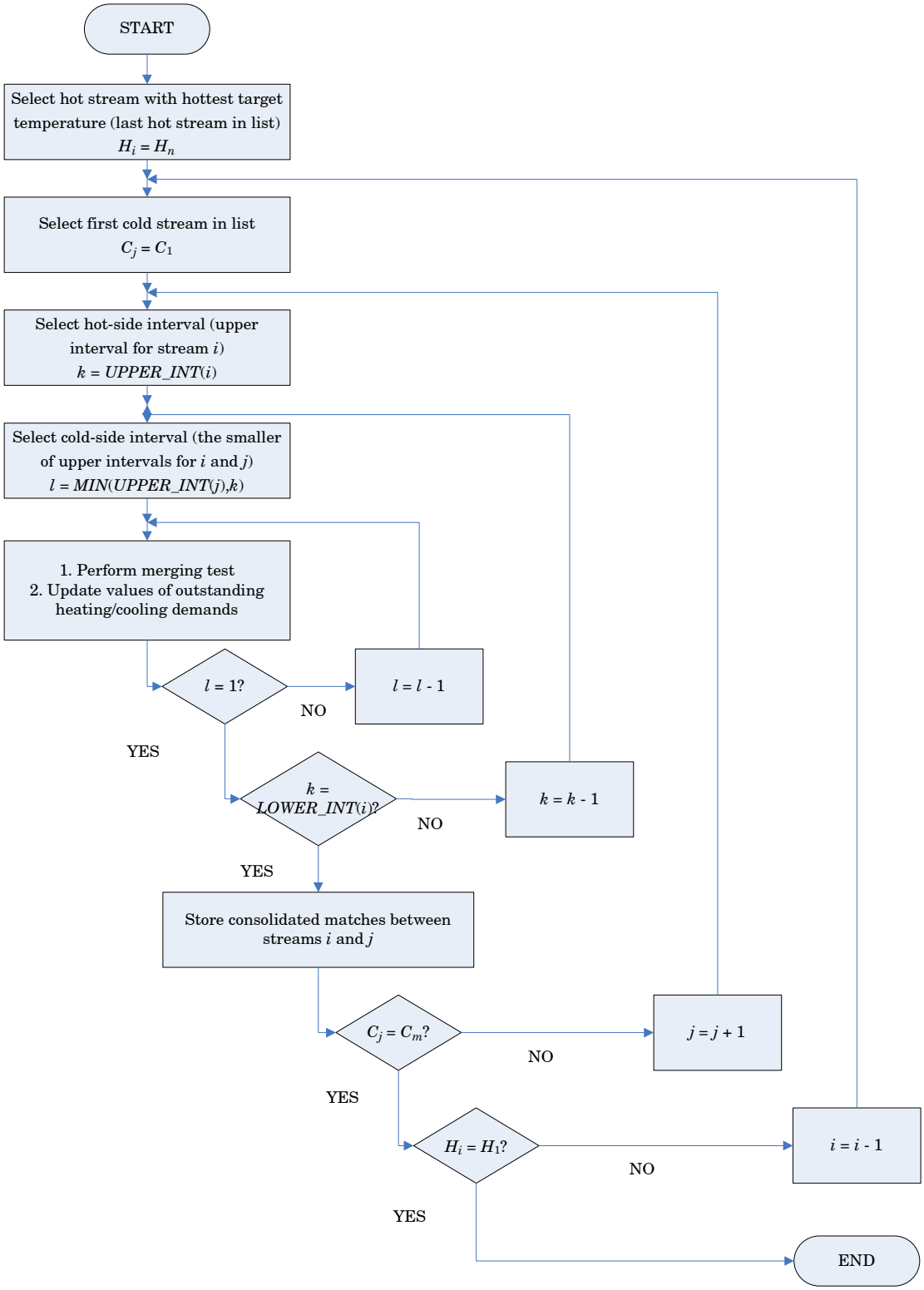

Figure 12.13: Schematics of the sequence of the match-merging procedure.

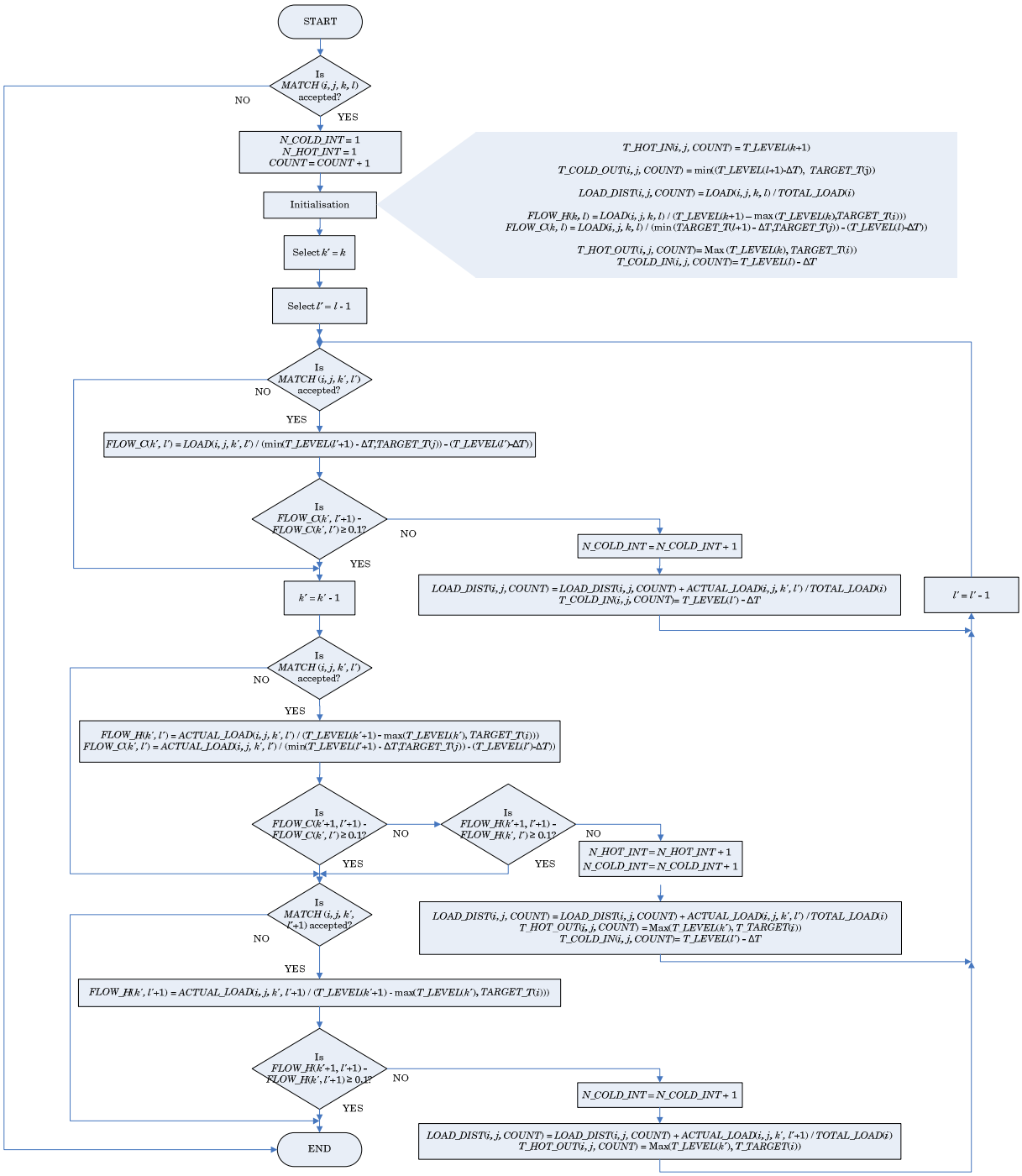

Figure 12.14: Schematics of the algorithm responsible for the match-merging test.

Figure 12.14 uses the following variables:

ACTUAL_LOAD(*i*, *j*, *k*, *l*)	=	Selected heat duty between streams H_i and C_j from hot-side interval k to cold-side interval l
COUNT	=	Intermediate counter of heat exchangers between streams H_i and C_j
FLOW_C(*k*, *l*)	=	Cold stream enthalpy-temperature profile for match between given pair of streams between intervals k and l
FLOW_H(*k*, *l*)	=	Hot stream enthalpy-temperature profile for match between given pair of streams between intervals k and l
LOAD_DIST(*i*, *j*, *COUNT*)	=	Ratio of the cumulative actual heat duty exchanged between streams H_i and C_j in heat exchanger *COUNT* to the total heat demand of hot stream H_i
N_COLD_INT	=	Number of cold-side intervals covered by heat exchanger *COUNT*

N_HOT_INT	=	Number of hot-side intervals covered by heat exchanger *COUNT*
T_COLD_IN(*i, j, COUNT*)	=	Effective inlet cold side temperature for the heat exchanger *COUNT*
T_HOT_OUT(*i, j, COUNT*)	=	Effective outlet hot side temperature for the heat exchanger *COUNT*
T_LEVEL(*k*)	=	Hot-side temperature level k
T_TARGET(*i*)	=	Temperature target of hot stream H_i

12.4 Appendix IV: Costing considerations

	£1800 ≤ *UnitCost* < £2700					
	C_1	C_2	C_3	C_4	C_5	C_6
F_{ER}	0.38	0.15	0.38	1800	2700	1800
F_P	1.76	1.4	1.76	1800	2700	1800
F_I	1	0.65	1	1800	2700	1800
F_{EL}	0.19	0.13	0.19	1800	2700	1800
F_C	0.35	0.28	0.35	1800	2700	1800
F_{SB}	0.08	0.06	0.08	1800	2700	1800
F_L	0.38	0.31	0.38	1800	2700	1800
	£2700 ≤ *UnitCost* < £7800					
	C_1	C_2	C_3	C_4	C_5	C_6
F_{ER}	0.15	0.13	0.15	2700	7800	2700
F_P	1.4	0.98	1.4	2700	7800	2700
F_I	0.65	0.49	0.65	2700	7800	2700
F_{EL}	0.13	0.1	0.13	2700	7800	2700
F_C	0.28	0.22	0.28	2700	7800	2700
F_{SB}	0.06	0.05	0.06	2700	7800	2700
F_L	0.31	0.21	0.31	2700	7800	2700
	£7800 ≤ *UnitCost* < £18000					
	C_1	C_2	C_3	C_4	C_5	C_6
F_{ER}	0.13	0.11	0.13	7800	18000	7800
F_P	0.98	0.66	0.98	7800	18000	7800
F_I	0.49	0.34	0.49	7800	18000	7800
F_{EL}	0.1	0.06	0.1	7800	18000	7800
F_C	0.22	0.17	0.22	7800	18000	7800
F_{SB}	0.05	0.04	0.05	7800	18000	7800
F_L	0.21	0.14	0.21	7800	18000	7800
	£18000 ≤ *UnitCost* < £42000					
	C_1	C_2	C_3	C_4	C_5	C_6
F_{ER}	0.11	0.1	0.11	18000	42000	18000
F_P	0.66	0.4	0.66	18000	42000	18000
F_I	0.34	0.22	0.34	18000	42000	18000
F_{EL}	0.06	0.03	0.06	18000	42000	18000
F_C	0.17	0.14	0.17	18000	42000	18000
F_{SB}	0.04	0.025	0.04	18000	42000	18000
F_L	0.14	0.08	0.14	18000	42000	18000
	£42000 ≤ *UnitCost* < £120000					
	C_1	C_2	C_3	C_4	C_5	C_6
F_{ER}	0.1	0.08	0.1	42000	120000	42000
F_P	0.4	0.26	0.4	42000	120000	42000
F_I	0.22	0.13	0.22	42000	120000	42000
F_{EL}	0.03	0.03	0.03	42000	120000	42000
F_C	0.14	0.1	0.14	42000	120000	42000
F_{SB}	0.025	0.025	0.025	42000	120000	42000
F_L	0.08	0.04	0.08	42000	120000	42000
	£120000 ≤ *UnitCost* < £180000					
	C_1	C_2	C_3	C_4	C_5	C_6
F_{ER}	0.08	0.05	0.08	120000	180000	120000
F_P	0.26	0.16	0.26	120000	180000	120000
F_I	0.13	0.09	0.13	120000	180000	120000
F_{EL}	0.03	0.03	0.03	120000	180000	120000
F_C	0.1	0.08	0.1	120000	180000	120000
F_{SB}	0.025	0.012	0.025	120000	180000	120000
F_L	0.04	0.03	0.04	120000	180000	120000

Table 12.2: Coefficients for calculation of the various factors of *InstCost* for Method 1.

	X_1	X_3	Y_1	Y_3
£6300 ≤ *UnitCost* < £9900	6300	9900	6.875	5.28
£9900 ≤ *UnitCost* < £11300	9900	11300	5.28	4.889
£11300 ≤ *UnitCost* < £13000	11300	13000	4.889	4.509
£13000 ≤ *UnitCost* < £15100	13000	15100	4.509	4.139
£15100 ≤ *UnitCost* < £17000	15100	17000	4.139	3.87
£17000 ≤ *UnitCost* < £24600	17000	24600	3.87	3.148
£24600 ≤ *UnitCost* < £27700	24600	27700	3.148	2.948
£27700 ≤ *UnitCost* < £60300	27700	60300	2.948	1.941
£60300 ≤ *UnitCost* < £158200	60300	158200	1.941	1.184

Table 12.3: Coefficients for calculation of the F_{total} required for calculation of *InstCost* for Method 2.

Material	$F_{material}$
CS	1
Al	1.3
SS Low Grade	2.4
SS High Grade	3.4
Hastelloy C	3.6
Monel	4.1
Ni	4.4
Inconel	4.4
Ti	5.8
CS & CS (S&T)	1
CS & Al (S&T)	1.3
CS & Monel (S&T)	2.1
CS & SS Low Grade (S&T)	1.7
SS Low Grade & SS Low Grade (S&T)	2.9

Table 12.4: Material factors for general equipment and for shell and tube heat exchangers (S&T) for Method 3.

Absolute design pressure, bar	$F_{pressure}$
0.01 ≤ Pressure < 0.1	2 + (1.3 - 2) / (0.1 - 0.01) · (Pressure - 0.01)
0.1 ≤ Pressure < 0.5	1.3 + (1 - 1.3) / (0.5 - 0.1) · (Pressure - 0.1)
0.5 ≤ Pressure ≤ 7	1
7 < Pressure < 50	1 + (1.5 - 1) / (50 - 7) · (Pressure - 7)
Pressure ≥ 50	1.5 + (1.9 - 1.5) / (100 - 50) · (Pressure - 50)

Table 12.5: Pressure factor for heat exchanger cost estimation for Method 3.

Maximum design temperature, °C	$F_{temperature}$
0 ≤ Temperature <= 100	1
100 < Temperature <= 300	1 + (1.6 - 1) / (300 - 100) · (Temperature - 100)
Temperature > 300	1.6 + (2.1 - 1.6) / (500 - 300) · (Temperature - 300)

Table 12.6: Temperature factor for heat exchanger cost estimation for Method 3.

Country	$F_{location}$
UK	1
US Gulf Coast	1 ÷ 1.15
US Other	1.2 ÷ 1.15
Alaska	2 ÷ 1.15
India	0.8 ÷ 1.15
Indonesia	0.7 ÷ 1.15

Table 12.7. Location factors for heat exchanger cost estimation for Method 3.

Direct Costs	Factor
f_{er}	0.4
f_{pip}	0.7
f_{inst}	0.2
f_{elec}	0.1
f_{util}	0.5
f_{os}	0.2
f_{build}	0.2
f_{sp}	0.1
Indirect Costs	
f_{dec}	1
f_{cont}	0.4
Working Capital	
f_{wc}	0.7

Table 12.8. Capital cost factors for new equipment in gases or liquids processing plants for Method 3.

12.5 Appendix V: Case Studies

		Feed	Top Product	Bottom Product
		ABC (DE)	A	BC (DE)
Composition, molar fraction	Nitrogen	0.0637	0.0724	0
	Methane	0.8264	0.9162	0.1713
	Ethane	0.0713	0.0114	0.5085
	Propane	0.0267	0	0.2211
	Isobutane	0.0120	0	0.0991
	n-Pentane	0	0	0
Flowrate, kmol/s		1.141	1.004	0.138
Product recoveries (overall feed = column feed)	Nitrogen		1	0
	Methane		0.975	0.025
	Ethane		0.14	0.86
	Propane		0	1
	Isobutane		0	1
	n-Pentane		-	-

Table 12.9: Stream characterisation for initial split (A/BC) in the direct sequence.

		Feed	Top Product	Bottom Product
		BC(DE)	B	C(DE)
Composition, molar fraction	Nitrogen	0	0	0
	Methane	0.1713	0.2558	0
	Ethane	0.5085	0.7376	0.0447
	Propane	0.2211	0.0066	0.6555
	Isobutane	0.0991	0	0.2998
	n-Pentane	0	0	0
Flowrate, kmol/s		0.138	0.092	0.046
Product recoveries (overall feed)	Nitrogen		0	0
	Methane		0.025	0
	Ethane		0.835	0.025
	Propane		0.02	0.98
	Isobutane		0	1
	n-Pentane		-	-
Product recoveries (column feed)	Nitrogen		0	0
	Methane		1.000	0.000
	Ethane		0.971	0.029
	Propane		0.020	0.980
	Isobutane		0	0
	n-Pentane		-	-

Table 12.10: Stream characterisation for secondary split (B/C) in the direct sequence.

		Feed	Top Product	Bottom Product
		ABC (DE)	AB	C (DE)
Composition, molar fraction	Nitrogen	0.0637	0.0663	0
	Methane	0.8264	0.8607	0
	Ethane	0.0713	0.0724	0.0447
	Propane	0.0267	0.0006	0.6555
	Isobutane	0.0120	0	0.2998
	n-Pentane	0	0	0
Flowrate, kmol/s		1.141	1.096	0.0455
Product recoveries (overall feed = column feed)	Nitrogen		1	0
	Methane		1	0
	Ethane		0.975	0.025
	Propane		0.02	0.98
	Isobutane		0	1
	n-Pentane		-	-

Table 12.11: Stream characterisation for initial split (AB/C) in the indirect sequence.

		Feed AB	Top Product A	Bottom Product B
Composition, molar fraction	Nitrogen	0.0663	0.0724	0
	Methane	0.8607	0.9162	0.2558
	Ethane	0.0724	0.0114	0.7376
	Propane	0.0006	0	0.0066
	Isobutane	0	0	0
	n-Pentane	0	0	0
Flowrate, kmol/s		1.096	1.004	0.092
Product recoveries (overall feed)	Nitrogen		1	0
	Methane		0.975	0.025
	Ethane		0.14	0.835
	Propane		0	0.02
	Isobutane		0	0
	n-Pentane		-	-
Product recoveries (column feed)	Nitrogen		1.000	0.000
	Methane		0.975	0.025
	Ethane		0.144	0.856
	Propane		0	1
	Isobutane		0	0
	n-Pentane		-	-

Table 12.12: Stream characterisation for secondary split (A/B) in the indirect sequence.

Direct sequence	Feed to split 1	1.141 kmol/s
	Methane recovery (top)	0.975·1.141·0.8264 = 0.919 kmol/s
	Top product	1.004 kmol/s
	Ethane recovery (bottoms)	0.86·1.141·0.0713 = 0.070 kmol/s
	Bottoms product	0.138 kmol/s
	Feed to split 2	0.138 kmol/s
	Ethane recovery (top)	0.971·0.138·0.5085 = 0.068 kmol/s
	Top product	0.092 kmol/s
	Propane recovery (bottoms)	0.980·0.138·0.2211 = 0.030 kmol/s
	Bottoms product	0.046 kmol/s
Indirect sequence	Feed to split 1	1.141 kmol/s
	Ethane recovery (top)	0.975·1.141·0.0713 = 0.079 kmol/s
	Top product	1.096 kmol/s
	Propane recovery (bottoms)	0.98·1.141·0.0267 = 0.030 kmol/s
	Bottoms product	0.0455 kmol/s
	Feed to split 2	1.096 kmol/s
	Methane recovery (top)	0.975·1.096·0.8607 = 0.920 kmol/s
	Top product	1.004 kmol/s
	Ethane recovery (bottoms)	0.856·1.096·0.0724 = 0.068 kmol/s
	Bottoms product	0.092 kmol/s

Table 12.13: Key material balance data for separation tasks in direct and indirect sequences.

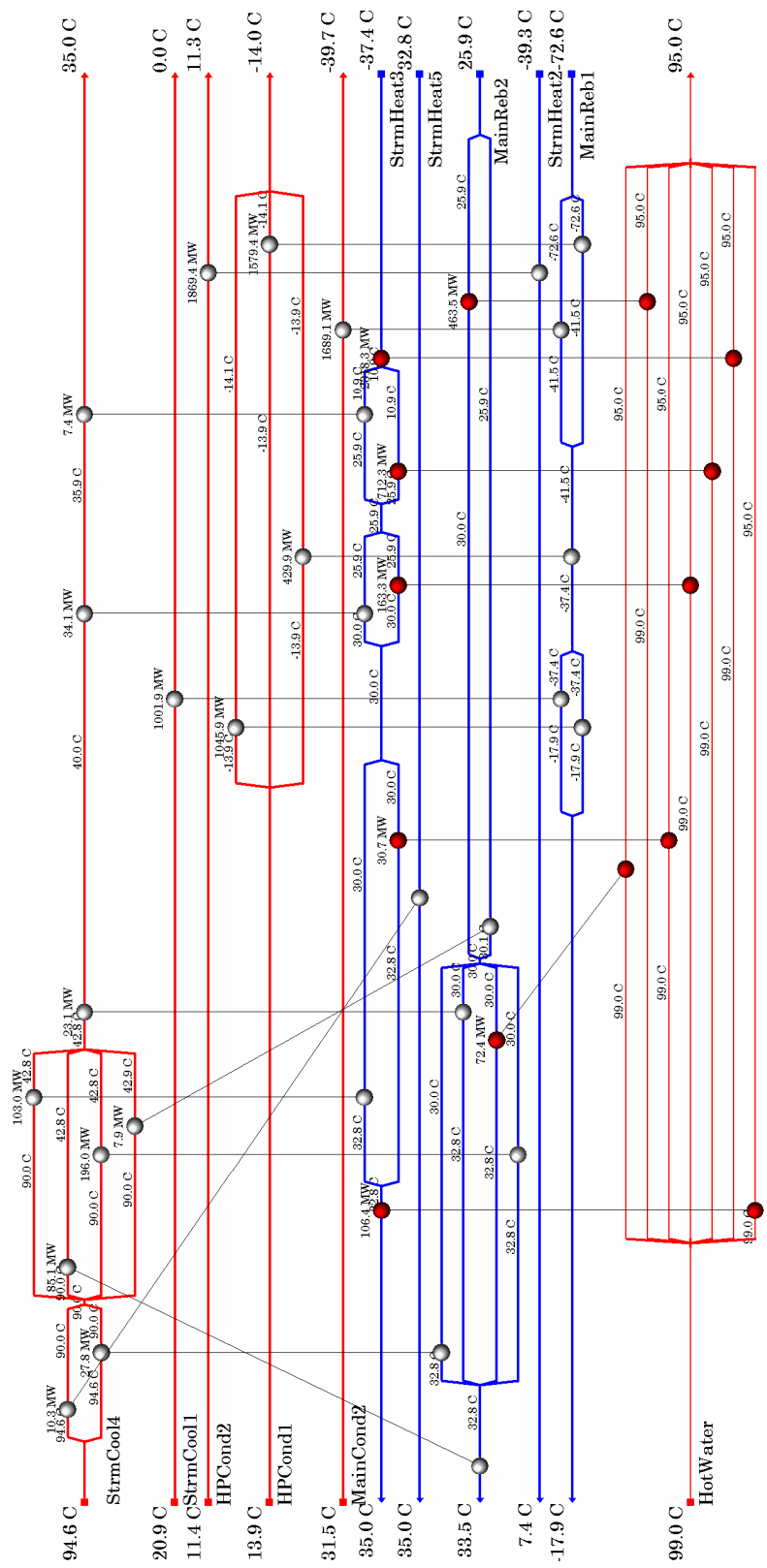

Figure 12.15: Config. No. 3 (Direct sequence – Distil. x 2): Heat integration network.

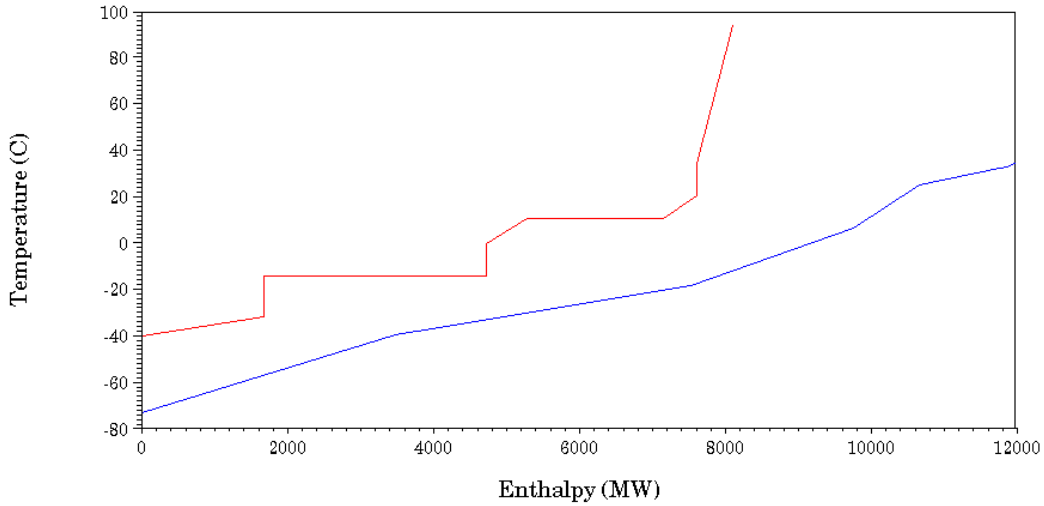

Figure 12.16: Config. No. 3 (Direct sequence – Distil. x 2): Composite curves for heat integration network of problem.

Number of real stages Absorber top section	Number of real stages (excluding reboiler) Absorber top section	Solvent-to-feed mol/mol	Boilup-to-feed mol/mol
10	10	0.694	0.657
10	14	0.695	0.664
10	18	0.693	0.663
10	22	0.693	0.663
14	10	0.699	0.668
14	14	0.694	0.664
14	18	0.693	0.663
14	22	0.693	0.663
18	10	0.698	0.668
18	14	0.694	0.663
18	18	0.693	0.663
18	22	0.693	0.663
22	10	0.698	0.667
22	14	0.694	0.663
22	18	0.693	0.663
22	22	0.693	0.663

Table 12.14: Sensitivity of solvent and boilup requirements to reboiled absorber height for Config. No. 1 of Case Study 2.